1-1-2013

Synthesis And Application Of Atp Analogs For Phosphorylation-Dependent Kinase-Substrate Crosslinking

Satish Kumar Garre Venkata Raghavendra
Wayne State University,

SYNTHESIS AND APPLICATION OF ATP ANALOGS FOR PHOSPHORYLATION-DEPENDENT KINASE-SUBSTRATE CROSSLINKING

by

SATISH KUMAR GARRE VENKATA RAGHAVENDRA

DISSERTATION

Submitted to the Graduate School

of Wayne State University,

Detroit, Michigan

in partial fulfillment of the requirements

for the degree of

DOCTOR OF PHILOSOPHY

2013

MAJOR: CHEMISTRY (Organic)

Approved by:

_____

Advisor Date

_____

_____

_____

DEDICATION

To my late mother

And

To my uncle, who died of metastatic liver cancer in July of 2013

In loving memory
Garre Family

ACKNOWLEDGMENTS

I would like to thank all the people who helped me and were part of my pursuits, in the past few years beyond research. I would like to mention some important people in this endeavor.

First, I would like to sincerely thank my advisor Prof. Mary Kay Pflum, who was a great mentor providing valuable guidance at all stages of my career and made this journey a memorable, learning experience. She is an outstanding teacher, who practices what she speaks and leads by example. I would like to thank my committee members Prof. Tamara L. Hendrickson, Prof. Zhongwu Guo and Prof. Russell L. Finley Jr. for their advice and suggestions.

I would like to thank my lab members who helped me and had fun with me over the past few years in the Pflum lab: Patrick Wloszczynski, Sujit Suwal, Sujith Weerasinghe, Emily Aubie, Sun Choi, Mostafa Aboutaleb, Joe Duran, Todd Faner, Anitha Chalasani, Geetha Padige, Magdalene Wambua, Tony Young, Thilani Anthony, Maheeka Embogama, Pavithra Dehigama, Ahmed Fauda, Danusha Nalawansha, Alex Stark and Ahmed Negmeldin.

Next, I would like to thank my wife Jyothsna, for all of her support over the past few years and my family members for their encouragement. I would like to thank Chandrasekhar, Ravi, Nilesh, Saptarshi, Srinivas, Shirin, Fathima, Amit, Rajesh, Rama, Raja, Appi, Pavan, Venkat and an unending list of friends at WSU.

I would like to acknowledge the Administrative staff of the Chemistry Department and the Science Stores personnel for their services. I would like to thank the technical staff of Lumigen Instrument Center for their support in NMR and MS analysis.

TABLE OF CONTENTS

LIST OF TABLES

LIST OF FIGURES

LIST OF SCHEMES

LIST OF ABBREVIATIONS

Amino Acids

A or Ala - alanine

C or Cys - cysteine

D or Asp - aspatate

E or Glu - glutamate

F or Phe - phenylalanine

G or Gly - gllycine

H or His - histidine

I or Ile - isoleucine

K or Lys - lysine

L or Leu - leucine

M or Met - methionine

N or Asn - asparagine

P or Pro - proline

Q or Gln - glutamine

R or Arg - arganine

S or Ser - serine

T or Thr - threonine

V or Val - valine

W or Trp - tryptophan

X- any amino acid

Y or Tyr - tyrosine

Z - hydrophobic residue

Nucleic Acids

AMP - adenosine 5'-monophosphate

ADP - adenosine 5'-diphosphate

ATP - adenosine 5'-triphosphate

ATP-γS - adenosine 5'-[γ-thio]triphosphate

CoA - coenzyme A

cAMP - cyclic 3',5'-monophosphate

DNA - deoxyribonucleic acid

GTP - guanine 5'-triphosphate

NADH - nicotinamide adenine dinucleotide

RNA - ribonucleic acid

Proteins

Abl - Abelson kinase

Arg - Abl related-gene

ATM - ataxia telangiectasia mutated kinase

ATR - ataxia-telangiectasia and Rad3 kinase related protein complex

BCR - breakpoint cluster region

BRCA1 - breast cancer susceptibility protein-1

CAMK4 - calcium/calmodulin-dependent protein kinase IV

CBP - CREB binding protein

CDK1- cyclin-dependent kinase1

CDK2- cyclin-dependent kinase 2

CDK7 - cyclin-dependent kinase 7

CHK1- checkpoint kinase 1

Chk2 - checkpoint kinase 2

CK2 - casein kinase 2

CK2 - casein kinase 2

CRE - cAMP response element

CREB - cAMP responsive element binding protein

Csk - C-terminal Src kinase

EGFR - endothelial growth factor receptor

EGFR - epithelial growth factor receptor

ELK1 - E 26 like protein

ERK2 - extracellular signal-regulated kinase 2

GAK - Cyclin G-associated kinase

GRK5 - G-protein coupled receptor kinase 5

GSK3β - glycogen synthase kinase 3 beta

JAK3 - janus kinase 3

MAPK - mitogen activated protein kinase

MRE 11- meiotic recombination-11

NBS1 - nijmegen breakage syndrome-1

PI3K - phosphatidylinositol-3-kinase

PKA - protein kinase A or cAMP regulated protein kinase

PKB - protein kinase B

PLK3 - polo-like kinase 3

SPK - serine/threonine protein kinase

SRC- v-src sarcoma (Schmidt-Ruppin A-2) viral oncogene homolog (avian)

Chapter 1

1.1 Introduction

Proteins undergo various types of modifications to orchestrate a myriad functions in a cell. Protein modifications occur after translation, so they are termed as post-translational modifications (PTMs). PTMs play a crucial role and affect diverse cellular processes.[1] Most of the proteins in a cell undergo at least one type of PTM at some point to carry out a biological function. So far, more than 100 different PTMs have been identified occurring on the protein side chains and some of them are listed in Table 1.1. Most of the essential amino acid residues undergo PTMs, which include phosphorylation, methylation, acetylation, adenylation, acylation, ADP-ribosylation, glycosylation, sulfation, prenylation, etc.[1] PTMs are carried out by a class of proteins called as enzymes. Dynamic regulation of these PTMs in nature is carried out by many enzyme families. These enzymes modify an amino acid of the protein, which triggers a sequence of activities, further influencing the cell function. One of the widely studied and important PTM in eukaryotes is protein phosphorylation, which also plays a major role in cell biology and disease formation.

Table 1.1: Protein post-translational modifications of amino acid side chains.[1]

Residue	Reaction	Example
Asp	Phosphorylation	Protein tyrosine phosphatases; response regulators in two component systems
	Isomerization to isoAsp	
Glu	Methylation	Chemotaxis receptor proteins
	Carboxylation	Gla residues in blood coagulation tubulin
	Polyglycination	Tubulin
	Polyglutamylation	
Ser	Phosphorylation	Protein serine kinases and phosphatases
	O-glycosylation	Notch O-glycosylation
	Phosphopantetheinylation	Fatty acid synthase
	Autocleavages	Pyruvamidyl enzyme formation

Thr	Phosphorylation	Protein threonine kinases/phosphatases
	O-glycosylation	
Tyr	Phosphorylation	Tyrosine kinases/phosphatases
	Sulfation	CCR5 receptor maturation
	Ortho-nitration	Inflammatory responses
	TOPA quinone	Amine oxidase maturation
His	Phosphorylation	Sensor protein kinases in two Component regulatory systems
	Aminocarboxypropylation	Diphthamide formation
	N-methylation	Methyl CoM reductase
Lys	N-methylation	Histone methylation
	N-acylation by acetyl, biotinyl, lipoyl, ubiquityl groups	Histone acetylation; swinging-arm Prosthetic groups; ubiquitin; SUMO (small ubiquitin-like modifier) tagging of proteins
	C-hydroxylation	Collagen maturation
Cys	S-hydroxylation (S-OH)	Sulfenate intermediates
	Disulfide bond formation	Protein in oxidizing environments
	Phosphorylation	PTPases
	S-acylation	Ras
	S-prenylation	Ras
	Protein splicing	Intein excisions
Met	Oxidation to sulfoxide	Met sulfoxide reductase
Arg	N-methylation	Histones
	N-ADP-ribosylation	GSa
Asn	N-glycosylation	N-glycoproteins
	N-ADP-ribosylation	eEF-2
	protein splicing	Intein excision step
Gln	Transglutamination	Protein cross-linking
Trp	C-mannosylation	Plasma-membrane proteins
Pro	C-hydroxylation	Collagen; HIF-1a
Gly	C-hydroxylation	C-terminal amide formation

No modifications of Leu, Ile, Val, Ala, Phe side chains are known

1.1 Protein Phosphorylation

Protein phosphorylation was first discovered by Levene and Alsberg in 1906 for the protein vitellin.[2] In 1932, the PTM on vitellin was mapped to serine phosphorylation.[3] To further identify the phenomenon and characterize phosphorylation as enzyme catalyzed, it took nearly 20 years.[4] In 1979, the Hunter group discovered tyrosine phosphorylation.[5] These early findings paved the way to elucidating many signaling pathways and cellular processes.[6-8,9,10] The discovery of the enzyme catalyzing phosphorylation was made possible with these early findings.

Protein phosphorylation is carried out by a class of enzymes called kinases. Phosphorylation occurs on hydroxyl containing amino acids serine, threonine and tyrosine. The reverse process of dephosphorylation is catalyzed by phosphatases, as shown in Scheme 1.1.[11] In addition, phosphorylation can occur on histidine, arginine, and lysine residues, generally known as N-phosphorylation, mainly in prokaryotes.[12-14] During phosphorylation, adenosine 5'-triphosphate (ATP) acts as a universal cosubstrate and phosphate donor. Approximately 30% of cellular proteins are found to be phosphorylated at a given time[15] and 2% of the genome is encoded for protein kinases.[16,17] Because of their major role in cell biology, it is important to study and understand kinase function in atomic detail. Next, role of phosphorylation in signaling pathways, other cellular events and diseases are discussed.

Scheme 1.1 Protein phosphorylation and dephosphorylation on hydroxyl containing amino acids

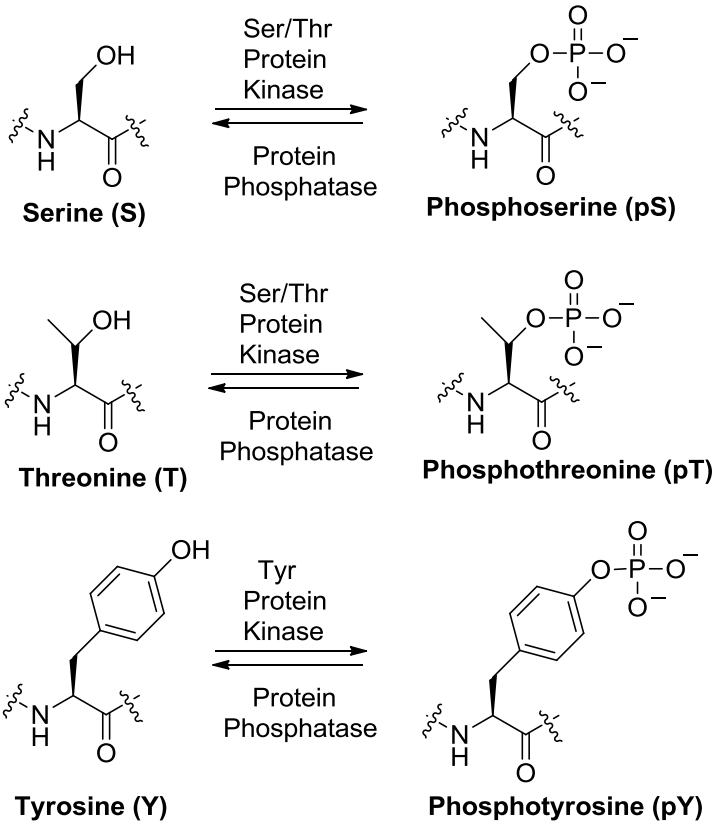

1.2 Phosphorylation and its role in signaling pathways

Phosphorylation plays a major role in the activity of proteins by stabilizing or triggering different signaling cascades, from the cell surface to the nucleus and vice versa. Signal transduction is a dynamic mechanism that involves a distinct set of proteins that conveys the signal downstream. The downstream signal can have a significant response or a harmful one in some instances. To illustrate the role of phosphorylation in signaling pathways, an example of ATM/ATR signaling pathway is discussed here (Figure 1.1). Under ionizing radiation (like UV or IR) causes changes in chromatin structure or DNA double strand breaks (DSBs) signaling for a DNA damage response. The DNA damage signal is primarily recognized by ataxia

telangiectasia mutated (ATM) kinase or by ataxia-telangiectasia and Rad3 (ATR) kinase related protein complex. The ATM and ATR kinases belong to the phosphatidylinositol-3-kinase (PI3K) family.[18,19] DNA DSBs or changes in chromatin structure lead to autophosphorylation of ATM and its activation. Upon activation ATM is recruited at the site of DSBs along with a protein complex containing Rad50, meiotic-recombination-11(MRE 11), Nijmegen breakage syndrome-1 (NBS1), and breast cancer susceptibility protein-1 (BRCA1), which signals for phosphorylation of checkpoint kinase (Chk2).[20,21] Chk2 kinase activity triggers the activity of its effector proteins, such as p53, through phosphorylation. Chk2 kinase phosphorylates serine 15 on p53.[22] Phosphorylation of p53 induces stabilization by dissociating from its negative regulator MDM2. Phosphorylation on other residues (serine 20, or serine 37) has been implicated in the stabilization and accumulation of p53.[23,24] Stabilization and accumulation of p53 leads to increased recruitment of transcription coactivators, such as p300 and CBP, which in turn help in the transactivation process and site-specific binding DNA-binding function of p53.[25] Depending on the type of stress signal and cofactors involved various downstream signaling events like DNA repair, cell-cycle checkpoint arrest, senescence, and apoptosis take place by translocating p53 into the nucleus and activation of gene transcription.[26,27] The signaling pathway discussed here is one of the possible pathways under IR stress. ATM was also known to directly phosphorylate p53 at serine 20 under stress conditions, but some reports demonstrated it as otherwise *in vivo*.[28,29] The role of p53, its activation and functions are highlighted with relevance to the studies and discussion in chapter 3.

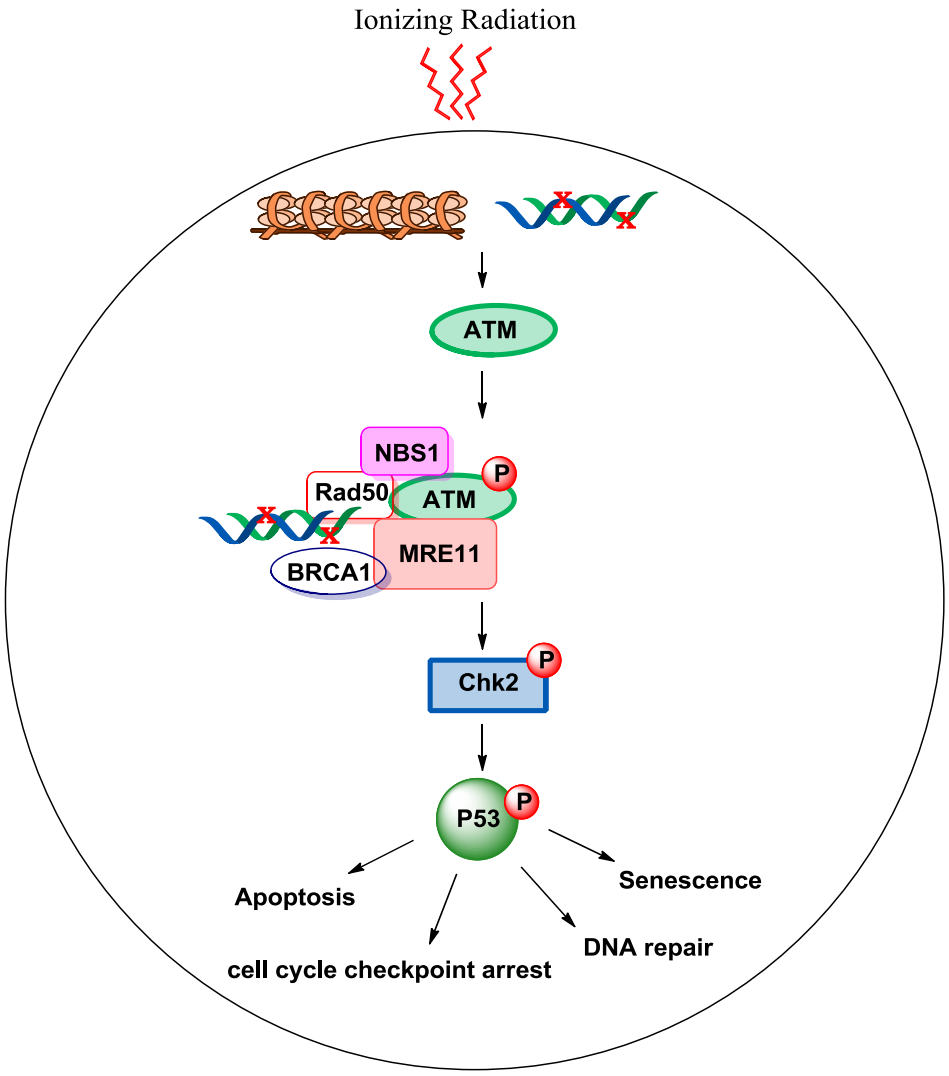

Figure 1.1: Phosphorylation mediated signaling pathway of ATM/ATR under IR. The DNA-damage signal from DSBs is recognized by ATM kinase and is recruited at the site of DNA damage by phosphorylation and activation. The phosphorylated ATM is recruited along with a protein complex containing RAD50, MRE11, NBS1 and BRCA1 at the site of the DSB.[20,21] This complex triggers the phosphorylation of chk2 kinase, which phosphorylates its effector proteins like p53. Phosphorylation of p53 on serine 15 signals its downstream effectors resulting in senescence, cell cycle arrest, apoptosis and DNA repair, depending on the extent of stress signal.[23-27]

1.3 Phosphorylation mediated protein-protein interactions

Protein phosphorylation changes the electronic environment around the site of modification, which influences protein electrostatic interactions with other proteins. Phosphorylation also plays a key role in promoting protein-protein interactions. One of the widely studied examples is the interaction between cyclic adenosine 3', 5'-monophosphate (cAMP) responsive element binding protein (CREB) and CREB binding protein (CBP). CREB binds to DNA through the cAMP response element (CRE) and regulates gene transcription, which induces cell proliferation, insulin response etc. Protein kinase A (PKA) phosphorylates CREB on serine 133, present in the kinase inducible domain (KID).[30,31] Phosphorylation of S133 changes the charge state from neutral to negative and from hydrogen bond donor to hydrogen bond acceptor. Phosphorylated S133 of CREB interacts with Y-658 in the KID interaction (KIX) domain of CBP, which is important for the transcriptional activation of CREB (Figure 1.2). Phosphorylation induced protein-protein interactions between CREB and CBP greatly enhance the transcriptional activity of CREB.

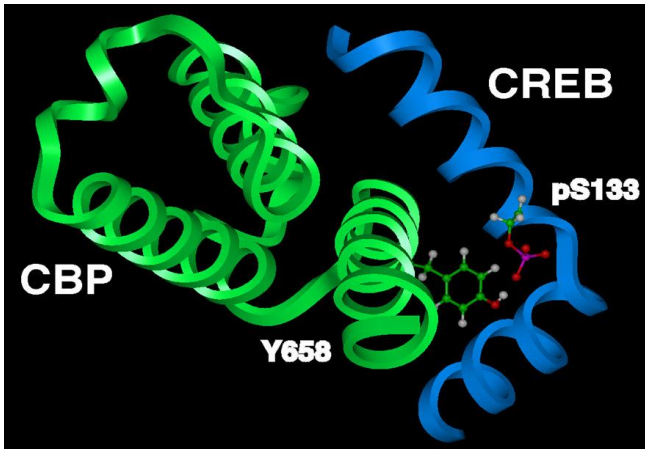

Figure 1.2: Phosphorylation mediated interaction between CREB and CBP. The CREB and CBP proteins are shown in blue and green ribbon respectively and the pSer-133 and Tyr-658 as ball and stick representations. The hydrogen bonding interaction between the phosphate (pS133) and hydroxyl group (Y658) of the two proteins regulates transcription of specific genes.[30, 31]

1.4 Role of phosphorylation and kinases in diseases

Kinases and phosphorylation play a key role in signal transduction. Aberrant activity in the signaling process and loss of dynamic equilibrium between the activity of phosphatases and kinases leads to formation of diseases. There are many kinases that are linked to disease formation like casein kinase 2 (CK2),[32] phosphoinositide 3-OH kinase (PI3K),[33] epithelial growth factor receptor (EGFR),[34] and protein kinase B (PKB)[35]. Kinase mediated signaling pathways like JAK-signal transducer and activator of transcription (STAT), PI3K-PKB etc, are known to have a role in cancer formation.[36,37]

A classic example for the role of kinases in the cancer formation is the chronic myelogenous leukemia (CML), which is myeloproliferative disorder of blood stem cells. CML is caused by genetic anomaly, which is called the Philadelphia chromosome.[38] Chromosomal translocation of the gene encoding Abelson kinase (Abl) on chromosome 9 and the break point cluster (BCR) gene on chromosome 22 results in a BCR-Abl gene. The BCR-Abl gene encodes for BCR-Abl fusion protein which has unusual tyrosine-kinase activity resulting in a signaling cascade leading to CML (Figure 1.3).[39-41] The mechanism of CML is very well understood but the cause of gene translocation is still unknown.[42] Gleevec (imatinib) is a FDA approved drug and widely used Abl kinase inhibitor for the treatment of CML.[43,44] Imatinib is a rationally designed, selective inhibitor of tyrosine kinase activity of BCR-Abl protein. Imatinib competitively binds the SH1 ATP domain of BCR-Abl fusion protein blocking the phosphorylation-mediated signaling pathway and progression of CML (Figure 1.3). As CML illustrates, kinases play a role in disease formation and have become attractive drug targets. Recent studies have focused on developing selective kinase inhibitors because of their roles in various diseases.

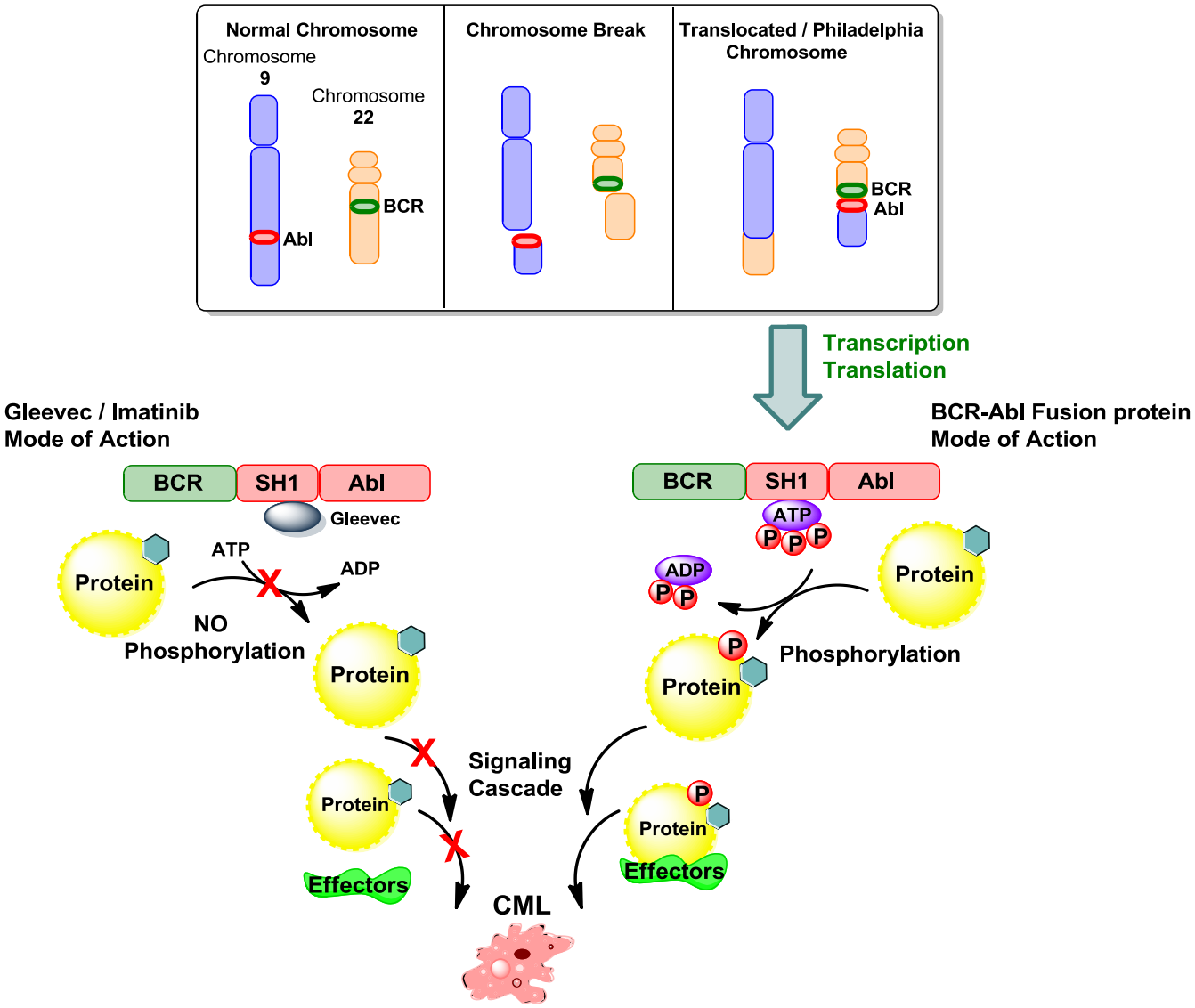

Figure 1.3: BCR-Abl gene formation and mode of action Cartoon depicting Philadelphia chromosome formation associated with CML (top). Signaling pathway of BCR-Abl fusion protein with hyperphosphorylation activity leads to CML (bottom right). Imatinib/Gleevec blocks ATP binding site, preventing hyperphosphorylation activity leading to CML and controls the disease (bottom left).

1.4.1 Kinase drugs and inhibitors

With recent advances in both *in vitro* and *in vivo* techniques, the role of phosphorylation in disease formation was better understood. As a result many kinases have been identified as potential drug targets. The challenge in the identification of selective, competitive inhibitors for kinases is due to their similarity in the highly conserved ATP binding site among different classes of kinases (kinase structure is discussed in Section 1.6).[7] Hence it is difficult to design inhibitors targeting a single kinase. However some drugs have been designed despite the challenge. Gleevec (Imatinib) was the first selective BCR-Abl tyrosine kinase inhibitor (See Figure 1.3 for mechanism of action, see Figure 1.4 for chemical structure), other examples include 5,6-Dichloro-1-β-D-ribofuranosyl benzimidazole (DRB), and N-[2-(methylamino)ethyl]-5-isoquinolonesulfonamide (H8), which selectively inhibit CK2 and PKA, respectively. Rapamycin and Everolimus are two natural products used to treat immunosupression by targeting mTOR. Staurosporine is also a natural product commonly used in research laboratories and is a non-selective kinase inhibitor (Figure 1.4). A list of FDA approved kinase inhibitors used to treat various diseases, mainly cancer, is shown in Table 1.2.[45,46]

Despite their selectivity and diversity in structural features (Figure 1.4), some inhibitors bind to off target kinases, this leads to adverse side effects. Gleevec, one successful kinase drug binds to the C-Kit receptor, PDGFR, resulting in serious side effects. In addition, gleevec drug resistance has also developed because of mutations in the gene/ target kinase affecting the binding of drug in the active site.[47-49] Hence, more selective kinase drugs are needed to treat diseases more effectively. Therefore, there is a need to understand and develop new methods to study the role of phosphorylation and the mechanism of kinases.

Table 1.2: List of some of the FDA approved, commercially available kinase inhibitors.[45,46]

Inhibitor/ Drug	Disease	Targeted Kinase	Company	Status
Fasudil/Eril	Cerebral vasospasm	ROCK	Eisai	Japan approved (1995)
Rapamycin/ Rapamune	Immunosuppression	m-TOR	Wyeth-Pfizer	FDA approved (1999)
Gleevec/ Imatinib	Cancer	Bcr-Abl	Novartis	FDA approved (2001)
Iressa	Cancer	EGFR	Astra-Zeneca	FDA approved (2003)
Tarceva	Cancer	EGFR	OSI Pharm.	FDA approved (2004)
Nexavar	Cancer	Raf-1	Bayer	FDA approved (2005)
Sunitinib	Cancer	VEGFR, PDGFR	Pfizer	FDA approved (2006)
Crizotinib	Cancer	ALK, ROS-1	Pfizer	FDA approved (2011)
Vemurafenib	Cancer	BRAF	Roche	FDA approved (2011)
Axitinib	Cancer	VEGFR, PDGFR	Pfizer	FDA approved (2012)
Bosutinib	Cancer	Bcr-Abl, Src	Pfizer	FDA approved (2012)
Tofacitinib	Rheumatoid Arthritis	JAKs	Pfizer	FDA approved (2012)

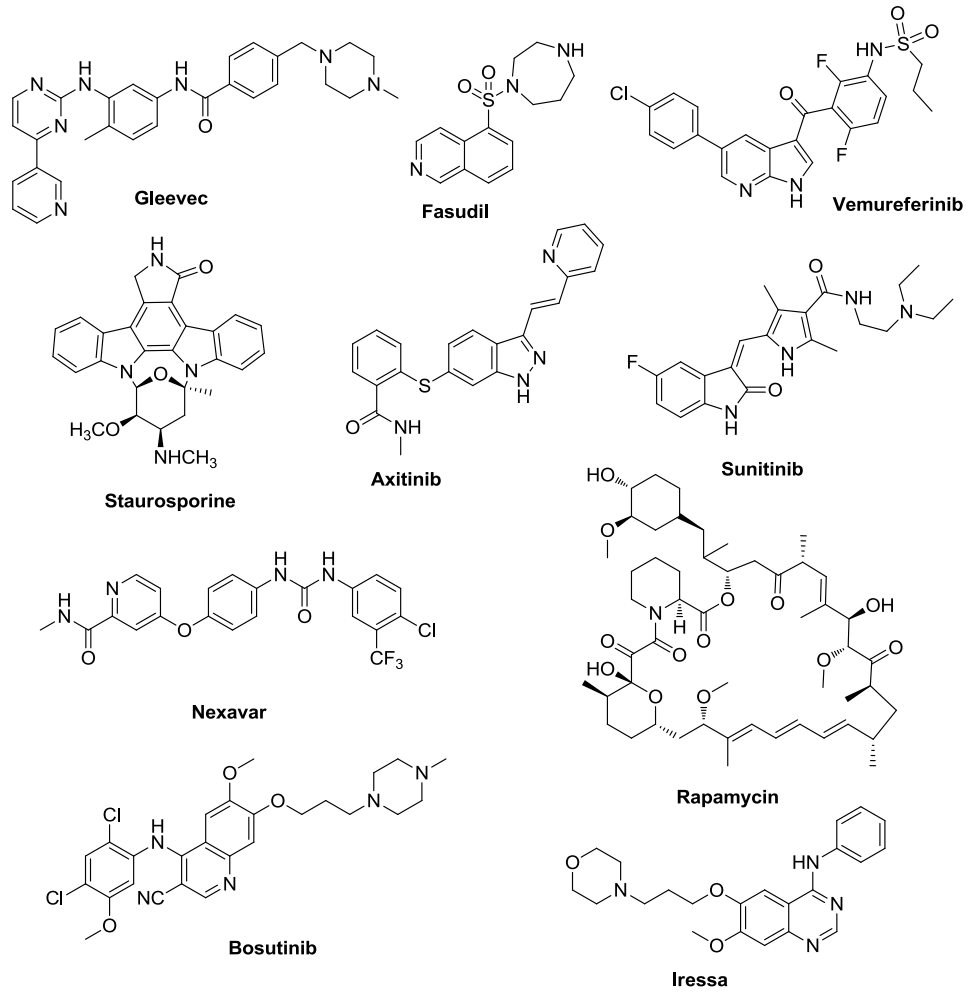

Figure 1.4: Chemical Structures of Some Kinase Inhibitors Staurosporine is used only for research purposes; all others are used for treatment of diseases (Table 1.2). [45,46]

1.5 Protein Kinases: Classification

Protein kinases catalyze protein phosphorylation and belong to a super family of enzymes called transferases. Over 500 human kinases are known, representing approximately 2% of the human genome.[17,50] Protein kinases are broadly classified into two classes based on their preferred amino acid substrates: serine/threonine protein kinases and tyrosine protein kinases. A third class of kinases exist that phosphorylate both serine/threonine and tyrosine residues, but

they are not well characterized. Protein kinases are further grouped into eight families based on sequence similarities in the catalytic site (Figure 1.5).[16] A second type of classification is based on the localization and activity of kinases, which are receptor (cell or nuclear membrane) and non-receptor (cytosolic) kinases.

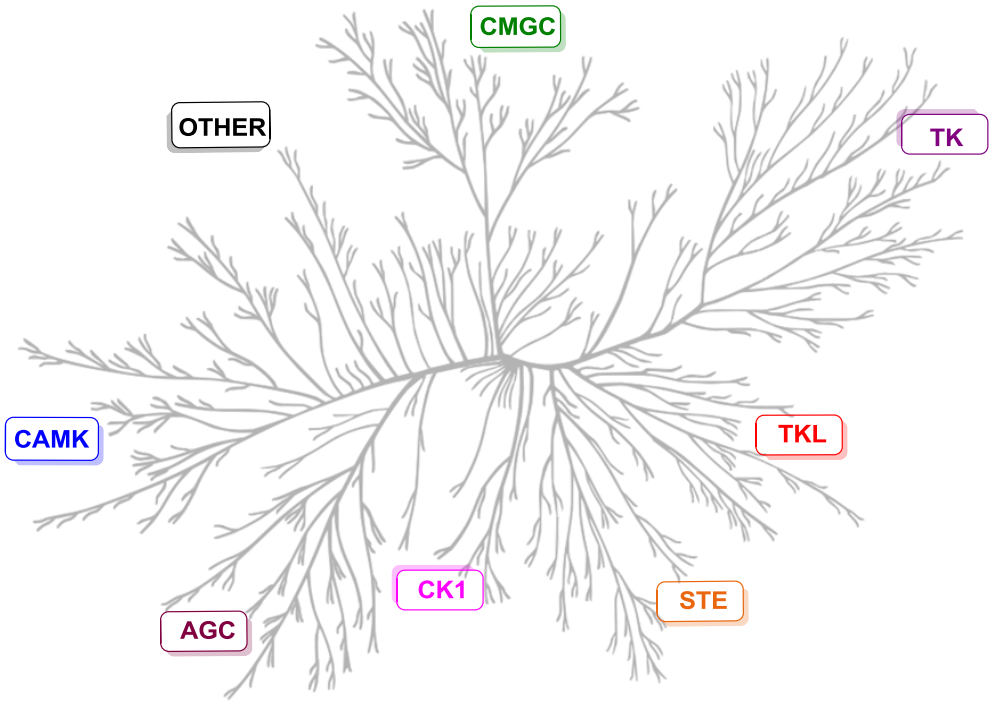

Figure 1.5: Classification of Human Kinases. Human kinases are mainly divided into 7 major groups including; **aAGC:** Containing PKA, PKG, PKC families; **CAMK:** Calcium/calmodulin-dependent protein kinase; **CK1:** Casein kinase 1; **CMGC:** Containing CDK, MAPK, GSK3, CLK families; **STE:** Homologs of yeast Sterile 7, Sterile 11, Sterile 20 kinases; **TK:** Tyrosine kinase; **TKL:** Tyrosine kinase-like. **Other:** kinases do not belong to any of the above groups.[16]

1.6 Protein Kinases: Structure, Mechanism and Specificity

Protein kinases consist of two domains, a catalytic and a regulatory domain, which work cooperatively to turn on and off phosphorylation events. Some kinases, like CK2, contain two catalytic and two regulatory units. But CK2 can exist and function independently with catalytic subunit only.[51] In the case of cSrc kinase, the catalytic domain is part of a large protein complex

that controls the phosphorylation activity.[52] The catalytic subunit consists of two domains, N-terminal and C-terminal domains, resulting in two conformations: open and closed conformations. The C-terminal domain, also called the larger lobe, consists of α-helices with substrate binding sites. The N-terminal domain, also called the smaller lobe, consists of β-sheets which assist in guiding the ATP to active site (Figure 1.6A). These two lobes are connected by a hydrophobic linker, which forms the binding site for an ATP molecule.[53] ATP binds to the active site by pointing the adenine moiety inside the conserved active site, with the triphosphate group pointed away from the active site. ATP binding into the active site brings both the N and C-terminal domains closer, along with the substrate and forms a ternary protein complex for enzymatic phosphorylation activity (Figure 1.6A). The catalytic core differs with respect to charge and hydrophobicity of the residues among serine/threonine and tyrosine kinases. Accordingly, serine/threonine kinases have a relatively shallow catalytic domain compared to tyrosine kinases, which have a deeper active site to accommodate the tyrosine side chain of the substrate.

The catalytic active sites of kinases display similar primary structures and contain nine conserved amino acid residues: G52, K72, Q91, D166, N171, D184, G186, Q208, and R280 (numbering as in PKA kinase).[54] These residues stabilize and interact with adenine base and triphosphate of ATP during catalysis (Figure 1.6B). Of the known > 500 kinases, some kinases lack catalytic activity due to the absence of some of the key amino acids in the active site, and are called atypical protein kinases.[55,56] Inactive protein kinases bind to active protein kinases which catalyze phosphorylation events. Inactive protein kinases also catalyze certain protein-protein mediated signaling in the cells.

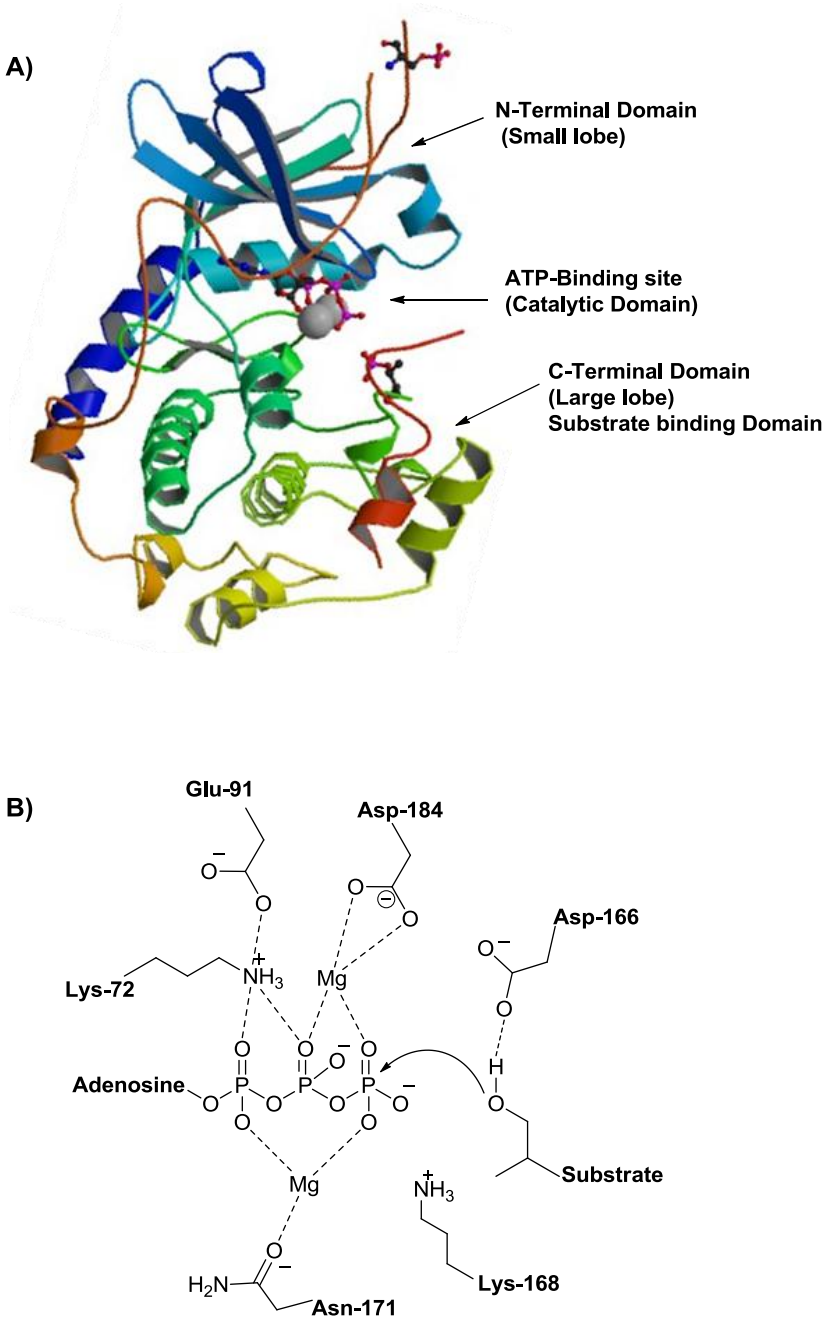

Figure 1.6: Crystal Structure of PKA Kinase. A) Crystal structure of PKA kinase (ribbon structure) bound to peptide substrate inhibitor (red ribbon structure) and ATP (ball and stick structure) complexed with Mn^{2+} (spheres) (PDB: 1ATP).[57] B) Kinase-catalyzed phosphorylation mechanism showing major interactions of ATP with the conserved amino acids in the active site of PKA kinase.

The ATP cosubstrate is stabilized in the active site by two divalent metal ions, either Mg^{+2} or Mn^{+2}, by chelating with phosphate groups and conserved amino acid residues in the active site. Aspartate (D166) acts as a base and deprotonates the hydroxyl group on the protein substrate, making it more nucleophilic. The ATP molecule is held tightly in the active site by the metal ions and amino acids (Scheme 1.2), which positions it for nucleophilic attack on its γ-phosphate by the protein substrate hydroxyl group. This results in the formation of phosphorylated protein substrate and ADP as a byproduct (Scheme 1.2).

Scheme 1.2: Mechanism of Protein Phosphorylation. Mechanism of protein phosphorylation illustrated with a serine amino acid, forming a phosphorylated serine product.

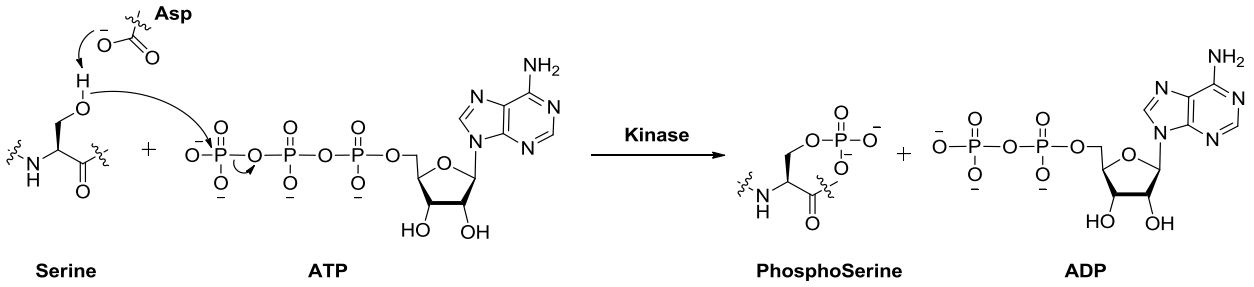

The enzymatic mechanism of protein phosphorylation was long debated and two possibilities were proposed. An associative mechanism was proposed first, which was similar to a bimolecular nucleophilic substitution reaction (S_N2).[58,59] In the transition state, bonds between the nucleophilic substrate oxygen and γ-phosphate of ATP are formed simultaneously when the ADP molecule is still bonded to the γ-phosphate (Figure 1.7, Path A). More recent evidence supports the dissociative type or unimolecular nucleophilic substitution reaction (S_N1) mechanism.[60-62] In the transition state, the ADP leaving group departs from the γ-phosphate group preceding nucleophilic attack of the substrate hydroxyl (Figure 1.7, Path B). Recently, many kinase inhibitors are designed based on the dissociative mechanism.[60]

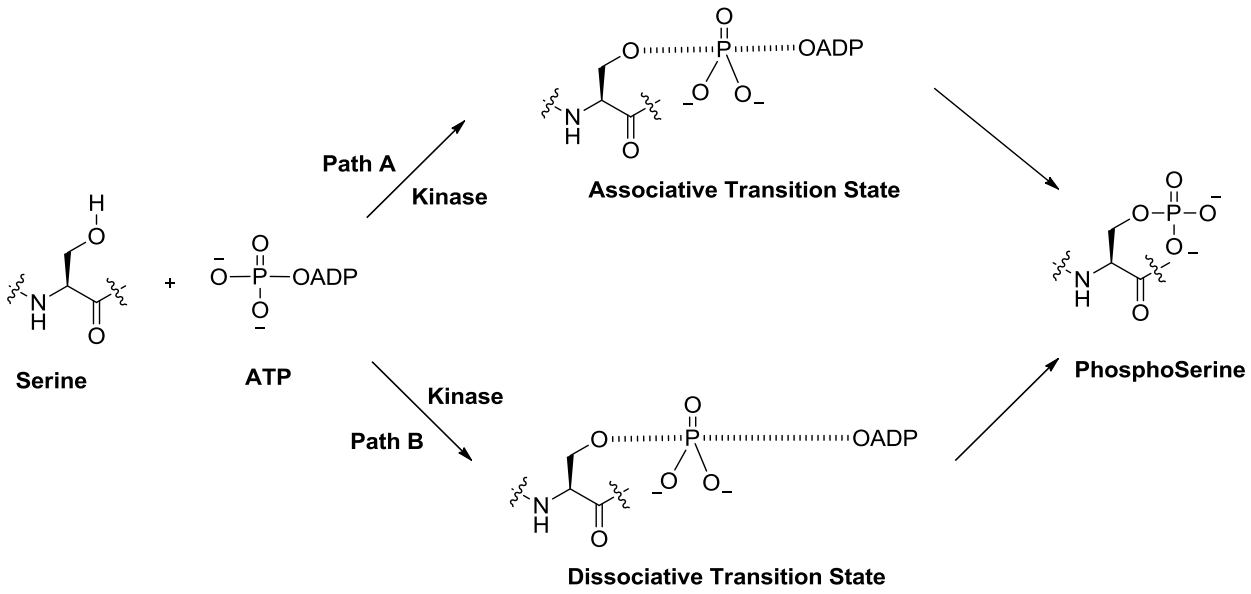

Figure 1.7: Proposed Transition States of Associative vs Dissociative Phosphorylation Mechanism. Path A: In the associative mechanism, the leaving group and incoming nucleophile remain attached to the reactive center. Path B: In the dissociative mechanism, the leaving group departs significantly before nucleophilic attack at the reactive center.

Kinases recognize their protein or peptide substrates through a specific consensus sequence. Various factors affect the binding interactions of kinases and substrates, like the distal docking domain or the presence of other protein partners during phosphorylation. However, a sequence of four amino acids that are toward the N or C terminus from the site of phosphorylation are critical for kinase recognition and phosphorylation (Table 1.3).[50] Consensus sequences for many kinases have been identified and kinases can specifically recognize acidic, basic, hydrophobic or proline residues in their substrates to direct phosphorylation. Abl protein kinase, a tyrosine kinase with a consensus sequence of I/V/L-Y-X-X-P/F (X represents any amino acid) phosphorylates tyrosine residues adjacent to hydrophobic residues.[63] CK2 kinase phosphorylates serine/threonine residues with a consensus sequence of S/T-D/E-X-D/E, near acidic amino acids.[64] c-AMP dependent protein kinase (PKA), preferentially phosphorylates

serine/threonine protein substrates which are flanked by basic amino acids, with R-R-X-S/T-Z consensus sequence.[65] Consensus sequence scanning is routinely used to identify the protein substrates of known kinases. But the consensus sites and sequences of the >500 kinases are not known and the presence of a particular consensus site does not necessarily establish a substrate/kinase pair. In addition to the consensus sequences, certain docking interactions and binding motifs outside of the site of phosphorylation influence the affinity of substrate and phosphorylation activity of the kinase. The factors which govern kinase substrate interactions are understood and the features that are important in cosubstrate interactions and identifications are discussed in the next section.

Table 1.3: Consensus Sequences of Selected Protein Kinases[50]

Kinase	Consensus Sequence
Abl	I/V/L-**Y**-X-X-P/F
AKT1	R-X-R-X-X-**S/T**
Aurora-A	R/K/N-R-X-**S/T**-B
CaMK2	R-X-X-**S/T**
CDK 1	**S/T**-P-X-R/K
CHK 1	R-X-X-**S/T**
CK1	pS-X-X-**S/T**
CK2	**S/T**-D/E-X-D/E
ERK 2	P-X-**S/T**-P
EGFR	E-E-E-**Y**-F
GRK 5	D/E$_n$-**S/T**-X-X-X
GSK 3	X-**S/T**-X-X-X-pS
IRK	**Y**-M-M-M
PKA	R-R-X-**S/T**-Z
SRC	E-E-I-**Y**-E/G-X-F

X – any residue, Z-hydrophobic residue, pS-phosphorylated serine, Red/Bold-site of phosphorylation

1.7 Kinase cosubstrate Promiscuity

Of the known PTM enzymes, many demonstrate cosubstrate promiscuity by accepting structurally similar cosubstrates.[66-72] A few examples of enzymes demonstrating cosubstrate promiscuity are acetyltransferase,[73] transglutaminase,[74] galactosyltransferase,[75] methyltransferase,[76] and farnesyltransferase.[77] Indeed, kinases also demonstrate cosubstrate promiscuity with modified ATP analogs. Adenosine 5'-[γ-thio]-triphosphate (ATP-γS) was the first reported modified ATP analog used as a kinase cosubstrate.[78-81] ATP-γS acts as a cosubstrate in kinase-catalyzed phosphorylation processes, resulting in a thiophosphorylated substrate (Scheme 1.3). The ATP-γS phosphorylation mechanism is similar to that of ATP, where the γ-phosphate group from ATP-γS is transferred onto the substrate hydroxyl group forming a thiophosphorylated product and ADP. The thiophosphate group can be used as a handle to identify and purify substrates. However, kinetic analyses with ATP-γS demonstrated poor catalytic efficiency compared to ATP, also known as thio effect.[82-85] In spite of low catalytic turnover, ATP-γS was used to study the proteome because of the stability of thiophosphorylated products towards phosphatases.[86-90] ATP-γS was also used in identification of novel and low abundant protein substrates.

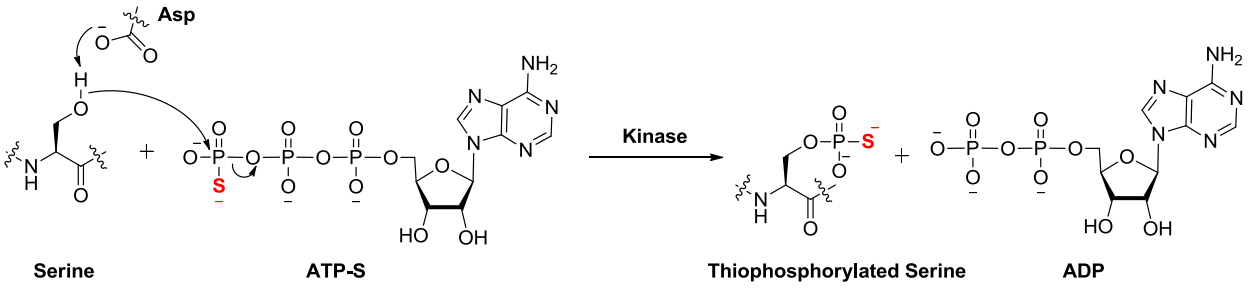

Scheme 1.3: Kinase-Catalyzed Protein Phosphorylation with ATP-γS. Serine, threonine and tyrosine hydroxyl groups on proteins attack the γ-thiophosphate group of ATP-γS to label proteins with a thiophosphoryl group.

In addition to the ATP-γS analog, other analogs were synthesized for selective phosphorylation with specific kinases by modifying both the adenine base and the γ-phosphate group.[91] One analog N^6-(benzyl) ATP-γS (Figure 1.9) was developed by the Shokat group, where in kinases were engineered to bind to base modified ATP analogs, which was helpful in purification and identification of substrates for a specific kinase by proteomic analysis.[90,86]

Analogous to ATP-γS, the Pflum lab was interested in developing γ-phosphate modified ATP analogs, which can aid in labeling kinase substrates, and identifying kinase substrate pairs. From the crystal structures analysis of CK2 and PKA kinase, it was clear that the γ-phosphate group of ATP is in the solvent exposed region (Figure 1.6 and 1.8). We hypothesized that ATP modified with other substituents on γ-phosphate can act as cosubstrate in a kinase-catalyzed labeling reaction. Accordingly, the Pflum group has demonstrated that several γ-phosphate modified ATP analogs can act as cosubstrates and transfer the modified phosphate group onto the substrate as described in the following sections.[92-94] These chemical probes will be helpful in understanding and characterizing signaling pathways in normal and diseased states.

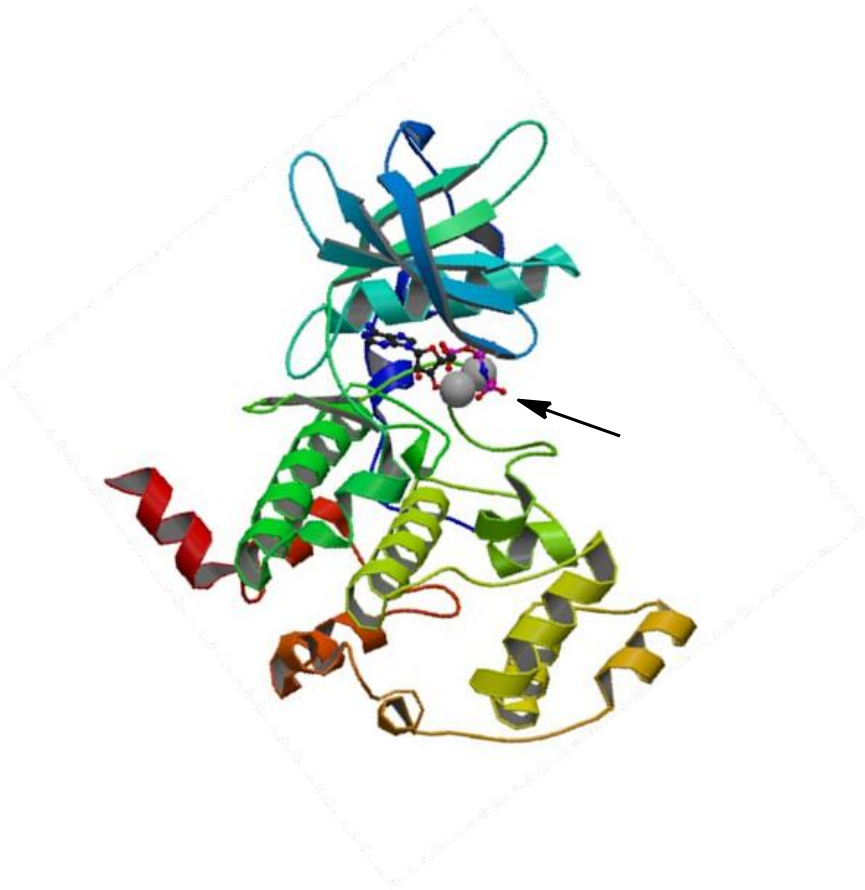

Figure 1.8: Crystal Structure of CK2 Kinase Bound to ATP Analog. Crystal structure of CK2 kinase complexed with ATP analog (Phosphoamino phosphonic acid adenylate ester) and Mg^{+2}. Solvent exposed phosphate group is pointed out as shown with an arrow (PDB-1LP4). [95]

1.7.1 ATP-Biotin

To initially validate cosubstrate promiscuity, kinase-catalyzed phosphorylation was carried out using an ATP-Biotin analog, along with a peptide substrate and recombinant kinase (Scheme 1.4). We found that kinases promiscuously accept ATP-Biotin and form biotinylated products with peptides containing serine (LRRA**S**LG), threonine (RRREEE**T**EEE), or tyrosine (EAI**Y**AAPFAKKK) along with corresponding PKA, CK2, and Abl kinase respectively. Biotinylation was quantified with respect to ATP (assuming 100% complete reaction) using quantitative mass spectrometry (QMS) analysis (Table 1.4).[96,97] Next, we tested the compatibility of ATP-Biotin with full length protein substrate (β-casein) and CK2 kinase. Biotinylation of the

substrates was analyzed using gel electrophoresis, followed by visualizing the biotin tag using streptavidin-horseradish peroxidase (SA-HRP) conjugate. In addition, when HeLa cell lysates were incubated with ATP-Biotin, we found that cellular kinases utilized ATP-Biotin to biotinylate cellular substrates.[96,97] These results demonstrate that kinase-catalyzed biotinylation can be generally applied to probe endogenous kinases and substrates.

Scheme 1.4: Kinase-Catalyzed Biotinylation using ATP-Biotin. Hydroxyl containing amino acids on peptides or proteins are biotinylated with ATP-biotin in the presence of kinases. See Table 1.4 for the structure of ATP-biotin.

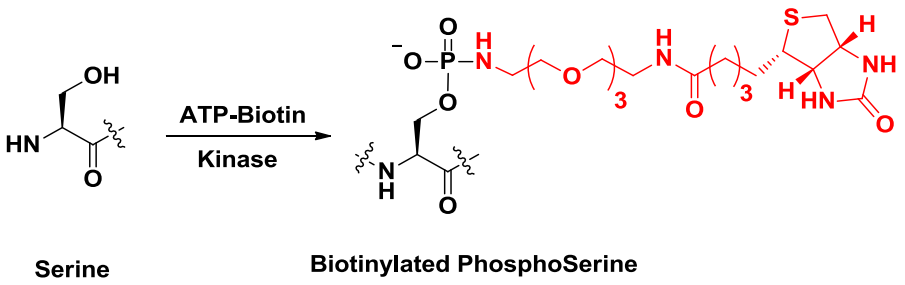

Table 1.4: Kinase-Catalyzed Labeling of Peptide Substrates using Previously Reported ATP analogs.[94,98,99]

ATP Analog	PKA	CK2	Abl
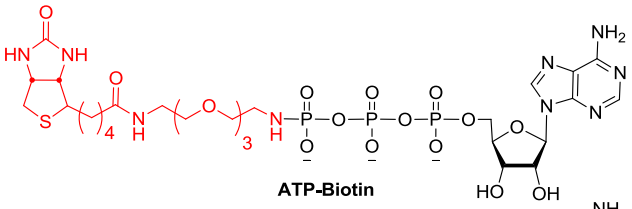 ATP-Biotin	79%	56%	80%
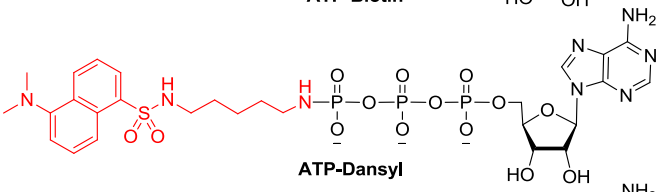 ATP-Dansyl	91%	81%	87%
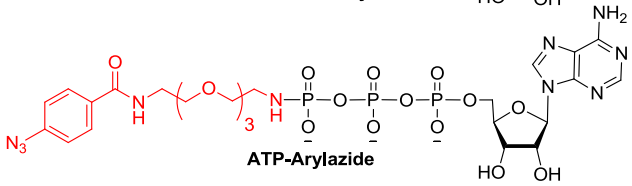 ATP-Arylazide	86%	51%	78%

1.7.2 ATP-Dansyl

After successful demonstration of kinase catalyzed biotinylation, we were interested in examining the compatibility of kinases with other γ-phosphate modified ATP analogs. Commercially available ATP-dansyl (Scheme 1.5) was used to test the compatibility in a kinase reaction. Similar to ATP-biotin, ATP-dansyl was incubated with peptides in the presence of their corresponding kinases and the efficiency of dansylation was analyzed using QMS (Table 1.4).[93] This data indicated that ATP-dansyl was successfully used as a cosubstrate in kinase-catalyzed phosphorylation.

To further characterize the kinase cosubstrate promiscuity of ATP-dansyl, kinetic studies were carried out. An absorbance assay was used to study the kinetics of ATP and ATP-dansyl with PKA kinase and a peptide substrate.[100,101] ATP-dansyl and ATP maintained similar K_M values (23 μM and 24 μM respectively), indicating that the γ-phosphate modification did not alter the binding of ATP in the active site. In contrast the k_{cat} of ATP-dansyl was 9-fold less compared to ATP, demonstrating that the kinase reaction with ATP-dansyl is slower than ATP.[93] Overall, this data demonstrates that γ-phosphate modified ATP analogs act as cosubstrate in kinase-catalyzed labeling reactions, and can be used for studying kinase substrates and kinase mediated signaling pathways.

Scheme 1.5: Kinase-Catalyzed Dansylation using ATP-Dansyl. Hydroxyl containing amino acids on peptides or proteins are dansylated with ATP-Dansyl in the presence of kinases. See Table 1.4 for the structure of ATP-Dansyl.

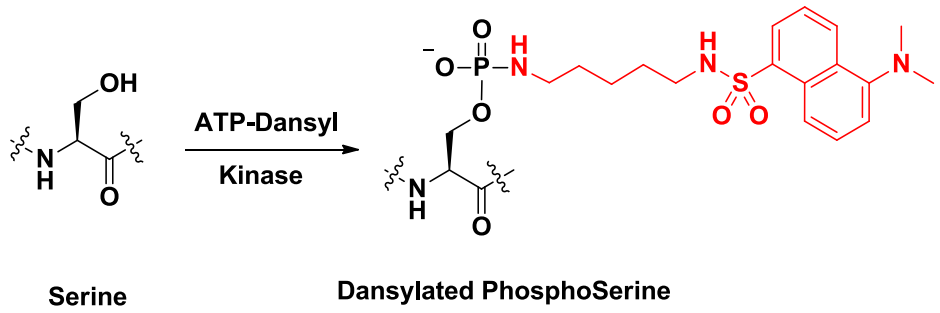

1.7.3 γ-phosphate Modified ATP analogs

In addition to the γ-phosphate modified analogs synthesized by the Pflum lab, other research groups have synthesized and studied the applications of the analogs. The Carlson group synthesized ATP-BODIPY, where the BODIPY fluorophore was attached to γ-phosphate of ATP using sulfur (Figure 1.9). ATP-BODIPY showed competitive binding with ATP and was used to study the autophosphorylation activity of histidine kinases.[102,103]

The Kraatz group synthesized an ATP-ferrocene analog, where the γ-phosphate is attached to a ferrocene moiety with a hydrocarbon linker (Figure 1.9). This ferrocene modification was used as a handle to detect kinase activity electrochemically and with anti-ferrocene antibodies. In addition, ATP-ferrocene was shown to compete with ATP for kinase binding and was used to profile kinase activity in complex mixtures and for kinase inhibitor profiling.[104-107]

Apart from profiling substrates, γ-phosphate modified ATP analogs were also used to label and identify kinases in complex mixtures. ATP-acyl-biotin analogs developed by Active X Biosciences were used to biotinylate kinases (Figure 1.9).[108,109] These analogs were designed based on ATP binding to the active site of kinases. The ATP binding site is highly conserved (with only a few exceptions) and contains two lysine residues. One of the lysine is found in the ATP binding region and the other one near the C-terminus closer to the γ- and β- phosphates of ATP. Once ATP-acyl-biotin was bound in the active site, the conserved lysine residue forms a covalent linkage with the acyl biotin group, displacing ATP. Formation of a stable covalent linkage with a biotin tag helps in the purification and identification of kinases selectively.[108,109] This method was applied to identify active kinases and kinase inhibitors. [108,109]

Figure 1.9: Structural Diversity of γ-Phosphate Modified ATP Analogs. γ-Phosphate modified ATP analogs synthesized and applied to study phosphorylation by various groups. Applications were briefly discussed in the text.

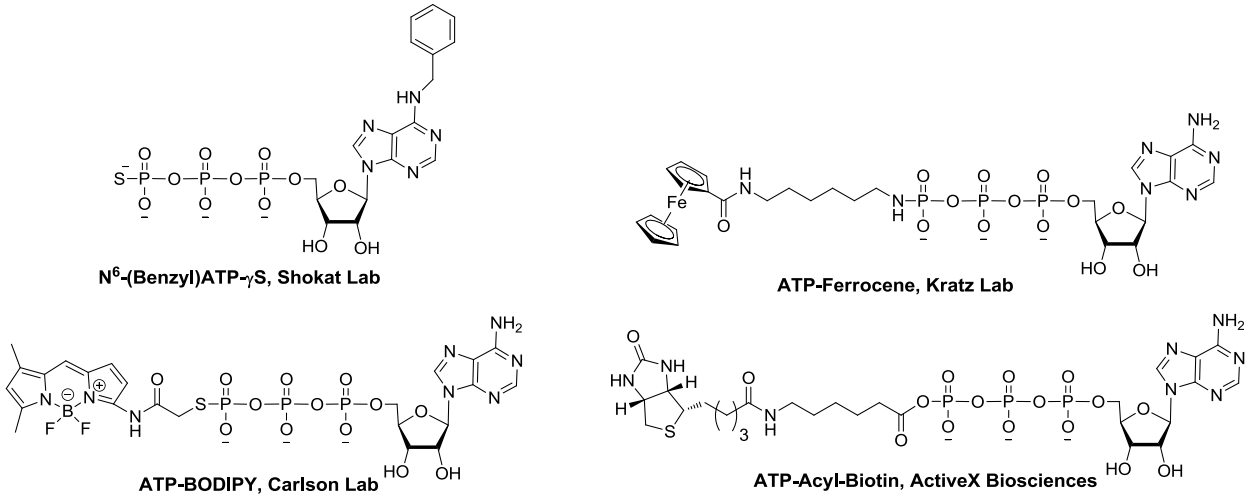

1.8 Photocrosslinking analog- ATP-ArN_3

Many ATP analogs were developed to characterize kinases and its substrates using proteomics. But identifying the genuine upstream kinase of a protein substrate in the normal and disease states is still challenging. Signaling pathways have multiple complimentary pathways and inhibition of a particular cascade can be compensated by others. In addition, one particular substrate can have multiple kinases depending on the cellular environment and *vice versa*. Besides, the interaction between kinase and its substrate is transient. Designing a γ-phosphate modified ATP analog that can identify kinase substrate pairs will be helpful in studying phosphorylation dependent signaling pathways. Such a chemical probe will allow us to map phosphorylation mediated signaling pathways in normal and diseased states of cells.

Accordingly, the Pflum lab wanted to develop an ATP analog modified at the γ-phosphate position with a photocrosslinking group. When the photocrosslinking ATP analog was incubated with a kinase and its substrate, kinases will promiscuously transfer the modified

phosphate group onto the substrate. With concurrent UV irradiation, the photocrosslinker is activated and covalently links kinase and its substrate in a phosphorylation dependent manner, as depicted in Figure 1.10. Previously Dr. Sujit Suwal from our lab synthesized ATP-arylazide (ATP-ArN_3), an ATP analog modified at the γ-phosphate with an aryl azide photolabel, to covalently link kinase and substrate upon phosphorylation and UV irradiation. Initial studies showed that ATP-ArN_3 acted as a kinase cosubstrate and modified the corresponding peptide substrates with high conversion efficiency (Table 1.4). Next, to test phosphorylation mediated kinase substrate crosslinking, we used CK2 kinase phosphorylation of casein protein substrate as a model system. CK2 kinase, ATP-ArN_3, and casein substrate were incubated under UV irradiation for 2 hours, followed by SDS-PAGE separation and western blot analysis with anti-CK2 to identify the kinase-substrate complex. Crosslinking was observed in an ATP-ArN_3 and UV dependent manner (Figure 1.11, lane 4), wherein a higher molecular weight complex corresponding to CK2 and casein was observed.[98] In contrast, no higher molecular weight bands were observed with ATP under similar conditions or with TFA treatment (Figure 1.11, lanes 3 and 5). These observations support the formation of kinase substrate complexes through phosphorylation-dependent kinase-substrate crosslinking.

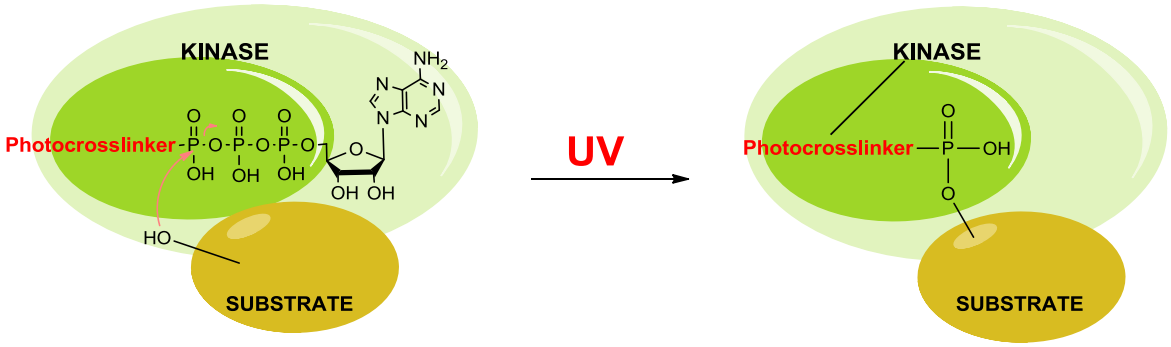

Figure 1.10: Phosphorylation-Dependent Kinase-substrate Crosslinking approach. Cartoon depicting phosphorylation-dependent kinase substrate crosslinking upon UV irradiation.

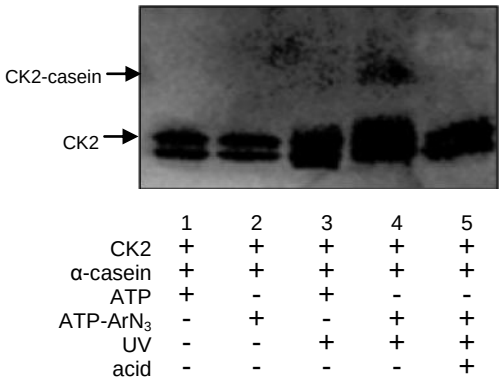

Figure 1.11: Kinase-Catalyzed Photocrosslinking with ATP-ArN_3. CK2 kinase was incubated with full length α-casein in the presence of ATP or ATP-ArN_3 before separation by SDS-PAGE and visualization with a CK2 antibody. Reactions were incubated either with or without exposure to 365 nm light (UV). Trifluoroacetic acid was added to a final concentration of 50% after crosslinking to cleave the phosphoramidate bond of the crosslink. The expected 68 kDa crosslinked complex is indicated as CK2-casein.[98]

1.9 Current methods to identify kinase-substrate pairs

Phosphorylation is an important PTM in cell signaling and affects various cellular functions, which emphasizes the need to develop new techniques to monitor phosphorylation as well as to identify the signaling partners. Techniques used to understand and monitor phosphorylation include radiolabel ^{32}P,[110] phospho specific antibodies,[111] immobilizing metal affinity chromatography,[112] Pro-Q diamond phosphate stain,[113] and covalent modifications of the phosphate, including the Pflum lab's γ-phosphate modified ATP analogs.[93,97,114,115] A variety of methods have been used to identify kinase-substrate pairs. The consensus sequences for many protein kinases have been determined using combinatorial peptide libraries.[116,117] Based on sequence preferences, kinase-substrate pairs are routinely revealed by consensus site searching.[116,117] Unfortunately, the consensus sequences of all 500 human protein kinases are not yet available. Techniques to identify protein-protein interactions are also used, including yeast two-hybrid and pull-down assays.[118,119] While these classical methods have shown success, the transient kinase-substrate interaction can be lost or overlooked during purification or gene expression. As alternatives, several chemical methods have been developed to convert the unstable kinase-substrate interaction into a covalent linkage, which facilitates purification and identification. The Shokat lab developed analog-sensitive kinase mutants[86] and a mechanism-based cross-linker[120]; the Cole group created a photocrosslinking ATP analog[121] to identify kinase substrate pairs. Some of these methods are further discussed in Chapter 2 and 3.

1.10 Thesis Projects

The Pflum lab has developed ATP-ArN_3, a phosphorylation-dependent kinase-substrate photocrosslinker, which crosslinks kinase and substrate in a phosphorylation dependent manner (Figure 1.10). To expand the scope and utility of other photolables in our approach, we wanted to

synthesize ATP analogs modified with different photocrosslinkers. Because of the difference in the properties of different photoprobes, comparative studies were performed and analyzed the crosslinking of kinase substrate pairs with ATP-ArN_3 (chapter 2). As a further application of these chemical probes, experiments were done to obtain optimum conditions for crosslinking in the presence of cell lysates. Next, to demonstrate the applicability of the analogs, p53 protein substrate was chosen as a model system. Experiments were carried out to identify kinases of p53 protein using cell lysates *in vitro.* Mass spectrometry analysis of the observed crosslinked bands revealed some novel and known kinases of p53 (chapter 3). This work highlights the utility of these chemical probes in identifying kinase substrate pairs using natural kinases and substrates. These probes are novel and will be useful in understanding the role of kinases in signaling pathways and biological processes.

Chapter 2

2. Comparative Study of Phosphorylation-Dependent Kinase-Substrate Photocrosslinkers

In this chapter, various aspects of photocrosslinking and photocrosslinking groups are discussed, with brief historical preview. Different types of photocrosslinking analogs were synthesized and tested with recombinant kinases. These analogs were successfully used to crosslink CK2 kinase and casein protein substrate. Autodock computational program was used for docking analysis and to analyze the factors governing crosslinking.

2.1 Introduction to photocrosslinking

In nature, living organisms contain various biomolecules like proteins, carbohydrates, nucleic acids, lipids, and metabolites. These biomolecules undergo various modifications like phosphorylation, acetylation, methylation etc to perform different functions. It is critical to understand the mechanism and nature of interactions between biomolecules involved, to promote a biological event. To study the complex network of protein interactions, many methods have been developed like affinity-based experiments, tandem affinity purifications (TAP) and mass spectrometry.[122,123] These methods have been powerful in studying protein-protein interactions using cell lysates, but there is a possibility of identifying false positives as well as loss of some weak interactions during the purification process. Alternatively, photoaffinity labeling (PAL) is used to identify interacting proteins by forming a covalent bond. In PAL a natural substrate is tagged with a photolabel and introduced into a system under investigation, upon irradiation the photolabel crosslinks interacting biomolecules (Figure 2.1).

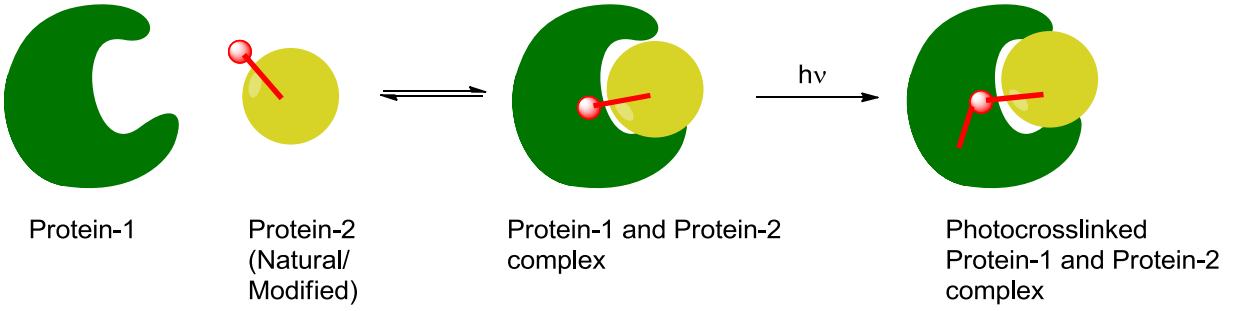

Figure 2.1: Scheme Depicting Protein-Protein Photocrosslinking.

PAL was first proposed by Prof. Westheimer in 1962 using a diazoacetyl group.[124] In the past few decades, many photoprobes have been developed and applied to study various biological systems, as shown in Table 2.1.[124-135] These photoprobes are broadly classified based on the reactive intermediate formed upon photolysis. They are divided into carbene-generating, nitrene-generating, radical-generating, and electrophilic carbon-generating photolabels. For successful PAL, the photoprobe needs to meet certain basic criteria.[136]

1. The photoprobe should be chemically inert towards other biological functionalities and in the absence of actinic light.
2. The photoprobe should be activated under mild conditions without causing damage to the biological system under study.
3. In order to capture the interacting biomolecules, the lifetime of the excited photolabel should be shorter than the lifetime of the interacting protein complex.
4. Upon irradiation the photoprobes should be able to form a covalent bond with any -CH, -NH, -OH, polar, non-polar or saturated groups present in proximity.

Depending on the biological system under study some other additional criteria can be considered. So far there are no ideal photoprobes that fit all criteria, but the compounds generating nitrenes, carbenes, diradicals and aryl cations upon photolysis meet most of these requirements.

Table 2.1: Chronology of Photoprobes Used to Study Biomolecules

Reactive Intermediate	First report	Reference	Reactive Intermediate	First report	Reference
Carbene			Nitrene		
N_2CHCO-	1962	2	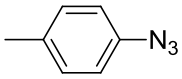	1969	3k
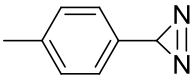	1973	3a	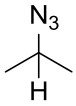	1978	3g
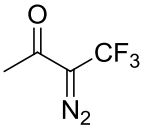	1976	3b	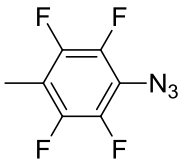	1989	3h
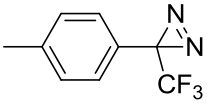	1980	3c	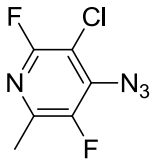	1999	3i
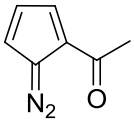	1983	3d			
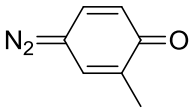	1989	3e	Electrophilic species (Aryldiazonium)		
Diradical (Benzophenone)			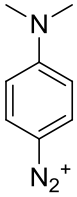	1980	3j
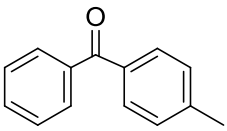	1973	3f			

2.1.1 Azides

Phenyl azides are widely used and studied compared to alkyl azides due to their stability. Aryl azides can be irradiated over a broad range (254-400 nm) depending on the substitution[137,138] and loss of a molecule of nitrogen produces a nitrene. The nitrene intermediate inserts into C-H and hetero atom (X)-H bonds (X = O, N, S) or it can undergo ring expansion to form a long lived intermediate ketenimine, which reacts with nucleophiles as shown in Figure 2.2.[139] The broad reactivity of nitrenes allows them to crosslink with a variety of biomolecules, but this high reactivity also leads to non-specific labeling especially, when the nitrene undergoes ring expansion.

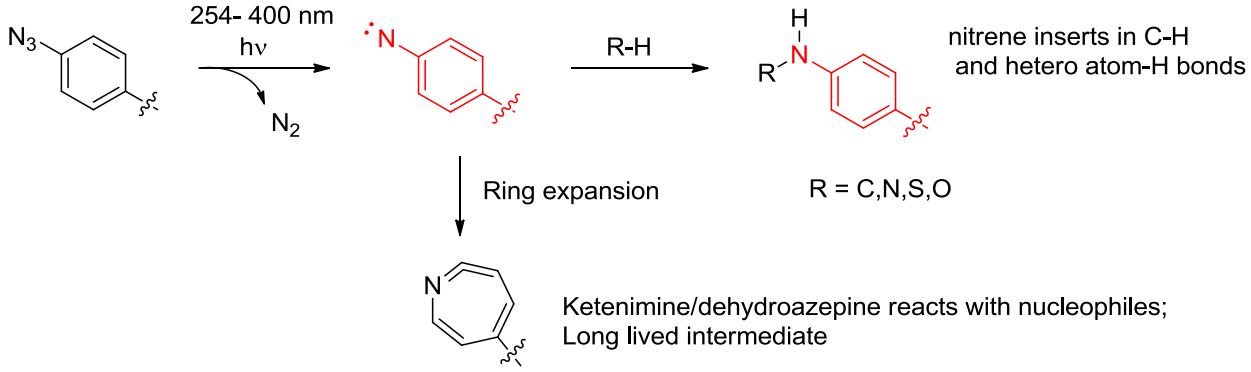

Figure 2.2: Reactivity of Aryl Azides under Photolysis

2.1.2 Diazirines

Diazirines require 350 nm light to form highly reactive carbene, which broadly reacts with biomolecules by C-H and X-H (X = O, N, S) insertions[140,141] as shown in Figure 2.3. Similar to aryl azides, carbenes can undergo Wolf type rearrangement to form a ketene, which reacts with nucleophiles like water to form carboxylic acids, reducing crosslinking efficiency.[142] The reactivity of the carbene is similar to that of a nitrene, but relatively smaller size of the diazirine doesn't perturb the biomolecules complex under study, which is advantageous.

Formation of a long lived ketene intermediate can react with nucleophiles producing nonspecific crosslinking. Despite these drawbacks, diazirine and aryl azides have been widely studied in various biological applications with different substitutions (Table 2.1).

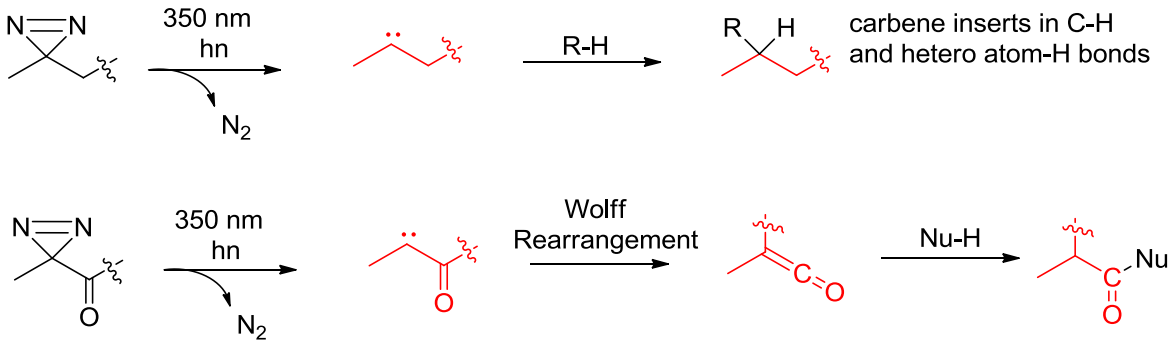

Figure 2.3: Reactivity of Diazirines under Photolysis

2.1.3 Benzophenones

Benzophenone upon photolysis at 350-360 nm produces a diradical species, which participates in crosslinking reactions by inserting in C-H and X-H (X = O, N, S). An advantage with benzophenone is that the diradical can crosslink with biomolecules in proximity or it can relax back to its ground state, which can be excited again as shown in Figure 2.4.[143] This results in high efficiency with benzophenone compared to others photolabels, but it also requires longer irradiation times.[144] Benzophenone was found to have a preference for methionine residues when they are in close proximity. Absence of methionine residue at the site of crosslinking might offset its use in some biological PAL studies.[145] Some other features of benzophenone like its bulky size and lipophilicity may also complicate its use in some studies.

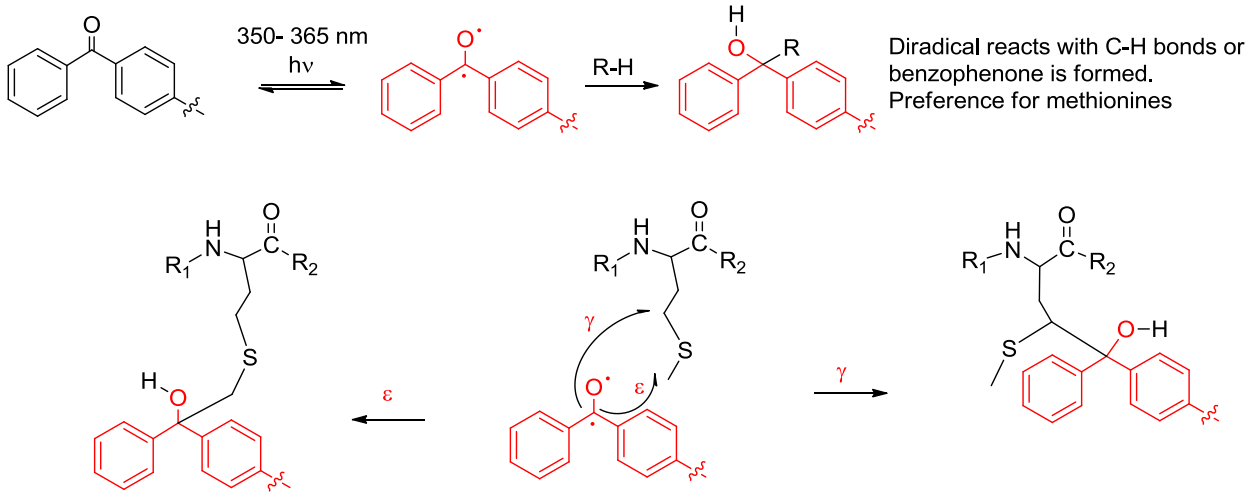

Figure 2.4: Reactivity of Benzophenone under Photolysis

To explore the nature and scope of these photoprobes in phosphorylation-dependent kinase-substrate crosslinking, we synthesized ATP analogs containing an aryl azide and a benzophenone. A summary of the current methods for identifying kinase-substrate pairs is discussed before the synthesis of ATP analogs and its application.

2.2 Existing methods for the identification of kinase-substrate pairs

The crystal structures of different kinases have provided significant input about the structure and mechanism of kinases (chapter 1). Similarly, techniques like *in vitro* phosphorylation, yeast two-hybrid systems, pull down assays, and chemical approaches like mechanism based crosslinkers, bifunctional photocrosslinkers were employed to identify kinase substrate pairs. Despite of these techniques mapping the entire kinome, determining the kinase activities, its effectors in the signaling pathways is still challenging. With increasing evidence from recent literature about the involvement of kinases in many diseases, there is a strong need

to develop new techniques that identify genuine kinase-substrate pairs. Therefore, tools that can identify kinase-substrate pairs in a phosphorylation dependent manner will be helpful in cell signaling studies. In the following section a few existing methods for identifying kinase-substrate pairs are discussed, emphasizing the chemical approaches due to their relevance to this work. In general, the techniques available to study kinase substrate pairs are broadly classified into four major groups.

1. *In vitro* phosphorylation
2. Physical association
3. Genetic approach
4. Chemical approach

2.2.1 *In Vitro* Phosphorylation

Of these methods, *in vitro* phosphorylation is the most traditionally used method. The substrate of a particular kinase can be identified by incubating a kinase of interest with radiolabeled [γ-^{32}P] ATP, with a purified substrate or cell lysates. The sites of phosphorylation are identified by resolution of the reaction mixture by SDS-PAGE analysis and Mass spectrometry. An alternative to the *in vitro* phosphorylation approach and using whole cell lysates mimicking cellular environment, was developed by the Shokat group.[146,147] In this method, ATP analog (N^6-benzyl-ATP-γS) was modified with a sterically bulky group on the adenine base, which prohibits binding to the kinase active site. A kinase of interest was mutated (as-Kinase: analog sensitive kinase) to accommodate the bulky group of N^6-benzyl-ATP-γS selectively. When an enzymatic reaction was carried out with as-kinase and N^6-benzyl-ATP-γS in the presence of cell lysates, the as-kinase selectively phosphorylated its substrates and the γ-thiophosphate group was transferred to its substrate (Figure 2.5). After phosphorylation, the sites

of phosphorylation and substrates can be characterized unambiguously, using 2D gel analysis, and phospho-specific antibodies, coupled with mass spectrometry. This As-kinase approach was used to label and identify substrates for JNK,[148] CDK7,[149] ERK2,[150] CDK1-Cyclin B[86] and CDK2-Cyclin A[151] kinases in human cells; c-Src,[152] v-Src,[153] PKA,[154] Abl related-gene (Arg),[155] and Erk2[90] kinases in murine cells; and Cdc28 (CDK1),[156] Hog1,[157] and Pho85-Pcl1[158] kinases in yeast cells.

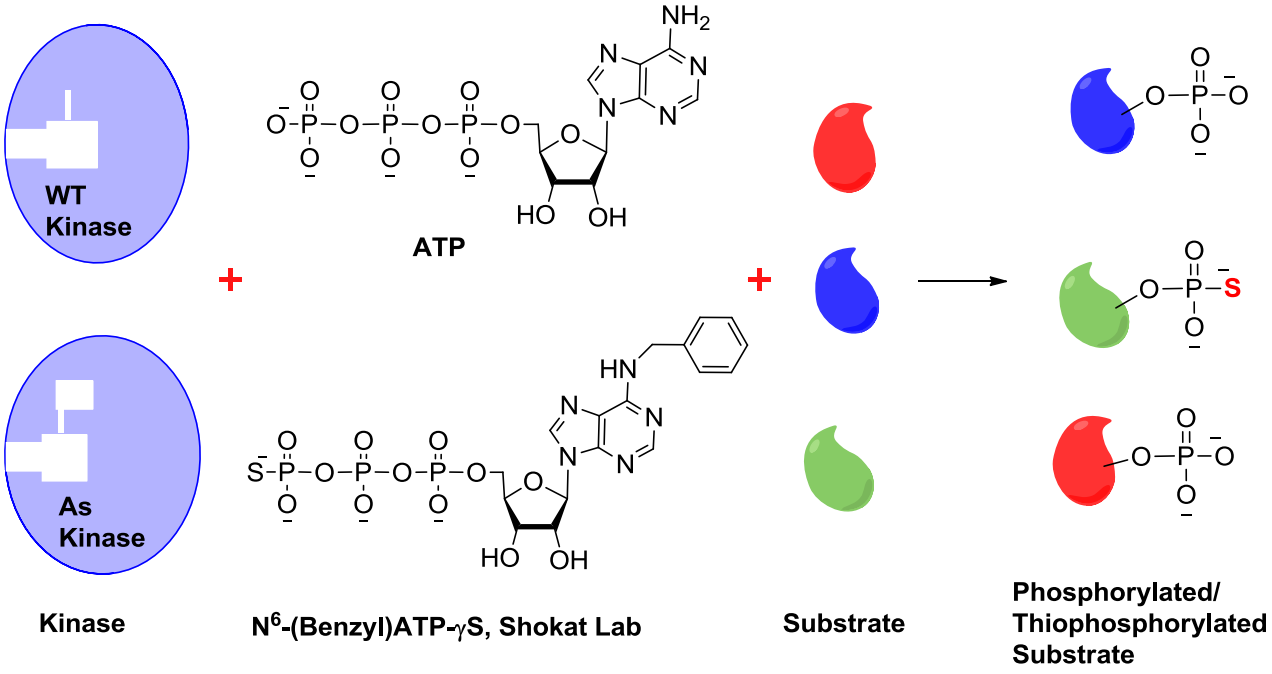

Figure 2.5: Schematic Representation of Phosphorylation by an Analog Sensitive Kinase (as-kinase). Cell lysates were incubated with mutant kinases, ATP and modified N^6-Benzyl-ATP-γS. Substrates for the mutant kinase were labeled as thiophosphorylated products. Thiophosphorylated products were purified and identified by MS analysis.

2.2.2. Physical Association

Another important method that is used to identify kinase substrate pairs is yeast two hybrid (Y2H) assay. Y2H is a physical interaction screen, which is mainly used to identify protein-protein interactions.[118] In Y2H approach, a fusion protein containing the catalytic site of a kinase and the DNA-binding domain of a transcription factor (for example, in yeast Gal4 or in bacteria LexA) is used as "bait". A set of substrates fused to an activation domain is used as "prey" to screen for interactions that turn on the transcription and promote growth and/or a color change or production of galactosidase (Figure 2.6). Y2H screens of kinase and substrate do not require primary information on the sequence specificity of the kinase and allows for identification from a cDNA library of the interacting proteins. In Y2H, the interacting kinase and substrate are likely to be in their native conformation since their entire screen is performed *in vivo*. For example, Y2H was successfully used in the identification of PICK1 as a substrate of PKC kinase,[159] and many others.[160,161] Y2H system is robust, rapid and sensitive, but due to some limitations, like over-expression of proteins and abnormal protein activities it is not widely used in kinase substrate pair identification.

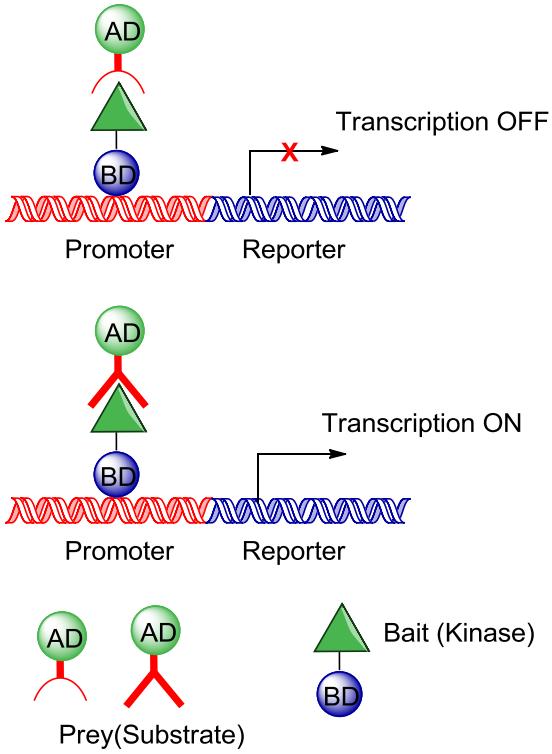

Figure 2.6: Yeast two-hybrid System Showing the Prey and Bait Interaction. When the bait containing DNA binding domain (BD) binds to the promoter, the prey is reunited with its activation domain (AD), as a result the expression will be turned ON. Transcription is turned OFF when there is no interaction between the bait and prey. Bait contains the kinase catalytic domain and prey contains the substrate sequence.[118]

2.2.3 Chemical approaches

A variety of chemical approaches have been developed to identify and confirm kinase substrate pairs. These chemical methods have commonly used a crosslinking strategy to transform the transient interaction of kinase and substrate into a covalent linkage, forming a kinase-substrate complex. The crosslinked kinase substrate protein complex can be identified using SDS-PAGE analysis, western blot and mass spectrometry. Covalent crosslinking can be achieved by modifying one of the interacting partners with a chemically reactive group or a photoreactive probe at the site of interaction. Chemically reactive probes like aldehydes or other electrophilic groups and photoreactive probes like azides, diazirine and benzophenone have been

extensively used in the crosslinking studies. Next some of the currently used chemical approaches for kinase substrate crosslinking are briefly explained.

2.2.3.1 Mechanism-based crosslinking approach

The mechanism-based crosslinking approach was reported by the Shokat group. In this approach a bi-functional crosslinker containing an *o*-phthaldialdehyde group attached to the 5'-hydroxyl of adenosine moiety was used. When this modified analog is bound in the ATP binding pocket of the kinase, the *o*-phthaldialdehyde substituent is positioned near a lysine residue in the active site (Figure 2.7). When in close proximity, the amino group of the lysine reacts with one of the aldehydes of ATP analog to form an imine. Incubation with a pseudo-substrate containing a cysteine in place of the reactive hydroxyl group initiates a cascade reaction with the imine and the remaining aldehyde of the ATP analog to form a covalent complex. This mechanism-based crosslinker approach was demonstrated with a few kinases and their corresponding biotinylated substrate peptides.[162] When crosslinking was performed between fluorophore-labeled peptide substrates and kinases in the presence of lysate, numerous non-specific fluorophore labeled products were observed because of the reactivity of the aldehyde ATP analog. To overcome these challenges, the Yao group has developed a second generation mechanism based crosslinker replacing *o*-phthaldialdehyde group with naphthalene-2, 3-dicarboxaldehyde (NDA, Figure 2.8).[163] The NDA modification was better accommodated in the kinase active site and compatible with serine/threonine and tyrosine kinases. This second generation analog was successfully used with various kinases and fluorophore labeled peptides in the presence and absence of cell lysates.

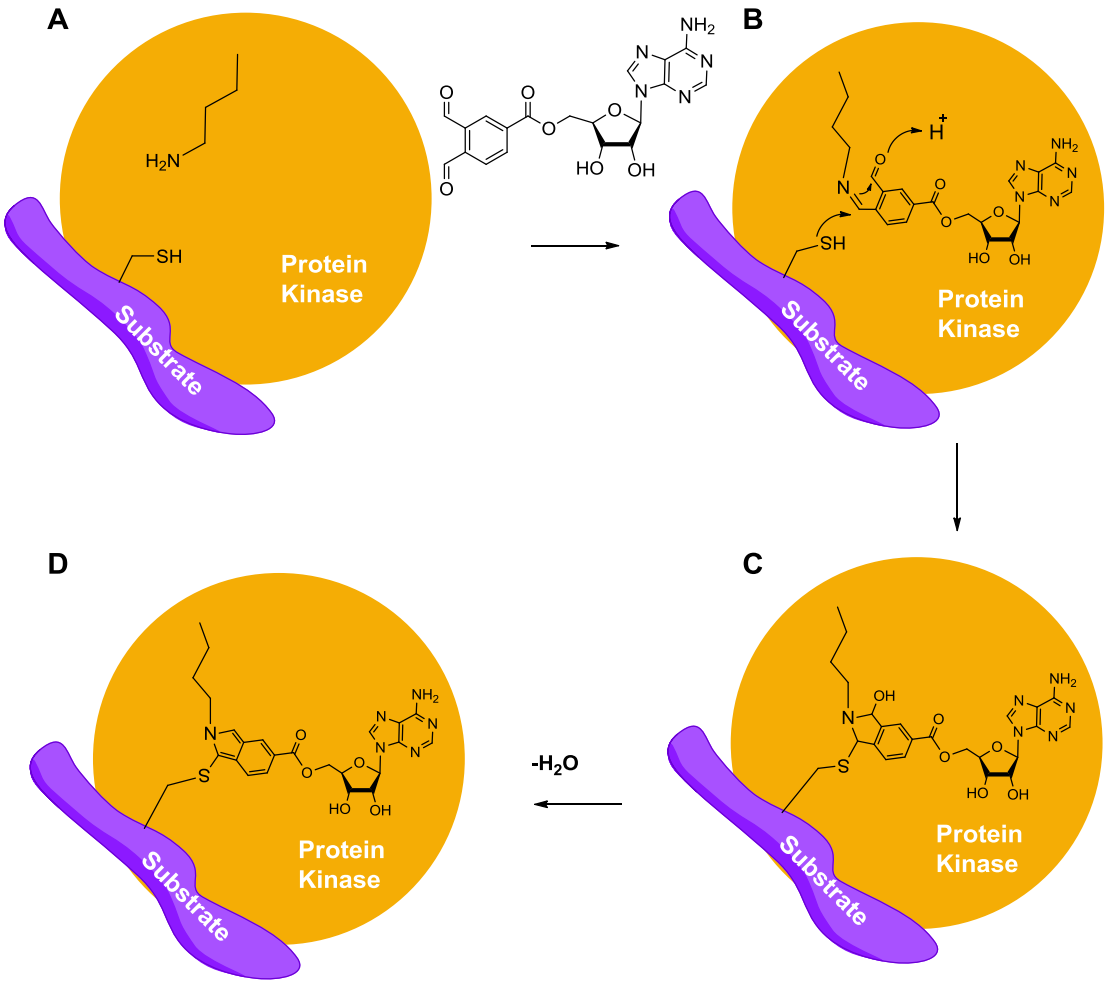

Figure 3.3: Schematic Representation of the Mechanism Based Crosslinking Approach. Reaction of lysine side chain and the mercapto group of the pseudo-substrate with the modified ATP analog in a three component reaction results in a crosslinked kinase-substrate complex.[162]

Recently, a third generation mechanism-based crosslinker was developed by the Shokat group (Figure 2.8).[164] In this crosslinker, adenosine moiety was replaced by a potent kinase inhibitor scaffold, 3-aminopyrazole, and the reactive *o*-phthaldialdehyde was replaced with the less reactive thiophene-2, 3-dialdehyde to reduce non-specific labeling in the presence of cell lysate. This new crosslinker was successfully used to crosslink Akt1 kinase selectively with fluorescein-labeled peptide substrate in the presence and absence of cell lysates. Some of the

drawbacks of this method are the requirement for mutation of serine to cysteine in the substrate, validation with other types of kinases, and possible side reactions between the mercapto group in the pseudo-substrate with peripheral residues of kinase and substrate.

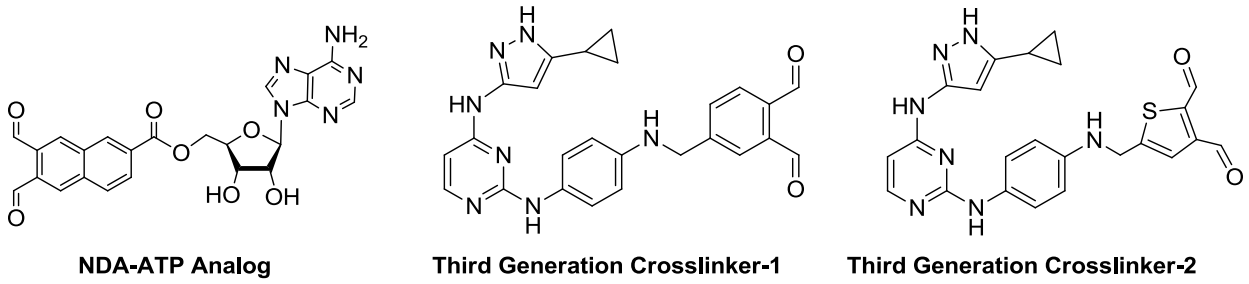

Figure 2.8: Chemical Structures of Mechanism Based Crosslinkers. The NDA-ATP analog was developed by the Yao group. The inhibitor based third generation crosslinkers were developed by the Shokat group.

2.2.3.2 Bifunctional photocrosslinking ATP analog

The Cole group developed a crosslinking ATP analog to identify kinase substrate pairs using an azide photoprobe.[165] ATP was modified with azide photoprobes on its phosphate and base portions. An azide moiety at the C-8 position of adenine could be easily accommodated into the kinase hydrophobic hinge region and upon photoactivation, covalently locked the ternary complex (Figure 2.9). This bi-functional photocrosslinker was successfully used to crosslink, Src kinase, with the protein substrate Csk. However, no further application of the bifunctional photocrosslinker ATP-analog has been reported. These methods have undoubtedly contributed to the study of kinases, but still there is a need to unambiguously identify genuine kinase-substrate pairs and the sites of phosphorylation. Novel chemical tools should be developed which are compatible with natural kinases and substrates in their native environment, maintaining the

activity of proteins during identification, and afford efficient covalent complex formation from transient proteins interaction.

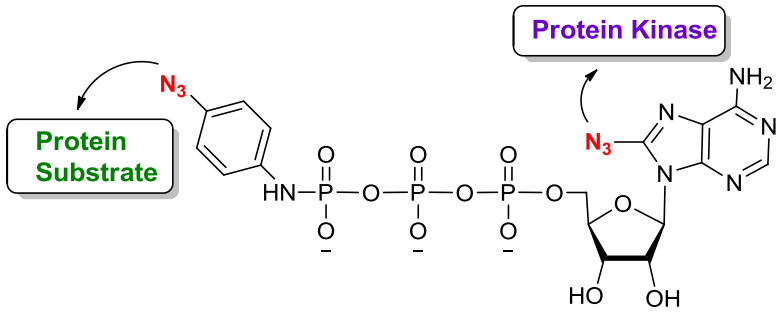

Figure 2.9: A Schematic Representation of a Bi-functional ATP Analog. The ATP analog is bound in the kinase active site and forms a ternary complex. Upon UV irradiation, both the azide groups are activated and one crosslinks to the kinase and the other with substrate.

2.3 Phosphorylation-Dependent Kinase-Substrate Crosslinking

Various methods have been developed to identify kinase substrate pairs as explained previously. Alternatively, the Pflum lab has developed phosphorylation-dependent kinase-substrate crosslinking using modified ATP analogs. This concept was based on the kinase cosubstrate promiscuity discussed earlier (Chapter 1). Briefly the kinase and substrate were incubated with an ATP analog attached to a photoprobe, the modified phosphate group was transferred onto the substrate. Then with simultaneous UV irradiation, the photolabel crosslinks to the kinase (Figure 2.10B). When the reaction mixtures are separated by SDS-PAGE followed by western blot analysis with an antibody, a higher molecular weight band corresponding to the kinase-substrate complex should be observed (Figure 2.10B). This crosslinking method employs the natural kinase and substrate without any modifications and serves as a powerful tool in profiling the phosphoproteome.

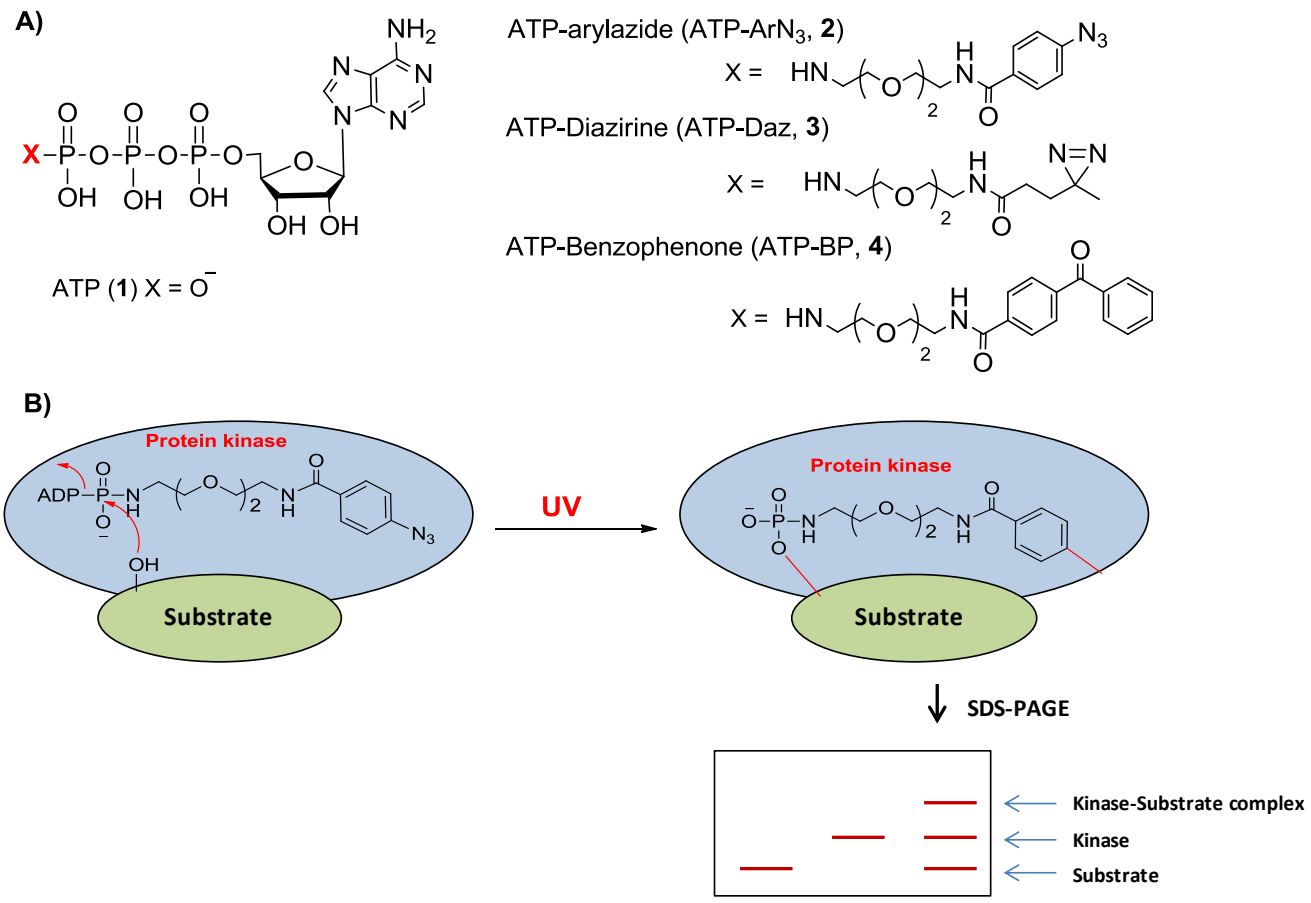

Figure 2.10: Scheme of Phosphorylation-Dependent Kinase-Substrate Photocrosslinking **A**) Chemical structures of ATP (**1**) and γ phosphate modified ATP analogs, ATP-arylazide (ATP-ArN_3, **2**), ATP-diazirine (ATP-DAz, **3**) and ATP-benzophenone (ATP-BP, **4**). **B**) Cartoon depicting kinase-catalyzed protein phosphorylation along with UV-mediated crosslinking of kinase and substrate.

To compare and contrast the applicability of various photoprobes in phosphorylation-dependent crosslinking, ATP-benzophenone (ATP-BP, **4**) was synthesized and compared to ATP-ArN_3. Because of the similarities in the reactivity of aryl azide and diazirine, ATP-diazirine (ATP-DAz, **3**) was used only for computational studies.

2.4 Synthesis of ATP-benzophenone (ATP-BP, 4) analog

The ATP-BP **4** was synthesized in two steps starting from 4-benzoyl benzoic acid **5** as shown in Scheme 2.1. Benzophenone amine linker **7** was prepared by activating 4-benzoyl benzoic acid **5** with EDCI, followed by reaction with the diamine linker **6.** Finally, ATP was coupled to benzophenone photolabel containing amine **7** using a reported procedure involving EDCI under controlled pH of 5.6-5.8 in aqueous medium. ATP-BP was obtained by purification of the reaction mixture by ion exchange chromatography.[166,167]

Scheme 2.1: Synthesis of ATP-Benzophenone (ATP-BP, 4)

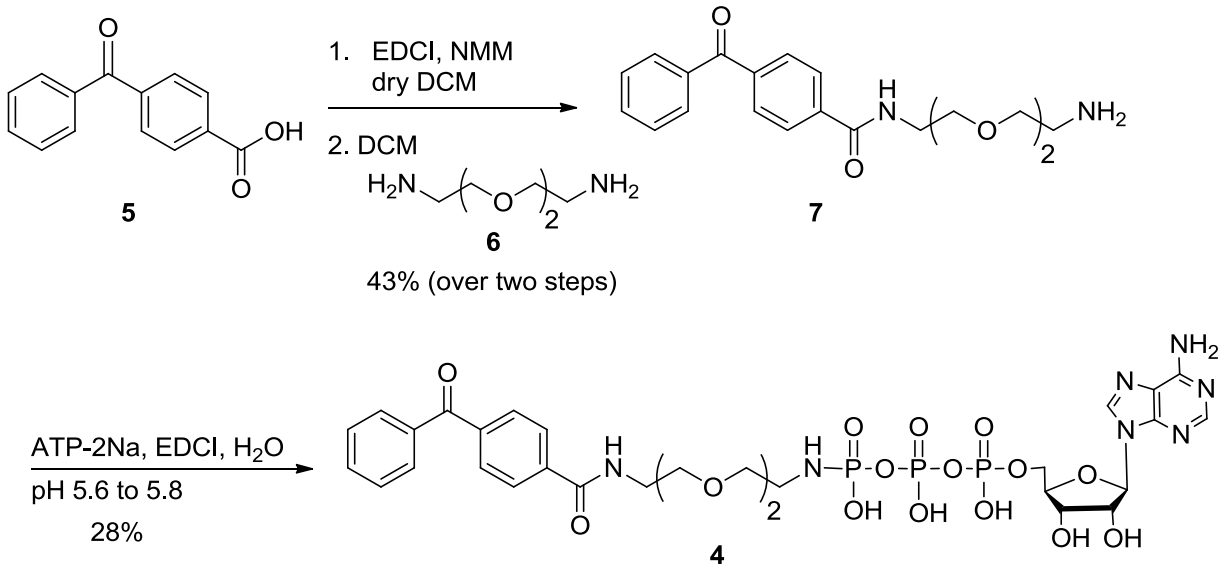

5 **6** **7** **4**

2.5 Kinase cosubstrate compatibility of ATP-BP analog using QMS analysis

We next investigated the compatibility of the ATP-BP analog in kinase-catalyzed labeling using quantitative mass spectrometric (QMS) analysis with peptide substrates.[96] QMS is isotopic differential labeling of peptide substrate and quantified using MALDI-TOF MS analysis.

Briefly, kinase catalysed labeling reaction was carried out with peptide substrate, recombinant kinase and ATP, followed by esterification with deuterated methanol, acetyl chloride (Figure 2.11). Similarly, in a separate eppendorf tube, kinase catalysed reaction was performed with ATP-BP and esterification with methanol, acetyl chloride (Figure 2.11). Methanol was evaporated and the residue is dissolved in a small volume of water (10µL). Equal volumes of sample from both ATP and ATP-BP reaction tubes were mixed and analyzed using a MALDI-TOF. Assuming 100% conversion in the kinase reaction with ATP, the relative percent conversion in the ATP-BP kinase reaction can be calculated from the peak areas obtained from the MALDI MS spectrum (Figure 2.12).

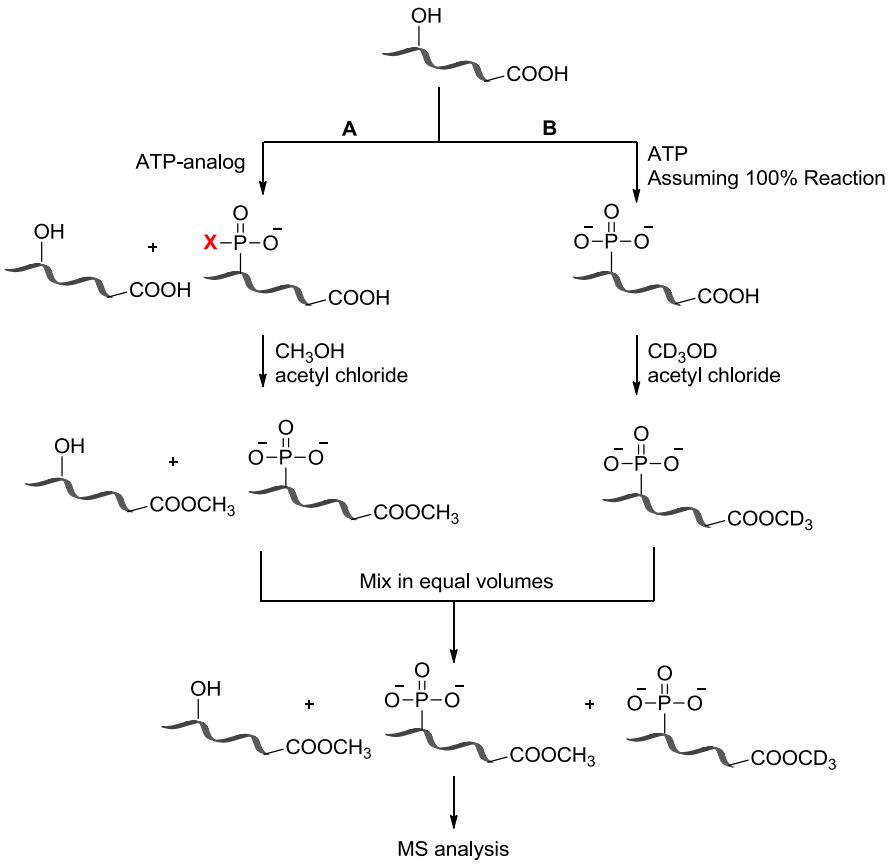

Figure 2.11: Scheme of Quantitative Mass Spectrometric (QMS) Analysis. A schematic representation of QMS analysis carried out with peptide substrate, recombinant kinase, ATP and ATP analog.

CK2 kinase was tested due to its variable conversions observed with several ATP analogs in our previous studies,[167] which make it an ideal model kinase. QMS data showed that both analogs were accepted by CK2. The CK2 peptide was modified with ATP-BP and CK2 kinase with 71% conversion. In earlier studies, ATP-ArN_3 demonstrated a labeling efficiency of 51% (Table 2).[166] Therefore, ATP-BP analog demonstrated enhanced labeling efficiency compared to ATP-ArN_3. Overall, QMS data suggest that the ATP-BP analog is compatible with kinase catalyzed labeling. Next we wanted to test whether the ATP-BP analog is capable of kinase-substrate crosslinking.

Table 2.2: MALDI-TOF MS analysis of CK2 peptide after incubation with ATP-BP and CK2 kinase.[a]

Analog	% Conversion
ATP-BP	71%
ATP-ArN_3	51%

[a]Percentage conversions were determined using quantitative MS by comparing to ATP phosphorylation (100%), as previously described.[96] Data reported previously with ATP-ArN3 are shown for comparison.

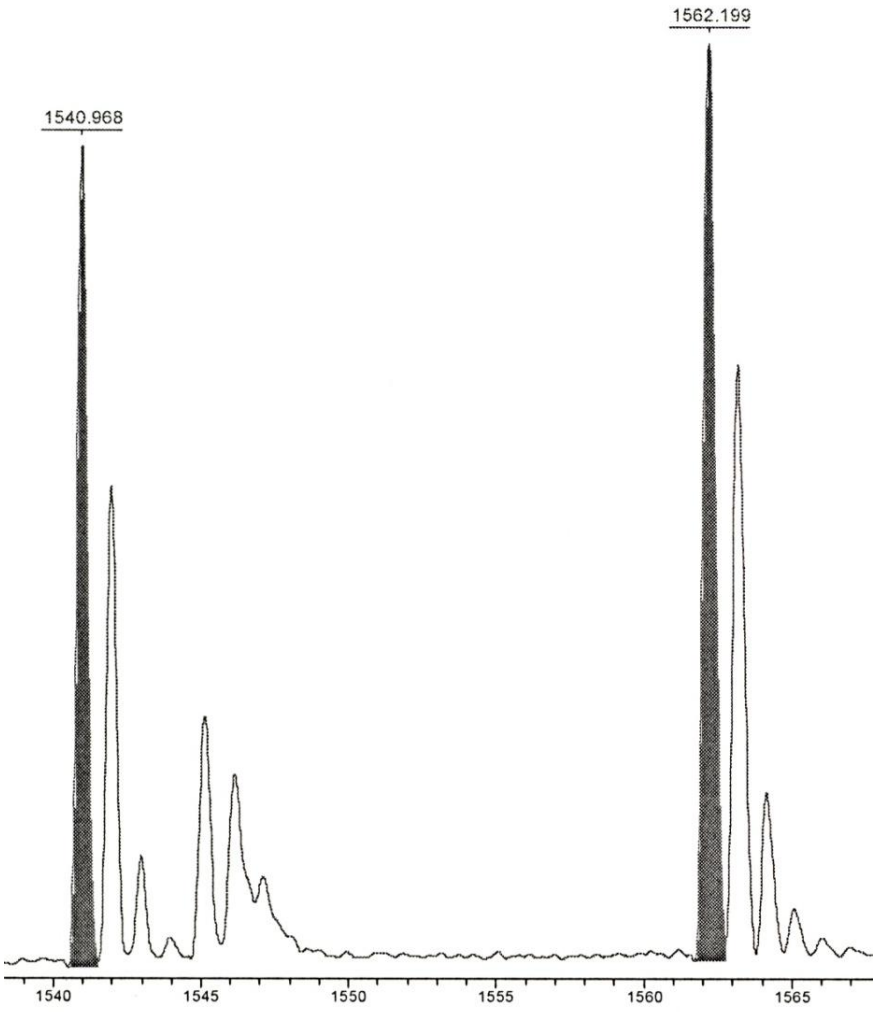

m/z	SN	Res.	Intens.	Area
1540.968	115.0	4094	813.42	317
1562.199	129.6	3420	916.66	431

Figure 2.12: QMS MADLI-TOF Spectrum of ATP-BP Analog Quantitative MALDI-TOF MS of peptide substrate (RRREEE**T**EEE) with CK2 kinase and either ATP **1** or ATP-BP **4.** The peak at m/z ~1541 corresponds to heptamethylated phosphopeptide after reaction with ATP-benzophenone and acidic cleavage of phosphoramide bond, while the peak at m/z ~1562 corresponds to the deuterated heptamethylated phosphopeptide after phosphorylation with ATP. Percent conversion of this single trial was 74% (Trial 1); Additional trials are shown in Appendix A, Figures A2.2.

2.6 Phosphorylation-dependent kinase-substrate photocrosslinking with ATP-BP analog

Phosphorylation-dependent kinase-substrate photocrosslinking studies were performed similar to the ATP-ArN_3 analog and purified protein substrate and recombinant CK2 kinase was used. α-casein was chosen as a model substrate because it is widely used as a substrate for CK2 kinase.[168] Crosslinking experiments were carried out by incubating CK2 kinase and α-casein with the ATP analog under UV light for 2 hours. The reaction mixtures were separated on SDS-PAGE and visualized by western blot analysis with CK2 antibody.

In the case of ATP-BP, CK2 kinase was incubated with α-casein protein and ATP-BP analog under UV irradiation. With separation of the reaction mixture on SDS-PAGE and western blot analysis with CK2 antibody, we found a CK2-reactive crosslinked band at ~68 kDa, corresponding to the catalytic α subunit of CK2 (45 kDa)[169,170] and β-casein (23 kDa) (Figure 2.13, lane 7). In addition to the expected 68 kDa crosslinked band, higher molecular weight complexes were also observed (Figure 2.13, lane 7). The crosslinked complex was not present in the absence of UV light (Figure 2.13, lane 4), in the presence of competitor ATP (Figure 2.13, lane 6) or when treated with TFA (Figure 2.13, lane 8). Prior work showed that genetically incorporated benzophenone was capable of producing multiply crosslinked protein complexes, suggesting that the higher molecular weight complexes are multimers.[171-173] These experiments show that ATP-BP is capable of phosphorylation-dependent crosslinking, although with formation of higher molecular weight complexes that were not observed with the ATP-ArN_3 analog (Chapter 1, Figure 1.11). To identify the factors causing differences in QMS studies and crosslinking efficiency of these analogs we sought to computational studies.

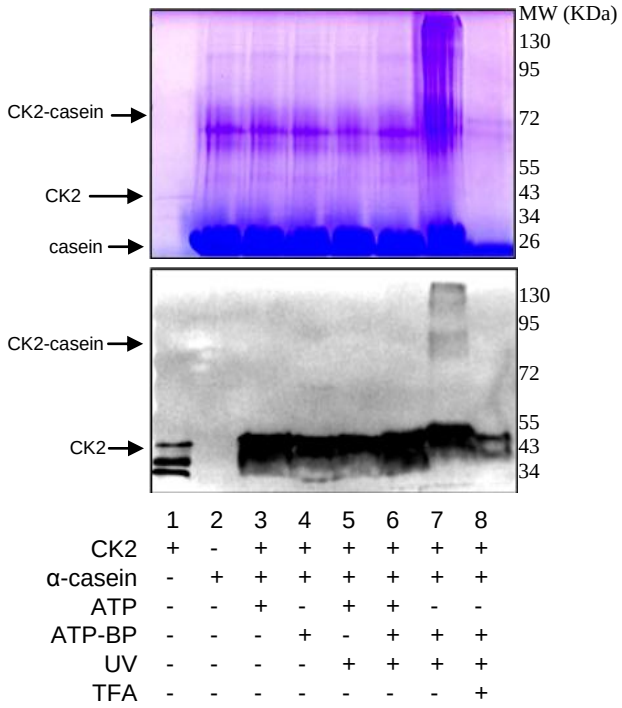

Figure 2.13: Kinase-Catalyzed Photocrosslinking with ATP-BP. CK2 kinase was incubated with α-casein in the presence of ATP or ATP-BP under UV for 2 hrs at 30 °C, the resulting mixtures were separated by SDS-PAGE and visualized by coomassie blue staining (top) and western blotting with anti-CK2 (bottom). The gels are representative of three independent trials (Appendix A, Figure A2.1). Refer to Chapter 1, Figure 1.11 for ATP-ArN_3 crosslinking experiment.

2.7 AutoDock studies of ATP-ArN_3, ATP-DAz, and ATP-BP

2.7.1 AutoDock analysis using CK2 kinase crystal structure

To understand the differences in the QMS and crosslinking efficiency data, we docked ATP-ArN_3, ATP-DAz, and ATP-BP into the active site of CK2 kinase (GenBank ID: 7766821, pdb:1DAW) using the Autodock Vina program (http://vina.scripps.edu/).[174] ATP-DAz analog was previously synthesized by Dr. Sujit Suwal, but complete analysis was not yet finished. ATP-DAz analog was used in computational studies for comparison. ATP-ArN_3 demonstrated the lowest binding energy amongst the three analogs (-8.1 kcal/mol, Appendix A, Table A2.1).

The most favorable binding mode positioned the phosphate group within 3.5-4.0 Å of G46 and G48 of CK2, while the linker of ATP-ArN_3 was located near K158 and H160 (Figure 2.14A). In the case of ATP-DAz, the docking study resulted in a higher binding energy of -6.5 kcal/mol (Appendix A, Table A2.2), perhaps due to fewer interactions observed compared to the other two analogs (Figure 2.14). The most favorable mode of ATP-BP maintained interactions similar to that of ATP-ArN_3 (Figure 2.14C), although with a reduced binding energy of -7.3 kcal/mol (Appendix A, Table A2.3). The docking data poorly mimic the observed kinase conversion (Table 2.2) or crosslinking efficiencies (Figure 2.13 and 1.11) of the ATP analogs. One possible cause for the discrepancy is the lack of a bound peptide substrate in the CK2 kinase structure, which could skew the analysis.

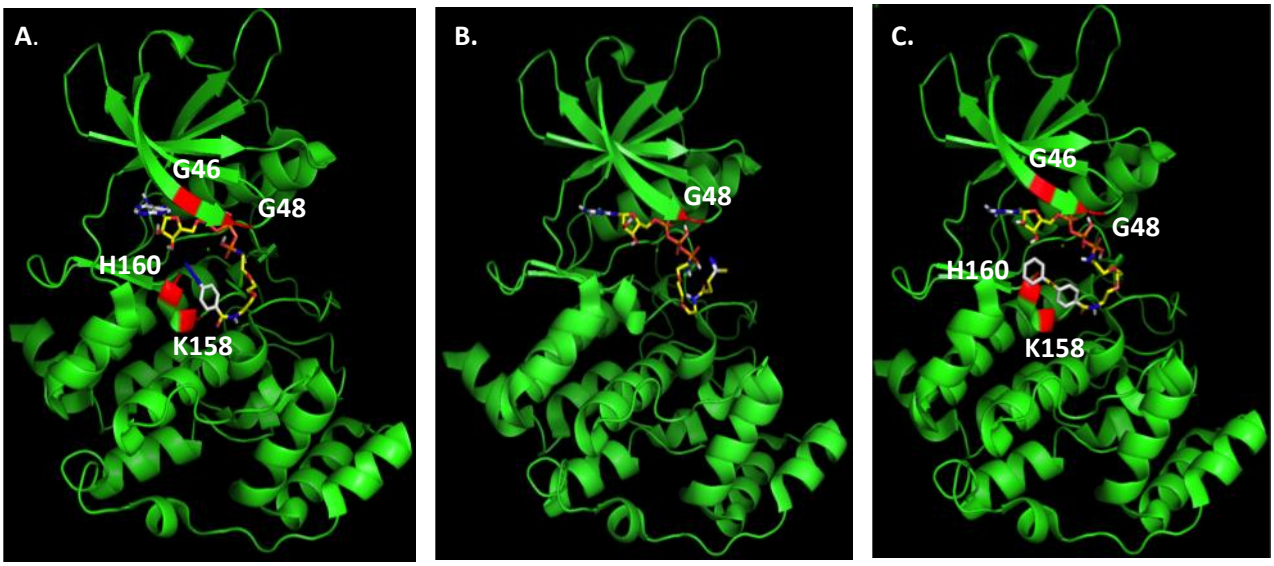

Figure 2.14: Docking of ATP-analogs into the Active Site of CK2 Kinase. The crosslinkers of the ATP-analogs (ball and stick structures) protrudes from the active site of CK2 kinase (green ribbon), but within close proximity to G46, G48, K158 and H160 (red). A) ATP-ArN_3, B) ATP-DAz, C) ATP-BP.

2.7.2 AutoDock analysis using PKA kinase crystal structure

To understand the influence of a peptide substrate on ATP analog binding, we also performed docking studies with PKA kinase. The PKA crystal structure contains a bound peptide inhibitor in the active site, in addition to an ATP mimic (Genbank ID 6755076, pdb: 1ATP). ATP-BP demonstrated the lowest binding energy of -9.7 kcal/mol among the three analogs (Appendix A, Table A2.6). The most favorable binding mode positioned the phosphate groups within 3.5-4.0 Å of G52 and T51 and the ethylene glycol linker 3.0-3.5 Å away from R18 and N20 in the peptide inhibitor (Figure 2.15C). Similar types of interactions were observed with ATP-ArN_3 and ATP-DAz, but with higher energy binding (-7.2 kcal/mol for both analogs, Figures 2.15A, 2.15B, and Appendix A, Table A2.4, A2.5).

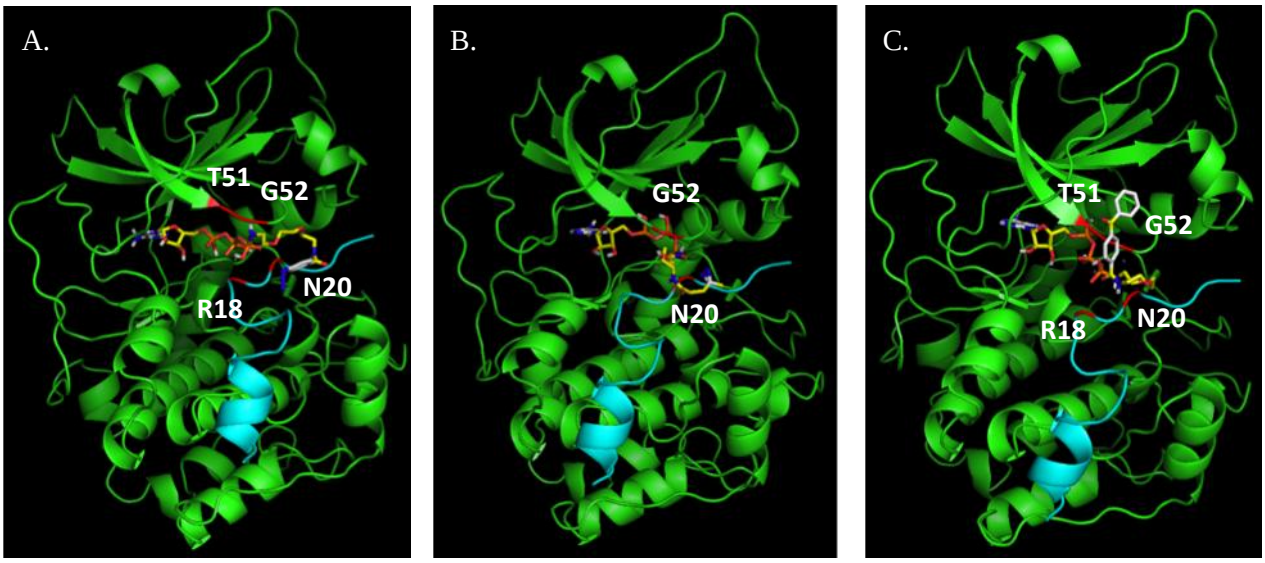

Figure 2.15: Docking of ATP-analogs into the Active Site of PKA Kinase. ATP-analogs (ball and stick structures), PKA kinase crystal structure consists of PKA kinase (green ribbon), and peptide substrate inhibitor (cyan). The modified group protrudes from the active site but within close proximity to G52, T51, R18, and N20 (red). A) ATP-ArN_3, B) ATP-DAz, C) ATP-BP.

In this case with PKA and its bound peptide inhibitor, the ATP analog binding energies are consistent with labeling efficiency data, where ATP-BP demonstrates the highest kinase conversions (71%, Table 2.2) and the lowest binding energy (-9.7 kcal/mol). Likewise, the ATP-

ArN_3 demonstrates kinase conversions (51%, Table 2.2) similar to binding energies (-7.2 kcal/mol) observed. These data strongly suggest that docking studies should utilize a kinase with a bound peptide to best reflect experimental results. In addition to binding energies, another key difference observed in the docking analysis was the positioning of the photocrosslinkers relative to the kinase structure. In the case of ATP-ArN_3, the aryl azide group was located within 3.2-4.4 Å of the protein complex in both the CK2 and PKA studies (Figure 2.16).

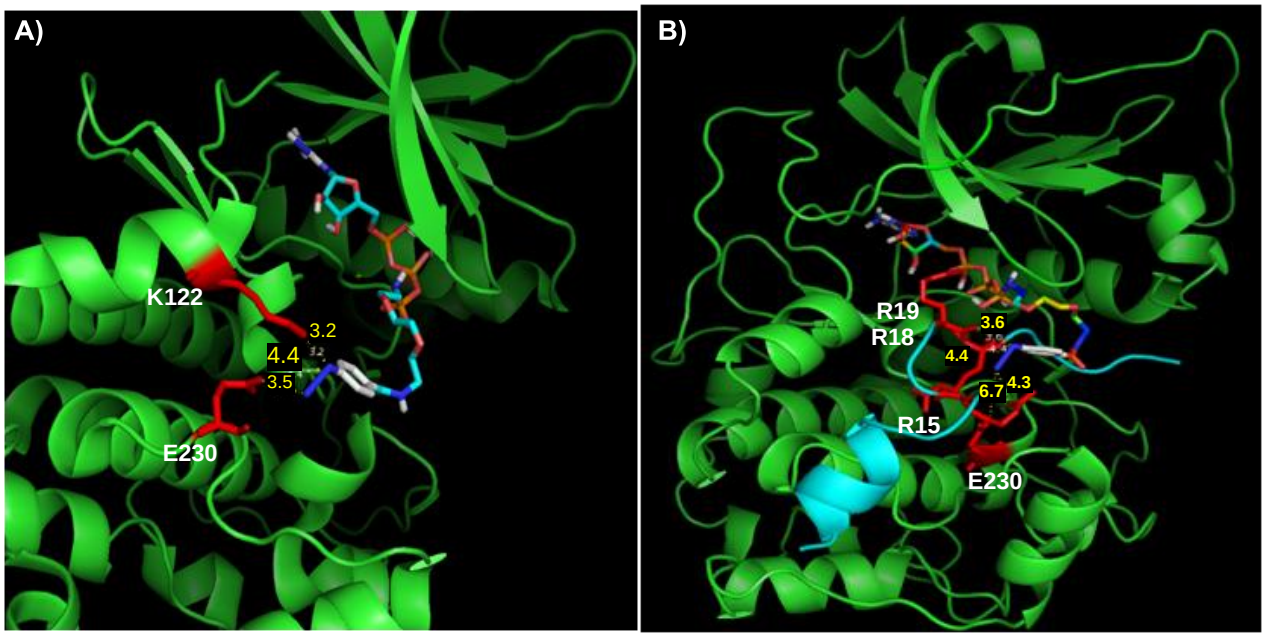

Figure 2.16: **Distance Measurements between Representative Amino Acid Residues in the Kinase and ATP-ArN_3 analog from the Autodock Analysis.** A) The distances shown are from the azide nitrogen of ATP-ArN_3 to the nearest atoms of K122 and E230 on CK2 kinase. B) The distances shown are from the azide nitrogen of ATP-ArN_3 to the nearest atoms of R15, R18, R19, and E203 on PKA kinase complex.

Similarly, with ATP-DAz, the diazirine group was located within 3.5-4.5 Å of either protein complex. In contrast, the benzophenone group of ATP-BP was positioned within 3.7-5.0 Å of the CK2 kinase, but 5.2-6.5 Å away from the PKA complex (Figure 2.17). This distance

analysis suggests that the large benzophenone group is positioned away from the kinase-substrate complex, which could result in reduced crosslinking efficiency. However, the smaller aryl azide or diazirine groups are located near the kinase active site for efficient crosslinking. Therefore, the docking studies point towards the size of the photocrosslinking group as a factor influencing the efficiency of kinase-mediated crosslinking.

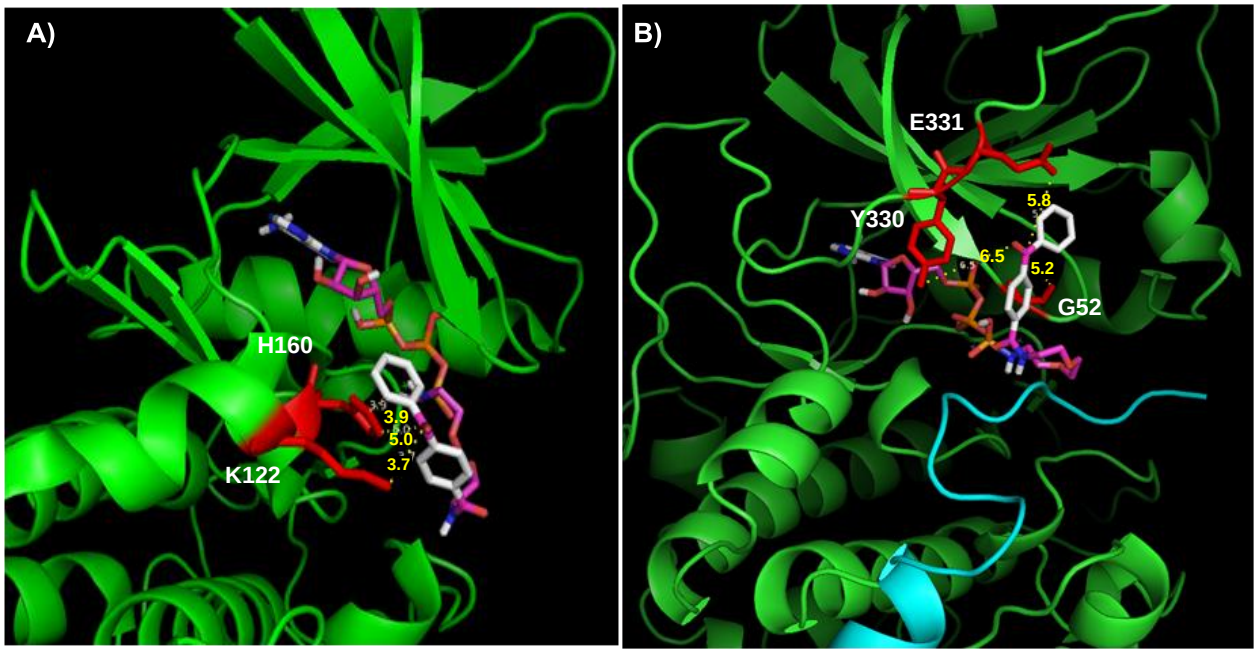

Figure 2.17: Distance Measurements between Representative Amino Acid Residues in the Kinase and ATP-BP analog from the Autodock Analysis. A) The distances shown are from the benzophenone carbonyl of ATP-BP to the nearest atoms of K122 and H160 on CK2 kinase B) The distances shown are from the benzophenone carbonyl of ATP-BP to the nearest atom of G52, Y330, and E331on PKA kinase complex.

2.8 Conclusions

In this chapter, we performed a comparative study of photocrosslinking ATP analogs for use in phosphorylation-dependent kinase-substrate crosslinking. These analogs were compatible with kinase-catalyzed labeling and appropriate for crosslinking CK2 with casein substrates. Interestingly, while the ATP-BP analog was the most efficient kinase cosubstrate, the ATP-ArN_3 analog produced the most distinct crosslinked complex. Docking studies indicated that the size of the crosslinking group could influence its position in the active site, and consequently crosslinking efficiency. Combined, this study revealed that ATP-ArN_3 and ATP-DAz (docking studies only) are excellent reagents for kinase-catalyzed photocrosslinking due to their small size and reasonable kinase compatibility. While ATP-BP was the best cosubstrate, it produced higher order crosslinked complexes with CK2 and casein. Photocrosslinking ATP analogs will serve as useful tools in dissecting kinase substrate specificity due to their phosphorylation-dependent mechanism and can play a role in studying signaling pathways.

2.9 Experimental

2.9.1 Materials

ATP, sodium azide and sodium nitrite were purchased from Fisher. CK2 was bought from New England Biolabs. CK2 peptide substrate (RRREEE**T**EEE) was purchased from Promega. 4-aminobenzoic acid, 2, 2'-ethylenedioxy bis-(ethylamine), 4-hydroxy-α-cyanocinnamic acid (4HCCA) and 1-(3-Dimethylaminopropyl)-3-ethylcarbodiimide hydrochloride (EDCI) were purchased from Acros. 4-benzoyl benzoic acid, *N*-hydroxy succinimide (NHS), *N*-methyl morpholine (NMM), 2-[4-(2-hydroxyethyl)piperazin-1-yl]ethanesulfonic acid (HEPES) were bought from SigmaAldrich. Tris-base, ethylenediamine tetra acetic acid (EDTA) and sodium chloride were obtained from JT Baker. D_4-MeOH, D_2O, $CDCl_3$ was purchased from Cambridge Isotope Lab. Inc. Flash chromatography was performed on silica gel, 200-400 mesh (Merck). A-25 sephadex was purchased from Aldrich. The anti-CK2 antibody was bought from Millipore and Sigma-Aldrich. Goat anti-Mouse IgG H&L (HRP) secondary antibody was purchased from Abcam. SuperSignal West Dura Chemiluminescent Substrate was purchased from Thermo Scientific. Sypro® Ruby protein stain was purchased from Invitrogen, and Coomassie blue stain was purchased from NuSep.

2.9.2 Instruments

^{1}H NMR, ^{13}C NMR, ^{31}P NMR (Varian Mercury-400) and ESI MS (Waters ZQ2000) were used to authenticate the synthesized compounds. The triethylamine counterion in ATP-BP **4** was observed at δ 1.18 and 2.8 in the ^{1}H NMR and δ 8.7 and 46.0 in ^{13}C NMR. The peaks around δ 4.95 and 3.31 in the ^{1}H NMR and δ 58.0 in ^{13}C NMR were due to CD_3OD solvent. Likewise, the peaks at δ 4.80 and 7.24 in the ^{1}H NMR were due to D_2O and $CDCl_3$, respectively. The peak at δ

77.0 in ^{13}C NMR was due to $CDCl_3$. IR spectra were recorded on an FT/IR-460 plus (JASCO DCo. Ltd.) spectrometer. Absorbance of intermediate compounds and the ATP-analog were measured on an HP 8452A Diode array UV-Vis spectrophotometer. High resolution mass spectra were obtained using LCT Premier XT (Waters). The concentration of the ATP analog was calculated using the UV-Vis spectrophotometer. Quantitative mass spectrometric analyses of phosphopeptides resulting from the kinase reactions were performed using a MALDI-TOF MS (Bruker Ultraflex) with 4-hydroxy-α-cyanocinnamic acid (4HCCA) matrix. A Thermo Scientific-Pierce UVP 3UV Ultraviolet lamp was used for crosslinking.

2.9.3 Synthesis of the ATP-ArN_3 (2) analog

ATP-ArN_3 was synthesized as reported earlier.[92] This analog was used for experiments discussed in chapter 3.

2.9.4 Synthesis of the ATP-BP (4) analog

(a) Synthesis of N-(2-(2-(2-aminoethoxy)ethoxy)ethyl)-4-benzoylbenzamide **7***:*

To a stirred solution of 4-benzoyl benzoic acid **5** (620 mg, 2.13 mmol) in dry DCM (10 mL) was added EDCI (713 mg, 3.73 mmol) and NMM (322 mg, 3.13 mmol) at room temperature. After stirring for 30 min, this solution was added drop wise to an ice cooled DCM solution (200 mL) of 2,2'-ethylenedioxy bis-(ethylamine) **6** (638 mg, 4.3 mmol) over a period of 30 min, followed by stirring for 2 hrs at room temperature. The solvent was evaporated to dryness and the residue was purified by flash chromatography using a stepwise solvent system, initially with DCM: EtOH (3:1) followed by DCM:EtOH:NH_4OH (3:1:0.05) to yield benzophenone linker **7** (43%, 420 mg, 1.2 mmol). ^1H NMR (400 MHz, $CDCl_3$): δ 3.15 (b, 2H), 3.62- 3.74 (m, 12H), 7.47 (t,

2H), 7.59 (t, 1H), 7.74 (m, 4H), 7.89 (b, 1H), 8.05 (d, 2H) ^{13}C NMR (100 MHz, $CDCl_3$): δ 40.1, 69.9, 70.1, 70.2, 127.5, 128.5, 129.9, 130.0, 132.9, 136.9, 137.5, 139.9, 167.0, 196.3. IR (neat, cm^{-1}): 658, 716, 768, 864, 926, 1117, 1277, 1541, 1649, 2872. HRMS [$M+H^+$] $C_{20}H_{25}N_2O_4$; cal: 357.1814 found: 357.1812. Spectra are in Appendix A, Figures A2.3 to A2.6.

(b) Synthesis of ATP-[γ] -N-(2-(2-(2-aminoethoxy)ethoxy)ethyl)-4-benzoylbenzamide **4***:*

ATP-2Na (30 mg, 0.05 mmol) was dissolved in water (5 mL) and the pH was adjusted to 7.0 with 1N aqueous HCl. EDCI (380 mg, 2 mmol) was added and the pH was adjusted to 5.6-5.8 with 1N aqueous HCl followed by addition of water (1 mL). Benzophenone amine linker **7** (400 mg, 1.1 mmol) was dissolved in water (1 mL), added to the reaction mixture, and incubated for 2 hours at room temperature while controlling the pH at 5.6-5.8. The reaction mixture was brought to pH 8.5 using 1 M triethylamine bicarbonate (TEAB) buffer and purified using an A-25 sephadex anion exchange column with a gradient of 0.1 M to 1.0 M TEAB buffer solution (pH=8.5) as the eluent. The purified product was lyophilized to dryness to obtain the TEA salt of ATP-BP **4** (28%, 11.83 mg, 0.014 mmol). The product was dissolved in 25 mM HEPES buffer, pH 7.2-7.5, aliquoted into single use fractions and stored at -80 °C until use (for up to several months). With the aid of UV absorbance, the concentration of the final product was calculated. λ = 261 nm, ε = 21000. ^{1}H NMR (400 MHz, D_2O): δ 3.54-3.74 (m, 12H), 4.15 (m, 1H), 4.21 (m, 1H), 4.28 (m, 1H), 4.50 (m, 1H), 4.67 (m, 1H), 5.98 (d, 1H), 7.50 (t, 2H), 7.67 (m, 3H), 7.75 (d, 2H), 7.83 (d, 2H), 8.10 (s, 1H), 8.43 (s, 1H). ^{31}P NMR (162 MHz, CD_3OD): δ -1.53 (d, γ-P), -11.69 (d, α-P), -23.08 (t, β-P). IR (cm^{-1}): 655, 715, 914, 991, 1060, 1222, 1647, 1707, 2366, 2981, 3275. HRMS: [$M-H^+$] $C_{30}H_{31}N_7O_{16}P_3$; cal: 844.1510; found: 844.1505. Spectra are in Appendix A, Figures A2.7 to A2.11.

2.9.5 Quantitative mass spectrometric (QMS) analysis:

Quantitative MALDI-TOF MS was performed using a previously described protocol.[96] Briefly, each reaction mixture contained ATP or a synthetic ATP-analog (1.0 mM final concentration), CK2 substrate peptide (40 μM), and CK2 kinase (10 units/μL) in the manufacturer-supplied buffer (1X). The final volume of the reaction was 10 μL. The reaction mixtures were incubated for 2 hours at 30 °C. The products formed after the enzymatic reaction was esterified at all carboxylic acids using acetyl chloride (50 μL) and either d_4-methanol (200 μL, for the ATP reaction) or d_0-methanol (200 μL, for the ATP-ArN_3 reaction). Reaction mixtures were incubated at room temperature for 2 hours. Under these conditions, the phosphoramidate bond of the ATP-BP product was cleaved to yield a phosphopeptide. The solvent in the resulting reaction mixtures was evaporated *in vacuo*. Phosphopeptide mixtures were separately dissolved in a minimum amount of water (5 μL). For MS analysis, the two phosphopeptide samples were mixed (2 μL of each) with 10 μL of a matrix solution (saturated solution of alpha-cyano-4-hydroxy cinnamic acid in 70 % acetonitrile, 30 % water and 0.1% TFA). The mixture (1 μL) was spotted on a MALDI plate (Standard 384 MTP, Bruker) and isotopically differentiated phosphopeptides were analyzed on MALDI-TOF MS instrument. MALDI-TOF MS spectra of three independent trials with ATP-BP **4** are shown in Appendix A, Figures A2.2. The mean of these three independent trials is reported in Table 2.2

2.9.6 Crosslinking experiment protocol

Crosslinking experiments were performed as reported previously.[92] Briefly, CK2 kinase (5 units/μL) was incubated with ATP-BP (2.5 mM) or ATP (2.5 mM) in CK2 buffer (20 mM HEPES, 50 mM KCl, 10 mM $MgCl_2$) for 5 minutes on ice, followed by the addition of α-casein

(100 μM). The final reaction volume was 20 μL. Equal concentrations (2.5 mM) of ATP-BP and ATP were added for competitive reaction control. The reaction mixtures were incubated for 2 hrs at 30 °C. Crosslinked protein was obtained by simultaneously irradiating the appropriate reaction tubes with a handheld UV lamp (365 nm). The presence of the phosphoramidate bond in the crosslinked product was confirmed by acid-mediated cleavage of the complex by adding 20 μL of trifluoroacetic acid (TFA) to the reaction mixture (final concentration of 50% TFA) and incubating at 30 °C for 1 hour. The sample tube containing TFA was neutralized using 100 mM Tris base (50 μL) and the volume was reduced *in vacuo*. The reaction products were separated by SDS-PAGE and the proteins were visualized with Coomassie blue stain or SyproRuby stain, or western blotting with an anti-CK2 antibody after electrotransfer onto PVDF membrane (Immobilon-P^{SQ}).

2.9.7. Sodium Dodecyl Sulfate-Polyacrylamide Gel Electrophoresis (SDS-PAGE)

The SDS-PAGE gels were prepared with a stacking layer and a separating layer (as described in *Molecular Cloning*, Appendix 8.40-8.45)[119]. The lower layer contained approximately 4 mL of solution resulting in a 10% separating layer. The separating layer consisted of 1 mL of 4X Tris/SDS separating buffer (0.4% w/v SDS, 1.5 M Tris, brought to pH 8.8 with HCl), 1 mL 40% w/v 37:1 acrylamide:bisacrylamide, 1.96 mL filtered water, and 40 μL of freshly prepared 10% ammonium persulfate (APS) (Fisher). Polymerization was initiated by the addition of 4 μL of tetramethylethylenediamine (TEMED) (Acros Organics) and poured into the sandwiched glass gel plates. Methanol was added on top of the separating layer, gently removing any air bubbles without disturbing the acrylamide layer. The upper stacking layer was prepared by mixing 0.5 mL 4X Tris/SDS stacking buffer (0.4% w/v SDS, 1.5% Tris, brought to pH 6.8 with HCl), 0.25 mL 40% w/v 37:1 acrylamide: bisacrylamide, 1.24 mL distilled water. The methanol was drained

and dried carefully. APS (10%, 10 µL) and TEMED (2 µL) were added, initiating polymerization and the solution was poured on top of the separating layer. A ten well comb was placed to create wells for loading proteins. The SDS-PAGE gel running chamber was filled with a 1X SDS running buffer, which was composed of 0.1% SDS, 0.025 M Tris, and 0.25 M glycine. A protein molecular weight marker (5 µL, EZ-RUN Pre-Stained Protein Marker, Fisher) was loaded onto the gel as a standard, using gel loading tips (Fisher). The gel was run using a mini-protean basic power pack unit at constant 200 Volt, 400 amps for 60-90 mins depending on the resolution of gel according to the protein of interest.

2.9.8. Western Blotting

Proteins separated by SDS-PAGE were transferred to a polyvinylidene difluoride (PVDF) membrane (Immobilon P, Millipore). The PVDF membrane was pre-wet with methanol and proteins were transferred using the Mini-Transblot Electrophoretic Transfer Cell apparatus from BioRad, with 0.01 M CAPS (*N*-cyclohexyl-3-aminopropanesulfonic acid) at pH 10.5, supplemented with 10% methanol as the buffer. The transfer process was done at constant 90 V for 90 mins. After the transfer was complete, the membrane was air dried for firm attachment of proteins. The membrane was re-wetted with methanol and incubated overnight in a blocking solution of 5% (w/v) non-fat dry milk powder in PBST (1X buffer contains 137 mM NaCl, 2.7 mM KCl, 10 mM Na_2HPO_4, 2 mM KH_2PO_4, pH 7.4 and 0.1% Tween-20). The membrane was washed with PBST and then incubated in recommended dilution of primary antibody (1: 500 to 1:1000) for one to two hours (longer incubation time can lead to non-specific labeling). The membrane was rinsed with PBST for 5 minutes, twice, to remove excess antibody. Secondary antibody (1: 1500 to 1:3000) was added and incubated for 1 to 2hr, and then washed with PBST (5 minutes two times). The PVDF membrane was developed using HRP substrate, in case of

HRP antibodies and visualized using the Typhoon 9400 scanner in chemiluminescence mode at 600 PTM. In case of fluorophore labeled antibodies the manufacturer instructions were followed using the Typhoon 9400 scanner in fluorescence mode.

2.9.9 Coomassie Blue Staining

The SDS-PAGE gel was gently placed into a clean container and 50 mL of commercially available Coomassie Brilliant Blue stain (NuSep) was added. The gel was incubated in the staining solution at room temperature overnight, with gentle rocking. The stain was removed and 50 mL of destaining solution (6% acetic acid) was added and incubated at room temperature for 1-2 hours. The Coomassie stained gel was imaged using a document scanner (HP Scanjet G4010).

2.9.10 Autodock analysis

The Autodock Vina program was designed by Dr. Oleg Trott of Molecular Graphics Lab at The Scripps Research Institute.[174] It was downloaded free from the website- http://vina.scripps.edu/index.html. The Autodock Vina program was executed as per the tutorial instructions found on the website. The crystal structures were downloaded from the RCSB Protein Data Bank (1ATP for PKA and 1DAW for CK2). The PyMOL program (Schrödinger Inc.) was used to delete ATP in the active site. The ATP analog structure was drawn in Chem 3D Pro (CambridgeSoft) and MM2 from Chem 3D pro was used for energy minimization. The output file of the different binding modes is shown in Appendix A, Tables A2.1 to A2.6. The lowest binding energy mode that conforms to the kinase-catalyzed phosphorylation mechanism is in bold for each docking experiment. The grid box dimensions used in all the analyses were the same or similar.

Chapter 3

Previous studies have demonstrated the utility of ATP-ArN_3 and ATP-BP photocrosslinking analogs for kinase-catalyzed labeling and crosslinking studies. In addition, we explored the important features of photolabels for photocrosslinking with AutoDock studies. In this chapter, experiments were done to find the optimum conditions for phosphorylation-dependent kinase-substrate photocrosslinking in the absence and presence of cell lysates. ATP-ArN_3 and ATP-BP photocrosslinking analogs were successfully used to identify novel kinases of p53 using natural kinase and substrate. A brief description of p53 and its importance is included at the beginning of the chapter.

3.1 Introduction

In order to demonstrate the novelty and applicability of the photocrosslinking ATP analogs in identifying known or novel kinases of a substrate, or vice-versa, we need to validate the chemical tool with a well studied protein. For this purpose p53, was chosen as the protein of interest because of its implication in various cancers and diseases.

3.1.1 p53 –"*Guardian of the Genome*"

p53 was discovered in 1979, independently reported by six groups[175-180] and characterized as tumor suppressor protein later in 1989.[181,182] Because of its central role in many cellular processes, p53 was dubbed the "cellular gatekeeper" [183] or "guardian of the genome".[184] p53, also known as tumor suppressor protein (TP53) is a 44 kDa protein containing 393 amino acids that is encoded by the TP53 gene on the short arm of chromosome 17 (17p13). Even though p53 is a 44 kDa protein, it migrates as a 53 kDa protein on SDS-PAGE due to high number of proline residues and it gained the name p53 (protein at 53 kDa).

The p53 protein is a tetramer, tied together with flexible side arms (Figure 3.1A). P53 consists of four functional domains: an N-terminal transactivation domain (TAD) also called the proline rich domain; a central DNA-binding domain (DBD), which binds to DNA and where most of the mutations observed in many cancers are found; a tetramerization domain (TD), where all the domains are attached; and a C-terminal domain (CD) that regulates p53 activity. Upon activation of p53 with stress signal, DNA is bound to the p53 DBD in a sequence specific manner where flexible residues are ready to act on DNA and assemble specific proteins for transcription (Figure 3.1B).[185]

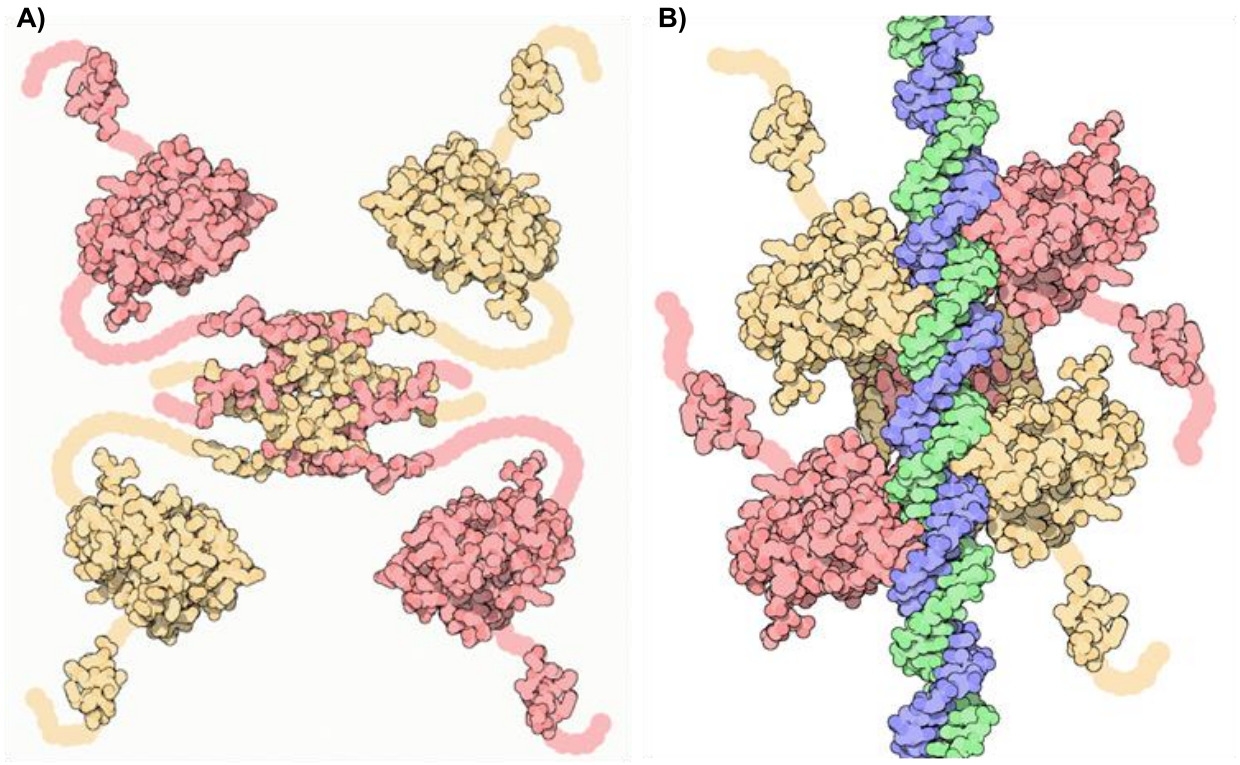

Figure 3.1: Illustration of p53 from crystal structures (a) Cartoon depicting p53 tetramer (b) Cartoon depicting DNA interacting with p53. These illustrations are rendered from the crystal structures of p53 domains (PDB ID- 1OLG,[186] 1YCQ,[187] 1TUP[188]). This figure was obtained from July 2002, RSC-PDB, molecule of the month by David S. Goodsell, (http://dx.doi.org/10.2210/rcsb_pdb/mom_2002_7). Copyright permission received from RSC-PDB to use the images.

P53 undergoes various PTMs, such as phosphorylation, acetylation, ubiquitination, glycosylation, sumoylation, ADP-ribosylation, neddylation and methylation, under various stress signals, leading to different cellular processes (Figure 3.2). PTM of p53 leads to various biological processes through stabilization, increased DNA binding of p53, and activation of transcription. An example of signaling pathway involving p53 was discussed in chapter 1 (Section 1.2). p53 plays a central role in mediating signaling processes critical for cell fate. Abnormalities in the function or mutations at the DNA binding domain of p53 can lead to diseases. In many types of cancers, mutations are commonly identified in the p53 DNA binding domain. Multiple phosphorylation sites have been identified on p53 and phosphorylation of each of these sites have further downstream effects in cell growth, proliferation and are also linked to diseases (Figure 3.2). Many *in vitro* kinases are known for p53 and some *in vivo* kinases have also been validated (Table 3.1).[189,190] Our goal was to use ATP-ArN_3 to identify kinases and proteins that interact with P53 by crosslinking after phosphorylation upon UV irradiation. By focusing on p53, we sought to uncover novel kinases of p53 and their functions and roles in disease formation. This approach allows us to establish a method for identification of true kinase-substrate pairs and also phosphorylation dependent protein-protein interactions.

One of the interesting phosphorylation sites on p53 is serine 392, which is phosphorylated by CK2 under stress conditions like UV irradiation (Table 3.1). There is a conflict regarding whether CK2 is both an *in vitro* as well as an *in vivo* kinase of p53.[191-193] ATP-ArN_3 crosslinker will be a good chemical tool to demonstrate and identify the true cellular kinase for Serine 392.

Table 3.1: List of some of the kinases known to phosphorylate p53.[194 195]

Kinase	Activated by	Phosphorylation site on p53	Molecular or cellular outcome
ATM	DNA damage	Ser15	Apoptosis
ATR	γ-radiation UV light	Ser15, Ser37	Apoptosis
CDK (CDC2/CDK2)	UV light	Ser315	Increased p53 transcription
AURKA	Overexpression of AURKA	Ser315	Ubiquitylation and degradation of p53
CHK1/CHK2	Ionizing radiation	Ser20	Disruption of the MDM2–p53 complex
CK2	UV light	Ser392	Increased p53 activity
CK1	Topoisomerase-directed drugs and DNA damage	Ser6, Ser9, Thr18(requires Stabilization of p53 through phosphorylation of	Stabilization of p53 by inhibition of MDM2
DNAPK	DNA damage	Ser15, Ser37	Disruption of the MDM2–p53
PKR	Interferon	Ser392	Not determined
CSN-associated kinase complex	Unstressed	Thr 150, Thr155, Ser149	Degradation
ERKs	UV light	Ser15	Apoptosis
ERK2	Doxorubicin	Thr55	Activation of p53
GSK3β	ER stress	Ser315, Ser376	Inhibition of p53 mediated apoptosis
HIPK2	UV light	Ser46	Facilitates CBP mediated acetylation of p53 (at Lys382); arrest and apoptosis
JNK	UV light	Ser20	Apoptosis
p38 kinase	UV light	Ser20	Apoptosis
p38	UV light	Ser 15	Apoptosis
p38 kinase	UV light DNA damage	Ser 392	Increased DNA-binding activity of p53

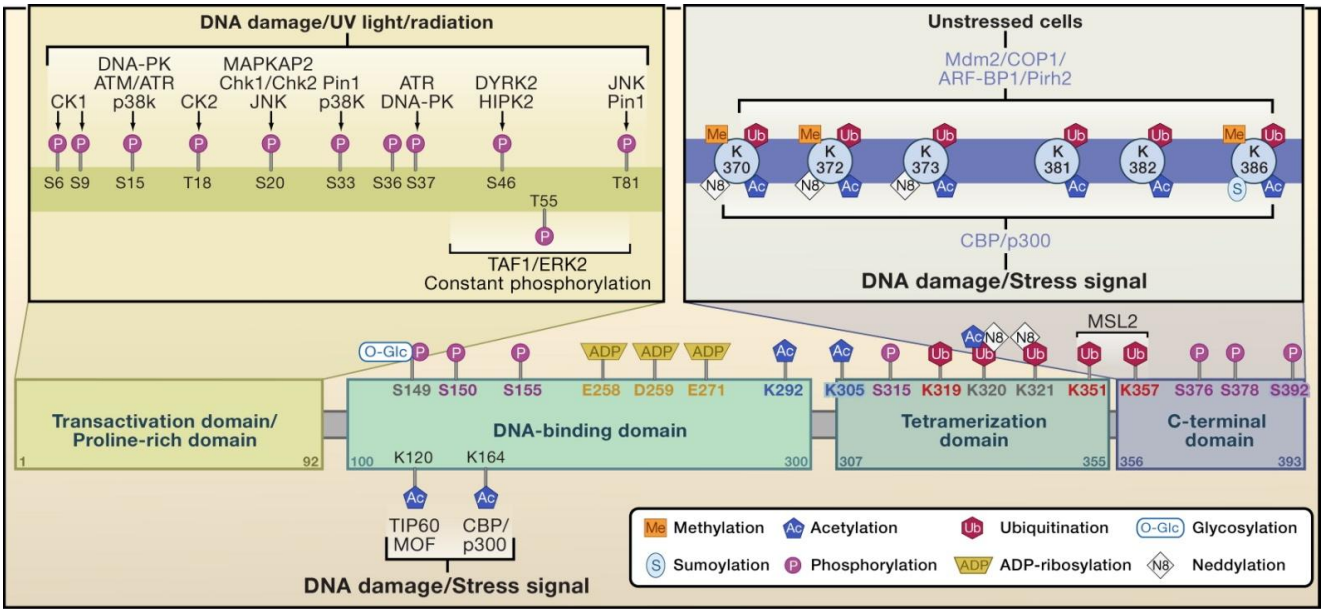

Figure 3.2: Overview of p53 Post-translational Modifications. p53 undergoes different PTMs like methylation (Me), acetylation (Ac), ubiquitination (Ub), glycosylation (o-Glc), sumoylation (S), phosphorylation (P), ADP-ribosylation (ADP) and neddylation (N8), of which phosphorylation is the major PTM. PTMs occur under different conditions and are carried out by different enzymes depending on the stress conditions as shown above, leading to a biological function. This figure was obtained with permission from Kruse, J.-P.; Gu, W., *Cell* **2009,** *137* (4), 609-622.[189] License Number: 3186091178308

3.2 Results and Discussion

Experiments were carried out to identify optimal conditions for crosslinking such as order of addition, UV irradiation time and concentration of ATP analog. Further explore the conditions for crosslinking in the presence of cell lysates and apply those conditions to identify novel kinases of p53 protein.

3.2.1 Optimization of CK2 kinase and casein photocrosslinking conditions

During phosphorylation-dependent kinase-substrate photocrosslinking studies of the CK2 kinase and casein protein substrate, a few important observations were made. First, the ATP-ArN_3 or

ATP-BP analogs obtained after lyophilization were resuspended in 25 mM HEPES buffer (pH 7.5) instead of Tris buffer because amine-containing buffers can quench the reactive intermediate formed during UV irradiation, inhibiting crosslinking. Second, the order of addition in the kinase reaction is critical. The optimal order is: water, CK2 kinase buffer, CK2 kinase, followed by addition of ATP-analog and incubation on ice for 5 minutes. Subsequently, α-casein substrate was added and incubated under UV for 2 hrs at 30 °C for crosslinking. Experiments were next performed to examine the optimal concentration of ATP analog and irradiation time needed for high levels of crosslinking.

To investigate the effect of UV irradiation time, as well as concentration of aryl azide on crosslinking efficiency, reactions were carried out with UV irradiation times of 30 minutes, 1 hour, and 2 hours using 1 mM, 2.5 mM and 5 mM concentrations of ATP-ArN_3 in the presence of CK2 kinase and casein substrate. SDS-PAGE separation and western blot analysis of the photocrosslinking reactions with CK2 antibody found that UV irradiation for 30 mins at any concentration of ATP-ArN_3 (Figure 3.3, lanes 3-5) produced only a faint band. With 1 hour UV irradiation, visible crosslink bands were observed at 1 mM and 2.5 mM concentration of ATP-ArN_3 (Figure 3.3, lane 6, 7) compared to 5 mM concentration of ATP-ArN_3 (Figure 3.3, lane 8). In the case of 2 hour UV irradiation, a significant crosslink band was observed at all concentrations of ATP-ArN_3 (Figure 3.3, lane 9-11). In conclusion, consistent crosslinked bands were observed with 1 mM and 2.5 mM concentration of ATP-ArN_3 and UV irradiation for 2 hours. Next, experiments were performed to identify conditions for phosphorylation-dependent kinase-substrate crosslinking in the presence of cell lysate.

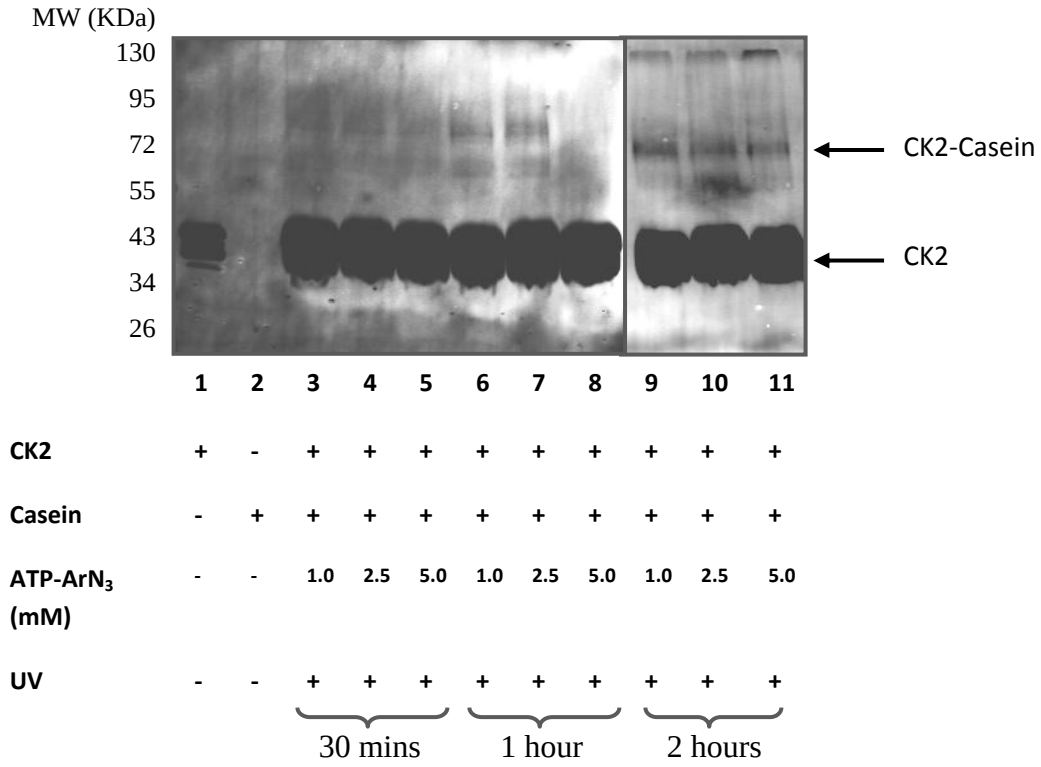

Figure 3.3: Photocrosslinking of CK2 and α-casein with Various Concentrations of ATP-ArN_3 and UV Irradiation times. Photocrosslinking reactions were performed with CK2 kinase and casein substrate in the presence of ATP-ArN_3 and UV at 30 °C, followed by SDS-PAGE separation and visualization with a CK2 antibody. ATP-ArN_3 concentrations and UV irradiation times are as indicated below each reaction lane. The expected ~68 kDa crosslinked band is indicated as CK2-Casein, and 45 kDa band of CK2 kinase as CK2.

3.2.2 Photocrosslinking kinase and full length protein substrate in the presence of cell lysates using ATP-ArN_3

To identify conditions for crosslinking in the presence of cell lysates, experiments were performed with ATP-ArN_3, CK2 kinase, α-casein substrate and Jurkat cell lysates similar to photocrosslinking with full length protein (Section 2.9.6). Briefly, CK2 kinase was incubated with α-casein and lysates in the presence of ATP or ATP-ArN_3 under UV for 2 hrs at 30 °C. The

resulting mixtures were separated by SDS-PAGE and visualized by western blotting with anti-CK2. In these photocrosslinking experiments, 10 μg of Jurkat cell lysate and 10 mM, 15 mM (final) concentration of ATP-ArN_3 were used to overcome the cellular ATP concentration and observe the crosslink between CK2 and casein. SDS-PAGE separation and western blot analysis of crosslinking between CK2 kinase and α-casein substrate in the presence of cell lysates is shown in Figure 3.4. A crosslinked band corresponding to the molecular weight of CK2 and α-casein was observed in the presence (Figure 3.4, lane 6) and absence (Figure 3.4, lane 4) of cell lysates. But the crosslinked band was not observed when the reaction was carried out with ATP (Figure 3.4, lane 5) or with CK2 only (Figure 3.4, lane 1), or lysate only (Figure 3.4, lane 2), or α-casein only (Figure 3.4, lane 3). Crosslinked complex was also not observed in the absence of exogenous CK2 kinase at 10 mM or 15 mM concentrations of ATP-ArN_3 (Figure 3.4, lane 8, 9 respectively). In addition, crosslinked complex was not significant when 15 mM concentration of ATP-ArN_3 was used in the presence of exogenous CK2 (Figure 3.4, lane 7). The optimum conditions were 10 mM of ATP-ArN_3 and 10 μg of total protein for crosslinking CK2 kinase and α-casein protein substrate. With the optimum conditions obtained for crosslinking kinase and substrate in the presence of cell lysate using ATP-ArN_3 in our model system, we wanted to demonstrate phosphorylation-dependent kinase-substrate crosslinking with other known kinase substrates using cell lysates.

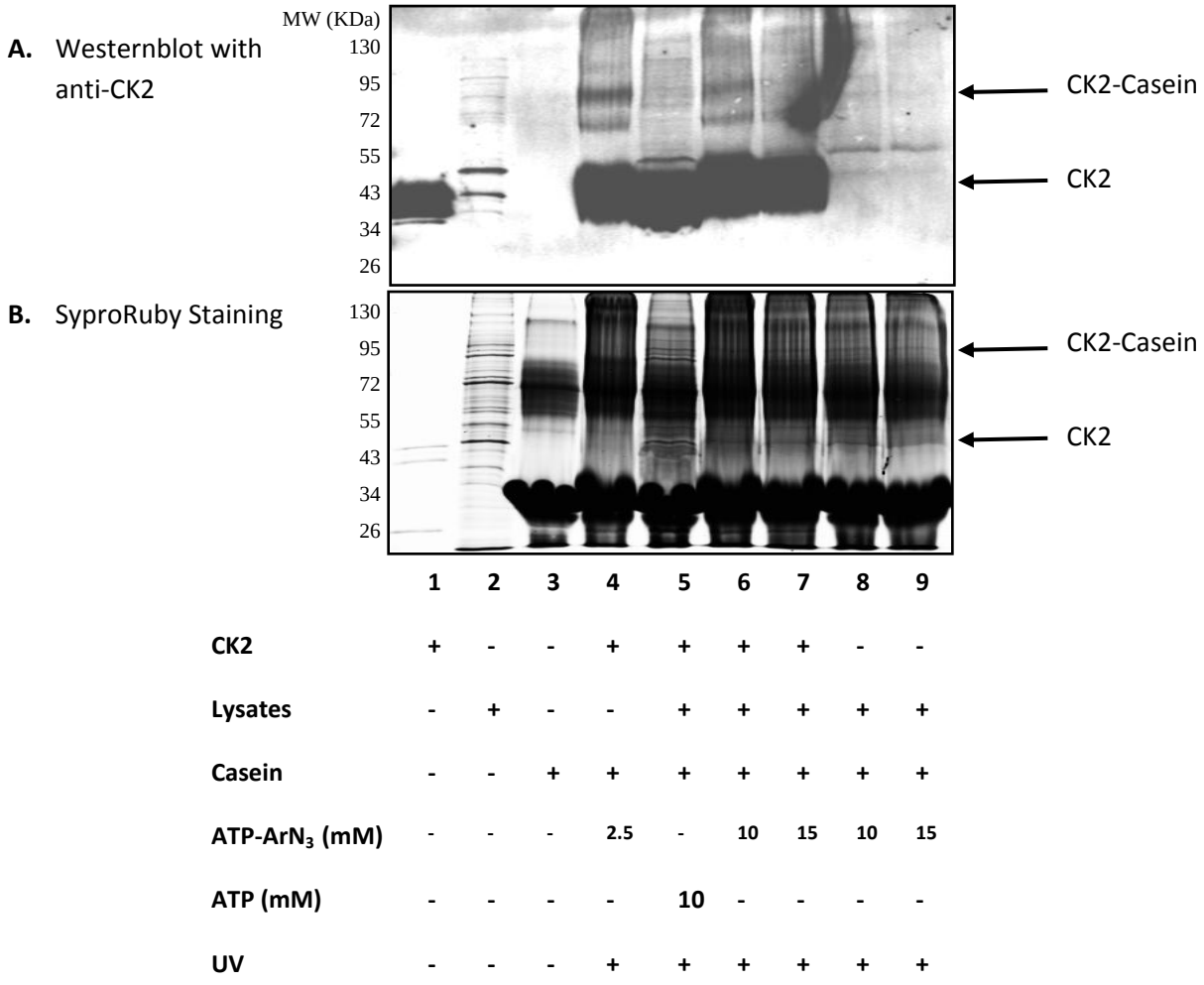

Figure 3.4: Photocrosslinking of CK2 and α-casein in the Presence of Jurkat Cell Lysates. Photocrosslinking reactions were performed with CK2 kinase, casein substrate, and ATP-ArN_3 in the presence of Jurkat cell lysates and UV at 30 °C, followed by SDS-PAGE separation and visualization with a CK2 antibody (top), SyproRuby protein staining (bottom). ATP-ArN_3 concentration and components of each reaction lane are as indicated.10 µg (total protein) of Jurkat cell lysates were used in each reaction. The expected ~68 kDa crosslinked band is indicated as CK2-Casein, and the 45 kDa band of CK2 kinase as CK2. Additional trials are shown in Appendix B, Figure A3.1.

3.3 Phosphorylation-dependent photocrosslinking of natural kinase and substrate using ATP-ArN_3 analog

After successful demonstration of kinase-substrate crosslinking in the presence of cell lysates using ATP-ArN_3, we wanted to demonstrate crosslinking with natural kinases and substrates. As described in the beginning of this chapter, p53 was chosen for this study, because of its role in signaling processes and diseases.

3.3.1 Photocrosslinking experiments with RKO cell lysate and ATP-ArN_3

Crosslinking experiments were carried out using RKO cell lysates. RKO cells are adherent colon cancer cells that have relatively high levels of wild type p53 protein. RKO cell lysates (30 µg of total protein) were incubated with ATP-ArN_3 (10 mM final concentration) and photocrosslinking was performed by incubating under UV for 2 hours at 30 °C. Initial crosslinking experiments were performed with RKO cell lysates in the presence of ATP-ArN_3 with and without exogenous CK2 kinase, to validate p53 as a substrate of CK2 kinase. Unfortunately, we did not observe any obvious higher molecular weight bands corresponding to crosslink between CK2 and p53 or with any other protein when probed with anti-p53 and anti-CK2 (Figure 3.5, lanes 6, 7, 8, and 9). High molecular weight protein complexes were also not observed in the presence and absence of exogenous CK2 kinase (Figure 3.5, lane 6, 8 vs. 7, 9). But the photocrosslinking reaction with CK2 kinase, ATP-ArN_3 (2.5 mM), and casein substrate formed the CK2 crosslinked complex both in the presence and absence of cell lysates (Figure 3.5A, lane 4 and 5), signifying that the phosphorylation-dependent kinase-substrate crosslinking reaction controls were successful. Importantly, p53 protein band at ~53 kDa was also not observed in the p53 western blot (Figure 3.5B, lane 1). Western blot analysis of various concentrations of RKO cell lysates with anti-p53 indicated that the presence of p53 in the lysate

sample was not noticeable. Therefore an insufficient level of p53 protein in the RKO cell lysates was prohibiting visualization of the crosslinking. The next goal was to identify conditions for increasing p53 protein levels in the RKO cell lysates or to find alternative model proteins for crosslinking studies.

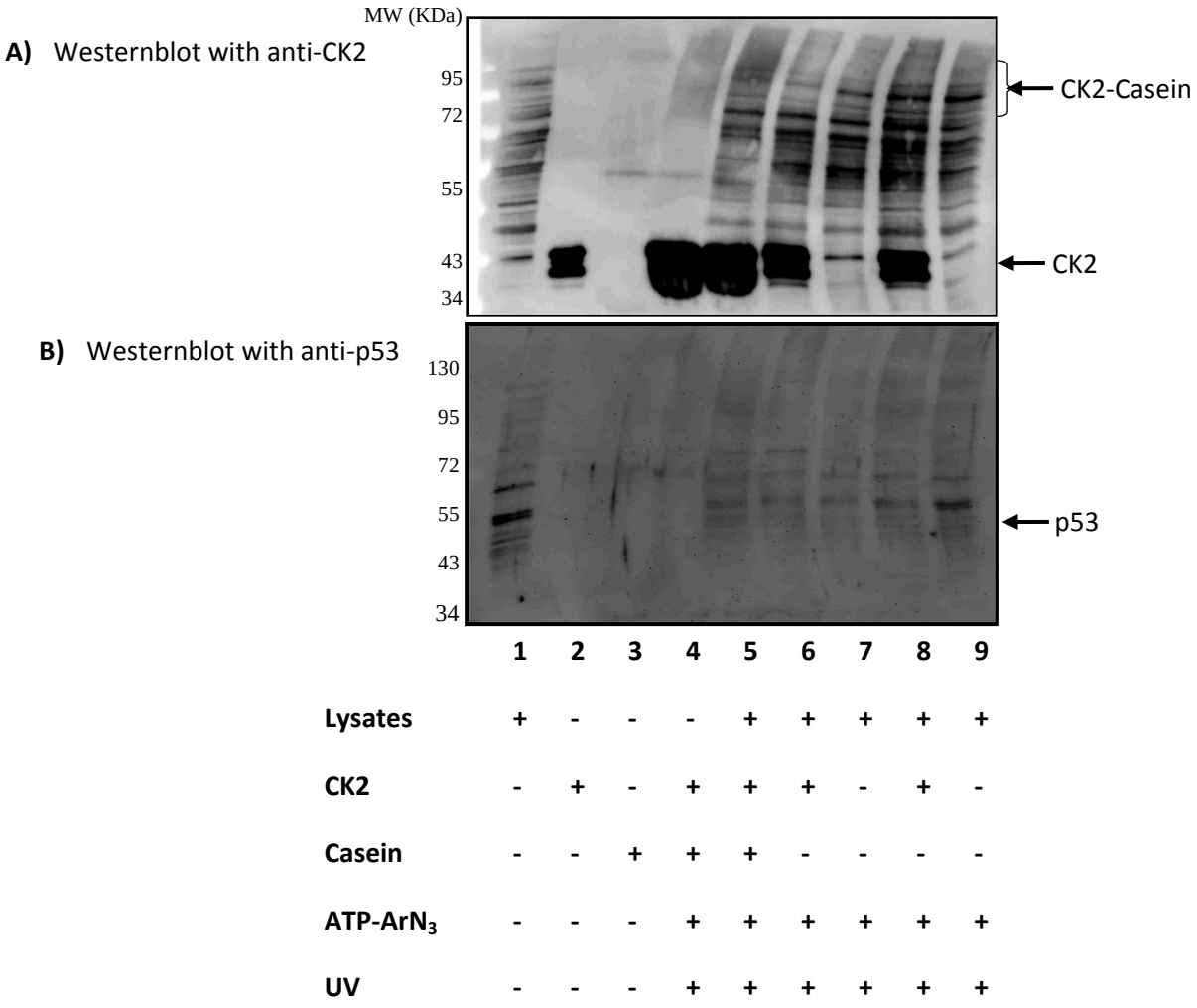

Figure 3.5: Photocrosslinking Reaction using ATP-ArN_3 and RKO cell lysates. Photocrosslinking reaction was performed by incubating the reaction components under UV as indicated for each lane, at 30 °C for 2 hrs, followed by SDS-PAGE separation and visualization with a CK2 antibody (top), and p53 antibody (bottom). The ATP-ArN_3 concentration was 10 mM except for lane 4 which contained 2.5 mM. RKO cell lysates (30 µg) were used in each reaction. The expected ~68 kDa crosslinked band for control reactions lane 4 and 5 was indicated as CK2-Casein, ~45 kDa band of CK2 kinase was labeled CK2 and the expected p53 protein at ~53 kDa was labeled p53.

3.3.2 MDM2 regulation of p53

To explore conditions for increasing p53 expression, we needed to understand the p53 regulation and activation pathways. Under normal conditions, p53 has a high turnover rate and its availability is low. Stress conditions like UV or IR radiation triggers a signaling event through ATM/ATR and CHK1/2 kinases, which phosphorylate MDM2 to disrupt the MDM2/p53 interaction. MDM2 is a negative regulator of p53. As a result, disruption of MDM2 and p53 interactions stabilizes p53 (Figure 3.6).[196] Once p53 is stabilized, it accumulates and carries out important functions, such as DNA repair and cell cycle arrest check points.[185,197] Because negative regulator MDM2 degrades p53, we treated RKO cells with the MDM2 inhibitor, (±)-Nutlin-3 (Figure 3.7A).[198,199] (±)-Nutlin-3 inhibits the MDM2 and p53 interaction by blocking the p53, MDM2 binding site. Although we use the racemic mixture, it was shown that only one enantiomer ((-)-Nutlin-3) (Figure 3.7B) is active and the stereochemical assignment for the enantiomers is arbitrary.[198]

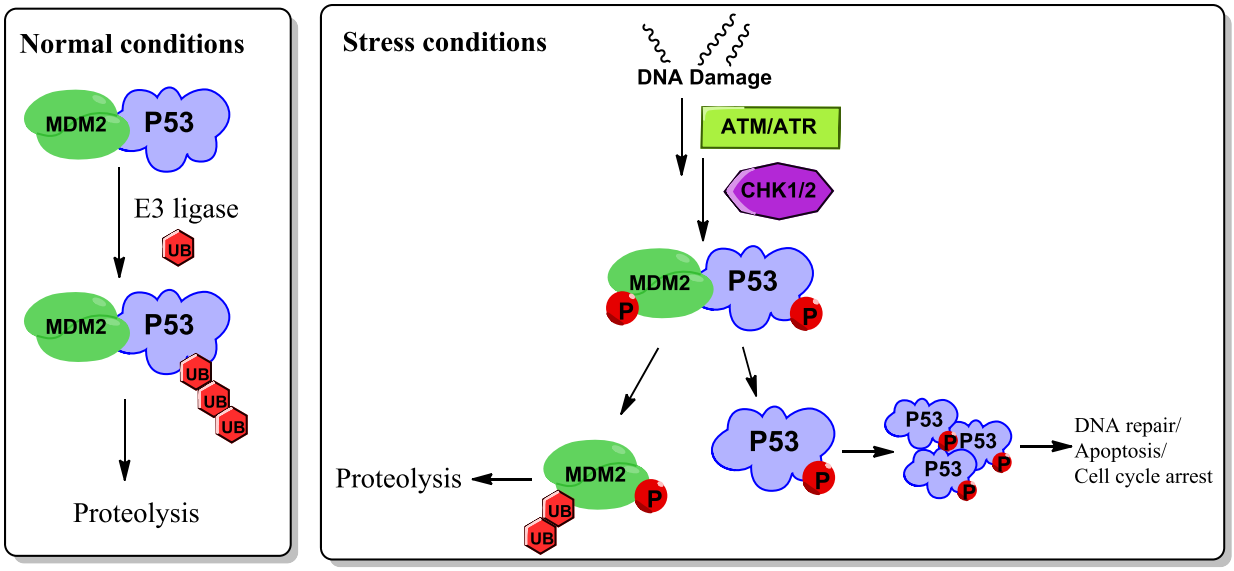

Figure 3.6: Cartoon Depicting the Regulation and Stabilization of p53 by MDM2 complex. In normal conditions p53 undergoes proteolysis by MDM2 (left), but during stress conditions p53 is stabilized through phosphorylation to decide cell fate (right).[196]

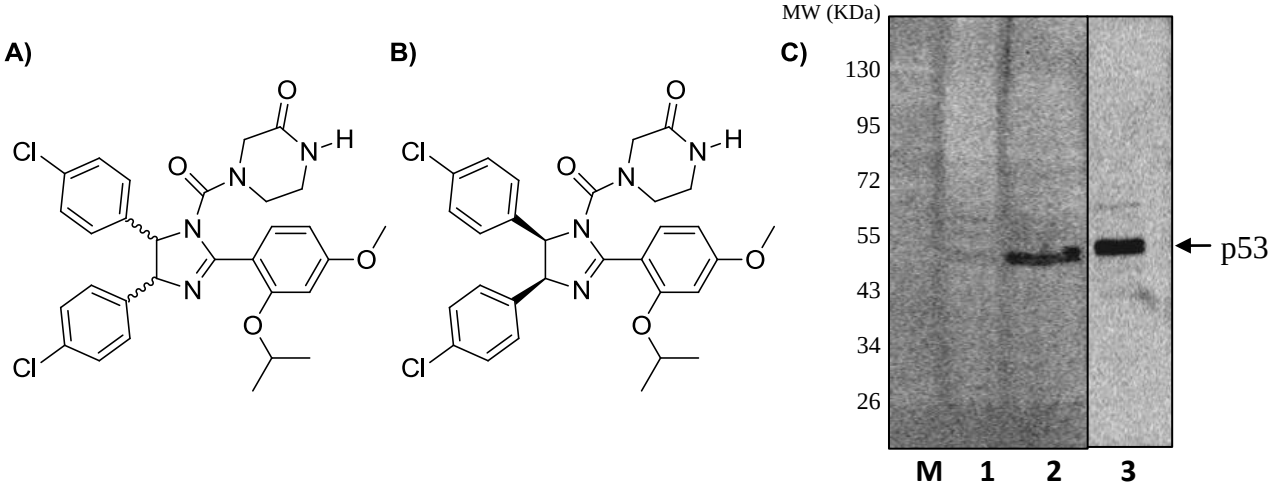

Figure 3.7: Treatment of RKO cells with (±)-Nutlin (A) Chemical structure of (±)-Nutlin-3 (B) Chemical structure of (-)-Nutlin-3, the active enantiomer (C) SDS-PAGE separation and western blot analysis with anti-p53, of lysates obtained after RKO cells were treated with (±)-Nutlin-3. The contents of each lane are molecular weight marker (M), DMSO treated control cell lysates (lane 1), 10 μM of (±)-Nutlin-3 treated cell lysates (lane 2), and 20 μM of (±)-Nutlin-3 treated cell lysates (lane 3). The expected 53 kDa p53 protein band is indicated as p53.

(±) Nutlin-3 was dissolved in DMSO solvent and supplemented to the growth media at either 10 or 20 μM concentrations overnight. Control cells were similarly treated but with DMSO alone. When RKO cells were treated with 10 μM or 20 μM of (±)-Nutlin-3, p53 expression was observed (Figure 3.7C, lane 2 and 3) incontrast to DMSO treated cells (Figure 3.7 C, lane 1). Because a racemic mixture of Nutlin was used for treatment, the effective concentration of the drug is only half of the concentrations (5 μM and 10 μM respectively). Lysates obtained from cells treated with 20 μM (±)-Nutlin-3 were used for the crosslink experiments; higher concentrations of Nutlin were not used because they can induce apoptosis.[198,199] Other drugs like Doxorubicin or Etoposide have also been used to increase the p53 levels in cells, but were found to phosphorylate some of the key amino acids on p53 to signal stress conditions.[199]

3.3.3 Photocrosslinking experiments with ATP-ArN_3 and (±)-Nutlin-3 treated RKO cells lysates

Crosslinking studies were carried out with RKO lysates obtained after Nutlin treatment. ATP-ArN_3 was incubated with Nutlin treated RKO lysates under UV for 2 hrs at 30 °C. Reaction mixtures were separated on SDS-PAGE and western blot analysis with anti-p53 was used to identify p53-specific higher molecular weight crosslink bands. In the presence of ATP-ArN_3 and UV, crosslinked bands specific to P53 were observed (Figure 3.8, lane 7), but not without UV (Figure 3.8, lane 3). As a control, when treated with acid the crosslinked bands were not observed due to cleavage of the phosphoramidate bond (Figure 3.8, lane 8). The crosslinked bands observed were also not present in other controls like lysates only (Figure 3.8, lane 1), lysates only in the presence of UV (Figure 3.8, lane 5), lysates treated with ATP in the presence (Figure 3.8, lane 6) and absence (Figure 3.8, lane 2) of UV. When heat denatured lysates were incubated with ATP-ArN_3 in the presence of UV (Figure 3.8, lane 4), no crosslinked bands were observed due to loss of protein activity. When the crosslinked experiment was carried out and probed with anti-CK2, unfortunately none of the higher molecular weight bands contained CK2 (Figure 3.8, lane 7), indicating that the higher molecular weight crosslinked bands do not contain CK2. After successful demonstration of phosphorylation-dependent kinase-substrate crosslinking with the ATP-ArN_3 analog using cellular proteins *in vitro*, our next goal was to identify the kinases or phosphorylation-dependent interacting proteins of p53.

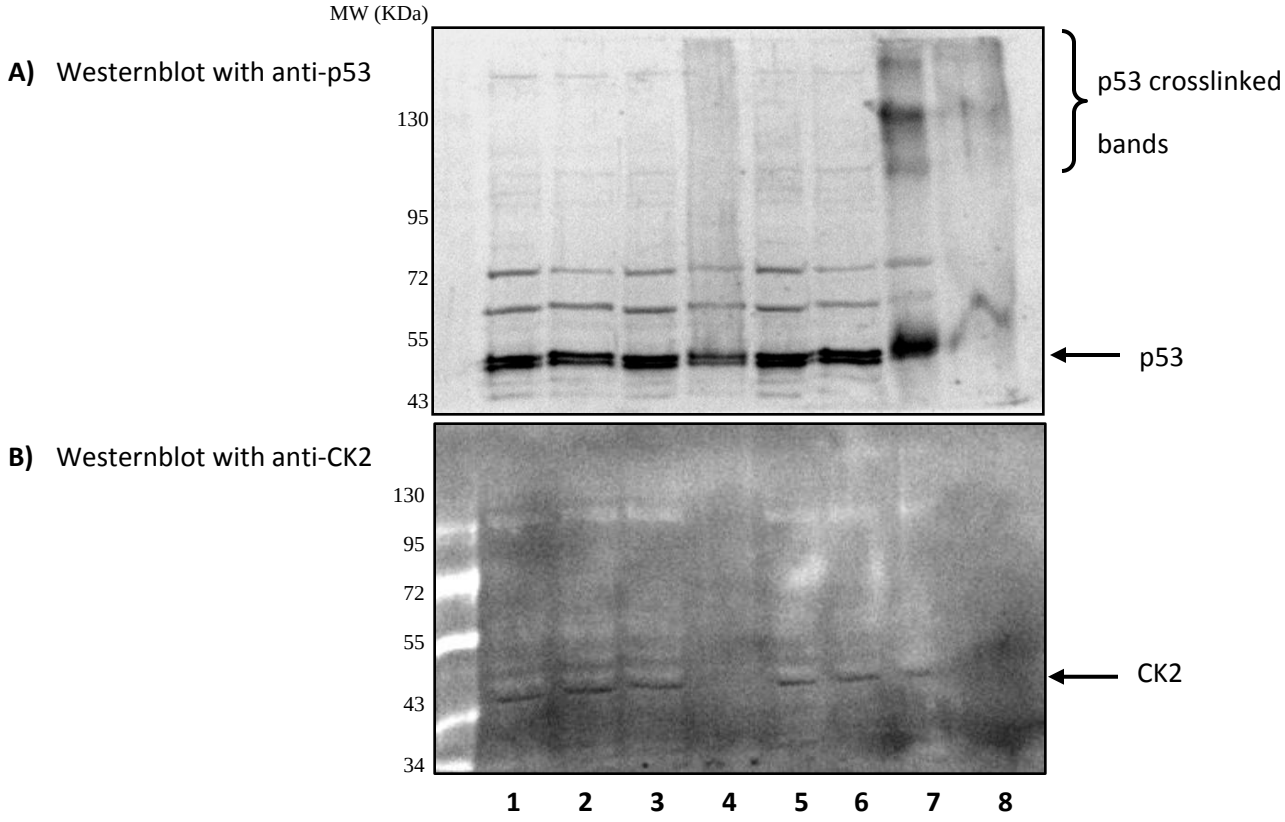

Figure 3.8: Photocrosslinking Experiment with ATP-ArN_3 and Nutlin Treated Cell Lysate. Photocrosslinking reactions were performed by incubating the reaction components under UV as indicated for each reaction, at 30 °C for 2 hrs, followed by SDS-PAGE separation and visualization with a p53 antibody (top), and CK2 antibody (bottom). An ATP-ArN_3 concentration of 10 mM (final) and 30 µg total protein from Nutlin treated RKO cell lysates were used in each reaction. As a control in lane 2, lysates were heated denatured for 5 minutes at 95 °C before the addition of ATP-ArN_3. As a control in lane 8, TFA was added to a final concentration of 50% after crosslinking to cleave the phosphoramidate band of crosslink. The high molecular weight crosslinked complex is indicated as p53 crosslinked bands, the 45 kDa band of CK2 kinase as CK2 and the 53 kDa band of p53 protein as p53. Additional trials are shown in Appendix B, Figure A3.2.

3.4 Experiments to validate phosphorylation of p53 by DNA-PK kinase

DNA-protein kinase (DNA-PK) belongs to a family of phosphatidylinositol 3-kinase-like (PI3K) protein kinases. DNA-PK's are well known for their role in V(D)J recombination for antibody diversity and normal immune development.[200,201] Recent studies show that DNA-PK is involved in p53 posttranslational modification in the ATM/ATR mediated pathway, controlling the cell fate in response to severe DNA damage.[202-204] A more recent study indicates that DNA-PK forms a complex with p53 and is recruited to the p21 promoter. This complex formation abrogates p21 transcription, inhibiting the cell cycle arrest pathway and triggering an apoptotic response to DNA damage.[205]

To identify if DNA-PK is one of the kinases of p53 in the crosslinked complex, crosslinking experiments were carried out as above, but with western blot analysis using p53 and DNA-PK antibodies (Figure 3.9). A higher molecular weight crosslinked band recognized by the p53 antibody was observed only in the presence of UV (Figure 3.9A, lane 7). The p53 crosslinked complex was not observed with ATP-ArN_3 in the absence of UV (Figure 3.10A, lane 3); or with ATP in the presence (Figure 3.10A, lane 6), or in the absence (Figure 3.10A, lane 2) of UV; or with ATP-ArN_3 and heat denatured lysates, in presence of UV (Figure 3.10A, lane 4). Absence of crosslinked bands in these controls implies that the crosslink is p53 specific in a UV and ATP-ArN_3-dependent manner.

When probed for the presence of DNA-PK in the p53 crosslink complex (Figure 3.9B), a higher molecular weight band reactive to the DNA-PK antibody was observed (Figure 3.9B, lane 7), but not observed in the absence of UV (Figure 3.9B, lane 3) or other controls (Figure 3.9B, lanes 1, 2, 5, 6, and 8). Heat denatured lysates with UV and ATP-ArN_3 also showed a higher molecular weight band (Figure 3.9B, lane 4) similar to the reaction lane (Figure 3.9B, lane 7).

Perhaps this can be attributed to ineffective heat inactivation of DNA-PK kinase activity. To overcome this challenge, lysates can be treated with kinase inhibitor Staurosporine, followed by incubating with ATP-ArN_3 under UV, which might result in loss of undesired crosslinking. Further studies with kinase inhibitor treatment will validate DNA-PK as one of the kinases in the crosslinked complex. In fact, when crosslinking was carried out with Staurosporine treated lysates, we observed a loss in higher molecular weight band (Appendix B, Figure A3.3, lane 4). Our, next goal was to validate some of the known kinases of p53 from the literature and the novel kinases identified in our MS analysis.

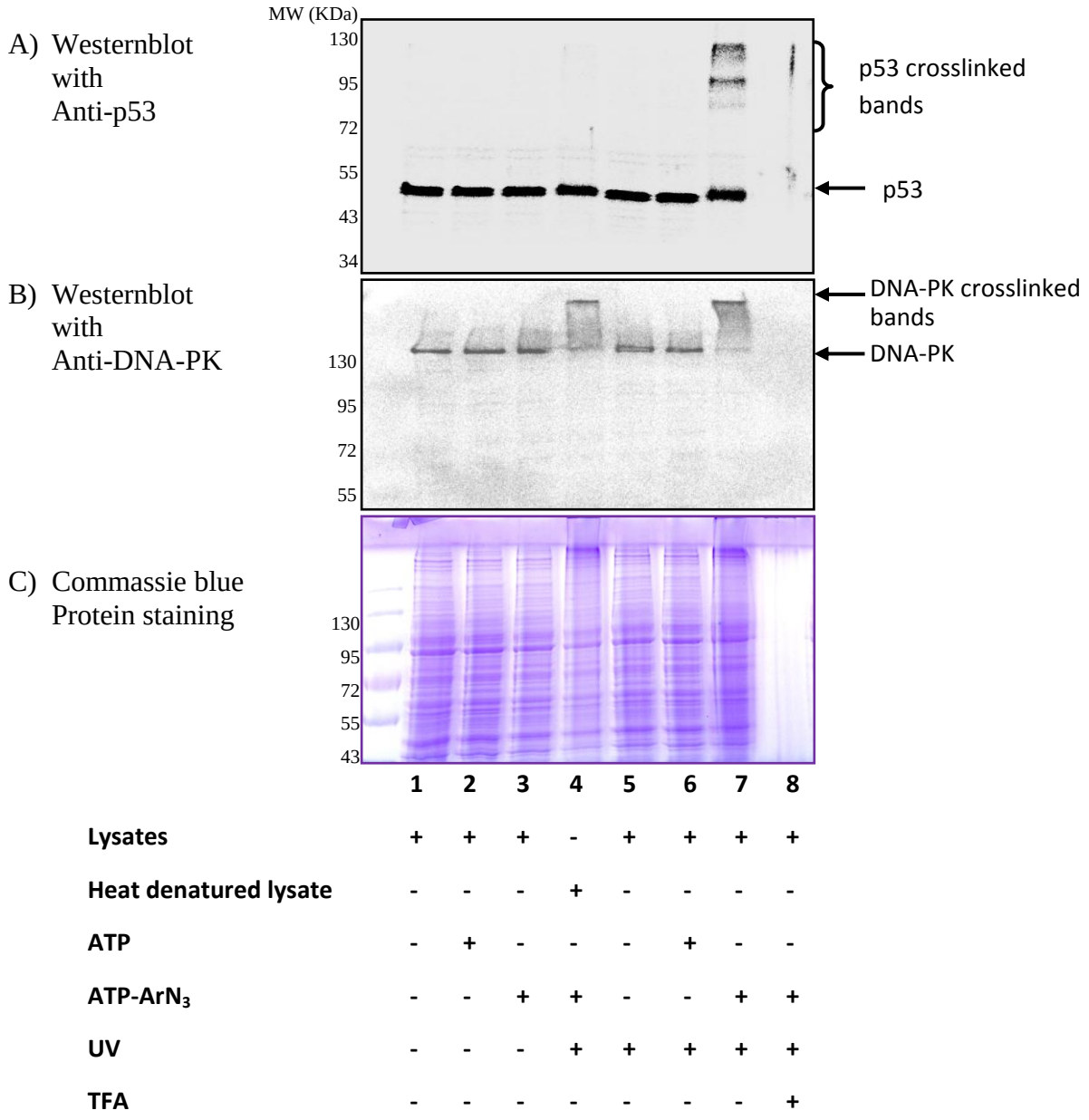

Figure 3.9: Photocrosslinking Experiments to validate Phosphorylation of p53 by DNA-PK kinase. The photocrosslinking reaction was performed by incubating the reaction components under UV as indicated for each reaction at 30 °C for 2 hrs, followed by SDS-PAGE separation and visualization with a p53 antibody (A), DNA-PK antibody (B), and Commassie blue staining (C). ATP-ArN_3 (10 mM) and 30 µg total proteins from Nutlin treated RKO cell lysates were used in each reaction. Lysates were heat denatured before the addition of ATP-ArN_3 for 5 minutes at 95 °C. TFA added to a final concentration of 50% after crosslinking to cleave the phosphoramidate band of crosslink. The high molecular weight crosslinked complex is indicated as p53 crosslinked bands, 53 kDa band of p53 protein as p53, DNA-PK protein band as DNA-PK, and the DNA-PK complex as DNA-PK crosslinked bands. Additional trials are in Appendix B, Figure A3.3.

3.5 Experiments to validate phosphorylation of p53 by FNK kinase

FNK kinase is a serine/threonine protein kinase and is a member of the polo-like kinase 3 (PLK3) family. PLK3 kinases are involved in cell cycle regulation and FNK is involved during the entry of cells into the cell cycle and during mitosis of cycling cells.[206] PLK3/FNK is known to phosphorylate p53 at serine 20 under oxidative stress conditions.[207,208] Since, FNK/PLK3 kinase is known to phosphorylate p53 experiments were carried out to investigate the presence of FNK kinase in the observed crosslinked bands.

Crosslinking experiments were carried out using optimized conditions as above, but using a western blot analysis with p53 and FNK antibody (Figure 3.10). Higher molecular weight complexes containing p53 were observed only in the presence of ATP-ArN_3 and UV (Figure 3.10A, lane 4) and not in the presence of ATP and UV (Figure 3.10A, lane 3). Crosslinked bands were not observed in the presence of UV with lysates (Figure 3.10A, lane 2), or with lysates in the absence of UV (Figure 3.10A, lane 1).

When probed for the presence of FNK in the p53 crosslinked complex, no FNK antibody reactive bands were observed (Figure 3.10B, lane 4). But in the crosslink reaction lane 4, there was a slight shift observed in the FNK band and with less intensity compared to controls (Figure 3.10B, lane 1, 2, and 3). Few possibilities for the lack of presence of FNK reactive band in the crosslinked complex are phosphorylation status of FNK[206] or the FNK-p53 crosslink was so minimal that could not be observed in the western blot or FNK is not a kinase of p53 under the reaction conditions. Therefore, these data clearly demonstrated the utility of ATP-ArN_3 analog as well as pointing towards the use of analytical techniques to unambiguously identify the protein partners. As a result, MS based crosslinking approach was used in identifying novel kinases or substrates of p53 protein, which is discussed next in this study.

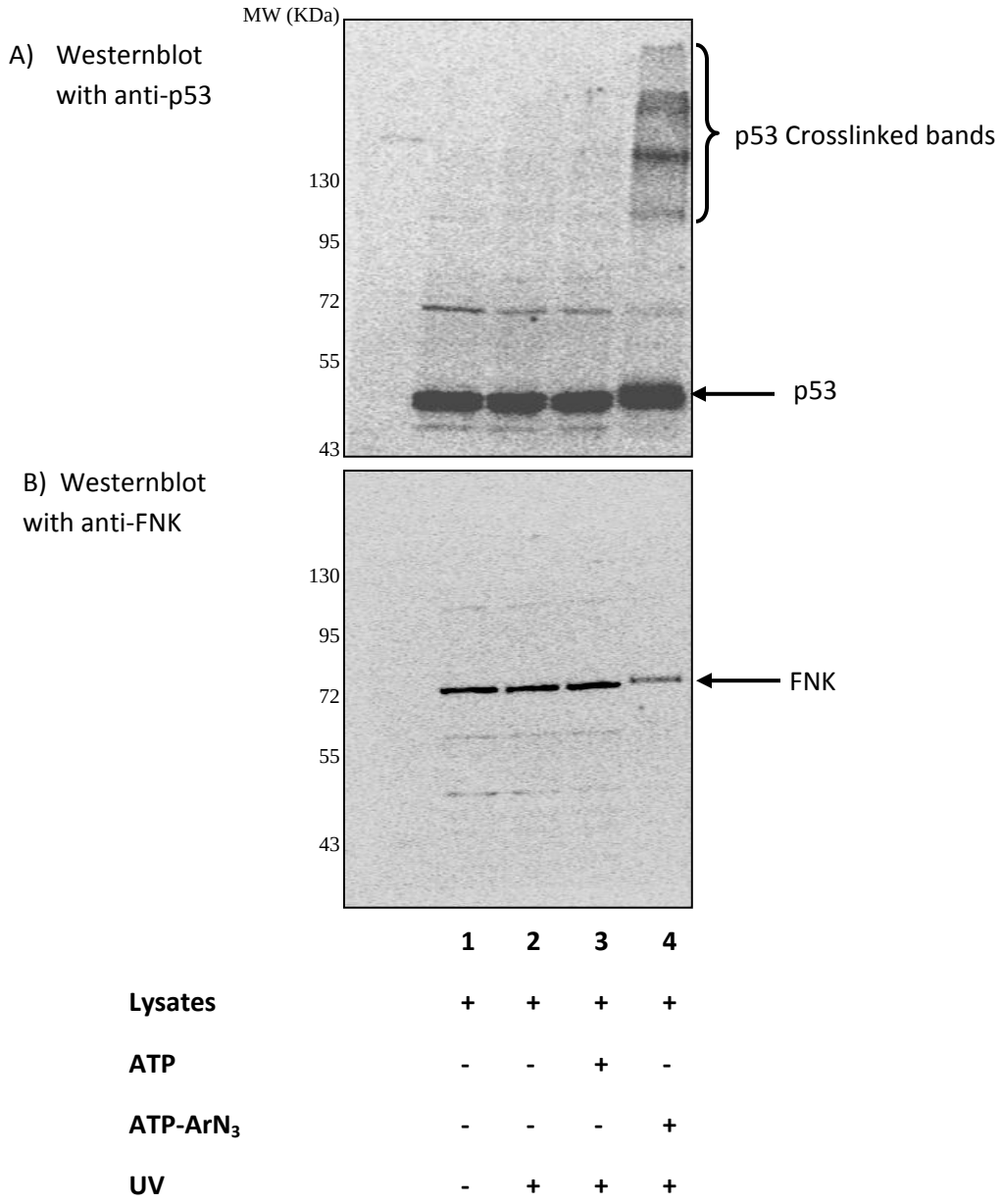

Figure 3.10: Photocrosslinking Experiments to Validate Phosphorylation of p53 by FNK Kinase. A Photocrosslinking reaction was performed by incubating the reaction components under UV as indicated for each reaction at 30 °C for 2 hrs, followed by SDS-PAGE separation and visualization with a p53 antibody (A) and an FNK antibody (B). ATP-ArN_3 (10 mM) and 30 µg total protein from Nutlin treated RKO cell lysates were used in each reaction. The high molecular weight crosslinked complex is indicated as p53 crosslinked bands, 53 kDa band of p53 protein as p53, FNK protein band as FNK.

3.6 Mass Spectrometry (MS) Coupled with Crosslinking Approach

3.6.1 Immunoprecipitation of p53 crosslinked complex

To identify the kinases in the p53 crosslinked complex in the earlier experiments, antibodies of some of the known kinases were used. However it is tedious and expensive to check the elaborate list of known kinases of p53 in the crosslinked complex using antibodies. To overcome this challenge, we sought to MS based crosslinking approach. Wherein the crosslinked complex has to be purified from the complex mixture of proteins, separated by SDS-PAGE, and processed to identify the proteins through mass spectrometry analysis. In general, an affinity purification method like immunoprecipitation (IP) is used to purify protein complexes of interest from complex cellular mixture. IP of p53 crosslinked complex was performed using mouse monoclonal and rabbit polyclonal antibodies because each of the antibodies recognizes different epitopes on the antigen. These epitopes on the antigen (p53) can be forbidden due to changes in structure or conformation on crosslinking or they could be blocked by the interacting protein. In order to identify all the possible crosslinked and interacting proteins of p53, IP was performed with two antibodies. Photocrosslinking was carried out with ATP-ArN_3, and Nutlin treated RKO cell lysates under UV for 2 hours at 30 °C. This reaction mixture, containing p53-crosslinked complexes was immunoprecipitated using A/G agarose beads and the p53 full length antibody from either rabbit or mouse. p53 immunoprecipitates from both crosslinked and uncrosslinked lysates were separated by SDS-PAGE before visualization by SyproRuby staining and western blot analysis with anti-p53 (Figure 3.11). As seen in figure 3.11A, several new bands were observed with crosslinking (lanes 4 and 8) compared to the IP of lysates incubated with ATP (lanes 3 and 7) and IP of lysates (lanes 2 and 6). In the western blot analysis, (Figure 3.11B) there were also a few specific bands present in the crosslinked lanes (Figure 3.11B, lanes 4, and

8) compared to the ATP control (Figure 3.11B, lanes 3, 7). Gradient SDS-PAGE (4-12%) gels[209] were made and used in this experiment for better resolution and migration of the crosslinked complexes. The next goal was to identify the p53 protein partners in the crosslinked complex using mass spectrometry.

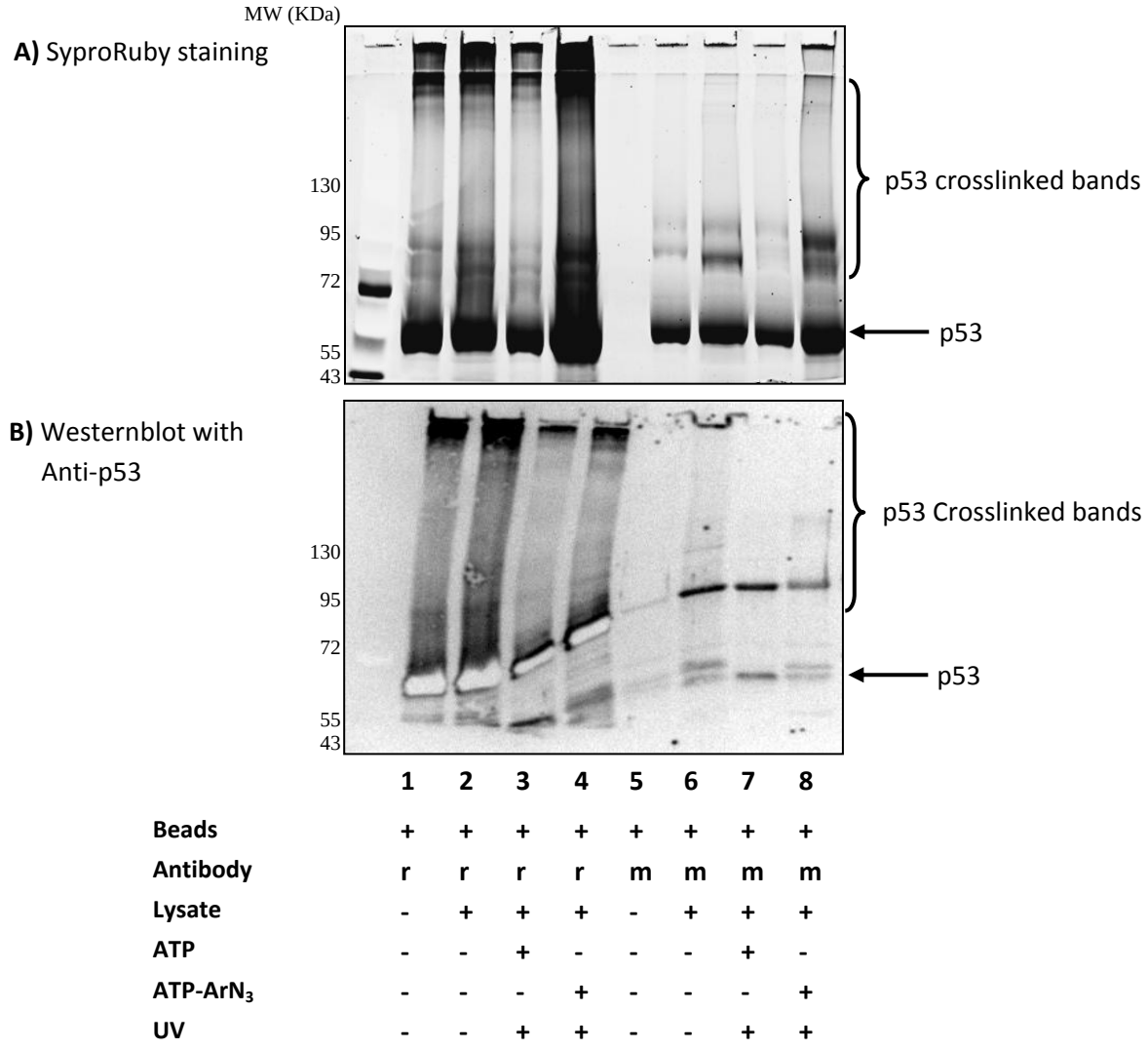

Figure 3.11: Immunoprecipitation (IP) of p53-Crosslinked Complexes

Photocrosslinking reactions were performed by incubating the reaction components under UV as indicated for each reaction, at 30 °C for 2 hrs, followed by immunoprecipitation with p53 antibody (rabbit polyclonal (r) or mouse monoclonal (m)) and SDS-PAGE separation and visualization with SyproRuby protein staining (top), and p53 antibody (1^0-rabbit polyclonal and 2^0 anti-rabbit HRP, bottom). ATP-ArN_3 (10 mM) and 30 µg total protein from Nutlin treated RKO cell lysates were used in each reaction. The high molecular weight crosslinked complex is indicated as p53 crosslinked bands, the 53 kDa band of p53 protein as p53.

3.6.2. Mass Spectrometry Analysis of p53 crosslinked complexes

Mass spectrometric studies were done in collaboration with my colleague Todd Faner. The SyproRuby stained gel (Figure 3.11A) was used for mass spectrometry studies where each lane (lanes 3 and 4; 7 and 8, Figure 3.11A) was cut into 1mm slices above the 50 kDa band, with equal and precise markings in all lanes. In-gel digestion and trypsinization was performed to extract peptide fragments of the proteins from the gel slices. The peptide mixture was separated on a nanoflow HPLC instrument and analyzed by MS analysis. The 12 most abundant ions from each injection were further fragmented using high energy collisional dissociation (HCD). The raw data was analyzed using the Proteome Discoverer and Mascot search algorithm programs. The peptide fragments identified were mapped to human protein sequence databases with strict parameters. The proteins identified from mass spectrometric analysis from both crosslinked and uncrosslinked lysates were tabulated. After removing proteins found in uncrosslinked lysates from crosslinked lysates, 5 kinases and more than 200 associated proteins unique to the crosslinked lysates were found from Q Exactive mass spectrometric analysis (Table 3.2 and Appendix B, Tables A3.1, A3.2).

The kinases and proteins were identified with high confidence and probability (Table 3.2). In addition, the kinases identified were observed in the high molecular weight gel slices unique to the crosslinked lanes (Appendix B, Table A3.2). Of the identified kinases in MS analysis, DNA-dependent protein kinase (DNA-PK),[202-204] Interferon-induced double-stranded RNA-activated protein kinase (EIF2AK2)[210] are known to phosphorylate p53. Interestingly, Serine/threonine-protein kinase MRCK beta (MRCKβ), SRSF protein kinase 1 (SRSF1), and Cyclin-dependent kinase 12 (CDK12) are novel kinases of p53 newly identified with this crosslinking approach. These experiments provide conditions for characterizing p53 associated

proteins as well as identification of endogenous kinases and substrates of interest. Previously, DNA-PK was identified as one of the kinase in the p53-crosslinked complex (Section 3.5) with westernblot analysis, the same was true from MS analysis. In addition, FNK kinase was not identified as the kinase in the p53-crosslinked complex (Section 3.6) either with westernblot analysis or with MS analysis. These two kinases highlight the consistent results observed both with westernblot and MS analysis. Therefore these photocrosslinking analogs can be successfully used to identify novel kinases of a substrate or *vice versa* and can play a role in elucidating signaling pathways. Next step was to validate few of the kinases and interacting proteins of p53 identified in this study.

Table 3.2: List of kinases identified with Q Exactive mass spectrometry analysis

No	**Identified Proteins**	**Accession Number/ Mol. Wt**	**Gel Slice** Mol. Wt. Range	**No. of peptides identified (Probability)**			
				Crosslinked lysates		Uncrosslinked lysates	
				R-AB	**M-AB**	**R-AB**	**M-AB**
1	DNA-dependent protein kinase catalytic subunit	PRKDC_ HUMAN/ 469 kDa	>170 kDa	**6** (100%)	**47**(100%)	-	-
2	Serine/threonine-protein kinase MRCK beta	MRCKB_ HUMAN/ 194 kDa	>170 kDa	**3** (100%)	**1** (98%)	-	-
3	Interferon-induced, double-stranded RNA-activated protein kinase	E2AK2_ HUMAN/ 62 kDa	>95 kDa	**1** (99%)	**3** (100%)	-	-
4	SRSF protein kinase 1	SRPK1_ HUMAN/ 74 kDa	~130 kDa	-	**2** (100%)	-	-
5	Cyclin-dependent kinase 12	CDK12_ HUMAN/ 164 kDa	>170 kDa	-	**2** (100%)	-	-

Crosslinked and uncrosslinked lysates were immunoprecipitated using Rabbit polyclonal antibody (R-AB) and Mouse monoclonal antibody (M-AB)

3.7 Photocrosslinking experiments with ATP-BP analog and (±)-Nutlin-3 treated RKO cells lysates

ATP-ArN_3 was successfully used as a phosphorylation-dependent kinase-substrate photocrosslinker to identify the novel kinases of p53 using Nutlin treated RKO cell lysates. Previously (chapter 2), an ATP-Benzophenone (ATP-BP) photocrosslinker was successfully used in phosphorylation-dependent kinase-substrate crosslinking of CK2 kinase and casein protein. Now we want to test the applicability of this ATP-BP analog in identifying novel kinases of p53.

To test the feasibility of the ATP-BP analog, crosslinking reactions were performed similar to that of ATP-ArN_3 and along with westernblot analysis using anti-DNA-PK, anti-GAK and anti-p53. DNA-PK was chosen because it was identified in the MS analysis with ATP-ArN_3 and was also validated by westernblot. Cyclin G-associated kinase (GAK), also known as auxilin II was also chosen, because it is one of the known kinase of p53.[211,212] GAK has a molecular weight of 160 kDa. GAK plays an important role in stabilization and transcription of p53, by forming a complex with other cofactors involved in the DNA repair process.[211,212]

Western blot analysis of crosslinking experiments with p53 antibody (Figure 3.12A, C) revealed high molecular weight complexes in the presence of UV and ATP-ArN_3 (Figure 3.12A, lane 7) and ATP-BP (Figure 3.12A, lane 8). Crosslinked bands were not observed in the absence of UV with ATP (Figure 3.12A, lane 3) or ATP-ArN_3 (Figure 3.12A, lane 4), or in lysates (Figure 3.12A, lane 1, 2). ATP-BP formed higher molecular weight crosslinked bands in an ATP-BP and UV dependent approach (Figure 3.12A, lane 8).

When probed with anti-GAK for the presence of GAK kinase in the p53-crosslinked complexes, no higher molecular weight bands were observed in the case of ATP-ArN_3

photoprobe (Figure 3.12B, lane 7). When the ATP-BP photocrosslinker was used, a high molecular weight crosslinked band was observed corresponding to the p53-GAK complex (Figure 3.12B, lane 8). The high molecular weight crosslinked complex was absent in lysates control (Figure 3.12B, lane 1, 2) and in the absence of UV (Figure 3.12B, lane 3, 4, 5). Another important observation made during these experiments was that washing the PVDF membrane with PBST after overnight blocking with 5% milk resulted in non specific signals and high background. To overcome this non-specific labeling, after overnight blocking, primary antibody was added without washing the membrane.

DNA-PK reactive band was observed in the higher molecular weight p53-crosslinked complex in the case of either ATP-ArN_3 photoprobe (Figure 3.12C, lane 7) or ATP-BP photo crosslinker (Figure 3.12C, lane 8) when probed with anti-DNA-PK. But the DNA-PK band intensity was reduced with ATP-BP compared to ATP-ArN_3 photocrosslinker. The higher molecular weight complex was absent in lysates (Figure 3.12C, lane 1, 2) and in the absence of UV (Figure 3.12C, lane 3, 4, 5). Therefore the ATP-BP analog was successfully used to demonstrate phosphorylation-dependent kinase-substrate photocrosslinking using cellular proteins *in vitro*. In addition, we validated GAK kinase as one of the protein found in the p53 crosslinked complex. Future studies would include performing MS analysis of p53-crosslinked complex to identify novel kinases or phosphorylation dependent interacting proteins of p53 similarly identified using ATP-ArN_3 photocrosslinker.

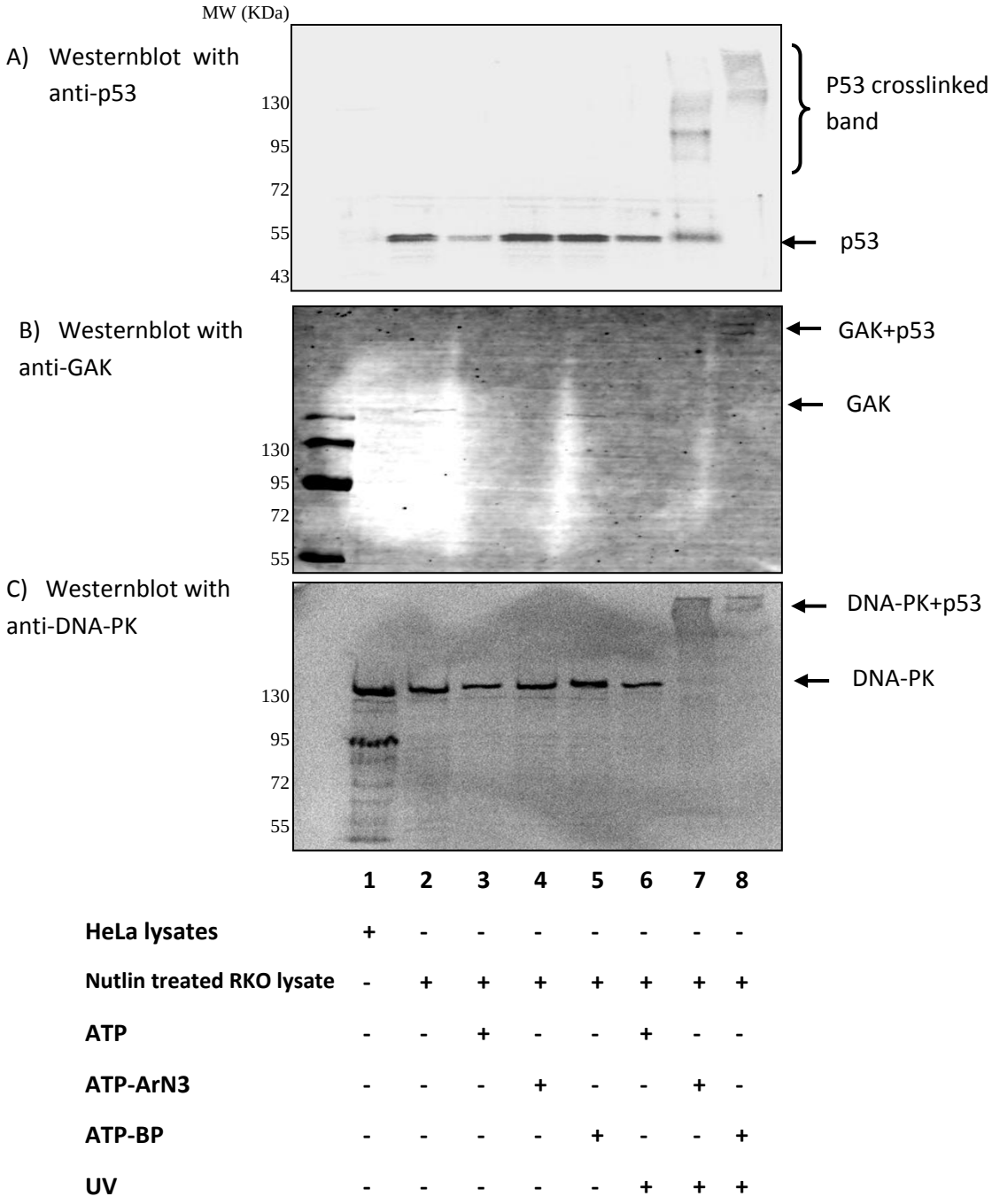

Figure 3.12: Photocrosslinking Experiments with ATP-BP and Nutlin treated RKO Cell lysates. Photocrosslinking reactions were performed by incubating the reaction components under UV as indicated for each reaction at 30 °C for 2 hrs, followed by SDS-PAGE separation and visualization with a p53 antibody (A), a GAK antibody (B), and a DNA-PK antibody (C). ATP-ArN_3, or ATP-BP analog (10 mM) and 30 µg of Nutlin treated RKO cell lysates were used in each reaction. The high molecular weight crosslinked complex is indicated as p53 crosslinked bands, 53 kDa band of p53 protein as p53, DNA-PK protein band as DNA-PK ; DNA-PK and p53 crosslinked complex as DNA-PK+P53; GAK protein band as GAK; GAK and p53 crosslinked complex as GAK+P53.

3.8 Conclusions and Future directions

In conclusion, ATP-ArN_3 was successfully used in photocrosslinking CK2 kinase and casein substrate in the presence of cell lysates. Further studies demonstrated that photocrosslinking with low concentration of ATP-ArN_3 for 2 hours yielded comparable crosslinking. With optimized crosslinking conditions in the presence of cell lysates, ATP-ArN_3 was successfully used to identify novel and known kinases of p53. Some of the interacting proteins of p53 were also identified using MS analysis. DNA-PK and GAK were validated as the kinases of p53 using ATP-ArN_3 and ATP-BP photocrosslinkers. The novel kinases identified in this study were MRCKβ, SRSF1 and CDK12. MRCKβ kinase plays a role in cytoskeleton organization and during mitosis.[213,214] p53 is known to be involved in the mitosis process,[215,216] but there is no known mechanism through which p53 and MRCKβ interact. In future, experiments will be performed on establishing the role of p53 and MRCKβ in the cellular function and cytoskeleton organization. Performing *in vitro* phosphorylation studies and establishing kinase-substrate relationship will be the first step in validating MRCKβ, CDK12, and SRSF1 as kinases of p53, further studies will be carried out to establish their role in cellular processes (Figure 3.13).

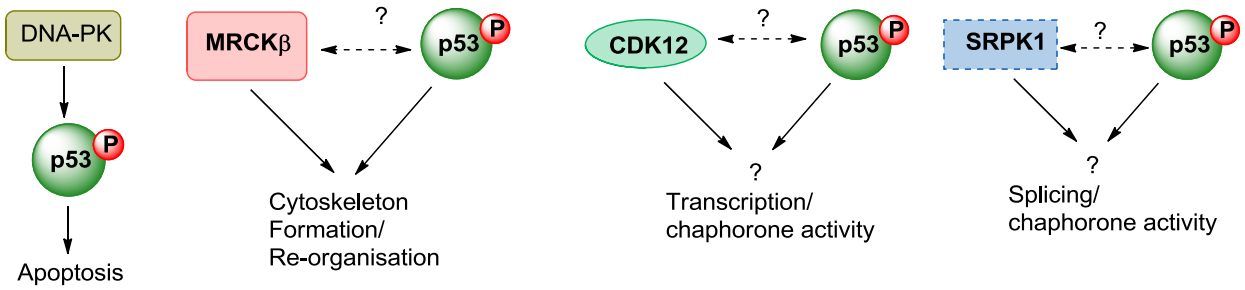

Figure 3.13: Cartoon Depicting the Possible Cellular Roles of Kinases (Identified in MS analysis) and p53

Developing next generation of ATP analogs such as affinity based crosslinking reagents and acid stable ATP analogs, will be helpful in the identification of kinase-substrate pairs as well as the site of crosslink. Specifically, these modified γ-phosphate ATP analogs require phosphorylation for crosslinking, in contrast to other kinase-substrate crosslinking approaches. Because these modified ATP analogs participate in phosphorylation, the crosslink will contain both kinase and substrate. One powerful feature of this methodology is that we can obtain an atomic level snapshot of the interactions between proteins, when coupled with analytical techniques like Mass Spectrometry (MS). These tools will help us in validating our understanding of protein-protein interactions, their role in signaling pathways and functioning of the cell.

3.9 Experimental

3.9.1 Materials

Cell culture grade dimethylsulfoxide (DMSO) was purchased from ATCC. The disodium salt of Adenosine 5'-triphosphate (ATP.2Na), glycerol, sodium hydroxide (NaOH), potassium chloride (KCl), magnesium chloride ($MgCl_2$), sodium chloride (NaCl), sodium dodecyl sulfate (SDS), and glacial acetic acid were purchased from Fisher. Ammonium bicarbonate, α-casein, tris(2-carboxyethyl) phosphine HCl (TCEP), iodoacetamide, and proteomics grade trypsin were bought from Sigma. CK2 was purchased from New England Biolabs. Triton X-100 was purchased from Fluka. Coomassie Brilliant Blue was obtained from NuSep. Trifluoroacetic acid (TFA) and Immobilion-P PVDF membrane were purchased from Millipore. SyproRuby stain was obtained from Invitrogen. Eagle's minimum essential medium (EMEM) (30-2003) and RKO cell culture sample (CRL-2577) were purchased from ATCC. Acrylamide/Bis acrylamide solution (40%, 37.5:1) was purchased from Bio-Rad. Proteomics grade formic acid was purchased from Proteochem. Anti-p53 (Rabbit) polyclonal antibody (SC-6243), anti-p53 (Mouse) monoclonal antibody (SC-55476), and protein A/G-PLUS agarose beads (SC-2003) were purchased from Santa Cruz Biotechnology Inc. Anti-DNA-PK antibody (4602P) and Anti-rabbit IgG HRP-linked secondary antibody (7074) were purchased from Cell Signaling Technology. Fetal bovine serum (FBS), antibiotic-antimycotic (100X), TrypLE™ Express (1X) with Phenol Red and Alexa Fluor® 647 Goat Anti-Rabbit IgG (H+L) (A-21244) were purchased from Life Technologies. Goat anti-mouse IgG (H+L) (HRP) (ab97040) secondary antibody was purchased from Abcam. Goat anti-mouse HiLyte Fluor™ 647-labeled secondary antibody was purchased from Anaspec. A free sample of anti-FNK antibody (GTX111495) was obtained from Genetex Inc. A free

sample of Anti-GAK antibody (H00002580-B01P) was obtained from Abnova. (±) Nutlin-3 was purchased from Cayman Chemicals.

3.9.2 Instrumentation

A SPD131 DDA ThermoSavant speedvac was used to evaporate solvents *in vacuo*. SDS-PAGE apparatus was purchased from BioRad (Protean III) and a mini-gel setup was used. Western blotting was carried out using the mini-transblot electrophoretic transfer Cell apparatus from Bio-Rad. Western blot and SDS-PAGE gel images were visualized using a Typhoon 9210 scanner (Amersham Biosciences).

3.9.3 Procedure for crosslinking of CK2 kinase and casein in the presence of cell lysates

The order of addition is important in crosslinking. The order used was water, CK2 buffer, CK2 kinase, ATP analog or ATP, followed by cell lysates or casein. Briefly, CK2 kinase (5 units/μL) was incubated with ATP-BP (10 mM) or ATP (10 mM) or ATP-ArN_3 (10 mM) in CK2 buffer (20 mM HEPES, 50 mM KCl, 10 mM $MgCl_2$, pH 7.2-7.5) for 5 minutes on ice, followed by the addition of α-casein (100 μM) and Jurkat cell lysates (10 μg total protein). The final reaction volume was 20 μL. Equal concentrations of ATP-analog and ATP were added for a competitive reaction control. The reaction mixtures were incubated for 2 hrs at 30 °C. Crosslinked protein was obtained by simultaneously irradiating the appropriate reaction tubes with a handheld UV lamp (365 nm). The presence of the phosphoramidate bond in the crosslinked product was confirmed by acid-mediated cleavage of the complex by adding 20 μL trifluoroacetic acid (TFA) to the reaction mixture (final concentration of 50% TFA) and incubating at 30 °C for 1 hour. The sample tube containing TFA was neutralized using 100 mM Tris base (50 μL) and the volume was reduced *in vacuo*. The reaction products were separated by SDS-PAGE and the proteins

were visualized with coomassie blue stain (Section 3.9.7) or SyproRuby stain (Section 3.9.8) or western blotting with an anti-CK2 antibody after electrotransfer onto PVDF membrane (Immobilon-P^{SQ}).

3.9.4 Procedure for crosslinking using ATP-Analog and RKO cell lysates

To an eppendorf tube containing the required amount of water, was added 2 µL CK2 buffer (20 mM HEPES, 50 mM KCl, 10 mM $MgCl_2$), 1 µL JLB buffer without protease inhibitor (50 mM HEPES, pH 8.0, 150 mM NaCl, 10% glycerol, 0.5% Triton X-100), 1 µL HEPES buffer (0.1 M), followed by addition of RKO cell lysates or Nutlin treated RKO cell lysates (30 µg total protein). Next, ATP-ArN_3 (10 mM), ATP-BP (10 mM) or ATP (10 mM) was added and the reaction mixture was incubated on ice for 3-5 minutes covered with aluminum foil. The reaction mixtures were incubated for 2 hrs at 30 °C. Crosslinked protein was obtained by simultaneously irradiating the appropriate reaction tubes with a handheld UV lamp (365 nm). The presence of the phosphoramidate bond in the crosslinked product was confirmed by acid-mediated cleavage of the complex by adding 20 µL trifluoroacetic acid (TFA) to the reaction mixture (final concentration: 50% TFA) and incubating at 30 °C for 1 hour. The sample tube containing TFA was neutralized using 100 mM Tris base (50 µL) and the volume was reduced *in vacuo*. The reaction products were separated by SDS-PAGE and the proteins were visualized with coomassie blue stain (Section 3.9.7) or SyproRuby stain (Section 3.9.8) or western blotting with an antibody after electrotransfer onto PVDF membrane (Immobilon-P^{SQ}).

3.9.5 Sodium Dodecyl Sulfate-Polyacrylamide Gel Electrophoresis (SDS-PAGE)

Refer to chapter 2, section 2.9.7.

3.9.6 Western Blotting

Refer to chapter 2, section 2.9.8.

3.9.7 Coomassie Blue Staining

Refer to chapter 2, section 2.9.9.

3.9.8 SyproRuby Staining

The SDS-PAGE gel was gently placed into a clean container containing 50 mL fixing solution (50% methanol and 7% acetic acid in water) and incubated with gentle rocking at room temperature for 30 minutes. Fixing solution was removed and the process was repeated for another 30 min, for a total of one hour. The fixing solution was poured off and 25 to 30 mL of SyproRuby protein stain (Invitrogen) was added in the absence of light. The container was covered in aluminum foil to protect from light and incubated with gentle shaking overnight at room temperature. Sypro Ruby stain was carefully decanted and saved for later use. The saved stain can be used up to ten times. The gel was then destained to remove excess stain and reduce background. Destaining solution (10% methanol and 7% acetic acid in water) was added and the gel was incubated at room temperature for 30 minutes. The destaining solution was discarded and the gel was rinsed with distilled water for 5 minutes to remove any excess acid and to prevent corrosive damage to the instrument used for visualization. The stained gel was imaged using the Typhoon 9400 scanner at an excitation wavelength of 450 nm and an emission of 610 nm.

3.9.9 Starting a New RKO Cell Culture

RKO cells obtained from ATCC (1.0 mL, 5×10^6 cells, ATCC CRL-2577) in cryogenic vials on dry ice and were stored in a liquid nitrogen storage tank (Thermolyne) upon receipt. EMEM media was supplemented with 10% FBS, 1% antibiotic-antimycotic and filtered through 0.22 μm

pore size sterile filters. When starting a new cell culture, a frozen aliquot was removed from the liquid nitrogen tank and thawed quickly in a 37 °C water bath. The contents of the vial were then transferred to a 15 mL centrifuge tube containing 5 ml of warm EMEM media (containing FBS and antibiotic). The cryogenic vial was rinsed with 5 mL of EMEM media to recover the contents and all the solution was mixed gently in the centrifuge tube. The tube was centrifuged at 1000 rpm for 5 minutes at 25 °C. The supernatant was carefully discarded without disturbing the cell pellet and the cell pellet was resuspended in 5 mL of EMEM media (containing FBS and antibiotic) and transferred to a tissue culture flask (25 cm^2 size). The cells were cultured in a 37 °C incubator under a 5% CO_2 environment with 95% relative humidity. Cell growth was checked periodically using microscopy or by counting the cells with a hemocytometer and the cell count was maintained between 0.5-1.0 × 10^6 cells per mL.

3.9.10 Banking of RKO cells for long term use

Confluent cells (1 × 10^6 cells per mL) were trypsinized off the flask and collected by centrifugation at 1000 rpm for 5 minutes at 4 °C. Trypsinization was done using TrypLE™ Express (1X) containing trypsin-like enzyme with phenol red indicator. TrypLE™ Express (1X) (5-10 mL) was added to the flask to cover the surface and incubated at 37 °C for 10 minutes. The presence of any growth media inhibits the action of the TrypLE™ Express, so it's essential to rinse with 1XPBS prior to trypsinization. After 10 minutes, when adherent RKO cells appeared to dissociate from the flask, EMEM media (5 to 10 mL) was added to stop the action of TrypLE™ Express. The media was carefully mixed and the flask was rinsed with an additional 5 to 10 mL of media to collect all the cells. The cell pellet obtained by centrifuging 50 mL of cell culture media (50 X 10^6 cells) was washed with 1XPBS (cell culture grade, phosphate buffered

saline consisting of 137 mM NaCl, 2.7 mM KCl, 10 mM Na_2HPO_4, 2 mM KH_2PO_4, pH 7.4). Cel pellet obtained after washing with PBS was resuspended in 10 mL of fresh EMEM media with a final concentration of 10% v/v DMSO (cell culture grade) and aliquoted into cryogenic vials (Corning, 5 X 10^6 to 10 X 10^6 cells in each vial). The cells were slowly cooled in a stepwise fashion starting at -20 °C overnight and then -80 °C overnight followed by storing in a liquid nitrogen storage tank (Thermolyne).

3.9.11 Treatment of cells with (±)-Nutlin-3 and collection of cells

For (±)-Nutlin-3 treatment, 1.5 X 10^6 cells were seeded in a 75 cm^2 tissue culture flasks in 10 mL of EMEM growth medium 24 hours prior to treatment. (±)-Nutlin-3 (Cayman Chemicals, 10 mM stock solution in DMSO) was added to the media at various concentrations (10 µM, 20 µM) and incubated for 24 hours. Control cells were treated with an equivalent amount of DMSO. After 24 hours, the growth media was carefully removed and the flask was rinsed with 1X PBS and trypsinized (see section 3.10.10). The media was transferred to a conical tube and centrifuged at 1000 rpm for 5 minutes at 4 °C. The supernatant was discarded and cells were gently washed with 10 mL of cold 1X PBS. The cell pellet can be used immediately or stored at -80 °C until needed.

3.9.12 Cell lysis procedure

Frozen control or (±)-Nutlin-3-treated RKO cell pellets were thawed and kept on ice, or fresh cell pellets were used directly. Cells were resuspended in lysis buffer (200 µL; 50 mM HEPES, pH 8.0, 150 mM NaCl, 10% glycerol, 0.5% Triton X-100 and freshly added 1X protease inhibitor cocktail V). Cells were mixed in lysis buffer by pipetting several times and lysis was

achieved by mixing with rotation at 4 °C for 10 minutes. The soluble fraction was separated from the cell debris by spinning at 15,000 rpm at 4 °C for 25 minutes. The supernatant was collected without any debris into a clean epitube. The concentration of total protein in the lysate was determined using a Bradford assay[217] and the lysate was distributed into single use aliquots, which were stored at -80 °C. To preserve the activity of proteins, the entire lysis process was carried out at 4 °C on ice and as quickly as possible.

3.9.13 In-Gel Protein Digestion

For MS analysis, proteins were excised from gels and digested with trypsin. The in-gel protein digestion method was adapted from Shevchenko, A *et al.*[218] Benchtop surfaces, gloves, and tools used during in-gel digestion were washed with 70% ethanol (Decon Laboratories) prior to use to avoid contamination with keratin. The gel from SDS-PAGE (Section 3.4.4) was stained with SYPRO® Ruby (Invitrogen) and scanned on a Typhoon 9210 variable mode imager (Amersham Biosciences). The gel was stored until processing (one week) in destaining solution (7% acetic acid (Mallinckrodt Chemicals), 10% methanol (EMD) in ultrapure H_2O). Prior to band excision, the gel was washed with 10% methanol in ultrapure water twice for a minimum of 2 hours. The proteins in the gel were visualized on an FBTIV-88 ultraviolet trans-illuminator briefly to aid in the excision of the lanes-of-interest. Gel lanes were excised and cut into 8 equal slices (0.7 cm x 0.4 cm) from the 55 kDa molecular weight marker to the top of gel, using a 1.5 inch straight razor (Stanley). Slices were then cut into approximately 1 mm^3 pieces which were placed into 1.5 mL Protein LoBind tubes (Eppendorf) after rinsing the tubes with HPLC grade acetonitrile (EMD). Gel slices were washed with 1:1 (v/v) solution of 50 mM ammonium bicarbonate (Fluka Analytical) and acetonitrile for 10 minutes (100 µL of total volume). The liquid was removed

and replaced with an equal volume of acetonitrile. After 5 minutes with manual agitation as needed, gel particles turned white and stuck together. Acetonitrile was removed and replaced with 100 µL 50 mM ammonium bicarbonate for 5 minutes. Acetonitrile (100 µL) was then added and incubated for 10 minutes. All liquid was removed and replaced with neat acetonitrile (100 µL) for 5 minutes. After gel pieces shrunk and turned opaque white, acetonitrile was removed and samples were dried in a speedvac concentrator (SDP131DDA, Thermo Scientific Savant) for 10 minutes. Dried gel pieces were rehydrated and cysteine's were reduced in 100 µL reducing buffer (50 mM TCEP and 25 mM ammonium bicarbonate) at 37 °C for 20 minutes. Samples were allowed to cool on the bench for 10 minutes before removing excess reducing buffer. Alkylation was performed by adding 100 µL 100 mM iodoacetamide (Sigma) in 25 mM ammonium bicarbonate buffer to samples and incubating at room temperature in the dark for 30 minutes. Alkylation buffer was removed and gel particles were washed with 100 µL solution of 50 mM ammonium bicarbonate and acetonitrile (1:1), twice for 15 minutes each on a rocking platform. All liquid was then removed and 100 µL of acetonitrile was added and incubated for 5 minutes. After gel particles shrank and became white, the liquid was removed and particles were dried in speedvac for 10 minutes. Activated proteomics grade trypsin (Sigma) in digestion buffer (40 mM ammonium bicarbonate, 9% acetonitrile) was added to each sample in sufficient volume (75 µL) to cover the particles. Samples were kept on ice for 1 hour and additional digestion buffer was added (50 µL) to keep particles covered. Tubes were transferred to 37 °C incubator for digestion overnight. Peptide solutions were removed with gel-loading tips and transferred to new, pre-rinsed 0.5 mL Protein LoBind tubes. Peptides were further extracted from gel particles with 75 µL 0.1% (v/v) formic acid (Proteochem) in water:acetonitrile (65:35) with bath sonication for 5 minutes. After sonication, extracted peptide solutions were combined with

overnight peptide solutions and frozen at -80°C. Samples were then dried in the speedvac for 2 hours and stored at -20 °C before analysis. Dry peptides were reconstituted by solubilizing in an aqueous solution containing 5% acetonitrile, 0.1% formic acid and 0.05% trifluoroacetic acid by sonicating for 1 minute in a total volume of 20 µL.

3.9.14 Mass Spectrometric Analysis

(Analysis was performed by Todd Faner at the Proteomics core facility)

Peptides were desalted in-line and separated by reverse phase chromatography (Acclaim PepMap100 C18 pre-column, Acclaim PepMapRSLC C18 analytical column, Thermo Scientific) on a nanoflow HPLC instrument (Easy-nLC 1000, Thermo Scientific), followed by ionization with a Nanospray Flex Ion Source (Proxeon Biosystems A/S) and introduced into a Q Exactive mass spectrometer (Thermo Scientific). A linear gradient of 95% buffer A (water, 0.1% formic acid) with 5% buffer B (acetonitrile) to 90% buffer A, with 10% buffer B over 2 minutes, followed by 68% buffer A, with 32% buffer B over 30 minutes at a flow rate of 300 nL/min, was used for separation. Pumps and instrument methods were controlled with Thermo Xcalibur 2.2 SP1.48 software (Thermo).

The instrument was operated in positive mode and data was acquired using a data-dependent top 12 method. The 12 most abundant ions from the full MS scan (375-1600 m/z) were selected for fragmentation by high energy collisional dissocation (HCD). Dynamic exclusion was enabled with 12.0 s duration and precursor isolation width set to 3.0 m/z. Resolution of full MS and HCD scans was 70,000 at 375 m/z and 17,500 at 200 m/z, respectively. Normalized collision energy for HCD spectra was 30 eV and data were acquired in profile mode. Isotope exclusion, singly charged and unrecognized charged ion exclusion was enabled.

3.9.15. Peptide Spectrum Matching and Data Analysis

Analysis of raw data was performed with Proteome Discoverer 1.4.0.288 (Thermo) using the Mascot search algorithm (Matrix Science). The SwissProt_2013_04 database was used against human protein sequences and the reverse decoy protein database used to calculate false discovery rates (FDR). Secondary analysis was performed using Scaffold 4.0.5 (Proteome Software) with X! Tandem software (The Global Proteome Machine Organization) for subset database searching. Minimum protein identification probability was set to ≥99% with 2 unique peptides per protein and ≥80% minimum peptide identification probability.

Mascot and X! Tandem algorithms were searched with a precursor mass tolerance of 10 ppm and fragment mass tolerance of 0.02 Da. Target FDR was set to 0.01 (strict) and 0.05 (relaxed). Carbamidomethylation of cysteine (+57) was set as a fixed modification. Variable modifications included oxidation of methionine (+16), protein n-terminal acetylation (+42), phosphorylation on serine, threonine, and tyrosine (+80). Enzyme specificity was defined for trypsin as c-terminal to lysine and arginine with 1 missed cleavage site allowed. The parameters for the data analysis of each set of proteins obtained were mentioned in the tables, if different.

APPENDIX A

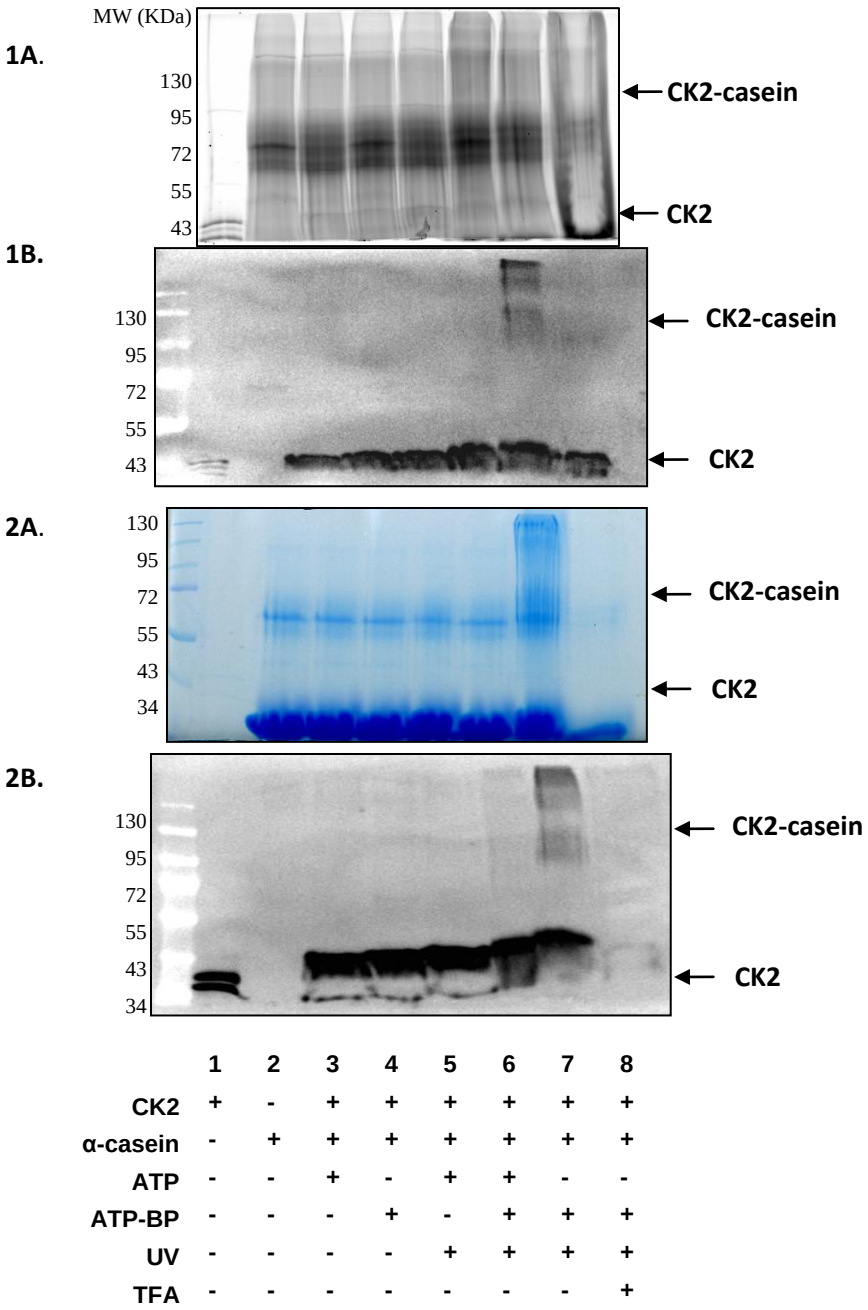

Figure A2.1: Kinase-catalyzed Photocrosslinking with ATP-BP. CK2 kinase was incubated with α-casein in the presence of ATP or ATP-BP under UV for 2 hrs at 30 °C. The resulting mixtures were separated by SDS-PAGE and visualized by coomassie blue staining (2A) or SyproRuby staining (1A) and western blotting with anti-CK2 (1B, 2B).

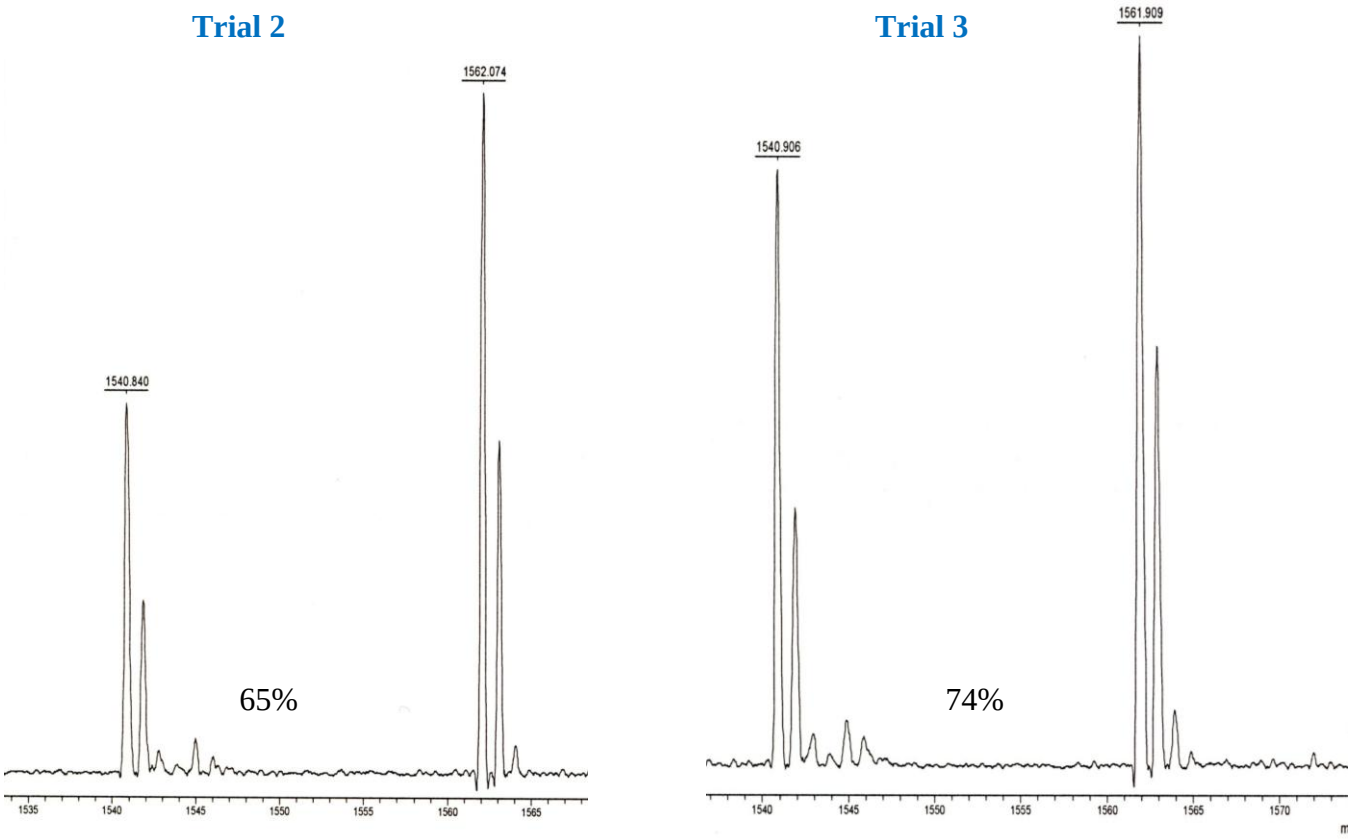

	m/z	SN	Res.	Intens.	Area	Conv%
Trial 2	1540.840	21.2	5016	55.36	18	65%
	1562.074	39.0	5803	101.99	28	
Trial 3	1540.906	42.7	5160	161.56	50	74%
	1561.909	52.3	4335	197.63	72	

Figure A2.2: Quantitative MALDI-TOF MS of peptide substrate (RRREEE**T**EEE) with CK2 kinase and either ATP **1** or ATP-BP **4.** The peak at m/z ~1541 corresponds to heptamethylated phosphopeptide after reaction with ATP-benzophenone and acidic cleavage of phosphoramide bond, while the peak at m/z ~1562 corresponds to the deuterated heptamethylated phosphopeptide after phosphorylation with ATP.

Compound Characterization:

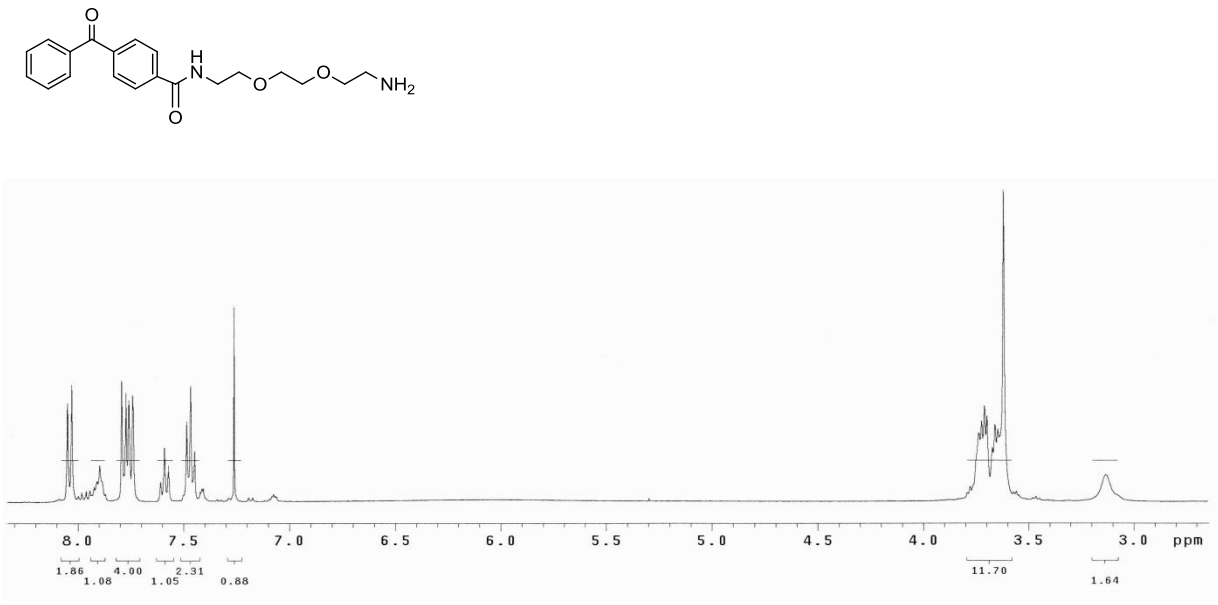

Figure A2.3: ^{1}H-NMR of compound **7** recorded in $CDCl_3$ solvent.

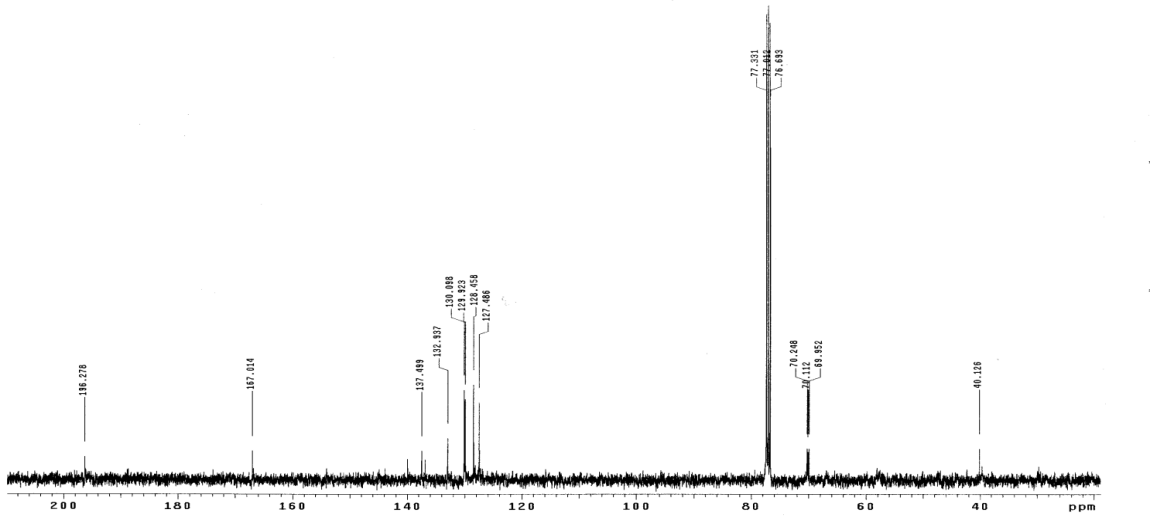

Figure A2.4: ^{13}C-NMR of compound **7** recorded in $CDCl_3$ solvent.

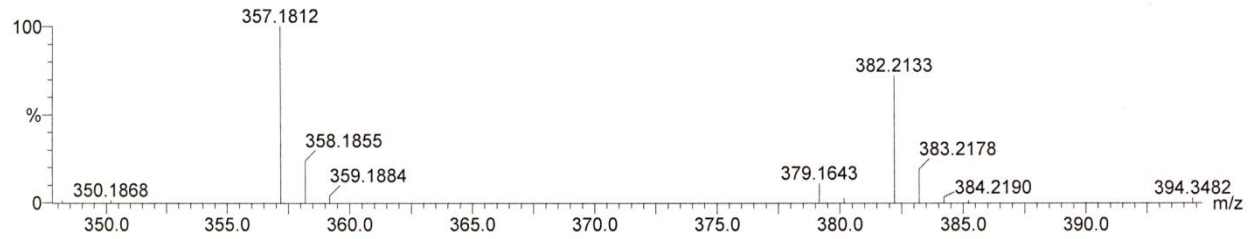

Minimum:				-1.5			
Maximum:		50.0	5.0	150.0			
Mass	Calc. Mass	mDa	PPM	DBE	i-FIT	i-FIT (Norm)	Formula
357.1812	357.1814	-0.2	-0.6	9.5	38.6	2.6	C20 H25 N2 O4
	357.1804	0.8	2.2	11.5	36.5	0.5	C19 H22 N6 23Na
	357.1822	-1.0	-2.8	-1.5	39.6	3.5	C7 H26 N8 O7 23Na
	357.1828	-1.6	-4.5	14.5	37.3	1.3	C21 H21 N6

Figure A2.5: HR-MS of compound **7** recorded with methanol solvent.

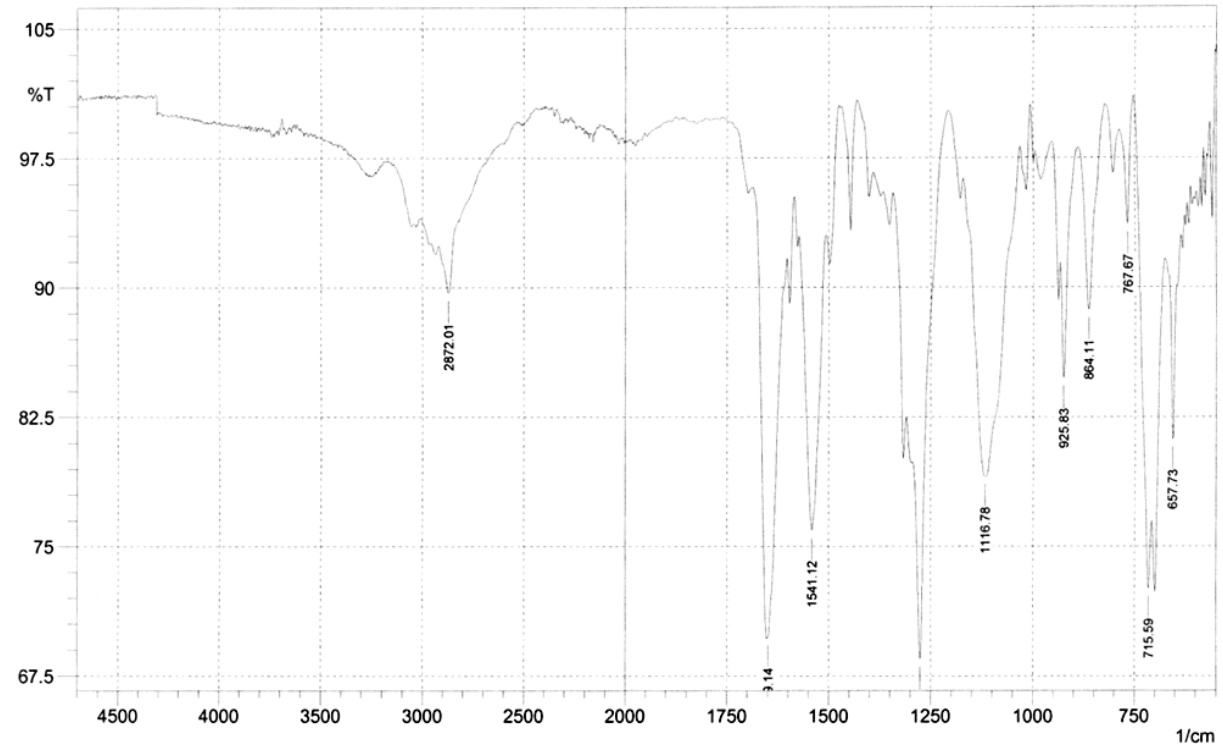

Figure A2.6: IR spectrum of compound **7**.

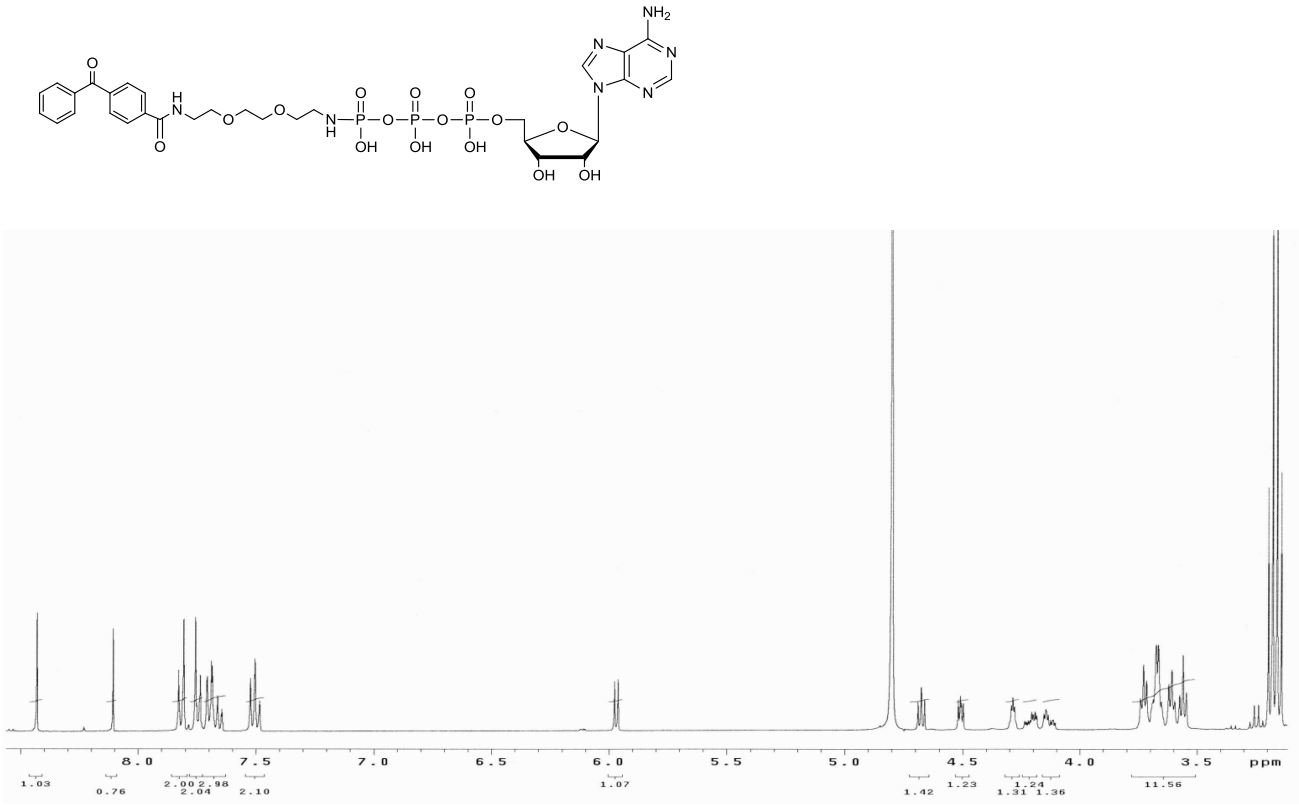

Figure A2.7: ^{1}H-NMR of ATP-BP **4** recorded in D_2O solvent.

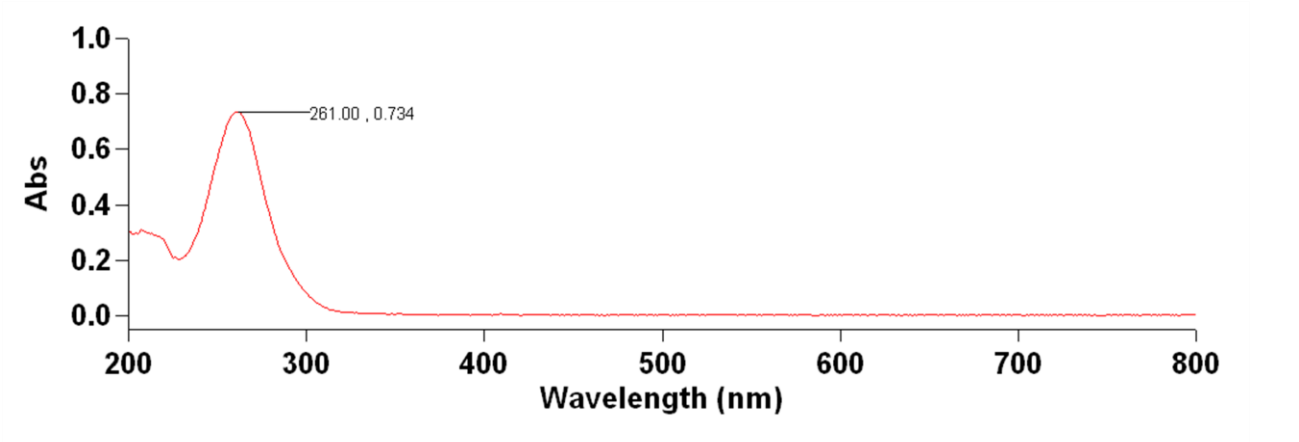

Figure A2.8: UV absorbance of ATP-BP **4**.

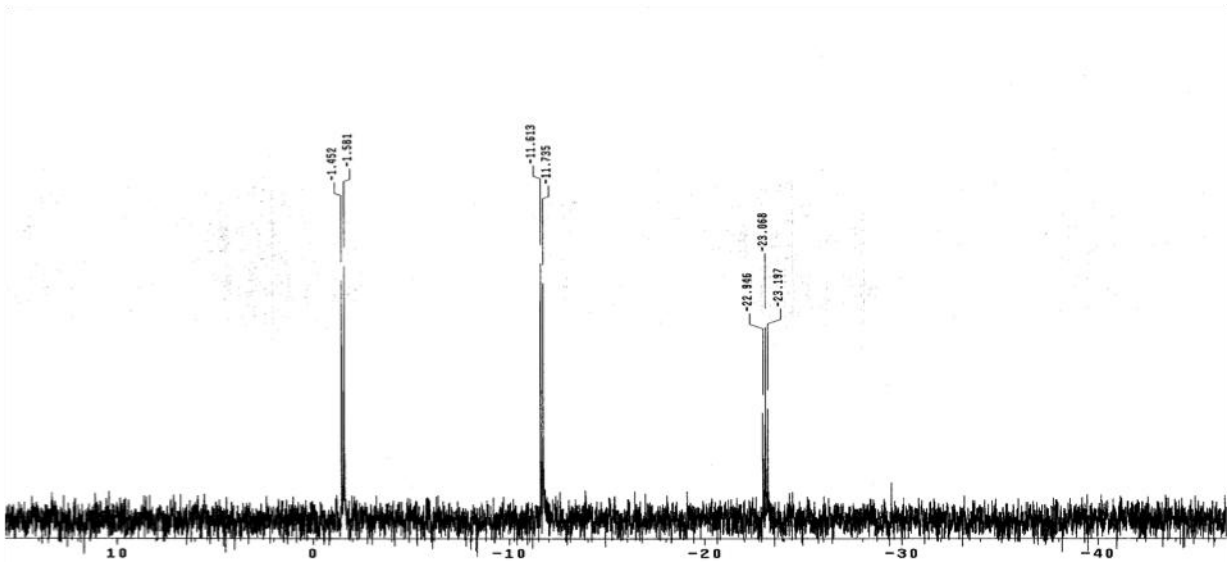

Figure A2.9: ^{31}P-NMR of ATP-benzophenone **4** recorded in D_2O solvent.

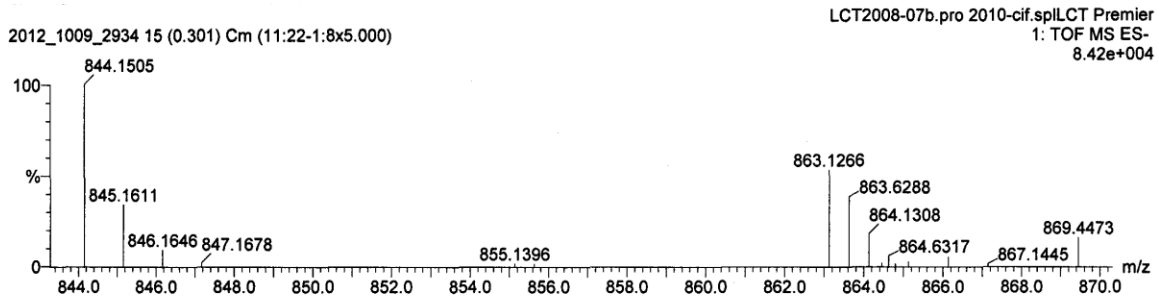

Minimum:				-1.5								
Maximum:		50.0	5.0	100.0								
Mass	Calc. Mass	mDa	PPM	DBE	i-FIT	i-FIT (Norm)	Formula					
844.1505	844.1505	0.0	0.0	35.5	53.1	3.0	C43	H29	N9	O5	P3	
	844.1507	-0.2	-0.2	31.5	53.4	3.3	C45 P3	H34	N3	O7	23Na	
	844.1510	-0.5	-0.6	17.5	52.8	2.7	C30	H37	N7	O16	P3	
	844.1512	-0.7	-0.8	13.5	53.1	2.9	C32 P3	H42	N	O18	23Na	

Figure A2.10: HR-MS of ATP-BP **4** recorded with methanol solvent.

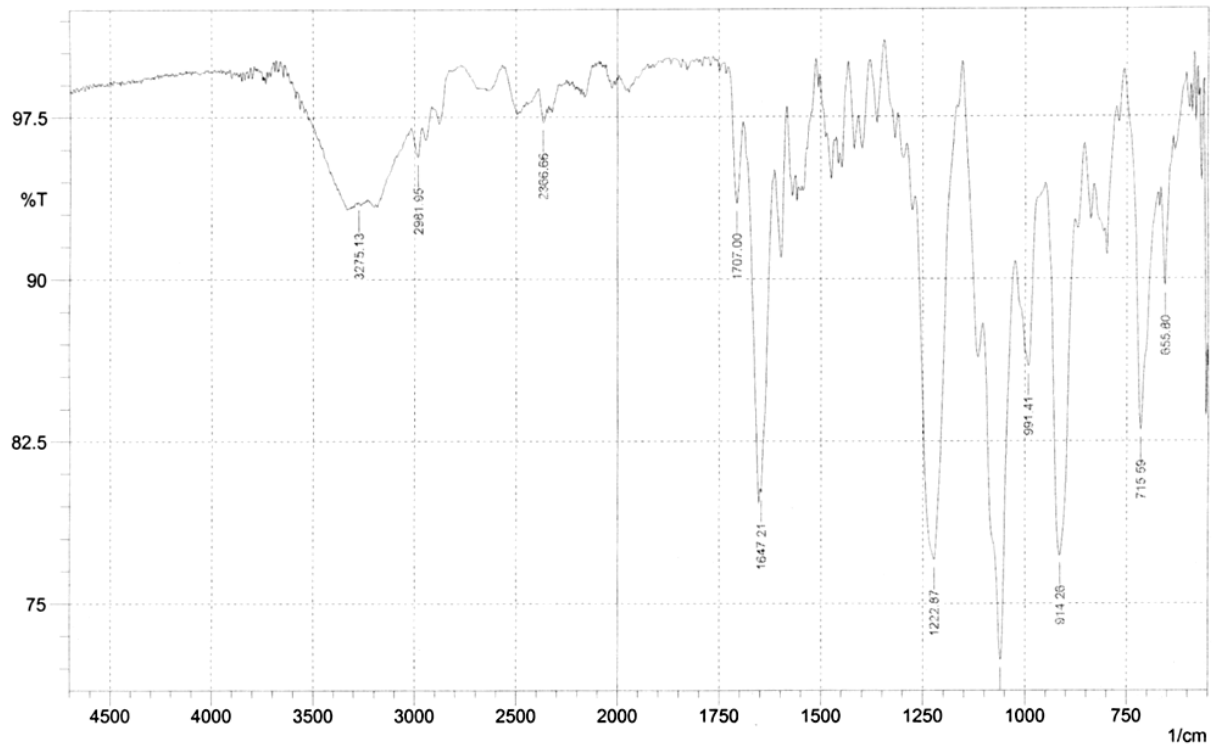

Figure A2.11: IR spectrum of compound ATP-BP **4**.

Autodock analysis:

The lowest binding energy mode that conforms to the kinase-catalyzed phosphorylation mechanism is in bold for each docking experiment. The grid box dimensions used in all the analysis were same or similar.

A) <u>CK2 kinase docking</u>

Table A2.1. The grid dimensions and output file with all the different binding modes obtained from docking of ATP-ArN_3 (2) and CK2 kinase.

center_x = 21.579 size_x = 22
center_y = 5.811 size_y = 30
center_z = 19.517 size_z = 18 exhaustiveness = 8.

mode	affinity (kcal/mol)	dist from best mode rmsd l.b.	rmsd u.b.
1	**-8.1**	**0.000**	**0.000**
2	-7.2	3.685	5.354
3	-7.2	8.785	10.991
4	-7.1	3.032	5.129
5	-7.1	4.889	7.208
6	-6.9	2.469	3.659
7	-6.9	3.559	5.621
8	-6.8	5.732	8.818
9	-6.7	10.940	13.509

Table A2.2. The grid dimensions and output file with all the different binding modes obtained from docking of ATP-DAz (3) and CK2 kinase.

center_x = 21.579 size_x = 22
center_y = 5.811 size_y = 30
center_z = 19.517 size_z = 18 exhaustiveness = 8

mode	affinity (kcal/mol)	dist from best mode rmsd l.b.	rmsd u.b.
1	-6.5	0.000	0.000
2	**-6.5**	**3.228**	**11.654**
3	-6.1	2.106	3.128
4	-5.8	4.891	12.286
5	-5.8	2.521	4.035
6	-5.7	3.274	11.896
7	-5.5	1.740	2.940
8	-5.4	2.944	5.893
9	-5.3	1.727	2.881

Table A2.3. The grid dimensions and output file with all the different binding modes obtained from docking of ATP-BP (4) and CK2 kinase.

center_x = 21.579 size_x = 22
center_y = 5.811 size_y = 30
center_z = 19.517 size_z = 18 exhaustiveness = 8

mode	affinity (kcal/mol)	dist from best mode rmsd l.b.	rmsd u.b.
1	**-7.3**	**0.000**	**0.000**
2	-7.3	4.706	11.056
3	-6.7	1.462	2.275
4	-5.3	3.205	8.800
5	-5.2	4.051	8.731
6	-5.1	4.015	8.548
7	-5.0	4.001	8.547
8	-4.9	3.656	4.845
9	-4.8	3.301	9.279

B) <u>PKA kinase docking</u>

Table A2.4. The grid dimensions and output file with all the different binding modes obtained from docking of ATP-ArN_3 (2) and PKA kinase.

center_x = 12.723 size_x = 28
center_y = 8.552 size_y = 20
center_z = 2.82 size_z = 16 exhaustiveness = 8

mode	affinity (kcal/mol)	dist from best mode rmsd l.b.	rmsd u.b.
1	-7.6	0.000	0.000
2	-7.6	2.552	4.617
3	**-7.2**	**3.196**	**15.716**
4	-7.2	2.061	3.817
5	-7.2	2.418	4.028
6	-7.2	2.202	14.849
7	-7.1	3.220	5.859
8	-7.0	2.486	4.993
9	-7.0	2.848	5.832

Table A2.5. The grid dimensions and output file with all the different binding modes obtained from docking of ATP-DAz (3) and PKA kinase.

center_x = 12.723 size_x = 28
center_y = 8.552 size_y = 20
center_z = 2.82 size_z = 16 exhaustiveness = 8

mode	affinity (kcal/mol)	dist from best mode rmsd l.b.	rmsd u.b.
1	-7.5	0.000	0.000
2	-7.3	1.233	2.256
3	**-7.2**	**2.663**	**14.449**
4	-7.2	1.440	2.310
5	-7.1	2.304	14.531
6	-6.9	2.774	4.834
7	-6.8	4.594	6.423
8	-6.8	2.376	14.876
9	-6.8	2.321	3.800

Table A2.6. The grid dimensions and output file with all the different binding modes obtained from docking of ATP-BP (4) and PKA kinase.

center_x = 12.886 size_x = 28
center_y = 8.549 size_y = 20
center_z = 2.924 size_z = 18 exhaustiveness = 8

mode	affinity (kcal/mol)	dist from best mode rmsd l.b.	rmsd u.b.
1	-10.2	0.000	0.000
2	-10.0	1.646	2.884
3	**-9.7**	**4.611**	**13.432**
4	-9.6	3.385	14.637
5	-9.6	4.480	14.024
6	-9.6	3.417	5.212
7	-9.6	3.992	6.090
8	-9.4	1.918	3.723
9	-9.2	2.214	4.154

APPENDIX B

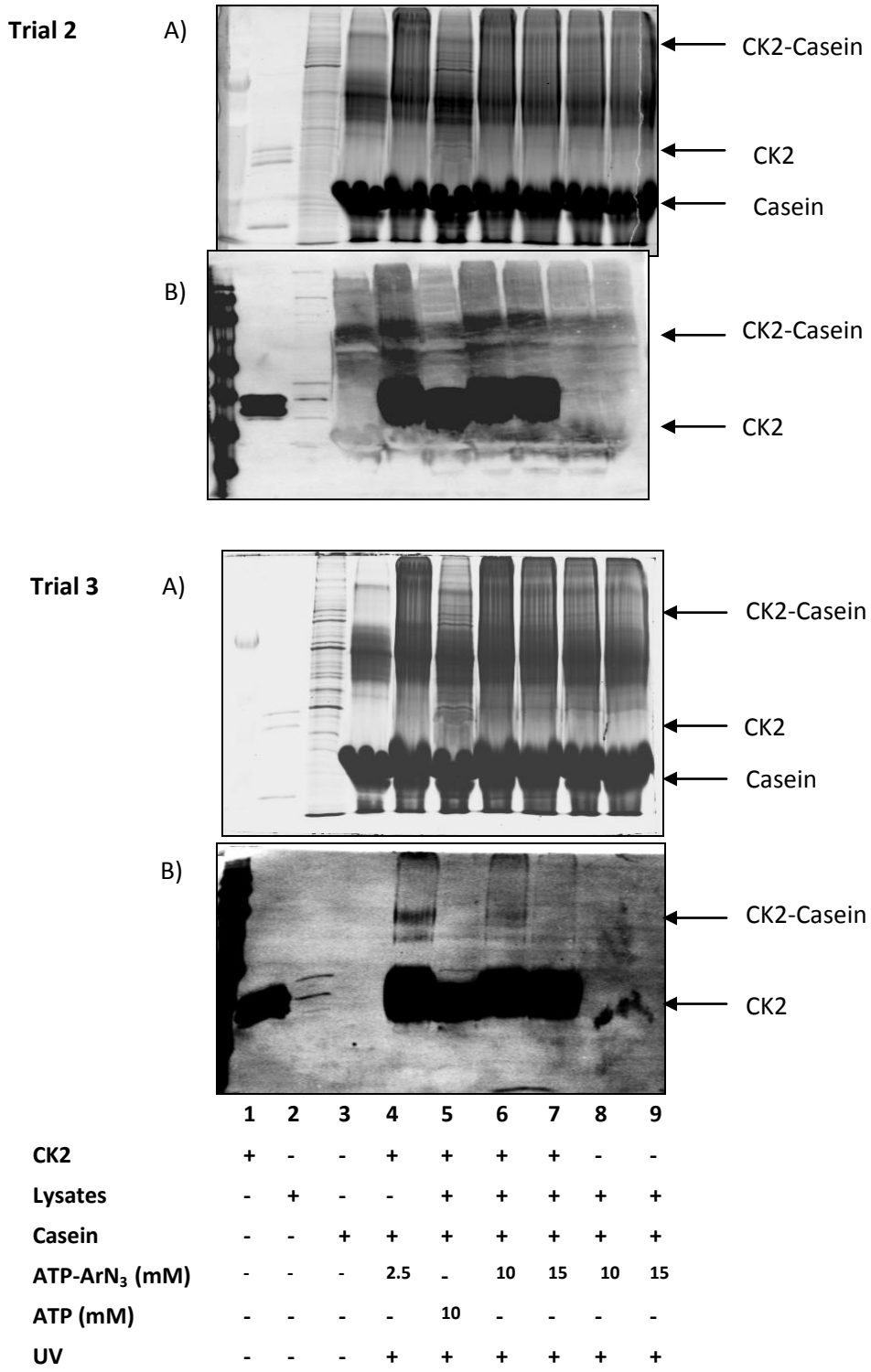

	1	2	3	4	5	6	7	8	9
CK2	+	-	-	+	+	+	+	-	-
Lysates	-	+	-	-	+	+	+	+	+
Casein	-	-	+	+	+	+	+	+	+
ATP-ArN$_3$ (mM)	-	-	-	2.5	-	10	15	10	15
ATP (mM)	-	-	-	-	10	-	-	-	-
UV	-	-	-	+	+	+	+	+	+

Figure A3.1: Photocrosslinking of CK2 and α-casein in the presence of Jurkat cell lysates. Photocrosslinking reactions were performed with CK2 kinase, casein substrate, ATP-ArN$_3$ in the presence of Jurkat cell lysates and UV at 30 ^{o}C, followed by SDS-PAGE separation and visualization with a CK2 antibody (B), SyproRuby protein staining (A). ATP-ArN$_3$ concentration and components of each reaction lane are as indicated. Jurkat cell lysates (10 µg) were used in each reaction. The expected ~68 kDa crosslinked band is indicated as CK2-Casein, the 45 kDa band of CK2 kinase as CK2, and 25 kDa band of α-casein as casein.

Trial-2: Westernblot with anti-p53

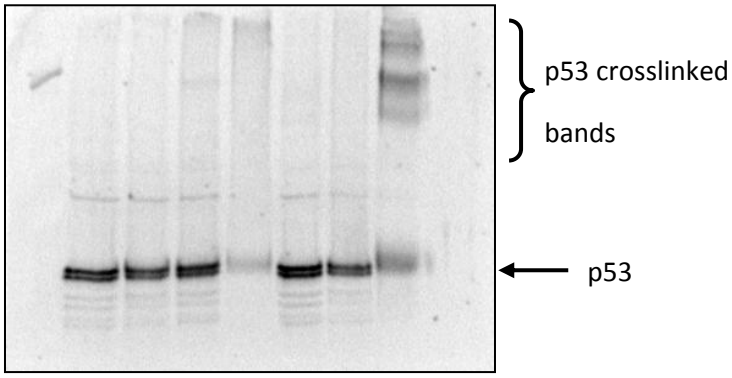

Trial-3: Westernblot with anti-p53

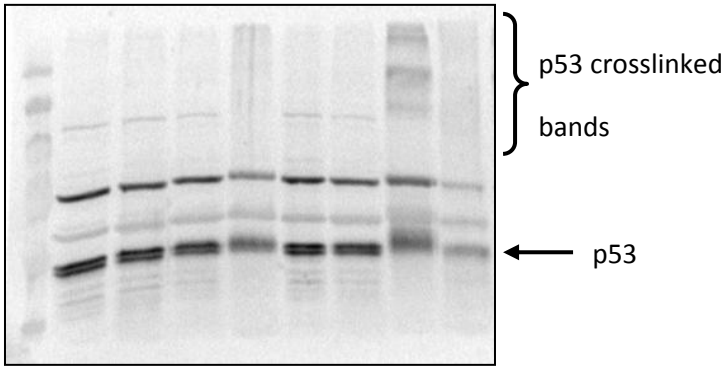

	1	2	3	4	5	6	7	8
Lysates	+	+	+	-	+	+	+	+
Heat denatured lysate	-	-	-	+	-	-	-	-
ATP	-	+	-	-	-	+	-	-
ATP-ArN3	-	-	+	+	-	-	+	+
UV	-	-	-	+	+	+	+	+
TFA	-	-	-	-	-	-	-	+

Figure A3.2: Photocrosslinking experiment with ATP-ArN_3 and Nutlin treated cell lysate. Photocrosslinking reactions were performed by incubating the reaction components under UV as indicated for each reaction, at 30 °C for 2 hrs, followed by SDS-PAGE separation and visualization with a p53 antibody (top), and CK2 antibody (bottom). ATP-ArN_3 (10 mM) and 30µg of total protein from Nutlin treated RKO cell lysates were used in each reaction. Lysates were heat denatured before the addition of ATP-ArN_3 for 5 minutes at 95 °C. TFA was added to a final concentration of 50% after crosslinking to cleave the phosphoramidate bond in the crosslink. The high molecular weight crosslinked complex is indicated as p53 crosslinked bands, and 53 kDa band of p53 protein as p53.

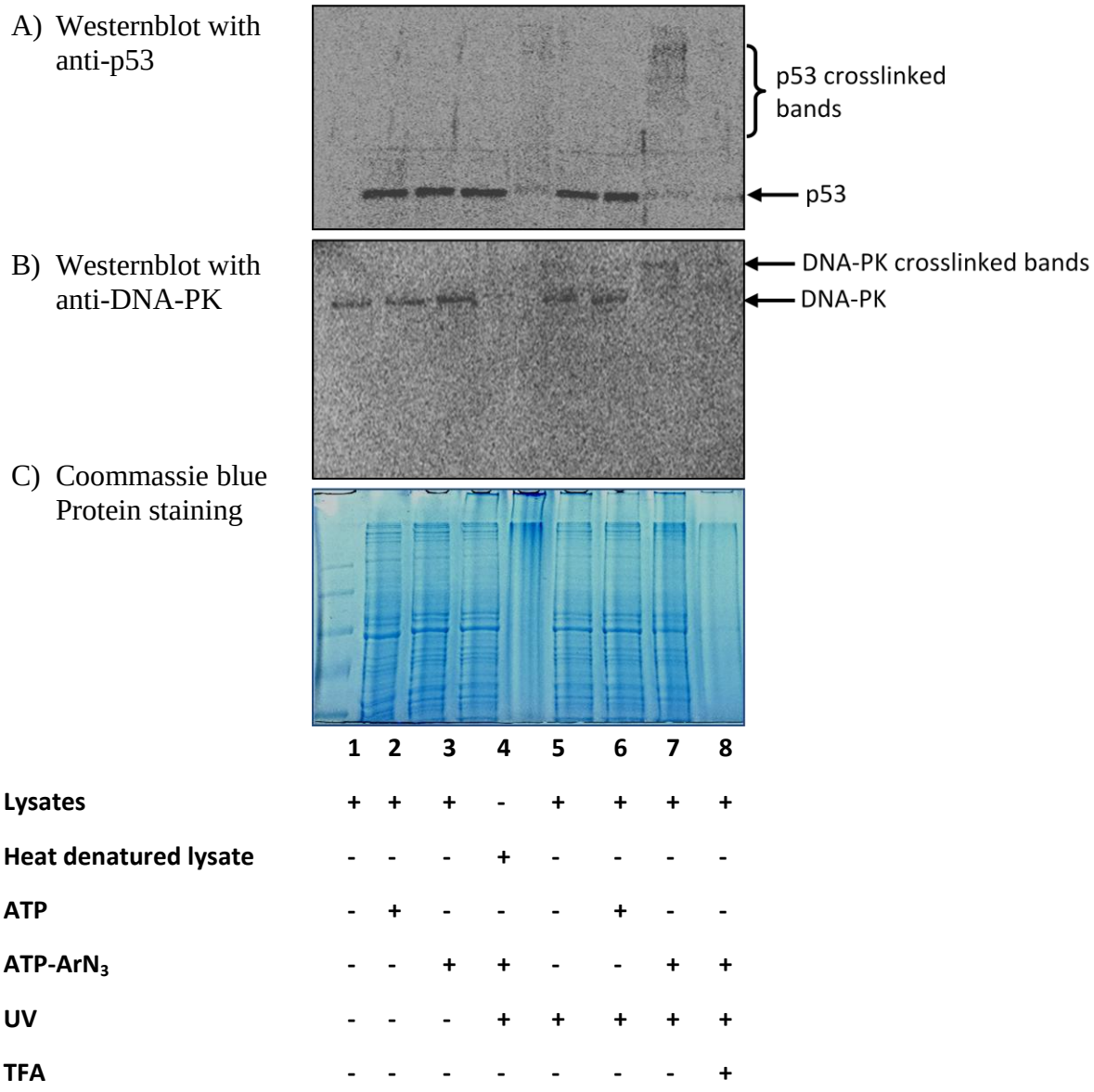

Figure A3.3: Photocrosslinking Experiments to validate Phosphorylation of p53 by DNA-PK kinase. The photocrosslinking reaction was performed by incubating the reaction components under UV as indicated for each reaction at 30 °C for 2 hrs, followed by SDS-PAGE separation and visualization with a p53 antibody (A), DNA-PK antibody (B), and Commassie blue staining (C). ATP-ArN_3 (10 mM) and 30 µg total proteins from Nutlin treated RKO cell lysates were used in each reaction. Lysates were heat denatured before the addition of ATP-ArN_3 for 5 minutes at 95 °C. TFA added to a final concentration of 50% after crosslinking to cleave the phosphoramidate band of crosslink. The high molecular weight crosslinked complex is indicated as p53 crosslinked bands, 53 kDa band of p53 protein as p53, DNA-PK protein band as DNA-PK, and the DNA-PK complex as DNA-PK crosslinked bands.

Table A3.1: Proteins identified in the crosslinking experiment with Q Exactive Mass Spectrometry

This table catalogs the number of unique peptides identified with respect to crosslinked and uncrosslinked lysates as well as with the use of rabbit antibody and mouse antibody for the IP of crosslinked complex. **A)** uncrosslinked lysates, IP with Rabbit Antibody; **B)** crosslinked lysates, IP with Rabbit Antibody; **C)** uncrosslinked lysates, IP with Mouse Antibody; **D)** crosslinked lysates, IP with Mouse Antibody. The parameters were set to a 90% protein threshold, 99.9% peptide threshold, with the minimum number of peptides set to 1. Absence of a number or presence of zero under the different reaction conditions (A, B, C, and D) implies that there are no unique peptides identified for that protein.

No.	Identified Proteins	Accession Number	Mol. Wt	No. of Uniques peptides identified			
				A	B	C	D
1	Cluster of 14-3-3 protein zeta/delta	1433Z_HUMAN [2]	28 kDa	1			7
2	40S ribosomal protein S13	RS13_HUMAN	17 kDa				1
3	60S ribosomal protein L11	RL11_HUMAN	20 kDa				1
4	A-kinase anchor protein SPHKAP	SPKAP_HUMAN	186 kDa				1
5	AFG3-like protein 2	AFG32_HUMAN	89 kDa				3
6	Adenylyl cyclase-associated protein 1	CAP1_HUMAN	52 kDa		1		2
7	Ankyrin repeat and KH domain-containing protein 1	ANKH1_HUMAN (+1)	269 kDa				1
8	Ataxin-2-like protein	ATX2L_HUMAN	113 kDa				2
9	Baculoviral IAP repeat-containing protein 6	BIRC6_HUMAN	530 kDa				1
10	Bifunctional protein NCOAT	NCOAT_HUMAN	103 kDa				1
11	Bifunctional purine biosynthesis protein PURH	PUR9_HUMAN	65 kDa				3
12	Brefeldin A-inhibited guanine nucleotide-exchange protein 1	BIG1_HUMAN (+1)	209 kDa				1
13	Bromodomain-containing protein 4	BRD4_HUMAN	152 kDa		2		
14	C2 domain-containing protein 2	CU025_HUMAN	76 kDa		3	1	18
15	CAD protein	PYR1_HUMAN	243 kDa		2		16
16	CDK5 regulatory subunit-associated protein 3	CK5P3_HUMAN	57 kDa				2
17	CUB domain-containing protein 1	CDCP1_HUMAN	93 kDa				1
18	Calcium-binding mitochondrial carrier protein Aralar1	CMC1_HUMAN	75 kDa				1

No.	Identified Proteins	Accession Number	Mol. Wt	No. of Uniques peptides identified			
				A	B	C	D
19	Calcium-binding mitochondrial carrier protein Aralar2	CMC2_HUMAN	74 kDa				1
20	Chloride intracellular channel protein 1	CLIC1_HUMAN	27 kDa				3
21	Cluster of Chromodomain-helicase-DNA-binding protein 4	CHD4_HUMAN	218 kDa				5
22	Clustered mitochondria protein homolog	CLU_HUMAN	147 kDa				1
23	Coiled-coil and C2 domain-containing protein 1A	C2D1A_HUMAN	104 kDa				4
24	Coiled-coil domain-containing protein 47	CCD47_HUMAN	56 kDa		1		
25	Constitutive coactivator of PPAR-gamma-like protein 1	F120A_HUMAN	122 kDa				2
26	Cytoplasmic FMR1-interacting protein 1	CYFP1_HUMAN	145 kDa				3
27	Cytoskeleton-associated protein 4	CKAP4_HUMAN	66 kDa		1		1
28	Cytoskeleton-associated protein 5	CKAP5_HUMAN	226 kDa				4
29	DNA damage-binding protein 1	DDB1_HUMAN	127 kDa		1	0	5
30	DNA repair protein XRCC4	XRCC4_HUMAN	38 kDa	5	12		
31	DNA-dependent protein kinase catalytic subunit	PRKDC_HUMAN	469 kDa		6		47
32	Developmentally-regulated GTP-binding protein 1	DRG1_HUMAN	41 kDa				1
33	Dolichyl-diphosphooligosaccharide--protein glycosyltransferase 48 kDa subunit	OST48_HUMAN	51 kDa		0		2
34	Dolichyl-diphosphooligosaccharide--protein glycosyltransferase subunit 1	RPN1_HUMAN	69 kDa		3		15
35	Dolichyl-diphosphooligosaccharide--protein glycosyltransferase subunit 2	RPN2_HUMAN	69 kDa		5		10
36	Dolichyl-diphosphooligosaccharide--protein glycosyltransferase subunit STT3A	STT3A_HUMAN	81 kDa				3
37	Dolichyl-diphosphooligosaccharide--protein glycosyltransferase subunit STT3B	STT3B_HUMAN	94 kDa				1

No.	Identified Proteins	Accession Number	Mol. Wt	No. of Uniques peptides identified			
				A	B	C	D
38	Dual specificity mitogen-activated protein kinase kinase 3	MP2K3_HUMAN	39 kDa				1
39	Dynamin-1-like protein	DNM1L_HUMAN	82 kDa				1
40	Dynamin-like 120 kDa protein, mitochondrial	OPA1_HUMAN	112 kDa		2		7
41	E3 UFM1-protein ligase 1	UFL1_HUMAN	90 kDa				2
42	E3 ubiquitin-protein ligase BRE1B	BRE1B_HUMAN	114 kDa				2
43	E3 ubiquitin-protein ligase HUWE1	HUWE1_HUMAN	482 kDa				4
44	E3 ubiquitin-protein ligase TRIM21	RO52_HUMAN	54 kDa	6	8	2	
45	E3 ubiquitin-protein ligase TRIM32	TRI32_HUMAN	72 kDa				1
46	E3 ubiquitin-protein ligase UBR4	UBR4_HUMAN	574 kDa				15
47	EH domain-containing protein 1	EHD1_HUMAN	61 kDa				1
48	ER membrane protein complex subunit 1	EMC1_HUMAN	112 kDa				1
49	Echinoderm microtubule-associated protein-like 4	EMAL4_HUMAN	109 kDa				1
50	Elongator complex protein 1	ELP1_HUMAN	150 kDa				2
51	Far upstream element-binding protein 1	FUBP1_HUMAN	68 kDa				2
52	Far upstream element-binding protein 2	FUBP2_HUMAN	73 kDa		1		6
53	Far upstream element-binding protein 3	FUBP3_HUMAN	62 kDa		3		3
54	Fragile X mental retardation syndrome-related protein 2	FXR2_HUMAN	74 kDa				1
55	GTP-binding protein 1	GTPB1_HUMAN	72 kDa				1
56	GTP-binding protein SAR1a	SAR1A_HUMAN (+1)	22 kDa				1
57	Gamma-interferon-inducible protein 16	IF16_HUMAN	88 kDa		4		20
58	Gem-associated protein 4	GEMI4_HUMAN	120 kDa				1
59	Glutamate-rich WD repeat-containing protein 1	GRWD1_HUMAN	49 kDa		1		1
60	Guanine nucleotide-binding protein G(I)/G(S)/G(T) subunit beta-1	GBB1_HUMAN (+3)	37 kDa				1
61	Guanine nucleotide-binding protein G(i) subunit alpha-1	GNAI1_HUMAN (+9)	40 kDa				1

No.	Identified Proteins	Accession Number	Mol. Wt	No. of Uniques peptides identified			
				A	B	C	D
62	Guanine nucleotide-binding protein-like 1	GNL1_HUMAN	69 kDa				2
63	H/ACA ribonucleoprotein complex non-core subunit NAF1	NAF1_HUMAN	54 kDa		1		
64	HEAT repeat-containing protein 3	HEAT3_HUMAN	75 kDa				1
65	Heat shock 70 kDa protein 4L	HS74L_HUMAN	95 kDa		6		13
66	Heterogeneous nuclear ribonucleoprotein A1	ROA1_HUMAN	39 kDa			0	4
67	Heterogeneous nuclear ribonucleoprotein D0	HNRPD_HUMAN	38 kDa				4
68	Heterogeneous nuclear ribonucleoprotein H	HNRH1_HUMAN	49 kDa				2
69	Heterogeneous nuclear ribonucleoprotein L	HNRPL_HUMAN	64 kDa		3		2
70	Heterogeneous nuclear ribonucleoprotein Q	HNRPQ_HUMAN	70 kDa				5
71	Heterogeneous nuclear ribonucleoprotein R	HNRPR_HUMAN	71 kDa		1		8
72	Heterogeneous nuclear ribonucleoprotein U	HNRPU_HUMAN	91 kDa		3		20
73	Heterogeneous nuclear ribonucleoprotein U-like protein 1	HNRL1_HUMAN	96 kDa	0			2
74	Heterogeneous nuclear ribonucleoprotein U-like protein 2	HNRL2_HUMAN	85 kDa		0		1
75	Heterogeneous nuclear ribonucleoproteins A2/B1	ROA2_HUMAN	37 kDa			0	7
76	Histone-binding protein RBBP4	RBBP4_HUMAN (+1)	48 kDa		1		1
77	Hsc70-interacting protein	F10A1_HUMAN (+1)	41 kDa				1
78	Hypoxia up-regulated protein 1	HYOU1_HUMAN	111 kDa				1
79	Insulin-like growth factor 2 mRNA-binding protein 2	IF2B2_HUMAN (+1)	66 kDa				1
80	Interferon-induced, double-stranded RNA-activated protein kinase	E2AK2_HUMAN	62 kDa		1		3
81	Kelch-like protein 22	KLH22_HUMAN	72 kDa		1		
82	Kinesin-like protein KIF13B	KI13B_HUMAN	203 kDa				1
83	Kinesin-like protein KIF3A	KIF3A_HUMAN	80 kDa				1
84	Large proline-rich protein BAG6	BAG6_HUMAN	119 kDa				1

No.	Identified Proteins	Accession Number	Mol. Wt	No. of Uniques peptides identified			
				A	B	C	D
85	Leucine-rich repeat-containing protein 47	LRC47_HUMAN	63 kDa				1
86	Leucine-rich repeat-containing protein 59	LRC59_HUMAN	35 kDa				1
87	Lipopolysaccharide-responsive and beige-like anchor protein	LRBA_HUMAN	319 kDa				3
88	Long-chain fatty acid transport protein 4	S27A4_HUMAN	72 kDa				2
89	Lymphoid-restricted membrane protein	LRMP_HUMAN	62 kDa				1
90	Lysosome-associated membrane glycoprotein 2	LAMP2_HUMAN	45 kDa				1
91	MMS19 nucleotide excision repair protein homolog	MMS19_HUMAN	113 kDa		2		3
92	Melanoma inhibitory activity protein 3	MIA3_HUMAN	214 kDa				2
93	Cluster of Metastasis-associated protein MTA2	MTA2_HUMAN [2]	75 kDa		1		6
94	Methyltransferase-like protein 13	MET13_HUMAN	79 kDa				1
95	Microtubule-associated protein 4	MAP4_HUMAN	121 kDa				2
96	Mitochondrial inner membrane protein	IMMT_HUMAN	84 kDa				2
97	Myb-binding protein 1A	MBB1A_HUMAN	149 kDa		1		14
98	Nck-associated protein 1	NCKP1_HUMAN	129 kDa				3
99	Neuroblast differentiation-associated protein AHNAK	AHNK_HUMAN	629 kDa				55
100	Niban-like protein 1	NIBL1_HUMAN	84 kDa		1		8
101	Non-POU domain-containing octamer-binding protein	NONO_HUMAN	54 kDa		2	0	4
102	Nuclear cap-binding protein subunit 1	NCBP1_HUMAN	92 kDa				1
103	Nuclear mitotic apparatus protein 1	NUMA1_HUMAN	238 kDa				3
104	Nuclear pore complex protein Nup155	NU155_HUMAN	155 kDa				1
105	Nuclear pore complex protein Nup205	NU205_HUMAN	228 kDa				1
106	Nuclear pore complex protein Nup93	NUP93_HUMAN	93 kDa				3
107	Nucleolar and coiled-body phosphoprotein 1	NOLC1_HUMAN	74 kDa		1		1
108	Nucleolar protein 56	NOP56_HUMAN	66 kDa				1

No.	Identified Proteins	Accession Number	Mol. Wt	No. of Uniques peptides identified			
				A	B	C	D
109	Nucleolar protein 58	NOP58_HUMAN	60 kDa				2
110	Nucleolar protein 6	NOL6_HUMAN	128 kDa				2
111	Nucleosome assembly protein 1-like 1	NP1L1_HUMAN	45 kDa		1		2
112	NudC domain-containing protein 1	NUDC1_HUMAN	67 kDa				1
113	Oxysterol-binding protein-related protein 3	OSBL3_HUMAN	101 kDa		3		
114	Oxysterol-binding protein-related protein 8	OSBL8_HUMAN	101 kDa		2		5
115	Pentatricopeptide repeat domain-containing protein 3, mitochondrial	PTCD3_HUMAN	79 kDa		1		2
116	Phosphate carrier protein, mitochondrial	MPCP_HUMAN	40 kDa				1
117	Phospholipase A-2-activating protein	PLAP_HUMAN	87 kDa				1
118	Polypyrimidine tract-binding protein 1	PTBP1_HUMAN	57 kDa		8		19
119	Pre-rRNA-processing protein TSR1 homolog	TSR1_HUMAN	92 kDa		1		
120	Programmed cell death 6-interacting protein	PDC6I_HUMAN	96 kDa		3		14
121	Programmed cell death protein 4	PDCD4_HUMAN	52 kDa				1
122	Protein FAM203A	F203A_HUMAN (+1)	42 kDa				1
123	Protein FAM83H	FA83H_HUMAN	127 kDa				2
124	Protein LYRIC	LYRIC_HUMAN	64 kDa		1		3
125	Protein RRP5 homolog	RRP5_HUMAN	209 kDa				1
126	Protein Red	RED_HUMAN	66 kDa				1
127	Protein S100-A14	S10AE_HUMAN	12 kDa				1
128	Protein S100-A2	S10A2_HUMAN	11 kDa				2
129	Protein TBRG4	TBRG4_HUMAN	71 kDa		1		1
130	Protein TFG	TFG_HUMAN	43 kDa		1		
131	Protein VAC14 homolog	VAC14_HUMAN	88 kDa		1		2
132	Protein arginine N-methyltransferase 5	ANM5_HUMAN	73 kDa				1
133	Protein disulfide-isomerase A4	PDIA4_HUMAN	73 kDa				4
134	Protein disulfide-isomerase A6	PDIA6_HUMAN	48 kDa		1		10
135	Protein scribble homolog	SCRIB_HUMAN	175 kDa				1

No.	Identified Proteins	Accession Number	Mol. Wt	No. of Uniques peptides identified			
				A	B	C	D
136	Protein transport protein Sec16A	SC16A_HUMAN	234 kDa				1
137	Cluster of Protein transport protein Sec23B	SC23B_HUMAN	86 kDa				3
138	Protein transport protein Sec24C	SC24C_HUMAN	118 kDa				1
139	Protein transport protein Sec61 subunit alpha isoform 1	S61A1_HUMAN	52 kDa				3
140	Protein unc-45 homolog A	UN45A_HUMAN	103 kDa		0		5
141	Protein-glutamine gamma-glutamyltransferase E	TGM3_HUMAN	77 kDa				1
142	Protein-methionine sulfoxide oxidase MICAL1	MICA1_HUMAN	118 kDa				1
143	RNA-binding protein 12	RBM12_HUMAN	97 kDa		1		6
144	RNA-binding protein 14	RBM14_HUMAN	69 kDa	0			3
145	RNA-binding protein FUS	FUS_HUMAN	53 kDa	0			3
146	RRP12-like protein	RRP12_HUMAN	144 kDa				2
147	Rab3 GTPase-activating protein non-catalytic subunit	RBGPR_HUMAN	156 kDa				2
148	Ran GTPase-activating protein 1	RAGP1_HUMAN	64 kDa				2
149	Ran-binding protein 10	RBP10_HUMAN	67 kDa				1
150	Ras GTPase-activating-like protein IQGAP1	IQGA1_HUMAN	189 kDa		2		19
151	Rho-associated protein kinase 2	ROCK2_HUMAN	161 kDa				1
152	Ribonucleases P/MRP protein subunit POP1	POP1_HUMAN	115 kDa				1
153	Ribosomal L1 domain-containing protein 1	RL1D1_HUMAN	55 kDa				1
154	Ribosomal RNA processing protein 1 homolog B	RRP1B_HUMAN	84 kDa				2
155	Ribosomal biogenesis protein LAS1L	LAS1L_HUMAN	83 kDa		1		
156	Ribosome-binding protein 1	RRBP1_HUMAN	152 kDa				1
157	SAM domain and HD domain-containing protein 1	SAMH1_HUMAN	72 kDa				1
158	SCY1-like protein 2	SCYL2_HUMAN	104 kDa		1		2
159	SRSF protein kinase 1	SRPK1_HUMAN	74 kDa				2
160	Serine/threonine-protein kinase 4	STK4_HUMAN	56 kDa		1		
161	Serine/threonine-protein kinase MRCK beta	MRCKB_HUMAN	194 kDa		3		1

No.	Identified Proteins	Accession Number	Mol. Wt	No. of Uniques peptides identified			
				A	B	C	D
162	Serine/threonine-protein kinase TBK1	TBK1_HUMAN	84 kDa				1
163	Serine/threonine-protein phosphatase 2A 56 kDa regulatory subunit delta isoform	2A5D_HUMAN	70 kDa		0		1
164	Serine/threonine-protein phosphatase 2A 65 kDa regulatory subunit A alpha isoform	2AAA_HUMAN	65 kDa		1		6
165	Signal recognition particle 54 kDa protein	SRP54_HUMAN	56 kDa				1
166	Signal recognition particle 68 kDa protein	SRP68_HUMAN	71 kDa				2
167	Signal recognition particle 72 kDa protein	SRP72_HUMAN	75 kDa				3
168	Sister chromatid cohesion protein PDS5 homolog B	PDS5B_HUMAN	165 kDa				1
169	Skin-specific protein 32	XP32_HUMAN	26 kDa				3
170	Spermatogenesis-associated protein 5-like protein 1	SPA5L_HUMAN	81 kDa				1
171	Staphylococcal nuclease domain-containing protein 1	SND1_HUMAN	102 kDa				17
172	Stomatin-like protein 2, mitochondrial	STML2_HUMAN	39 kDa	0			1
173	Stress-induced-phosphoprotein 1	STIP1_HUMAN	63 kDa		2		6
174	Structural maintenance of chromosomes flexible hinge domain-containing protein 1	SMHD1_HUMAN	226 kDa				1
175	Structural maintenance of chromosomes protein 3	SMC3_HUMAN	142 kDa				2
176	Submaxillary gland androgen-regulated protein 3B	SMR3B_HUMAN	8 kDa				2
177	Succinate dehydrogenase [ubiquinone] flavoprotein subunit, mitochondrial	DHSA_HUMAN	73 kDa		1		2
178	Surfeit locus protein 4	SURF4_HUMAN	30 kDa		0		5
179	T-complex protein 1 subunit epsilon	TCPE_HUMAN	60 kDa	1	5		6
180	TATA-binding protein-associated factor 172	BTAF1_HUMAN	207 kDa				1
181	Thioredoxin domain-containing protein 5	TXND5_HUMAN	48 kDa				1
182	Torsin-1A-interacting protein 1	TOIP1_HUMAN	66 kDa		1		1
183	Torsin-1A-interacting protein 2	TOIP2_HUMAN	51 kDa		1		

No.	Identified Proteins	Accession Number	Mol. Wt	No. of Uniques peptides identified			
				A	B	C	D
184	Trans-Golgi network integral membrane protein 2	TGON2_HUMAN	51 kDa				1
185	Translocating chain-associated membrane protein 1	TRAM1_HUMAN	43 kDa				1
186	Transmembrane protein 33	TMM33_HUMAN	28 kDa				2
187	Trifunctional purine biosynthetic protein adenosine-3	PUR2_HUMAN	108 kDa		3		11
188	Tubulin--tyrosine ligase-like protein 12	TTL12_HUMAN	74 kDa				3
189	Tuftelin-interacting protein 11	TFP11_HUMAN	97 kDa				1
190	Tyrosine-protein phosphatase non-receptor type 1	PTN1_HUMAN	50 kDa				6
191	Tyrosine-protein phosphatase non-receptor type 11	PTN11_HUMAN	68 kDa				1
192	U2 snRNP-associated SURP motif-containing protein	SR140_HUMAN	118 kDa		1		1
193	U4/U6.U5 small nuclear ribonucleoprotein 27 kDa protein	SNR27_HUMAN	19 kDa				1
194	U4/U6.U5 tri-snRNP-associated protein 2	SNUT2_HUMAN	65 kDa				1
195	U5 small nuclear ribonucleoprotein 200 kDa helicase	U520_HUMAN	245 kDa	0	3		13
196	UV excision repair protein RAD23 homolog B	RD23B_HUMAN	43 kDa		1		1
197	Ubiquitin-protein ligase E3A	UBE3A_HUMAN	101 kDa		1		
198	Ubiquitin-protein ligase E3C	UBE3C_HUMAN	124 kDa		1		3
199	Vacuolar protein sorting-associated protein 13C	VP13C_HUMAN	422 kDa				1
200	Vacuolar protein sorting-associated protein 16 homolog	VPS16_HUMAN	95 kDa				1
201	Vacuolar protein sorting-associated protein 35	VPS35_HUMAN	92 kDa				3
202	Vasodilator-stimulated phosphoprotein	VASP_HUMAN	40 kDa				1
203	Very-long-chain (3R)-3-hydroxyacyl-[acyl-carrier protein] dehydratase 3	HACD3_HUMAN	43 kDa				2
204	WD repeat-containing protein 26	WDR26_HUMAN	72 kDa				1
205	Wiskott-Aldrich syndrome protein family member 2	WASF2_HUMAN	54 kDa				1
206	X-ray repair cross-complementing protein 5	XRCC5_HUMAN	83 kDa		1		18

No.	Identified Proteins	Accession Number	Mol. Wt	No. of Uniques peptides identified			
				A	B	C	D
207	X-ray repair cross-complementing protein 6	XRCC6_HUMAN	70 kDa		2		30
208	Zinc finger CCCH-type antiviral protein 1	ZCCHV_HUMAN	101 kDa				1
209	Zinc finger HIT domain-containing protein 2	ZNHI2_HUMAN	43 kDa				1
210	Zinc finger protein 207	ZN207_HUMAN	51 kDa		1		
211	Zymogen granule protein 16 homolog B	ZG16B_HUMAN	23 kDa		1		1

Table A3.2: Overview of MS data of p53 and kinases identified

	Identified Proteins	Accession Number	Mol.Wt	No. of unique peptides identified																													
				Uncrosslinked Lysate Rabbit Antibody								Crosslinked Lysate Rabbit Antibody								Uncrosslinked Lysate Mouse Antibody								Crosslinked Lysate Mouse Antibody							
				A	B	C	D	E	F	G	H	A	B	C	D	E	F	G	H	A	B	C	D	E	F	G	H	A	B	C	D	E	F	G	H
1	Cellular tumor antigen p53	P53_HUMAN	44 kDa		4	1							3	7		2	1	1			1	2	0						1	1				2	
2	DNA-dependent protein kinase catalytic subunit	PRKDC_HUMAN	469 kDa																6																47
3	Casein kinase II subunit alpha	CSK21_HUMAN	45 kDa	1																1	6							1							
4	Serine/threonine-protein kinase MRCK beta	MRCKB_HUMAN	194 kDa														3																		1
5	SRSF protein kinase 1	SRPK1_HUMAN	74 kDa																											2					
6	Interferon-induced, double-stranded RNA-activated protein kinase	E2AK2_HUMAN	62 kDa											1															2						1
7	Cyclin-dependent kinase 12	CDK12_HUMAN	164 kDa																																2

A to H are the eight SDS-PAGE gel slices of each lane of interest. **A** being 50 kDa Mol wt, with increasing molecular weight and **H** being the highest molecular weight. This table shows the no. of unique peptides identified with respect to crosslinked and uncrosslinked lysates as well as use of rabbit antibody and mouse antibody for the IP of crosslinked complex. The parameters set were protein threshold-90%, peptide threshold-99.9%, with minimum number of peptides set to 1.

P53_HUMAN (100%), 43,653.4 Da
Cellular tumor antigen p53 OS=Homo sapiens GN=TP53 PE=1 SV=4
7 exclusive unique peptides, 7 exclusive unique spectra, 14 total spectra, 85/393 amino acids (22% coverage)

M E E P Q S D P S V E P P L S Q E T F S D L W K L L P E N N V L S P L P S Q A M D D L M L S P D D I
E Q W F T E D P G P D E A P R M P E A A P P V A P A P A A P T P A A P A P A P S W P L S S S V P S Q
K T Y Q G S Y G F R L G F L H S G T A K **S V T C T Y S P A L** **N K** M F C Q L A K T C P V Q L W V D S T
P P P G T R V R A M A I Y K Q S Q H M T E V V R R C P H H E R **C S D S D G L A P** **P Q H L I R** V E G N
L R **V E Y L D D R N** **T F R** H S V V V P Y E P P E V G S D C T T I H Y N Y M C N S S C M G G M N R **R P**
I L T I I T L E D S **S G N L L G R** N S F E V R V C A C P G R D R R T E E E N L R K K G E P H H E L P
P G S T K R **A L P N** **N T S S S P Q P K** K K P L D G E Y F T L Q I R G R E R F E M F R **E L N E A L E L**
K D A Q A G K E P G G S R A H S S H L K S K K G Q S T S R H K K L M F K T E G P D S D

Figure A3.4: Primary sequence of p53 proteins identified in crosslinked and uncrosslinked IP experiments. Amino acids observed in the MS/MS analysis are highlighted in yellow, while modified amino acids are in green (phosphorylation (S or T) or oxidation (M)). The parameters set were protein threshold-90%, peptide threshold-99.9%, with minimum number of peptides set to 1.

Peptide Sequence: (R)LGFLHSGTAK(S)

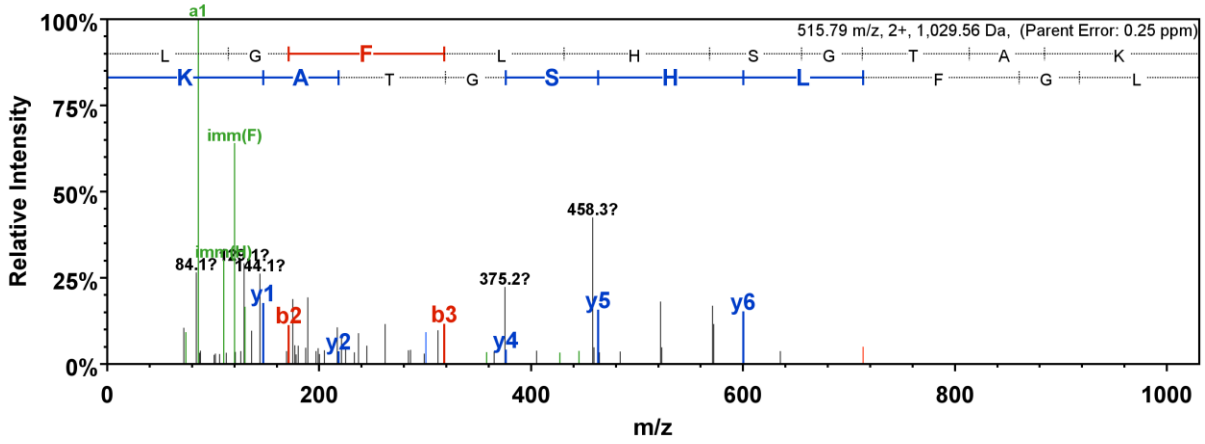

Peptide Sequence: (R)VEYLDDRNTFR(H)

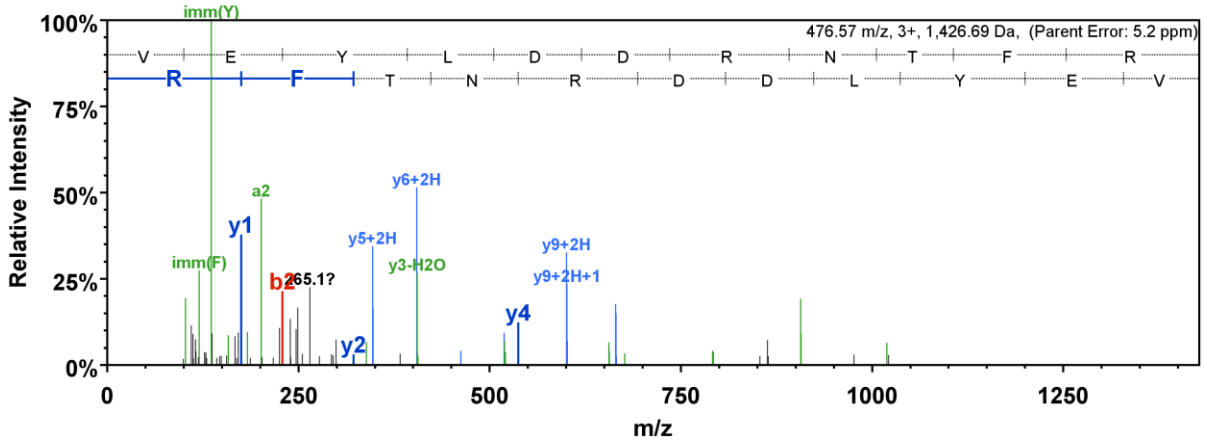

Peptide Sequence: (K)SVTcTYSPALNK(M)

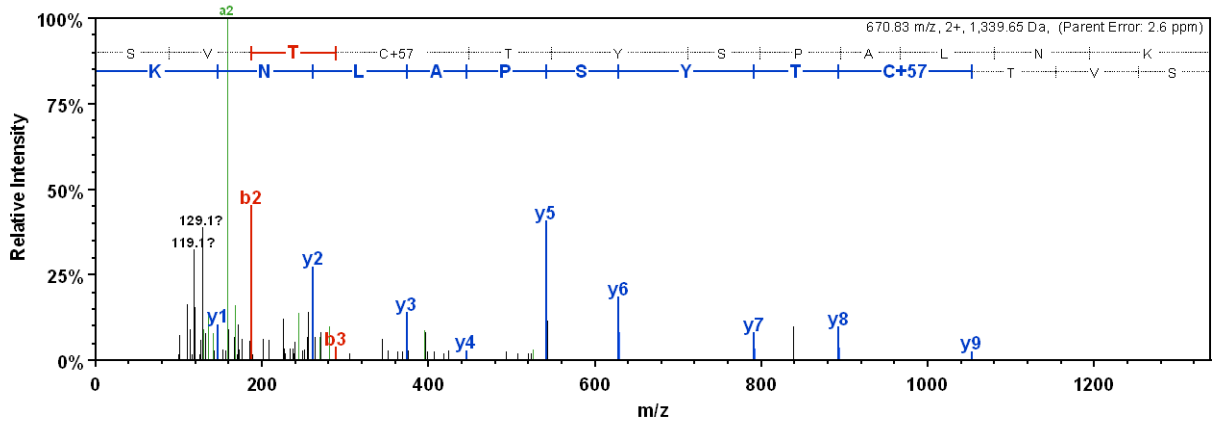

Peptide Sequence: (R)cSDSDGLAPPQHLIR(V)

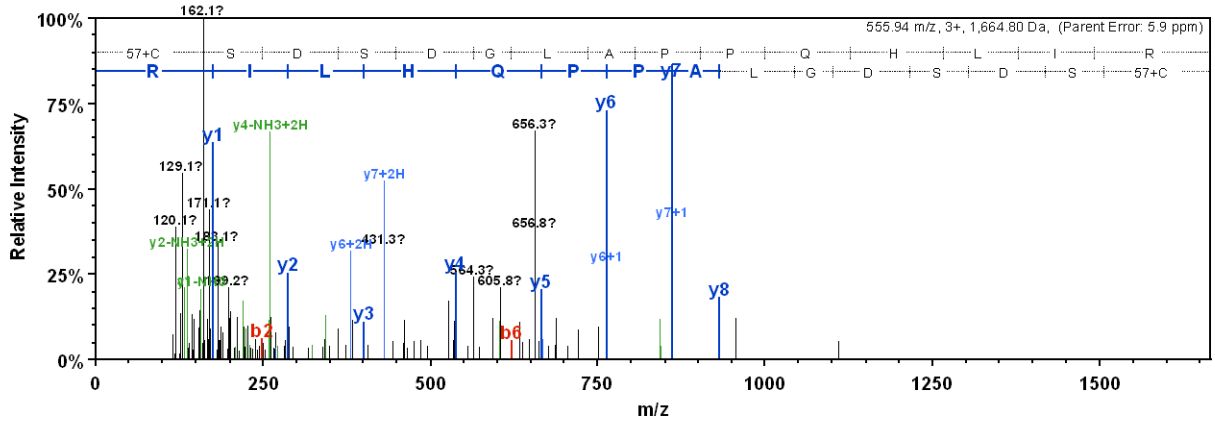

Peptide Sequence: (R)RPILTIITLEDSSGNLLGR(N)

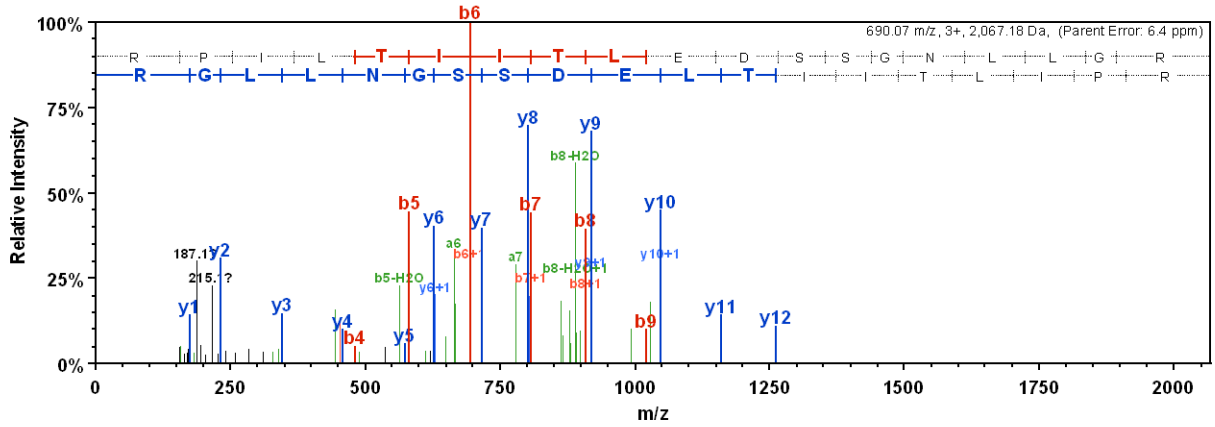

Peptide Sequence: (R)ALPNNTSSSPQPK(K)

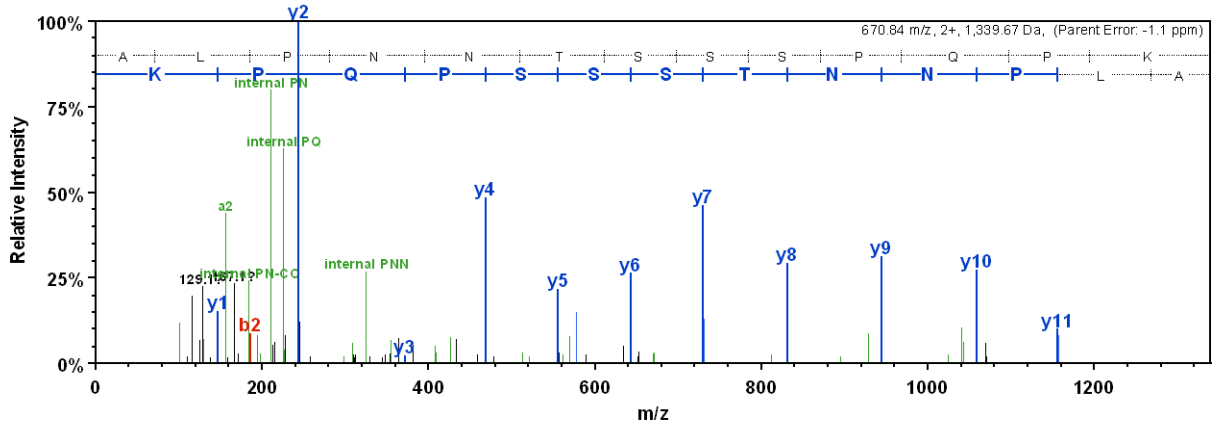

Peptide Sequence: (R)ELNEALELK(D)

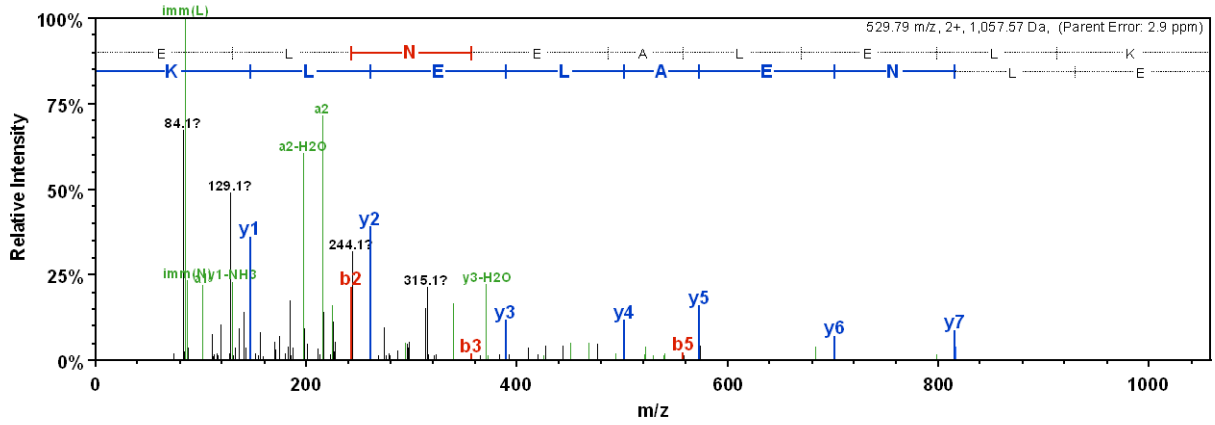

Peptide Sequence: (R)ELNEALELKDAQAGK(E)

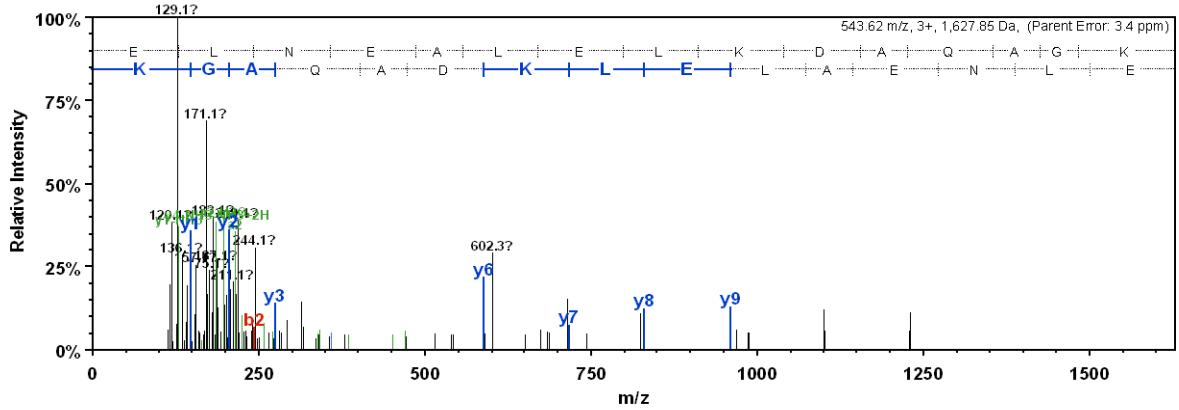

Figure A3.5: The annotated spectra of p53 peptides identified by MS/MS analysis shown in figure A3.1. A representation of the peptide fragments identified is shown with the peptide sequence on top of each spectrum.

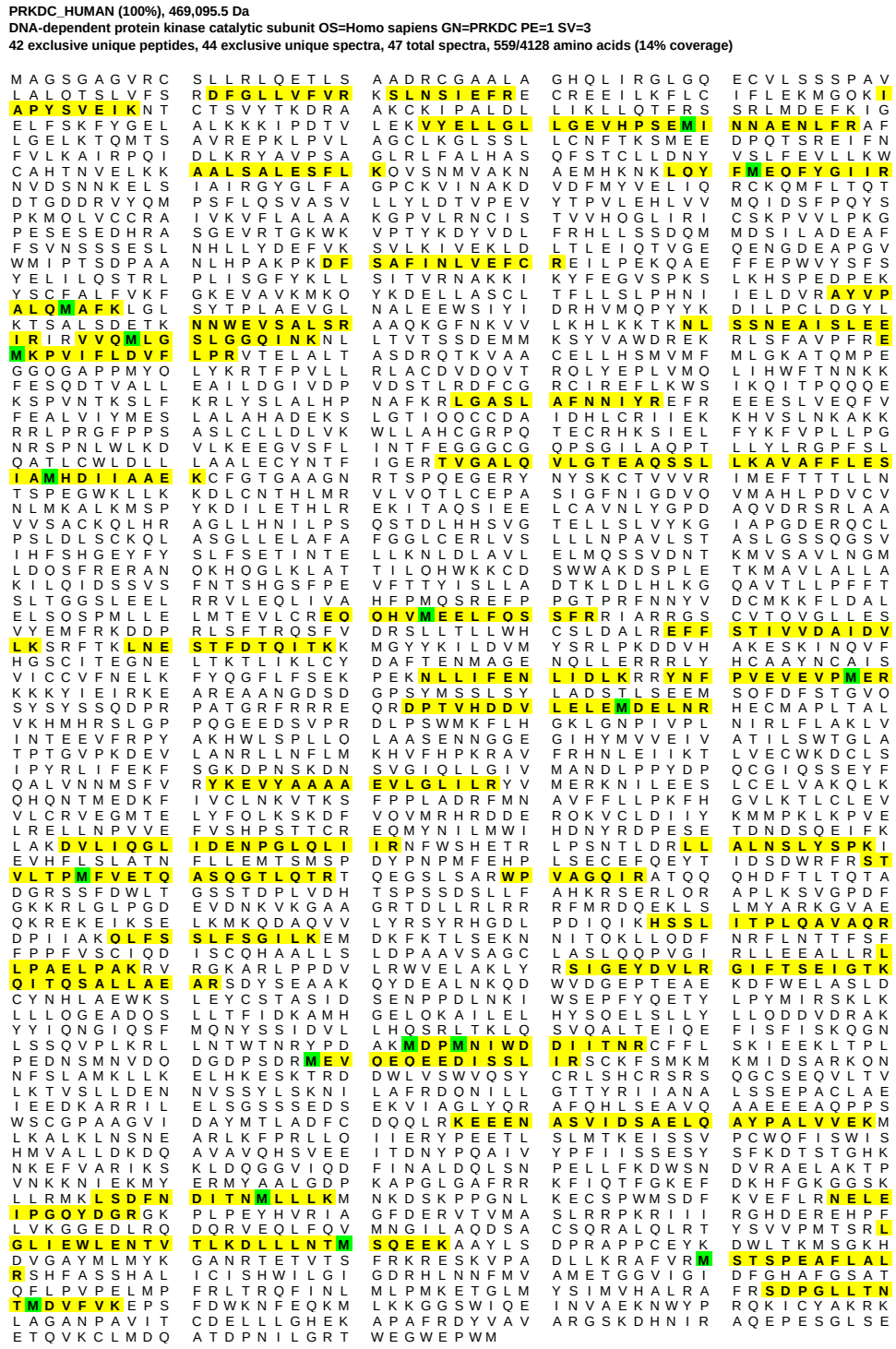

Figure A3.6: Primary sequence of DNA-PK protein identified in the crosslinked IP experiments. Amino acids observed in the MS/MS analysis are highlighted in yellow, while modified amino acids are in green (phosphorylation (S or T) or oxidation (M)). The parameters set were protein threshold-90%, peptide threshold-99.9%, with minimum number of peptides set to 1.

Peptide Sequence: (R)DPTVHDDVLELEMDELNR(H)

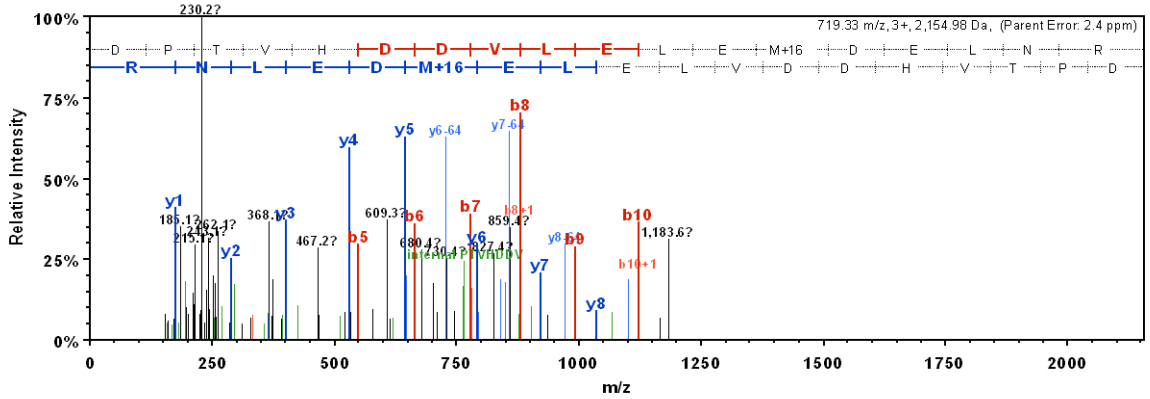

Peptide Sequence: (R)MEVQEQEEDISSLIR(S)

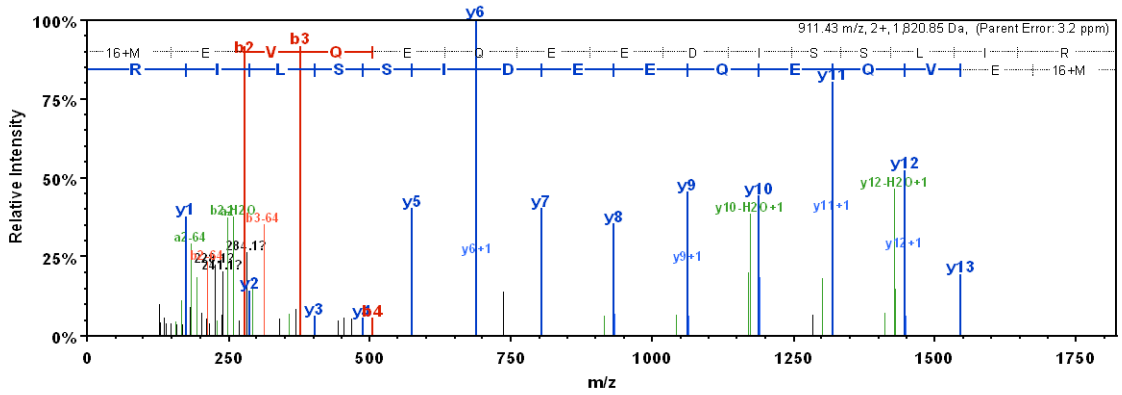

Peptide Sequence: (R)TVGALQVLGTEAQSSLLK(A)

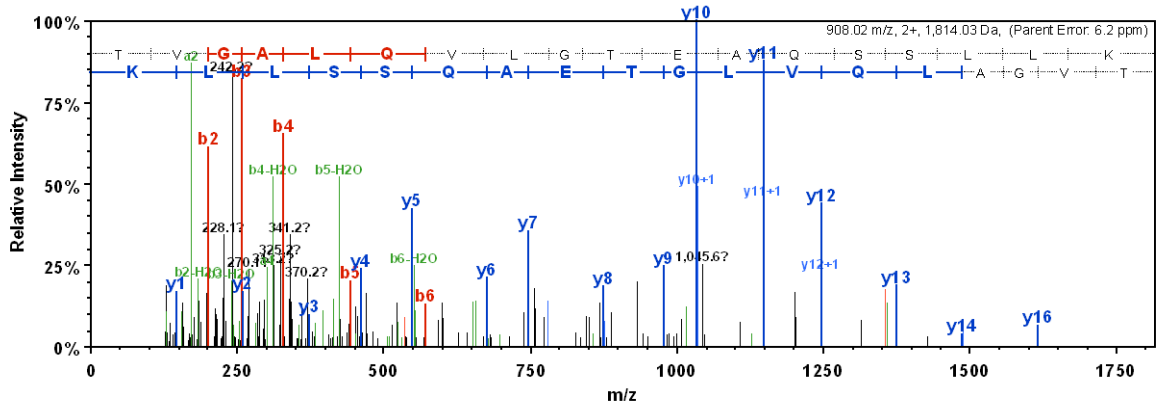

Figure A3.7: The annotated spectra of DNA-PK peptides identified by MS/MS analysis, shown in figure A3.3. A representation of the peptide fragments identified is shown with the peptide sequence on top of each spectrum. MS spectra of only three of 47 unique peptides are shown as a representation here.

MRCKB_HUMAN (100%), 194,318.0 Da
Serine/threonine-protein kinase MRCK beta OS=Homo sapiens GN=CDC42BPB PE=1 SV=2
3 exclusive unique peptides, 3 exclusive unique spectra, 3 total spectra, 39/1711 amino acids (2% coverage)

M S A K V R L K K L E Q L L L D G P W R N E S A L S V E T L L D V L V C L Y T E C S H S A L R R D K
Y V A E F L E W A K P F T Q L V K E M Q L H R E D F E I I K V I G R G A F G E V A V V K M K N T E R
I Y A M K I L N K W E M L K R A E T A C F R E E R D V L V N G D C Q W I T A L H Y A F Q D E N H L Y
L V M D Y Y V G G D L L T L L S K F E D K L P E D M A R F Y I G E M V L A I D S I H Q L H Y V H R D
I K P D N V L L D V N G H I R L A D F G S C L K M N D D G T V Q S S V A V G T P D Y I S P E I L Q A
M E D G M G K Y G P E C D W W S L G V C M Y E M L Y G E T P F Y A E S L V E T Y G K I M N H E E R F
Q F P S H V T D V S E E A K D L I Q R L I C S R E R R L G Q N G I E D F K K H A F F E G L N W E N I
R N L E A P Y I P D V S S P S D T S N F D V D D D V L R N T E I L P P G S H T G F S G L H L P F I G
F T F T T E S C F S D R G S L K S I M Q S N T L T K D E D V Q R D L E H S L Q M E A Y E R R I R R L
E Q E K L E L S R K L Q E S T Q T V Q S L H G S S R A L S N S N R D K E I K K L N E E I E R L K N K
I A D S N R L E R Q L E D T V A L R Q E R E D S T Q R L R G L E K Q H R V V R Q E K E E L H K Q L V
E A S E R L K S Q A K E L K D A H Q Q R K **L A L Q E F S E L** **N E R** M A E L R A Q K Q K V S R Q L R D
K E E E M E V A T Q K V D A M R Q E M R R A E K L R K **E L E** **A Q L D D A V A E A** **S K** E R K L R E H S
E N F C K Q M E S E L E A L K V K Q G G R G A G A T L E H Q Q E I S K I K S E L E K K V L F Y E E E
L V R R E A S H V L E V K N V K K E V H D S E S H Q L A L Q K E I L M L K D K L E K S K R E R H N E
M E E A V G T I K D K Y E R E R A M L F D E N K K L T A E N E K L C S F V D K L T A Q N R Q L E D E
L Q D L A A K K E S V A H W E A Q I A E I I Q W V S D E K D A R G Y L Q A L A S K M T E E L E A L R
S S S L G S R T L D P L W K V R R S Q K L D M S A R L E L Q S A L E A E I R A K Q L V Q E E L R K V
K D A N L T L E S K L K D S E A K N R E L L E E M E I L K K K M E E K F R A D T G L K L P D F Q D S
I F E Y F N T A P L A H D L T F R T S S A S E Q E T Q A P K P E A S P S M S V A A S E Q Q E D M A R
P P Q R P S A V P L P T T Q A L A L A G P K P K A H Q F S I K S F S S P T Q C S H C T S L M V G L I
R Q G Y A C E V C S F A C H V S C K D G A P Q V C P I P P E Q S K R P L G V D V Q R G I G T A Y K G
H V K V P K P T G V K K G W Q R A Y A V V C D C K L F L Y D L P E G K S T Q P G V I A S Q V L D L R
D D E F S V S S V L A S D V I H A T R R D I P C I F R V T A S L L G A P S K T S S L L I L T E N E N
E K R K W V G I L E G L Q S I L H K N R L R N Q V V H V P L E A Y D S S L P L I K **A I L T A A I V D**
A D R I A V G L E E G L Y V I E V T R D V I V R A A D C K K V H Q I E L A P R E K I V I L L C G R N
H H V H L Y P W S S L D G A E G S F D I K L P E T K G C Q L M A T A T L K R N S G T C L F V A V K R
L I L C Y E I Q R T K P F H R K F N E I V A P G S V Q C L A V L R D R L C V G Y P S G F C L L S I Q
G D G Q P L N L V N P N D P S L A F L S Q Q S F D A L C A V E L E S E E Y L L C F S H M G L Y V D P
Q G R R A R A Q E L M W P A A P V A C S C S P T H V T V Y S E Y G V D V F D V R T M E W V Q T I G L
R R I R P L N S E G T L N L L N C E P P R L I Y F K S K F S G A V L N V P D T S D N S K K Q M L R T
R S K R R F V F K V P E E E R L Q Q R R E M L R D P E L R S K M I S N P T N F N H V A H M G P G D G
M Q V L M D L P L S A V P P S Q E E R P G P A P T N L A R Q P P S R N K P Y I S W P S S G G S E P S
V T V P L R S M S D P D Q D F D K E P D S D S T K H S T P S N S S N P S G P P S P N S P H R S Q L P
L E G L E Q P A C D T

Figure A3.8: Primary sequence of MRCKB protein identified in the crosslinked IP experiments. Amino acids observed in the MS/MS analysis are highlighted in yellow, while modified amino acids are in green (phosphorylation (S or T) or oxidation (M)). The parameters were, protein threshold-90%, peptide threshold-99.9%, with minimum number of peptides set to 1.

Peptide Sequence: (K)LALQEFSELNER(M)

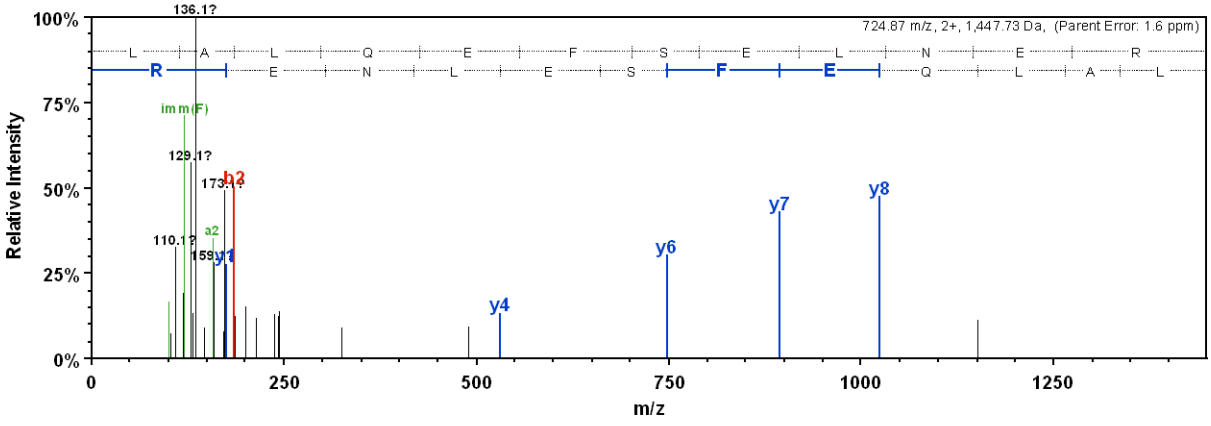

Peptide Sequence: (K)ELEAQLDDAVAEASK(E)

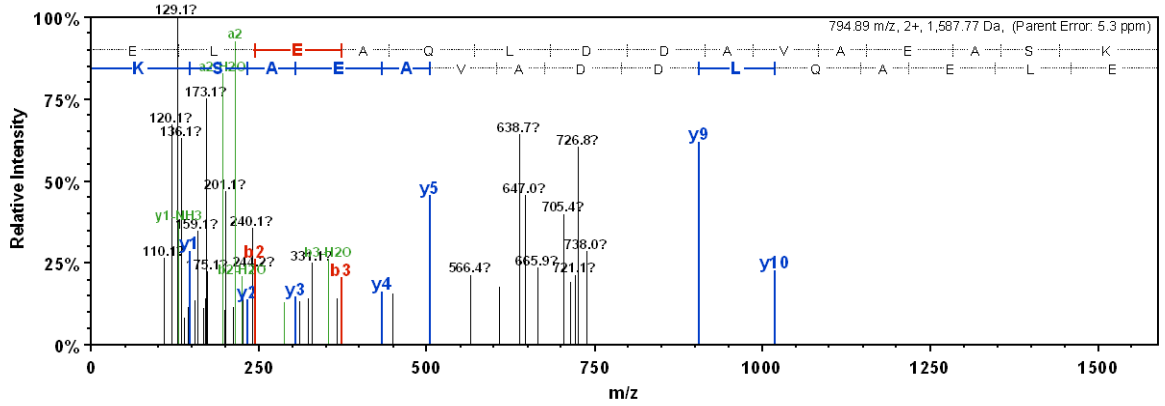

Peptide Sequence: (K)AILTAAIVDADR(I)

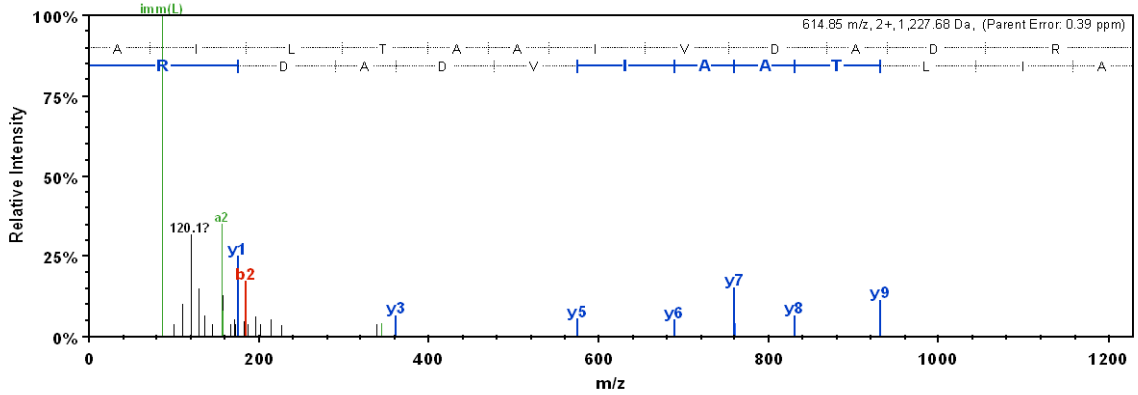

Figure A3.9: The annotated spectra of MRCKB peptides identified by MS/MS analysis, shown in figure A3.5. A representation of the peptide fragments identified is shown with the peptide sequence on top of each spectrum.

SRPK1_HUMAN (100%), 74,326.0 Da
SRSF protein kinase 1 OS=Homo sapiens GN=SRPK1 PE=1 SV=2
3 exclusive unique peptides, 3 exclusive unique spectra, 3 total spectra, 39/655 amino acids (6% coverage)

M E R K V L A L Q A R K K R T K A K K D K A Q R K S E T Q H R G S A P H S E S D L P E Q E E E E I L G
S D D D E Q E D P N D Y C K G G Y H L V K I G D L F N G R Y H V I R K L G W G H F S T V W L S W D I
Q G K K F V A M K V V K **S A E H Y T E T** **A L D E I R** L L K S V R N S D P N D P N R **E M V V Q L L D D**
F K I S G V N G T H I C M V F E V L G H H L L K W I I K S N Y Q G L P L P C V K K I I Q Q V L Q G L
D Y L H T K C R I I H T D I K P E N I L L S V N E Q Y I R R L A A E A T E W Q R S G A P P P S G S A
V S T A P Q P K P A D K M S K N K K K K L K K K Q K R Q A E L L E K R M Q E I E E M E K E S G P G Q
K R P N K Q E E S E S P V E R P L K E N P P N K M T Q E K L E E S S T I G Q D Q T L M E R D T E G G
A A E I N C N G V I E V I N Y T Q N S N N E T L R H K E D L H N A N D C D V Q N L N Q E S S F L S S
Q N G D S S T S Q E T D S C T P I T S E V S D T M V C Q S S S T V G Q S F S E Q H I S Q L Q E S I R
A E I P C E D E Q E Q E H N G P L D N K G K **S T A G N F L V** **N P L E P K** N A E K L K V K I A D L G N
A C W V H K H F T E D I Q T R Q Y R S L E V L I G S G Y N T P A D I W S T A C M A F E L A T G D Y L
F E P H S G E E Y T R D E D H I A L I I E L L G K V P R K L I V A G K Y S K E F F T K K G D L K H I
T K L K P W G L F E V L V E K Y E W S Q E E A A G F T D F L L P M L E L I P E K R A T A A E C L R H
P W L N S

Figure A3.10: Primary sequence of SRPK1 protein identified in the crosslinked IP experiments. Amino acids observed in the MS/MS analysis are highlighted in yellow, while modified amino acids are in green (phosphorylation (S or T) or oxidation (M)). The parameters set were protein threshold-90%, peptide threshold-99.9%, with minimum number of peptides set to 1.

Peptide sequence: (K)SAEHYTETALDEIR(L)

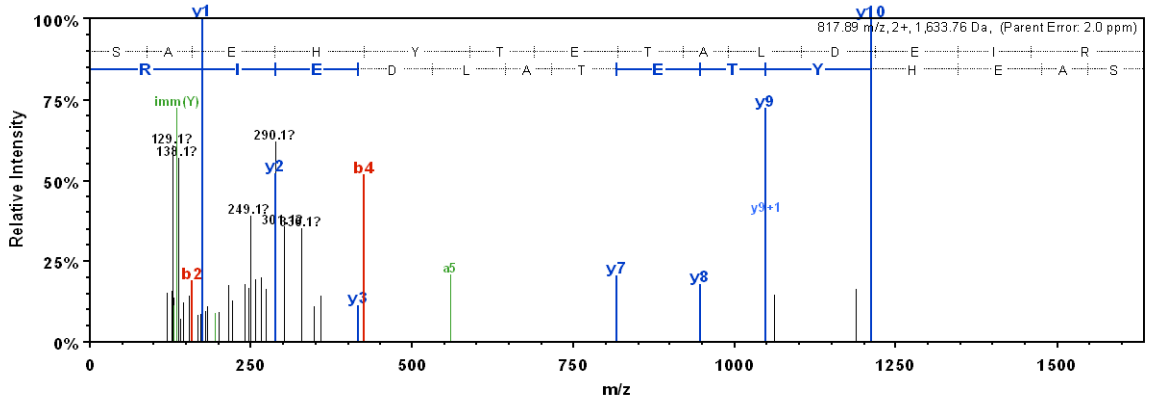

Peptide sequence: (R)EMVVQLLDDFK(I)

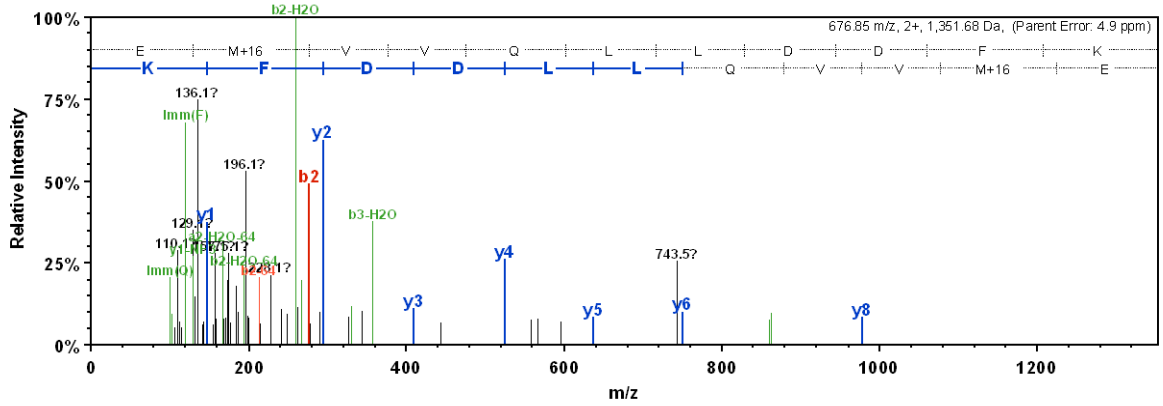

Peptide sequence: (K)STAGNFLVNPLEPK(N)

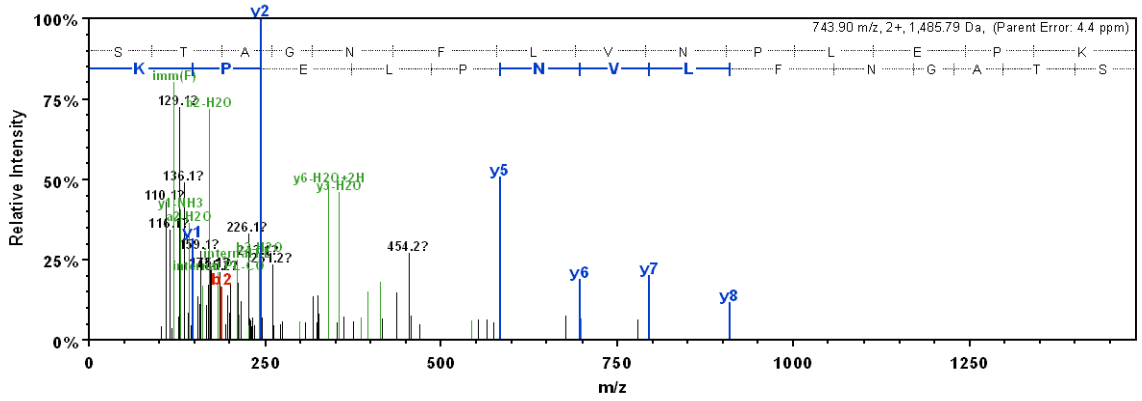

Figure A3.11: The annotated spectra of SRPK1 peptides identified by MS/MS analysis, shown in figure A3.7. A representation of the peptide fragments identified is shown with the peptide sequence on top of each spectrum.

E2AK2_HUMAN (100%), 62,097.1 Da
Interferon-induced, double-stranded RNA-activated protein kinase OS=Homo sapiens GN=EIF2AK2 PE=1 SV=2
2 exclusive unique peptides, 2 exclusive unique spectra, 3 total spectra, 23/551 amino acids (4% coverage)

M A G D L S A G F F M E E L N T Y R Q K Q G V V L K Y Q E L P N S G P P H D R R F T F Q V I I D G R
E F P E G E G R S K K E A K N A A A K L A V E I L N K E K K A V S P L L L T T T N S S E G L S M G N
Y I G L I N R I A Q K K R L T V N Y E Q C A S G V H G P E G F H Y K C K M G Q K E Y S I G T G S T K
Q E A K Q L A A K L A Y L Q I L S E E T S V K S D Y L S S G S F A T T C E S Q S N S L V T S T L A S
E S S S E G D F S A D T S E I N S N S D S L N S S S L L M N G L R N N Q R K A K R S L A P R F D L P
D M K E T K Y T V D K R F G M D F K E I E L I G S G G F G Q V F K A K H R I D G K T Y V I K R V K Y
N N E K A E R E V K A L A K L D H V N I V H Y N G C W D G F D Y D P E T S D D S L E S S D Y D P E N
S K N S S R S K T K C L F I Q M E F C D K G T L E Q W I E K R R G E K L D K **V L** **A L E L F E Q I T K**
G V D Y I H S K K L I H R D L K P S N I F L V D T K Q V K **I** **G D F G L V T S L K** N D G K R T R S K G
T L R Y M S P E Q I S S Q D Y G K E V D L Y A L G L I L A E L L H V C D T A F E T S K F F T D L R D
G I I S D I F D K K E K T L L Q K L L S K K P E D R P N T S E I L R T L T V W K K S P E K N E R H T
C

Figure A3.12: Primary sequences of E2AK2 protein identified in the crosslinked IP experiments. Amino acids observed in the MS/MS analysis were highlighted in yellow, while modified amino acids were in green (phosphorylation (S or T) or oxidation (M)). The parameters set were protein threshold-90%, peptide threshold-99.9%, with minimum number of peptides set to 1.

Peptide Sequence: (K)VLALELFEQITK(G)

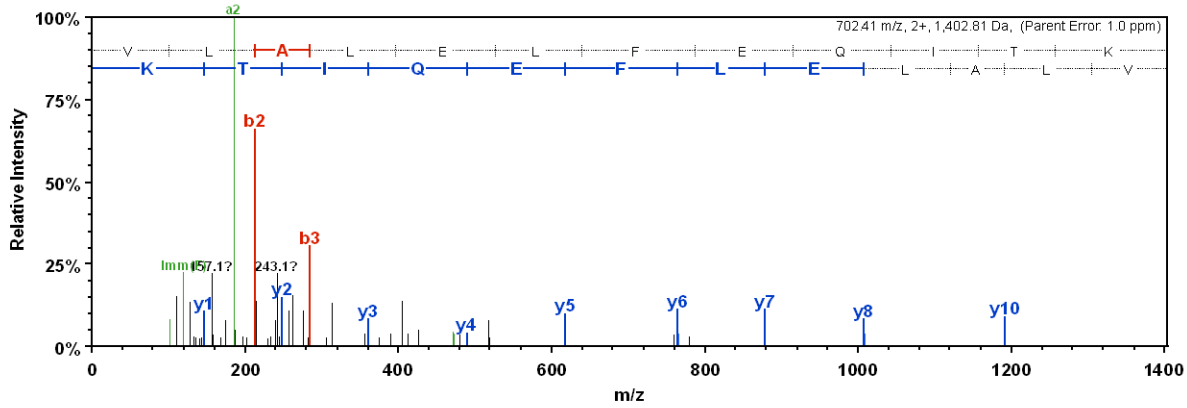

Peptide Sequence: (K)VLALELFEQITK(G)

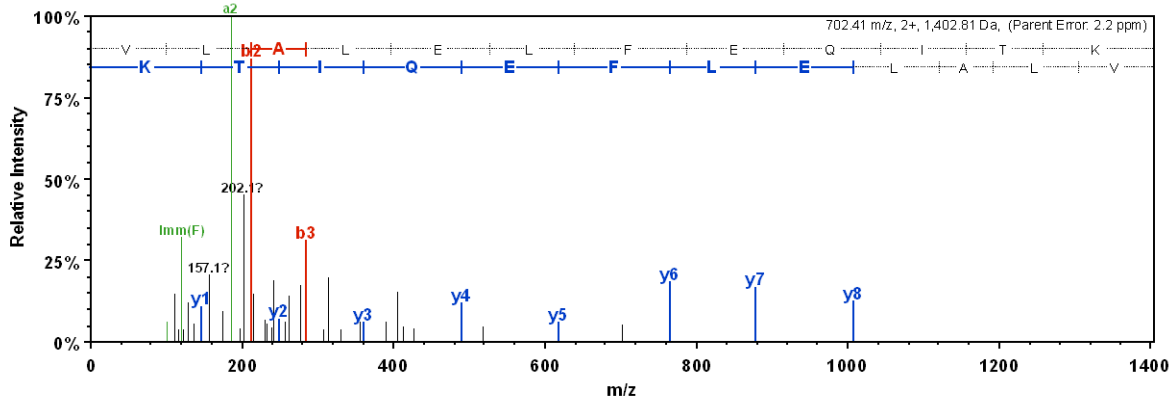

Peptide Sequence: (K)IGDFGLVTSLK(N)

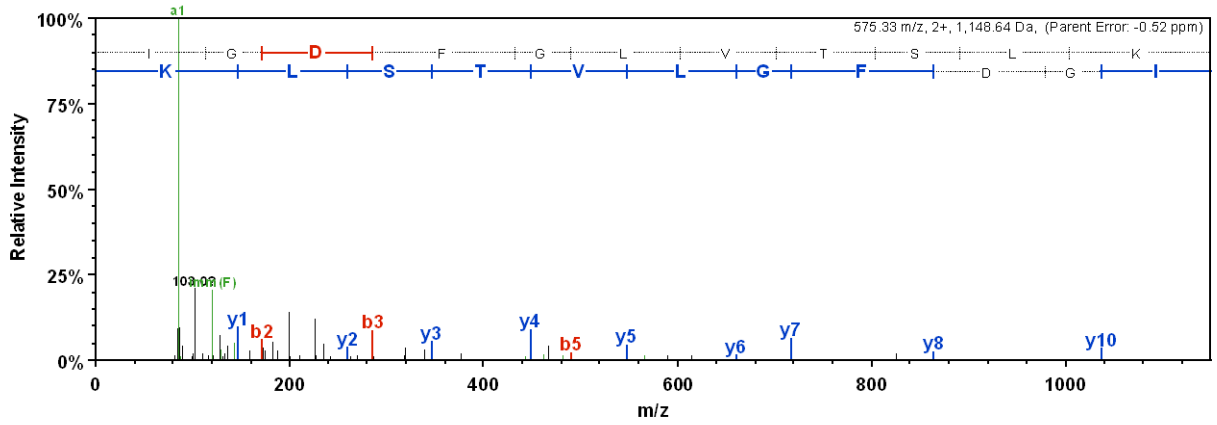

Figure A3.13: The annotated spectra of E2AK2 peptides identified by MS/MS analysis, shown in figure A3.9. A representation of the peptide fragments identified is shown with the peptide sequence on top of each spectrum.

CDK12_HUMAN (100%), 164,159.1 Da
Cyclin-dependent kinase 12 OS=Homo sapiens GN=CDK12 PE=1 SV=2
2 exclusive unique peptides, 2 exclusive unique spectra, 2 total spectra, 27/1490 amino acids (2% coverage)

M P N S E R H G G K K D G S G G A S G T L Q P S S G G G G S S N S R E R H R L V S K H K R H K S K H S
K D M G L V T P E A A S L G T V I K P L V E Y D D I S S D S D T F S D D M A F K L D R R E N D E R R
G S D R S D R L H K H R H H Q H R R S R D L L K A K Q T E K E K S Q E V S S K S G S M K D R I S G S
S K R S N E E T D D Y G K A Q V A K S S S K E S R S S K L H K E K T R K E R E L K S G H K D R S K S
H R K R E T P K S Y K T V D S P K R R S R S P H R K W S D S S K Q D D S P S G A S Y G Q D Y D L S P
S R S H T S S N Y D S Y K K S P G S T S R R Q S V S P P Y K E P S A Y Q S S T R S P S P S Y S R R Q R
S V S P Y S R R R S S S Y E R S G S Y S G R S P S P Y G R R R S S S P F L S K R S L S R S P L P S R
K S M K S R S R S P A Y S R H S S S H S K K K R S S S R S R H S S I S P V R L P L N S S L G A E L S
R K K K E R A A A A A A K M D G K E S K G S P V F L P R K E N S S V E A K D S G L E S K K L P R S
V K L E K **S A P D T** **E L V N V T H L N T** **E V K** N S S D T G K V K L D E N S E K H L V K D L K A Q G T
R D S K P I A L K E E I V T P K E T E T S E K E T P P P L P T I A S P P P P L P T T T P P P Q T P P
L P P L P P I P A L P Q Q P P L P P S Q P A F S Q V P A S S T S T L P P S T H S K T S A V S S Q A N
S O P P V O V S V K T O V S V T A A I P H L K T S T L P P L P L P P L L P G D D D M D S P K E T L P
S K P V K K E K E Q R T R H L L T D L P L P P E L P G G D L S P P D S P E P K A I T P P Q Q P Y K K
R P K I C C P R Y G E R R Q T E S D W G K R C V D K F D I I G I I G E G T Y G Q V Y K A K D K D T G
E L V A L K K V R L D N E K **E G F P I T** **A I R** E I K I L R Q L I H R S V V N M K E I V T D K Q D A L
D F K K D K G A F Y L V F E Y M D H D L M G L L E S G L V H F S E D H I K S F M K Q L M E G L E Y C
H K K N F L H R D I K C S N I L L N N S G Q I K L A D F G L A R L Y N S E E S R P Y T N K V I T L W
Y R P P E L L L G E E R Y T P A I D V W S C G C I L G E L F T K K P I F Q A N L E L A Q L E L I S R
L C G S P C P A V W P D V I K L P Y F N T M K P K K Q Y R R R L R E E F S F I P S A A L D L L D H M
L T L D P S K R C T A E Q T L Q S D F L K D V E L S K M A P P D L P H W Q D C H E L W S K K R R R Q
R Q S G V V V E E P P P S K T S R K E T T S G T S T E P V K N S S P A P P Q P A P G K V E S G A G D
A I G L A D I T Q Q L N Q S E L A V L L N L L Q S Q T D L S I P Q M A Q L L N I H S N P E M Q Q Q L
E A L N Q S I S A L T E A T S Q Q Q D S E T M A P E E S L K E A P S A P V I L P S A E Q T T L E A S
S T P A D M Q N I L A V L L S Q L M K T Q E P A G S L E E N N S D K N S G P Q G P R R T P T M P Q E
E A A A C P P H I L P P E K R P P E P P G P P P P P P P P P L V E G D L S S A P Q E L N P A V T A A
L L Q L L S Q P E A E P P G H L P H E H Q A L R P M E Y S T R P R P N R T Y G N T D G P E T G F S A
I D T D E R N S G P A L T E S L V Q T L V K N R T F S G S L S H L G E S S S Y Q G T G S V Q F P G D
Q D L R F A R V P L A L H P V V G Q P F L K A E G S S N S V V H A E T K L Q N Y G E L G P G T T G A
S S S G A G L H W G G P T Q S S A Y G K L Y R G P T R V P P R G G R G R G V P Y

Figure A3.14: Primary sequences of CDK12 protein identified in the crosslinked IP experiments. Amino acids observed in the MS/MS analysis are highlighted in yellow, while modified amino acids are in green (phosphorylation (S or T) or oxidation (M)). The parameters set were protein threshold-90%, peptide threshold-99.9%, with minimum number of peptides set to 1.

Peptide Sequence: (K)SAPDTELVNVTHLNTEVK(N)

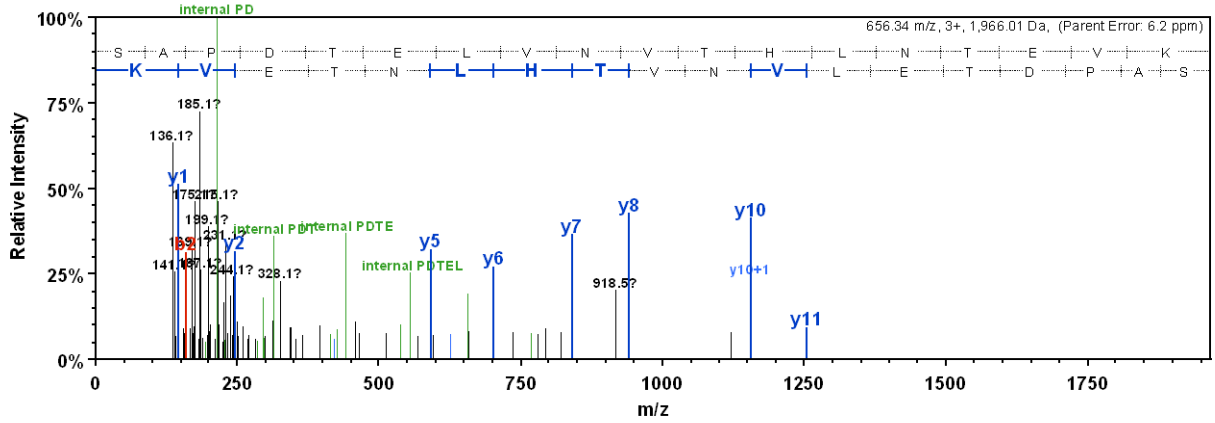

Peptide Sequence: (K)EGFPITAIR(E)

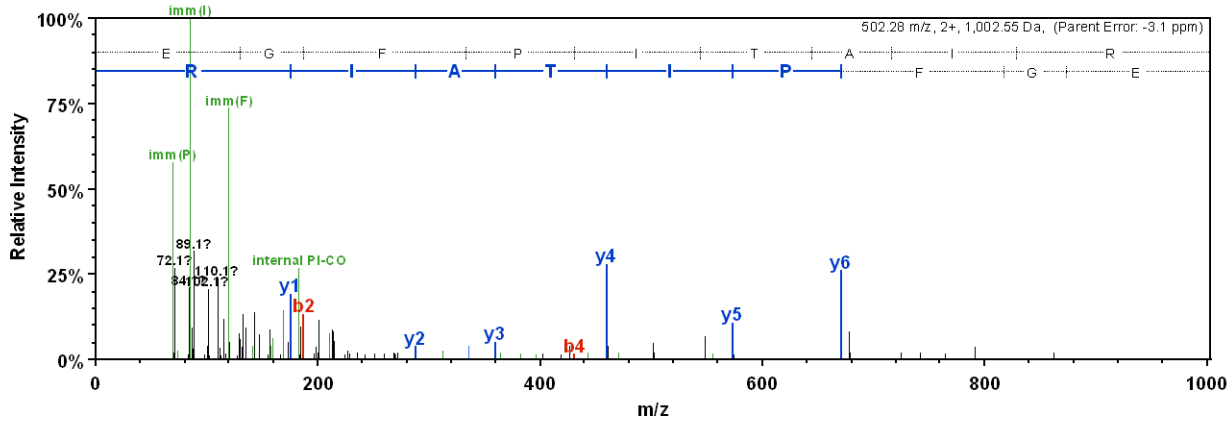

Figure A3.15: The annotated spectra of CDK12 peptides identified by MS/MS analysis, shown in figure A3.11. A representation of the peptide fragments identified is shown with the peptide sequence on top of each spectrum.

APPENDIX C

ELSEVIER LICENSE
TERMS AND CONDITIONS

Nov 11, 2013

This is a License Agreement between Satish Garre ("You") and Elsevier ("Elsevier") provided by Copyright Clearance Center ("CCC"). The license consists of your order details, the terms and conditions provided by Elsevier, and the payment terms and conditions.

All payments must be made in full to CCC. For payment instructions, please see information listed at the bottom of this form.

Supplier	Elsevier Limited The Boulevard,Langford Lane Kidlington,Oxford,OX5 1GB,UK
Registered Company Number	1982084
Customer name	Satish Garre
Customer address	4757 anthony wayne dr, apt 10 DETROIT, MI 48201
License number	3186091178308
License date	Jul 11, 2013
Licensed content publisher	Elsevier
Licensed content publication	Cell
Licensed content title	Modes of p53 Regulation
Licensed content author	Jan-Philipp Kruse,Wei Gu
Licensed content date	15 May 2009
Licensed content volume number	137
Licensed content issue number	4
Number of pages	14
Start Page	609
End Page	622
Type of Use	reuse in a thesis/dissertation
Portion	figures/tables/illustrations
Number of figures/tables/illustrations	1
Format	both print and electronic
Are you the author of this Elsevier article?	No
Will you be translating?	No

Title of your thesis/dissertation	SYNTHESIS AND APPLICATION OF ATP ANALOGS FOR PHOSPHORYLATION-DEPENDENT KINASE-SUBSTRATE CROSSLINKING
Expected completion date	Aug 2013
Estimated size (number of pages)	
Elsevier VAT number	GB 494 6272 12
Permissions price	0.00 USD
VAT/Local Sales Tax	0.00 USD / 0.00 GBP
Total	0.00 USD
Terms and Conditions	

INTRODUCTION

1. The publisher for this copyrighted material is Elsevier. By clicking "accept" in connection with completing this licensing transaction, you agree that the following terms and conditions apply to this transaction (along with the Billing and Payment terms and conditions established by Copyright Clearance Center, Inc. ("CCC"), at the time that you opened your Rightslink account and that are available at any time at http://myaccount.copyright.com).

GENERAL TERMS

2. Elsevier hereby grants you permission to reproduce the aforementioned material subject to the terms and conditions indicated.

3. Acknowledgement: If any part of the material to be used (for example, figures) has appeared in our publication with credit or acknowledgement to another source, permission must also be sought from that source. If such permission is not obtained then that material may not be included in your publication/copies. Suitable acknowledgement to the source must be made, either as a footnote or in a reference list at the end of your publication, as follows:

"Reprinted from Publication title, Vol /edition number, Author(s), Title of article / title of chapter, Pages No., Copyright (Year), with permission from Elsevier [OR APPLICABLE SOCIETY COPYRIGHT OWNER]." Also Lancet special credit - "Reprinted from The Lancet, Vol. number, Author(s), Title of article, Pages No., Copyright (Year), with permission from Elsevier."

4. Reproduction of this material is confined to the purpose and/or media for which permission is hereby given.

5. Altering/Modifying Material: Not Permitted. However figures and illustrations may be altered/adapted minimally to serve your work. Any other abbreviations, additions, deletions and/or any other alterations shall be made only with prior written authorization of Elsevier Ltd. (Please contact Elsevier at permissions@elsevier.com)

6. If the permission fee for the requested use of our material is waived in this instance, please be advised that your future requests for Elsevier materials may attract a fee.

JOHN WILEY AND SONS LICENSE TERMS AND CONDITIONS

Nov 11, 2013

This is a License Agreement between Satish Garre ("You") and John Wiley and Sons ("John Wiley and Sons") provided by Copyright Clearance Center ("CCC"). The license consists of your order details, the terms and conditions provided by John Wiley and Sons, and the payment terms and conditions.

All payments must be made in full to CCC. For payment instructions, please see information listed at the bottom of this form.

License Number	3197680615278
License date	Jul 28, 2013
Licensed content publisher	John Wiley and Sons
Licensed content publication	Angewandte Chemie International Edition
Licensed content title	Phosphorylation-Dependent Kinase–Substrate Cross-Linking
Licensed copyright line	Copyright © 2010 WILEY-VCH Verlag GmbH & Co. KGaA, Weinheim
Licensed content author	Sujit Suwal,Mary Kay H. Pflum
Licensed content date	Jan 27, 2010
Start page	1627
End page	1630
Type of use	Dissertation/Thesis
Requestor type	University/Academic
Format	Electronic
Portion	Figure/table
Number of figures/tables	1
Original Wiley figure/table number(s)	Figure 2
Will you be translating?	No
Total	0.00 USD
Terms and Conditions	

TERMS AND CONDITIONS

This copyrighted material is owned by or exclusively licensed to John Wiley & Sons, Inc. or one of its group companies (each a "Wiley Company") or a society for whom a Wiley Company has exclusive publishing rights in relation to a particular journal (collectively "WILEY"). By clicking "accept" in connection with completing this licensing transaction, you agree that the following terms and conditions apply to this transaction (along with the billing and payment terms and conditions

Date: Tue, 30 Jul 2013 06:20:20 -0600 [07/30/2013 08:20:20 AM EST]
From: Rachel Kramer Green <kramer@rcsb.rutgers.edu>

To: gvrsatish@chem.wayne.edu
Cc: info@rcsb.org

Reply-To: info <info@rcsb.org>
Subject: Re: Permission to use molecule of the month illustration (help-4367)

Thank you for your email message.

You have our permission. Please provide attribution to David S. Goodsell and the RCSB PDB.

For example: Image from the RCSB PDB September 2008 Molecule of the Month feature by David Goodsell (doi: 10.2210/rcsb_pdb/mom_2008_9).

Our policies and citation information are available at:
http://www.pdb.org/pdb/static.do?p=general_information/about_pdb/policies_references.html

High resolution tif images can be found at:
http://www.rcsb.org/pdb/static.do?p=education_discussion/molecule_of_the_month/images.jsp

Sincerely,
Rachel Green

Rachel Kramer Green, Ph.D.

RCSB PDB

kramer@rcsb.rutgers.edu

Twitter: https://twitter.com/#!/buildmodels

Facebook: http://www.facebook.com/RCSBPDB

On 7/29/2013 9:02 AM, gvrsatish@chem.wayne.edu wrote:

> Hi,
> My name is Satish Garre, PhD student at Wayne State University. I would like to get permission to use figures in the molecule of the month-p53, for my thesis.
> http://www.rcsb.org/pdb/101/motm.do?momID=31
>
> I would use only the two illustrations.
>
> I would like to know if I need any copyright permission to use crystal structure images from PDB, after I cite the PDB ID and original article.
>
> Thank you
> Satish

REFERENCES

(1) Walsh, C. T.; Garneau-Tsodikova, S.; Gatto, G. J.: Protein Posttranslational Modifications: The Chemistry of Proteome Diversifications. *Angewandte Chemie International Edition* **2005**, *44*, 7342-7372.

(2) Levene, P. A.; Alsberg, C. L.: The Cleavage Products Of Vitellin. *Journal of Biological Chemistry* **1906**, *2*, 127-133.

(3) Lipmann, F. A.; Levene, P. A.: Serinephosphoric Acid Obtained On Hydrolysis Of Vitellinic Acid. *Journal of Biological Chemistry* **1932**, *98*, 109-114.

(4) Burnett, G.; Kennedy, E. P.: The Enzymatic Phosphorylation Of Proteins. *Journal of Biological Chemistry* **1954**, *211*, 969-980.

(5) Eckhart, W.; Hutchinson, M. A.; Hunter, T.: An activity phosphorylating tyrosine in polyoma T antigen immunoprecipitates. *Cell* **1979**, *18*, 925-933.

(6) Hunter, T.: Protein kinases and phosphatases: the yin and yang of protein phosphorylation and signaling. *Cell* **1995**, *80*, 225-36.

(7) Cohen, P.: Protein kinases--the major drug targets of the twenty-first century? *Nature reviews. Drug discovery* **2002**, *1*, 309-15.

(8) Barford, D.: Protein phosphatases. *Current opinion in structural biology* **1995**, *5*, 728-34.

(9) Lawrence, D. S.: Chemical biology of signal transduction. *Accounts of chemical research* **2003**, *36*, 353-4.

(10) Lawrence, D. S.: Chemical probes of signal-transducing proteins. *Accounts of chemical research* **2003**, *36*, 401-9.

(11) Ingebritsen, T. S.; Cohen, P.: Protein phosphatases: properties and role in cellular regulation. *Science* **1983**, *221*, 331-8.

(12) Wolanin, P.; Thomason, P.; Stock, J.: Histidine protein kinases: key signal transducers outside the animal kingdom. *Genome Biology* **2002**, *3*, reviews3013.1 - reviews3013.8.

(13) Besant, P.: Focus on Phosphoarginine and Phospholysine. *Current protein & peptide science* **2009**, *10*, 536-550.

(14) Matthews, H. R.; Huebner, V. D.: Nuclear protein kinases. *Molecular and cellular biochemistry* **1984**, *59*, 81-99.

(15) Cohen, P.: The regulation of protein function by multisite phosphorylation--a 25 year update. *Trends in biochemical sciences* **2000**, *25*, 596-601.

(16) Manning, G.; Whyte, D. B.; Martinez, R.; Hunter, T.; Sudarsanam, S.: The protein kinase complement of the human genome. *Science* **2002**, *298*, 1912-34.

(17) Manning, G.; Plowman, G. D.; Hunter, T.; Sudarsanam, S.: Evolution of protein kinase signaling from yeast to man. *Trends in biochemical sciences* **2002**, *27*, 514-20.

(18) Sengupta, S.; Harris, C. C.: p53: traffic cop at the crossroads of DNA repair and recombination. *Nature reviews. Molecular cell biology* **2005**, *6*, 44-55.

(19) Yosef, S.: ATM and related protein kinases: safeguarding genome integrity. *Nature Reviews Cancer* **2003**, *3*, 155-168.

(20) Zha, S.; Boboila, C.; Alt, F. W.: Mre11: roles in DNA repair beyond homologous recombination. *Nature structural & molecular biology* **2009**, *16*, 798-800.

(21) Matsuoka, S.; Huang, M.; Elledge, S. J.: Linkage of ATM to cell cycle regulation by the Chk2 protein kinase. *Science* **1998**, *282*, 1893-7.

(22) Shieh, S. Y.; Ahn, J.; Tamai, K.; Taya, Y.; Prives, C.: The human homologs of checkpoint kinases Chk1 and Cds1 (Chk2) phosphorylate p53 at multiple DNA damage-inducible sites. *Genes & development* **2000**, *14*, 289-300.

(23) Chehab, N. H.; Malikzay, A.; Stavridi, E. S.; Halazonetis, T. D.: Phosphorylation of Ser-20 mediates stabilization of human p53 in response to DNA damage. *Proceedings of the National Academy of Sciences* **1999**, *96*, 13777-13782.

(24) Shieh, S. Y.; Ikeda, M.; Taya, Y.; Prives, C.: DNA damage-induced phosphorylation of p53 alleviates inhibition by MDM2. *Cell* **1997**, *91*, 325-34.

(25) Dumaz, N.; Meek, D. W.: Serine15 phosphorylation stimulates p53 transactivation but does not directly influence interaction with HDM2. *The EMBO journal* **1999**, *18*, 7002-10.

(26) de Lange, J.; Verlaan-de Vries, M.; Teunisse, A. F.; Jochemsen, A. G.: Chk2 mediates RITA-induced apoptosis. *Cell death and differentiation* **2012**, *19*, 980-9.

(27) Meek, D. W.: Tumour suppression by p53: a role for the DNA damage response? *Nature reviews. Cancer* **2009**, *9*, 714-23.

(28) Chehab, N. H.; Malikzay, A.; Stavridi, E. S.; Halazonetis, T. D.: Phosphorylation of Ser-20 mediates stabilization of human p53 in response to DNA damage. *Proc Natl Acad Sci U S A* **1999**, *96*, 13777-82.

(29) Banin, S.; Moyal, L.; Shieh, S.-Y.; Taya, Y.; Anderson, C. W.; Chessa, L.; Smorodinsky, N. I.; Prives, C.; Reiss, Y.; Shiloh, Y.; Ziv, Y.: Enhanced Phosphorylation of p53 by ATM in Response to DNA Damage. *Science* **1998**, *281*, 1674-1677.

(30) Chrivia, J. C.; Kwok, R. P.; Lamb, N.; Hagiwara, M.; Montminy, M. R.; Goodman, R. H.: Phosphorylated CREB binds specifically to the nuclear protein CBP. *Nature* **1993**, *365*, 855-9.

(31) Parker, D.; Ferreri, K.; Nakajima, T.; LaMorte, V. J.; Evans, R.; Koerber, S. C.; Hoeger, C.; Montminy, M. R.: Phosphorylation of CREB at Ser-133 induces complex formation with

CREB-binding protein via a direct mechanism. *Molecular and cellular biology* **1996**, *16*, 694-703.

(32) Munstermann, U.; Fritz, G.; Seitz, G.; Lu, Y. P.; Schneider, H. R.; Issinger, O. G.: Casein kinase II is elevated in solid human tumours and rapidly proliferating non-neoplastic tissue. *European journal of biochemistry / FEBS* **1990**, *189*, 251-7.

(33) Chang, H. W.; Aoki, M.; Fruman, D.; Auger, K. R.; Bellacosa, A.; Tsichlis, P. N.; Cantley, L. C.; Roberts, T. M.; Vogt, P. K.: Transformation of chicken cells by the gene encoding the catalytic subunit of PI 3-kinase. *Science* **1997**, *276*, 1848-50.

(34) Mendelsohn, J.; Baselga, J.: Status of epidermal growth factor receptor antagonists in the biology and treatment of cancer. *Journal of clinical oncology : official journal of the American Society of Clinical Oncology* **2003**, *21*, 2787-99.

(35) Zdychova, J.; Komers, R.: Emerging role of Akt kinase/protein kinase B signaling in pathophysiology of diabetes and its complications. *Physiological research / Academia Scientiarum Bohemoslovaca* **2005**, *54*, 1-16.

(36) Blume-Jensen, P.; Hunter, T.: Oncogenic kinase signalling. *Nature* **2001**, *411*, 355-65.

(37) Karin, M.; Hunter, T.: Transcriptional control by protein phosphorylation: signal transmission from the cell surface to the nucleus. *Current biology : CB* **1995**, *5*, 747-57.

(38) Nowell, P. C.; Hungerford, D.: A Minute Chromosome in Human Chronic Granulocytic Leukemia. *Science* **1960**, *132*, 1497.

(39) Heisterkamp, N.; Groffen, J.; Stephenson, J. R.; Spurr, N. K.; Goodfellow, P. N.; Solomon, E.; Carritt, B.; Bodmer, W. F.: Chromosomal localization of human cellular homologues of two viral oncogenes. *Nature* **1982**, *299*, 747-749.

(40) Daley, G. Q.; Van Etten, R. A.; Baltimore, D.: Induction of chronic myelogenous leukemia in mice by the P210bcr/abl gene of the Philadelphia chromosome. *Science* **1990**, *247*, 824-830.

(41) Ren, R.: Mechanisms of BCR-ABL in the pathogenesis of chronic myelogenous leukaemia. *Nature Reviews Cancer* **2005**, *5*, 172-183.

(42) Hehlmann, R.; Hochhaus, A.; Baccarani, M.: Chronic myeloid leukaemia. *Lancet* **2007**, *370*, 342-50.

(43) Druker, B. J.; Tamura, S.; Buchdunger, E.; Ohno, S.; Segal, G. M.; Fanning, S.; Zimmermann, J.; Lydon, N. B.: Effects of a selective inhibitor of the Abl tyrosine kinase on the growth of Bcr-Abl positive cells. *Nature medicine* **1996**, *2*, 561-6.

(44) Capdeville, R.; Buchdunger, E.; Zimmermann, J.; Matter, A.: Glivec (STI571, imatinib), a rationally developed, targeted anticancer drug. *Nature reviews. Drug discovery* **2002**, *1*, 493-502.

(45) Garber, K.: The second wave in kinase cancer drugs. *Nature biotechnology* **2006**, *24*, 127-30.

(46) Cohen, P.; Alessi, D. R.: Kinase Drug Discovery – What's Next in the Field? *ACS chemical biology* **2012**, *8*, 96-104.

(47) Berman, E.; Nicolaides, M.; Maki, R. G.; Fleisher, M.; Chanel, S.; Scheu, K.; Wilson, B. A.; Heller, G.; Sauter, N. P.: Altered bone and mineral metabolism in patients receiving imatinib mesylate. *The New England journal of medicine* **2006**, *354*, 2006-13.

(48) Heinrich, M. C.; Griffith, D. J.; Druker, B. J.; Wait, C. L.; Ott, K. A.; Zigler, A. J.: Inhibition of c-kit receptor tyrosine kinase activity by STI 571, a selective tyrosine kinase inhibitor. *Blood* **2000**, *96*, 925-32.

(49) Mughal, T. I.; Schrieber, A.: Principal long-term adverse effects of imatinib in patients with chronic myeloid leukemia in chronic phase. *Biologics : targets & therapy* **2010**, *4*, 315-23.

(50) Ubersax, J. A.; Ferrell, J. E., Jr.: Mechanisms of specificity in protein phosphorylation. *Nature reviews. Molecular cell biology* **2007**, *8*, 530-41.

(51) Allende, J. E.; Allende, C. C.: Protein kinases. 4. Protein kinase CK2: an enzyme with multiple substrates and a puzzling regulation. *FASEB journal : official publication of the Federation of American Societies for Experimental Biology* **1995**, *9*, 313-23.

(52) Roskoski, R., Jr.: Src protein-tyrosine kinase structure and regulation. *Biochemical and biophysical research communications* **2004**, *324*, 1155-64.

(53) Adams, J. A.: Kinetic and catalytic mechanisms of protein kinases. *Chemical reviews* **2001**, *101*, 2271-90.

(54) Hanks, S.; Quinn, A.; Hunter, T.: The protein kinase family: conserved features and deduced phylogeny of the catalytic domains. *Science* **1988**, *241*, 42-52.

(55) Zervas, C. G.; Brown, N. H.: Integrin Adhesion: When Is a Kinase a Kinase? *Current Biology* **2002**, *12*, R350-R351.

(56) Kroiher, M.; Miller, M. A.; Steele, R. E.: Deceiving appearances: signaling by "dead" and "fractured" receptor protein-tyrosine kinases. *BioEssays : news and reviews in molecular, cellular and developmental biology* **2001**, *23*, 69-76.

(57) Zheng, J.; Trafny, E. A.; Knighton, D. R.; Xuong, N. H.; Taylor, S. S.; Ten Eyck, L. F.; Sowadski, J. M.: 2.2 A refined crystal structure of the catalytic subunit of cAMP-dependent protein kinase complexed with MnATP and a peptide inhibitor. *Acta crystallographica. Section D, Biological crystallography* **1993**, *49*, 362-5.

(58) Knighton, D. R.; Zheng, J. H.; Ten Eyck, L. F.; Ashford, V. A.; Xuong, N. H.; Taylor, S. S.; Sowadski, J. M.: Crystal structure of the catalytic subunit of cyclic adenosine monophosphate-dependent protein kinase. *Science* **1991**, *253*, 407-14.

(59) Madhusudan; Trafny, E. A.; Xuong, N. H.; Adams, J. A.; Ten Eyck, L. F.; Taylor, S. S.; Sowadski, J. M.: cAMP-dependent protein kinase: crystallographic insights into substrate recognition and phosphotransfer. *Protein science : a publication of the Protein Society* **1994**, *3*, 176-87.

(60) Cole, P. A.; Courtney, A. D.; Shen, K.; Zhang, Z.; Qiao, Y.; Lu, W.; Williams, D. M.: Chemical approaches to reversible protein phosphorylation. *Accounts of chemical research* **2003**, *36*, 444-52.

(61) Grant, B. D.; Adams, J. A.: Pre-steady-state kinetic analysis of cAMP-dependent protein kinase using rapid quench flow techniques. *Biochemistry* **1996**, *35*, 2022-9.

(62) Ablooglu, A. J.; Till, J. H.; Kim, K.; Parang, K.; Cole, P. A.; Hubbard, S. R.; Kohanski, R. A.: Probing the catalytic mechanism of the insulin receptor kinase with a tetrafluorotyrosine-containing peptide substrate. *The Journal of biological chemistry* **2000**, *275*, 30394-8.

(63) Wu, J. J.; Afar, D. E.; Phan, H.; Witte, O. N.; Lam, K. S.: Recognition of multiple substrate motifs by the c-ABL protein tyrosine kinase. *Combinatorial chemistry & high throughput screening* **2002**, *5*, 83-91.

(64) Meggio, F.; Marin, O.; Pinna, L. A.: Substrate specificity of protein kinase CK2. *Cellular & molecular biology research* **1994**, *40*, 401-409.

(65) Kemp, B. E.; Graves, D. J.; Benjamini, E.; Krebs, E. G.: Role of multiple basic residues in determining the substrate specificity of cyclic AMP-dependent protein kinase. *The Journal of biological chemistry* **1977**, *252*, 4888-94.

(66) Charron, G.; Zhang, M. M.; Yount, J. S.; Wilson, J.; Raghavan, A. S.; Shamir, E.; Hang, H. C.: Robust fluorescent detection of protein fatty-acylation with chemical reporters. *J Am Chem Soc* **2009**, *131*, 4967-75.

(67) Grammel, M.; Luong, P.; Orth, K.; Hang, H. C.: A chemical reporter for protein AMPylation. *J Am Chem Soc* **2011**, *133*, 17103-5.

(68) Hang, H. C.; Wilson, J. P.; Charron, G.: Bioorthogonal chemical reporters for analyzing protein lipidation and lipid trafficking. *Accounts of chemical research* **2011**, *44*, 699-708.

(69) Hwang, Y.; Thompson, P. R.; Wang, L.; Jiang, L.; Kelleher, N. L.; Cole, P. A.: A selective chemical probe for coenzyme A-requiring enzymes. *Angewandte Chemie (International ed. in English)* **2007**, *46*, 7621-4.

(70) Kostiuk, M. A.; Corvi, M. M.; Keller, B. O.; Plummer, G.; Prescher, J. A.; Hangauer, M. J.; Bertozzi, C. R.; Rajaiah, G.; Falck, J. R.; Berthiaume, L. G.: Identification of palmitoylated mitochondrial proteins using a bio-orthogonal azido-palmitate analogue. *FASEB journal : official publication of the Federation of American Societies for Experimental Biology* **2008**, *22*, 721-32.

(71) Lee, B. W.; Sun, H. G.; Zang, T.; Kim, B. J.; Alfaro, J. F.; Zhou, Z. S.: Enzyme-catalyzed transfer of a ketone group from an S-adenosylmethionine analogue: a tool for the functional analysis of methyltransferases. *J Am Chem Soc* **2010**, *132*, 3642-3.

(72) Luo, M.: Current chemical biology approaches to interrogate protein methyltransferases. *ACS chemical biology* **2012**, *7*, 443-63.

(73) Yu, M.; de Carvalho, L. P.; Sun, G.; Blanchard, J. S.: Activity-based substrate profiling for Gcn5-related N-acetyltransferases: the use of chloroacetyl-coenzyme A to identify protein substrates. *J Am Chem Soc* **2006**, *128*, 15356-7.

(74) Lin, C. W.; Ting, A. Y.: Transglutaminase-catalyzed site-specific conjugation of small-molecule probes to proteins in vitro and on the surface of living cells. *J Am Chem Soc* **2006**, *128*, 4542-3.

(75) Khidekel, N.; Arndt, S.; Lamarre-Vincent, N.; Lippert, A.; Poulin-Kerstien, K. G.; Ramakrishnan, B.; Qasba, P. K.; Hsieh-Wilson, L. C.: A chemoenzymatic approach toward the rapid and sensitive detection of O-GlcNAc posttranslational modifications. *J Am Chem Soc* **2003**, *125*, 16162-3.

(76) Dalhoff, C.; Lukinavicius, G.; Klimasauskas, S.; Weinhold, E.: Direct transfer of extended groups from synthetic cofactors by DNA methyltransferases. *Nature chemical biology* **2006**, *2*, 31-2.

(77) Duckworth, B. P.; Zhang, Z.; Hosokawa, A.; Distefano, M. D.: Selective labeling of proteins by using protein farnesyltransferase. *Chembiochem* **2007**, *8*, 98-105.

(78) Goody, R. S.; Eckstein, F.: Thiophosphate analogs of nucleoside di- and triphosphates. *Journal of the American Chemical Society* **1971**, *93*, 6252-6257.

(79) Cassel, D.; Glaser, L.: Resistance to phosphatase of thiophosphorylated epidermal growth factor receptor in A431 membranes. *Proc Natl Acad Sci U S A* **1982**, *79*, 2231-5.

(80) Facemyer, K. C.; Cremo, C. R.: A new method to specifically label thiophosphorylatable proteins with extrinsic probes. Labeling of serine-19 of the regulatory light chain of smooth muscle myosin. *Bioconjug Chem* **1992**, *3*, 408-13.

(81) Gratecos, D.; Fischer, E. H.: Adenosine 5'-O(3-thiotriphosphate) in the control of phosphorylase activity. *Biochemical and biophysical research communications* **1974**, *58*, 960-7.

(82) Parker, L. L.; Schilling, A. B.; Kron, S. J.; Kent, S. B.: Optimizing thiophosphorylation in the presence of competing phosphorylation with MALDI-TOF-MS detection. *Journal of proteome research* **2005**, *4*, 1863-6.

(83) Sun, I. Y.; Johnson, E. M.; Allfrey, V. G.: Affinity purification of newly phosphorylated protein molecules. Thiophosphorylation and recovery of histones H1, H2B, and H3 and the high mobility group protein HMG-1 using adenosine 5'-O-(3-thiotriphosphate) and cyclic AMP-dependent protein kinase. *The Journal of biological chemistry* **1980**, *255*, 742-7.

(84) Cole, P. A.; Burn, P.; Takacs, B.; Walsh, C. T.: Evaluation of the catalytic mechanism of recombinant human Csk (C-terminal Src kinase) using nucleotide analogs and viscosity effects. *The Journal of biological chemistry* **1994**, *269*, 30880-7.

(85) Grace, M. R.; Walsh, C. T.; Cole, P. A.: Divalent ion effects and insights into the catalytic mechanism of protein tyrosine kinase Csk. *Biochemistry* **1997**, *36*, 1874-81.

(86) Blethrow, J. D.; Glavy, J. S.; Morgan, D. O.; Shokat, K. M.: Covalent capture of kinase-specific phosphopeptides reveals Cdk1-cyclin B substrates. *Proc Natl Acad Sci U S A* **2008**, *105*, 1442-7.

(87) Kwon, S. W.; Kim, S. C.; Jaunbergs, J.; Falck, J. R.; Zhao, Y.: Selective enrichment of thiophosphorylated polypeptides as a tool for the analysis of protein phosphorylation. *Molecular & cellular proteomics : MCP* **2003**, *2*, 242-7.

(88) Hiriyanna, K. T.; Baedke, D.; Baek, K. H.; Forney, B. A.; Kordiyak, G.; Ingebritsen, T. S.: Thiophosphorylated substrate analogs are potent active site-directed inhibitors of protein-tyrosine phosphatases. *Anal Biochem* **1994**, *223*, 51-8.

(89) Endo, S.; Critz, S. D.; Byrne, J. H.; Shenolikar, S.: Protein phosphatase-1 regulates outward K+ currents in sensory neurons of Aplysia californica. *Journal of neurochemistry* **1995**, *64*, 1833-40.

(90) Allen, J. J.; Li, M.; Brinkworth, C. S.; Paulson, J. L.; Wang, D.; Hubner, A.; Chou, W. H.; Davis, R. J.; Burlingame, A. L.; Messing, R. O.; Katayama, C. D.; Hedrick, S. M.; Shokat, K. M.: A semisynthetic epitope for kinase substrates. *Nature methods* **2007**, *4*, 511-6.

(91) Allen, J. J.; Lazerwith, S. E.; Shokat, K. M.: Bio-orthogonal affinity purification of direct kinase substrates. *J Am Chem Soc* **2005**, *127*, 5288-9.

(92) Suwal, S.; Senevirathne, C.; Garre, S.; Pflum, M. K. H.: Structural Analysis of ATP Analogues Compatible with Kinase-Catalyzed Labeling. *Bioconjugate Chemistry* **2012**, *23*, 2386-2391.

(93) Green, K. D.; Pflum, M. K.: Exploring kinase cosubstrate promiscuity: monitoring kinase activity through dansylation. *Chembiochem* **2009**, *10*, 234-7.

(94) Green, K. D.; Pflum, M. K. H.: Kinase-Catalyzed Biotinylation for Phosphoprotein Detection. *Journal of the American Chemical Society* **2006**, *129*, 10-11.

(95) Yde, C. W.; Ermakova, I.; Issinger, O. G.; Niefind, K.: Inclining the purine base binding plane in protein kinase CK2 by exchanging the flanking side-chains generates a preference for ATP as a cosubstrate. *Journal of molecular biology* **2005**, *347*, 399-414.

(96) Senevirathne, C.; Green, K. D.; Pflum, M. K. H.: Kinase-Catalyzed Biotinylation of Peptides, Proteins, and Lysates. In *Current Protocols in Chemical Biology*; John Wiley & Sons, Inc., 2009.

(97) Green, K. D.; Pflum, M. K.: Kinase-catalyzed biotinylation for phosphoprotein detection. *J Am Chem Soc* **2007**, *129*, 10-1.

(98) Suwal, S.; Pflum, M. K. H.: Phosphorylation-Dependent Kinase–Substrate Cross-Linking. *Angewandte Chemie International Edition* **2010**, *49*, 1627-1630.

(99) Green, K. D.; Pflum, M. K. H.: Exploring Kinase Cosubstrate Promiscuity: Monitoring Kinase Activity through Dansylation. *ChemBioChem* **2009**, *10*, 234-237.

(100) Cheng, K. Y.; Noble, M. E.; Skamnaki, V.; Brown, N. R.; Lowe, E. D.; Kontogiannis, L.; Shen, K.; Cole, P. A.; Siligardi, G.; Johnson, L. N.: The role of the phospho-CDK2/cyclin A recruitment site in substrate recognition. *The Journal of biological chemistry* **2006**, *281*, 23167-79.

(101) Cook, P. F.; Neville, M. E., Jr.; Vrana, K. E.; Hartl, F. T.; Roskoski, R., Jr.: Adenosine cyclic 3',5'-monophosphate dependent protein kinase: kinetic mechanism for the bovine skeletal muscle catalytic subunit. *Biochemistry* **1982**, *21*, 5794-9.

(102) Wilke, K. E.; Francis, S.; Carlson, E. E.: Activity-based probe for histidine kinase signaling. *J Am Chem Soc* **2012**, *134*, 9150-3.

(103) Attwood, P. V.; Piggott, M. J.; Zu, X. L.; Besant, P. G.: Focus on phosphohistidine. *Amino acids* **2007**, *32*, 145-56.

(104) Martic, S.; Tackenburg, S.; Bilokin, Y.; Golub, A.; Bdzhola, V.; Yarmoluk, S.; Kraatz, H. B.: Electrochemical screening of the indole/quinolone derivatives as potential protein kinase CK2 inhibitors. *Anal Biochem* **2012**, *421*, 617-21.

(105) Kerman, K.; Song, H.; Duncan, J. S.; Litchfield, D. W.; Kraatz, H. B.: Peptide biosensors for the electrochemical measurement of protein kinase activity. *Analytical chemistry* **2008**, *80*, 9395-401.

(106) Martic, S.; Beheshti, S.; Kraatz, H. B.; Litchfield, D. W.: Electrochemical investigations of Tau protein phosphorylations and interactions with Pin1. *Chemistry & biodiversity* **2012**, *9*, 1693-702.

(107) Martic, S.; Gabriel, M.; Turowec, J. P.; Litchfield, D. W.; Kraatz, H. B.: Versatile strategy for biochemical, electrochemical and immunoarray detection of protein phosphorylations. *J Am Chem Soc* **2012**, *134*, 17036-45.

(108) Patricelli, M. P.; Szardenings, A. K.; Liyanage, M.; Nomanbhoy, T. K.; Wu, M.; Weissig, H.; Aban, A.; Chun, D.; Tanner, S.; Kozarich, J. W.: Functional interrogation of the kinome using nucleotide acyl phosphates. *Biochemistry* **2007**, *46*, 350-8.

(109) Patricelli, M. P.; Nomanbhoy, T. K.; Wu, J.; Brown, H.; Zhou, D.; Zhang, J.; Jagannathan, S.; Aban, A.; Okerberg, E.; Herring, C.; Nordin, B.; Weissig, H.; Yang, Q.; Lee, J. D.; Gray, N. S.; Kozarich, J. W.: In situ kinase profiling reveals functionally relevant properties of native kinases. *Chemistry & biology* **2011**, *18*, 699-710.

(110) Garcia, B. A.; Shabanowitz, J.; Hunt, D. F.: Analysis of protein phosphorylation by mass spectrometry. *Methods (San Diego, Calif.)* **2005**, *35*, 256-64.

(111) Sun, T.; Campbell, M.; Gordon, W.; Arlinghaus, R. B.: Preparation and application of antibodies to phosphoamino acid sequences. *Biopolymers* **2001**, *60*, 61-75.

(112) Muszynska, G.; Andersson, L.; Porath, J.: Selective adsorption of phosphoproteins on gel-immobilized ferric chelate. *Biochemistry* **1986**, *25*, 6850-3.

(113) Steinberg, T. H.; Agnew, B. J.; Gee, K. R.; Leung, W. Y.; Goodman, T.; Schulenberg, B.; Hendrickson, J.; Beechem, J. M.; Haugland, R. P.; Patton, W. F.: Global quantitative phosphoprotein analysis using Multiplexed Proteomics technology. *Proteomics* **2003**, *3*, 1128-44.

(114) Reinders, J.; Sickmann, A.: State-of-the-art in phosphoproteomics. *Proteomics* **2005**, *5*, 4052-61.

(115) Mann, M.; Ong, S. E.; Gronborg, M.; Steen, H.; Jensen, O. N.; Pandey, A.: Analysis of protein phosphorylation using mass spectrometry: deciphering the phosphoproteome. *Trends in biotechnology* **2002**, *20*, 261-8.

(116) Amanchy, R.; Periaswamy, B.; Mathivanan, S.; Reddy, R.; Tattikota, S. G.; Pandey, A.: A curated compendium of phosphorylation motifs. *Nature biotechnology* **2007**, *25*, 285-6.

(117) Pflum, M. K.; Tong, J. K.; Lane, W. S.; Schreiber, S. L.: Histone deacetylase 1 phosphorylation promotes enzymatic activity and complex formation. *The Journal of biological chemistry* **2001**, *276*, 47733-41.

(118) Fields, S.; Song, O.: A novel genetic system to detect protein-protein interactions. *Nature* **1989**, *340*, 245-6.

(119) Sambrook, J.; Russell, D. W.: *Molecular cloning : a laboratory manual*; 3rd ed.; Cold Spring Harbor Laboratory Press: NewYork., 2011.

(120) Maly, D. J.; Allen, J. A.; Shokat, K. M.: A Mechanism-Based Cross-Linker for the Identification of Kinase−Substrate Pairs. *Journal of the American Chemical Society* **2004**, *126*, 9160-9161.

(121) Parang, K.; Kohn, J. A.; Saldanha, S. A.; Cole, P. A.: Development of photo-crosslinking reagents for protein kinase–substrate interactions. *FEBS letters* **2002**, *520*, 156-160.

(122) Gavin, A. C.; Bosche, M.; Krause, R.; Grandi, P.; Marzioch, M.; Bauer, A.; Schultz, J.; Rick, J. M.; Michon, A. M.; Cruciat, C. M.; Remor, M.; Hofert, C.; Schelder, M.; Brajenovic, M.; Ruffner, H.; Merino, A.; Klein, K.; Hudak, M.; Dickson, D.; Rudi, T.; Gnau, V.; Bauch, A.; Bastuck, S.; Huhse, B.; Leutwein, C.; Heurtier, M. A.; Copley, R. R.; Edelmann, A.; Querfurth,

E.; Rybin, V.; Drewes, G.; Raida, M.; Bouwmeester, T.; Bork, P.; Seraphin, B.; Kuster, B.; Neubauer, G.; Superti-Furga, G.: Functional organization of the yeast proteome by systematic analysis of protein complexes. *Nature* **2002**, *415*, 141-7.

(123) Babu, M.; Butl, G.; Pogoutse, O.; Li, J.; Greenblatt, J. F.; Emili, A.: Sequential Peptide Affinity Purification System for the Systematic Isolation and Identification of Protein Complexes from Escherichia coli. 2009; Vol. 564; pp 373-400.

(124) Singh, A.; Thornton, E. R.; Westheimer, F. H.: The Photolysis of Diazoacetylchymotrypsin. *Journal of Biological Chemistry* **1962**, *237*, PC3006-PC3008.

(125) Smith, R. A.; Knowles, J. R.: Letter: Aryldiazirines. Potential reagents for photolabeling of biological receptor sites. *J Am Chem Soc* **1973**, *95*, 5072-3.

(126) Chowdhry, V.; Vaughan, R.; Westheimer, F. H.: 2-diazo-3,3,3-trifluoropropionyl chloride: reagent for photoaffinity labeling. *Proceedings of the National Academy of Sciences of the United States of America* **1976**, *73*, 1406-8.

(127) Brunner, J.; Senn, H.; Richards, F. M.: 3-Trifluoromethyl-3-phenyldiazirine. A new carbene generating group for photolabeling reagents. *The Journal of biological chemistry* **1980**, *255*, 3313-8.

(128) Nielsen, P. E.; Hansen, J. B.; Thomsen, T.; Buchardt, O.: Reagents for photoaffinity labeling. I. Photobinding efficiency of aryl azido-, diazocyclopentadienyl-and ethyl diazomalonyl-derivatives of 9-aminoacridine. *Experientia* **1983**, *39*, 1063-1072.

(129) Goeldner, M. P.; Hawkinson, J. E.; Casida, J. E.: Diazocyclohexadienones as photoaffinity ligands: Syntheses of trioxabicyclooctane probes for the convulsant binding site of the GABAA receptor. *Tetrahedron Letters* **1989**, *30*, 823-826.

(130) Galardy, R. E.; Craig, L. C.; Printz, M. P.: Benzophenone triplet: a new photochemical probe of biological ligand-receptor interactions. *Nature: New biology* **1973**, *242*, 127-8.

(131) Stoffel, W.; Schreiber, C.; Scheefers, H.: Lipids with photosensitive groups as chemical probes for the structural analysis of biological membranes. On the localization of the G- and M-protein of vesicular stomatitis virus. *Hoppe-Seyler's Zeitschrift fur physiologische Chemie* **1978**, *359*, 923-31.

(132) Young, M. J. T.; Platz, M. S.: Polyfluorinated aryl azides as photoaffinity labelling reagents; the room temperature CH insertion reactions of singlet pentafluorophenyl nitrene with alkanes. *Tetrahedron Letters* **1989**, *30*, 2199-2202.

(133) Kolpashchikov, D. M.; Zakharenko, A. L.; Dezhurov, S. V.; Rechkunova, N. I.; Khodyreva, S. N.; Degtiarev, S.; Litvak, V. V.; Lavrik, O. I.: [New reagents for affinity modification of biopolymers. Photoaffinity modification of Tte-DNA polymerase]. *Bioorganicheskaia khimiia* **1999**, *25*, 129-36.

(134) Goeldner, M. P.; Hirth, C. G.: Specific photoaffinity labeling induced by energy transfer: application to irreversible inhibition of acetylcholinesterase. *Proceedings of the National Academy of Sciences* **1980**, *77*, 6439-6442.

(135) Vodovozova, E. L.: Photoaffinity labeling and its application in structural biology. *Biochemistry (Moscow)* **2007**, *72*, 1-20.

(136) Vodovozova, E. L.: Photoaffinity labeling and its application in structural biology. *Biochemistry. Biokhimiia* **2007**, *72*, 1-20.

(137) Reiser, A.; Willets, F. W.; Terry, G. C.; Williams, V.; Marley, R.: Photolysis of aromatic azides. Part 4.-Lifetimes of aromatic nitrenes and absolute rates of some of their reactions. *Transactions of the Faraday Society* **1968**, *64*, 3265-3275.

(138) Geiger, M. W.; Elliot, M. M.; Karacostas, V. D.; Moricone, T. J.; Salmon, J. B.; Sideli, V. L.; Onge, M. A. S.: ARYL AZIDES AS PROTEIN PHOTOLABELS: ABSORPTION SPECTRAL PROPERTIES AND QUANTUM YIELDS OF PHOTODISSOCIATION. *Photochemistry and Photobiology* **1984**, *40*, 545-548.

(139) Hall, J. H.; Hill, J. W.; Tsai, H.-c.: Insertion reactions of aryl nitrenes. *Tetrahedron Letters* **1965**, *6*, 2211-2216.

(140) Blencowe, A.; Hayes, W.: Development and application of diazirines in biological and synthetic macromolecular systems. *Soft Matter* **2005**, *1*, 178-205.

(141) Dürr, H.: Carbenes, Nitrenes and Arynes. Von T. L. Gilchrist u. C. W. Rees. Th. Nelson and Sons Ltd., London 1969. 1. Aufl., 131 S., geb. $ 21.—. *Angewandte Chemie* **1971**, *83*, 812-812.

(142) Weber, P. J.; Beck-Sickinger, A. G.: Comparison of the photochemical behavior of four different photoactivatable probes. *The journal of peptide research : official journal of the American Peptide Society* **1997**, *49*, 375-83.

(143) Bayley, H.: *Photogenerated reagents in biochemistry and molecular biology / Hagan Bayley*; Elsevier: Amsterdam ; New York, 1983.

(144) Dorman, G.; Prestwich, G. D.: Benzophenone photophores in biochemistry. *Biochemistry* **1994**, *33*, 5661-73.

(145) Wittelsberger, A.; Thomas, B. E.; Mierke, D. F.; Rosenblatt, M.: Methionine acts as a "magnet" in photoaffinity crosslinking experiments. *FEBS Letters* **2006**, *580*, 1872-1876.

(146) Bishop, A. C.; Ubersax, J. A.; Petsch, D. T.; Matheos, D. P.; Gray, N. S.; Blethrow, J.; Shimizu, E.; Tsien, J. Z.; Schultz, P. G.; Rose, M. D.; Wood, J. L.; Morgan, D. O.; Shokat, K.

M.: A chemical switch for inhibitor-sensitive alleles of any protein kinase. *Nature* **2000**, *407*, 395-401.

(147) Bishop, A. C.; Shah, K.; Liu, Y.; Witucki, L.; Kung, C.; Shokat, K. M.: Design of allele-specific inhibitors to probe protein kinase signaling. *Current biology : CB* **1998**, *8*, 257-66.

(148) Habelhah, H.; Shah, K.; Huang, L.; Burlingame, A. L.; Shokat, K. M.; Ronai, Z.: Identification of new JNK substrate using ATP pocket mutant JNK and a corresponding ATP analogue. *The Journal of biological chemistry* **2001**, *276*, 18090-5.

(149) Larochelle, S.; Batliner, J.; Gamble, M. J.; Barboza, N. M.; Kraybill, B. C.; Blethrow, J. D.; Shokat, K. M.; Fisher, R. P.: Dichotomous but stringent substrate selection by the dual-function Cdk7 complex revealed by chemical genetics. *Nature structural & molecular biology* **2006**, *13*, 55-62.

(150) Eblen, S. T.; Kumar, N. V.; Shah, K.; Henderson, M. J.; Watts, C. K.; Shokat, K. M.; Weber, M. J.: Identification of novel ERK2 substrates through use of an engineered kinase and ATP analogs. *The Journal of biological chemistry* **2003**, *278*, 14926-35.

(151) Chi, Y.; Welcker, M.; Hizli, A. A.; Posakony, J. J.; Aebersold, R.; Clurman, B. E.: Identification of CDK2 substrates in human cell lysates. *Genome Biol* **2008**, *9*, R149.

(152) Chaudhary, A.; Brugge, J. S.; Cooper, J. A.: Direct phosphorylation of focal adhesion kinase by c-Src: evidence using a modified nucleotide pocket kinase and ATP analog. *Biochemical and biophysical research communications* **2002**, *294*, 293-300.

(153) Shah, K.; Shokat, K. M.: A chemical genetic screen for direct v-Src substrates reveals ordered assembly of a retrograde signaling pathway. *Chemistry & biology* **2002**, *9*, 35-47.

(154) Schauble, S.; King, C. C.; Darshi, M.; Koller, A.; Shah, K.; Taylor, S. S.: Identification of ChChd3 as a novel substrate of the cAMP-dependent protein kinase (PKA) using an analog-sensitive catalytic subunit. *The Journal of biological chemistry* **2007**, *282*, 14952-9.

(155) Boyle, S. N.; Koleske, A. J.: Use of a chemical genetic technique to identify myosin IIb as a substrate of the Abl-related gene (Arg) tyrosine kinase. *Biochemistry* **2007**, *46*, 11614-20.

(156) Ubersax, J. A.; Woodbury, E. L.; Quang, P. N.; Paraz, M.; Blethrow, J. D.; Shah, K.; Shokat, K. M.; Morgan, D. O.: Targets of the cyclin-dependent kinase Cdk1. *Nature* **2003**, *425*, 859-64.

(157) Kim, S.; Shah, K.: Dissecting yeast Hog1 MAP kinase pathway using a chemical genetic approach. *FEBS Lett* **2007**, *581*, 1209-16.

(158) Dephoure, N.; Howson, R. W.; Blethrow, J. D.; Shokat, K. M.; O'Shea, E. K.: Combining chemical genetics and proteomics to identify protein kinase substrates. *Proc Natl Acad Sci U S A* **2005**, *102*, 17940-5.

(159) Staudinger, J.; Zhou, J.; Burgess, R.; Elledge, S. J.; Olson, E. N.: PICK1: a perinuclear binding protein and substrate for protein kinase C isolated by the yeast two-hybrid system. *The Journal of Cell Biology* **1995**, *128*, 263-271.

(160) Wankhede, D. P.; Misra, M.; Singh, P.; Sinha, A. K.: Rice Mitogen Activated Protein Kinase Kinase and Mitogen Activated Protein Kinase Interaction Network Revealed by <italic>In-Silico</italic> Docking and Yeast Two-Hybrid Approaches. *PLoS ONE* **2013**, *8*, e65011.

(161) Liang, W.; Yang, B.; Yu, B.-J.; Zhou, Z.; Li, C.; Jia, M.; Sun, Y.; Zhang, Y.; Wu, F.; Zhang, H.; Wang, B.; Deyholos, M.; Jiang, Y.-Q.: Identification and analysis of MKK and MPK gene families in canola (Brassica napus L.). *BMC Genomics* **2013**, *14*, 392.

(162) Maly, D. J.; Allen, J. A.; Shokat, K. M.: A mechanism-based cross-linker for the identification of kinase-substrate pairs. *J Am Chem Soc* **2004**, *126*, 9160-1.

(163) Liu, K.; Kalesh, K. A.; Bing Ong, L.; Yao, S. Q.: An Improved Mechanism-Based Cross-Linker for Multiplexed Kinase Detection and Inhibition in a Complex Proteome. *ChemBioChem* **2008**, *9*, 1883-1888.

(164) Statsuk, A. V.; Maly, D. J.; Seeliger, M. A.; Fabian, M. A.; Biggs, W. H., 3rd; Lockhart, D. J.; Zarrinkar, P. P.; Kuriyan, J.; Shokat, K. M.: Tuning a three-component reaction for trapping kinase substrate complexes. *J Am Chem Soc* **2008**, *130*, 17568-74.

(165) Parang, K.; Kohn, J. A.; Saldanha, S. A.; Cole, P. A.: Development of photo-crosslinking reagents for protein kinase-substrate interactions. *FEBS Lett* **2002**, *520*, 156-60.

(166) Suwal, S.; Pflum, M. H.: Phosphorylation-dependent kinase-substrate cross-linking. *Angew Chem Int Ed Engl* **2010**, *49*, 1627-30.

(167) Suwal, S.; Senevirathne, C.; Garre, S.; Pflum, M. K.: Structural Analysis of ATP Analogues Compatible with Kinase-Catalyzed Labeling. *Bioconjug Chem* **2012**, *23*, 2386–2391.

(168) Mackinlay, A. G.; West, D. W.; Manson, W.: Specific Casein Phosphorylation by a Casein Kinase from Lactating Bovine Mammary Gland. *European Journal of Biochemistry* **1977**, *76*, 233-243.

(169) Litchfield, D. W.: Protein kinase CK2: structure, regulation and role in cellular decisions of life and death. *The Biochemical journal* **2003**, *369*, 1-15.

(170) Allende, J. E.; Allende, C. C.: Protein kinases. 4. Protein kinase CK2: an enzyme with multiple substrates and a puzzling regulation. *The FASEB Journal* **1995**, *9*, 313-23.

(171) Mahmood, R.; Yount, R. G.: Photochemical probes of the active site of myosin. Irradiation of trapped 3'-O-(4-benzoyl)benzoyladenosine 5'-triphosphate labels the 50-kilodalton heavy chain tryptic peptide. *The Journal of biological chemistry* **1984**, *259*, 12956-9.

(172) Farrell, I. S.; Toroney, R.; Hazen, J. L.; Mehl, R. A.; Chin, J. W.: Photo-cross-linking interacting proteins with a genetically encoded benzophenone. *Nature methods* **2005**, *2*, 377-84.

(173) Yan, P.; Wang, T.; Newton, G. J.; Knyushko, T. V.; Xiong, Y.; Bigelow, D. J.; Squier, T. C.; Mayer, M. U.: A targeted releasable affinity probe (TRAP) for in vivo photocrosslinking. *ChemBioChem* **2009**, *10*, 1507-18.

(174) Trott, O.; Olson, A. J.: AutoDock Vina: improving the speed and accuracy of docking with a new scoring function, efficient optimization, and multithreading. *J Comput Chem* **2010**, *31*, 455-61.

(175) Lane, D. P.; Crawford, L. V.: T antigen is bound to a host protein in SV40 transformed cells. *Nature* **1979**, *278*, 261-263.

(176) Linzer, D. I. H.; Levine, A. J.: Characterization of a 54K dalton cellular SV40 tumor antigen present in SV40 transformed cells and uninfected embryonal carcinoma cells. *Cell* **1979**, *17*, 43-52.

(177) DeLeo, A. B.; Jay, G.; Appella, E.; Dubois, G. C.; Law, L. W.; Old, L. J.: Detection of a transformation-related antigen in chemically induced sarcomas and other transformed cells of the mouse. *Proceedings of the National Academy of Sciences of the United States of America* **1979**, *76*, 2420-2424.

(178) Kress, M.; May, E.; Cassingena, R.; May, P.: Simian virus 40-transformed cells express new species of proteins precipitable by anti-simian virus 40 tumor serum. *Journal of virology* **1979**, *31*, 472-83.

(179) Smith, A. E.; Smith, R.; Paucha, E.: Characterization of different tumor antigens present in cells transformed by simian virus 40. *Cell* **1979**, *18*, 335-346.

(180) Melero, J.; Stitt, D. T.; Mangel, W. F.; Carroll, R. B.: Identification of new polypeptide species (48–55K) immunoprecipitable by antiserum to purified large T antigen and present in SV40-infected and -transformed cells. *Virology* **1979**, *93*, 466-480.

(181) Finlay, C. A.; Hinds, P. W.; Levine, A. J.: The p53 proto-oncogene can act as a suppressor of transformation. *Cell* **1989**, *57*, 1083-1093.

(182) Baker, S. J.; Fearon, E. R.; Nigro, J. M.; Hamilton, S. R.; Preisinger, A. C.; Jessup, J. M.; Van Tuinen, P.; Ledbetter, D. H.; Barker, D. F.; Nakamura, Y.; White, R.; Vogelstein, B.: Chromosome 17 deletions and p53 gene mutations in colorectal carcinomas. *Science* **1989**, *244*, 217-221.

(183) Levine, A. J.: p53, the cellular gatekeeper for growth and division. *Cell* **1997**, *88*, 323-331.

(184) Lane, D. P.: p53, guardian of the genome. *Nature* **1992**, *358*, 15-16.

(185) Vogelstein, B.; Lane, D.; Levine, A. J.: Surfing the p53 network. *Nature* **2000**, *408*, 307-10.

(186) Clore, G. M.; Omichinski, J. G.; Sakaguchi, K.; Zambrano, N.; Sakamoto, H.; Appella, E.; Gronenborn, A. M.: High-resolution structure of the oligomerization domain of p53 by multidimensional NMR. *Science* **1994**, *265*, 386-91.

(187) Kussie, P. H.; Gorina, S.; Marechal, V.; Elenbaas, B.; Moreau, J.; Levine, A. J.; Pavletich, N. P.: Structure of the MDM2 oncoprotein bound to the p53 tumor suppressor transactivation domain. *Science* **1996**, *274*, 948-53.

(188) Cho, Y.; Gorina, S.; Jeffrey, P. D.; Pavletich, N. P.: Crystal structure of a p53 tumor suppressor-DNA complex: understanding tumorigenic mutations. *Science* **1994**, *265*, 346-55.

(189) Kruse, J.-P.; Gu, W.: Modes of p53 Regulation. *Cell* **2009**, *137*, 609-622.

(190) Maclaine, N. J.; Hupp, T. R.: The regulation of p53 by phosphorylation: a model for how distinct signals integrate into the p53 pathway. *Aging* **2009**, *1*, 490-502.

(191) Sakaguchi, K.; Sakamoto, H.; Lewis, M. S.; Anderson, C. W.; Erickson, J. W.; Appella, E.; Xie, D.: Phosphorylation of Serine 392 Stabilizes the Tetramer Formation of Tumor Suppressor Protein p53. *Biochemistry* **1997**, *36*, 10117-10124.

(192) Filhol, O.; Baudier, J.; Chambaz, E. M.; Cochet, C.: Casein kinase 2 inhibits the renaturation of complementary DNA strands mediated by p53 protein. *The Biochemical journal* **1996**, *316 (Pt 1)*, 331-5.

(193) Meek, D. W.; Simon, S.; Kikkawa, U.; Eckhart, W.: The p53 tumour suppressor protein is phosphorylated at serine 389 by casein kinase II. *The EMBO journal* **1990**, *9*, 3253-60.

(194) Ha, G.-H.; Breuer, E.-K. Y.: Mitotic Kinases and p53 Signaling. *Biochemistry Research International* **2012**, *2012*, 14.

(195) Bode, A. M.; Dong, Z.: Post-translational modification of p53 in tumorigenesis. *Nature reviews. Cancer* **2004**, *4*, 793-805.

(196) Michael, D.; Oren, M.: The p53-Mdm2 module and the ubiquitin system. *Seminars in cancer biology* **2003**, *13*, 49-58.

(197) Levine, A. J.: p53, the cellular gatekeeper for growth and division. *Cell* **1997**, *88*, 323-31.

(198) Vassilev, L. T.; Vu, B. T.; Graves, B.; Carvajal, D.; Podlaski, F.; Filipovic, Z.; Kong, N.; Kammlott, U.; Lukacs, C.; Klein, C.; Fotouhi, N.; Liu, E. A.: In Vivo Activation of the p53 Pathway by Small-Molecule Antagonists of MDM2. *Science* **2004**, *303*, 844-848.

(199) Thompson, T.; Tovar, C.; Yang, H.; Carvajal, D.; Vu, B. T.; Xu, Q.; Wahl, G. M.; Heimbrook, D. C.; Vassilev, L. T.: Phosphorylation of p53 on Key Serines Is Dispensable for Transcriptional Activation and Apoptosis. *Journal of Biological Chemistry* **2004**, *279*, 53015-53022.

(200) Lu, H.; Shimazaki, N.; Raval, P.; Gu, J.; Watanabe, G.; Schwarz, K.; Swanson, P. C.; Lieber, M. R.: A biochemically defined system for coding joint formation in V(D)J recombination. *Molecular cell* **2008**, *31*, 485-97.

(201) Smith, G. R.: How homologous recombination is initiated: unexpected evidence for single-strand nicks from v(d)j site-specific recombination. *Cell* **2004**, *117*, 146-8.

(202) Woo, R. A.; Jack, M. T.; Xu, Y.; Burma, S.; Chen, D. J.; Lee, P. W.: DNA damage-induced apoptosis requires the DNA-dependent protein kinase, and is mediated by the latent population of p53. *The EMBO journal* **2002**, *21*, 3000-8.

(203) Woo, R. A.; McLure, K. G.; Lees-Miller, S. P.; Rancourt, D. E.; Lee, P. W.: DNA-dependent protein kinase acts upstream of p53 in response to DNA damage. *Nature* **1998**, *394*, 700-4.

(204) Achanta, G.; Pelicano, H.; Feng, L.; Plunkett, W.; Huang, P.: Interaction of p53 and DNA-PK in response to nucleoside analogues: potential role as a sensor complex for DNA damage. *Cancer research* **2001**, *61*, 8723-9.

(205) Hill, R.; Madureira, P. A.; Waisman, D. M.; Lee, P. W.: DNA-PKCS binding to p53 on the p21WAF1/CIP1 promoter blocks transcription resulting in cell death. *Oncotarget* **2011**, *2*, 1094-108.

(206) Chase, D.; Feng, Y.; Hanshew, B.; Winkles, J. A.; Longo, D. L.; Ferris, D. K.: Expression and phosphorylation of fibroblast-growth-factor-inducible kinase (Fnk) during cell-cycle progression. *The Biochemical journal* **1998**, *333 (Pt 3)*, 655-60.

(207) Xie, S.; Wu, H.; Wang, Q.; Cogswell, J. P.; Husain, I.; Conn, C.; Stambrook, P.; Jhanwar-Uniyal, M.; Dai, W.: Plk3 functionally links DNA damage to cell cycle arrest and apoptosis at least in part via the p53 pathway. *The Journal of biological chemistry* **2001**, *276*, 43305-12.

(208) Xie, S.; Wang, Q.; Wu, H.; Cogswell, J.; Lu, L.; Jhanwar-Uniyal, M.; Dai, W.: Reactive oxygen species-induced phosphorylation of p53 on serine 20 is mediated in part by polo-like kinase-3. *The Journal of biological chemistry* **2001**, *276*, 36194-9.

(209) Cubillos-Rojas, M.; Amair-Pinedo, F.; Tato, I.; Bartrons, R.; Ventura, F.; Rosa, J. L.: Simultaneous electrophoretic analysis of proteins of very high and low molecular mass using Tris-acetate polyacrylamide gels. *Electrophoresis* **2010**, *31*, 1318-21.

(210) Cuddihy, A. R.; Wong, A. H.; Tam, N. W.; Li, S.; Koromilas, A. E.: The double-stranded RNA activated protein kinase PKR physically associates with the tumor suppressor p53 protein and phosphorylates human p53 on serine 392 in vitro. *Oncogene* **1999**, *18*, 2690-702.

(211) Okamoto, K.; Beach, D.: Cyclin G is a transcriptional target of the p53 tumor suppressor protein. *The EMBO journal* **1994**, *13*, 4816-22.

(212) Sato, J.; Shimizu, H.; Kasama, T.; Yabuta, N.; Nojima, H.: GAK, a regulator of clathrin-mediated membrane trafficking, localizes not only in the cytoplasm but also in the nucleus. *Genes to cells : devoted to molecular & cellular mechanisms* **2009**, *14*, 627-41.

(213) Leung, T.; Chen, X. Q.; Tan, I.; Manser, E.; Lim, L.: Myotonic dystrophy kinase-related Cdc42-binding kinase acts as a Cdc42 effector in promoting cytoskeletal reorganization. *Molecular and cellular biology* **1998**, *18*, 130-40.

(214) Wilkinson, S.; Paterson, H. F.; Marshall, C. J.: Cdc42-MRCK and Rho-ROCK signalling cooperate in myosin phosphorylation and cell invasion. *Nature cell biology* **2005**, *7*, 255-61.

(215) Jebelli, J. D.; Hooper, C.; Garden, G. A.; Pocock, J. M.: Emerging roles of p53 in glial cell function in health and disease. *Glia* **2012**, *60*, 515-25.

(216) Qin, Q.; Liao, G.; Baudry, M.; Bi, X.: Role of calpain-mediated p53 truncation in semaphorin 3A-induced axonal growth regulation. *Proc Natl Acad Sci U S A* **2010**, *107*, 13883-7.

(217) Bradford, M. M.: A rapid and sensitive method for the quantitation of microgram quantities of protein utilizing the principle of protein-dye binding. *Anal Biochem* **1976**, *72*, 248-54.

(218) Shevchenko, A.; Wilm, M.; Vorm, O.; Mann, M.: Mass spectrometric sequencing of proteins silver-stained polyacrylamide gels. *Analytical chemistry* **1996**, *68*, 850-8.

ABSTRACT

SYNTHESIS AND APPLICATION OF ATP ANALOGS FOR PHOSPHORYLATION-DEPENDENT KINASE-SUBSTRATE CROSSLINKING

by

SATISH KUMAR GARRE VENKATA RAGHAVENDRA

December 2013

Advisor: Prof. Mary Kay Pflum

Major: Chemistry (Organic)

Degree: Doctor of Philosophy

Phosphorylation is an important post-translational modification that plays a key role in a variety of signaling cascades and cellular functions. Kinases phosphorylate protein substrates in a highly regulated manner and also demonstrate substrate promiscuity. Understanding kinase-substrate specificity has been challenging and there is a need for new chemical tools. To this end, we developed γ-phosphate modified ATP photocrosslinking analogs ATP-ArN_3 and ATP-BP that crosslink substrate and kinase in a phosphorylation-dependent manner. We have successfully demonstrated that ATP-ArN_3 and ATP-BP can be used with natural kinase and substrates using cell lysates *in vitro*. We used our approach to identify novel kinases of p53. One powerful feature of this methodology is that we can obtain atomic level snapshots of the interactions between proteins when coupled with analytical techniques like mass spectrometry (MS). These tools will help us in validating our understanding of kinase-substrate interactions, their roles in signaling pathways, and in the cellular processes.

AUTOBIOGRAPHICAL STATEMENT

SATISH KUMAR GARRE VENKATA RAGHAVENDRA

Education

2008-2013 **Ph.D.** (Organic Chemistry), Wayne State University, Detroit, MI, USA

2005-2007 **M.S.** (Chemistry), Texas A&M University-Commerce, Commerce, TX, USA

2001-2003 **M.Sc.** Osmania University, Hyderabad, India

1997-2000 **B.Sc. (Hons)**, Sri Sathya Sai Institute of Higher Learning, Puttaparthy, India

Fellowships

- Summer Dissertation Fellowship, Graduate School, Wayne State University, **2013**.
- Summer Research Fellowship, Graduate School, Texas A&M University-Commerce, **2007**.
- Robert A. Welch Graduate Research Assistantship, Texas A&M University-Commerce, **2006**.
- Robert A. Welch Scholarship, Department of Chemistry, Texas A&M University-Commerce, **2005**.
- Andhra Pradesh State Government Educational Merit Scholarship, India, **1992** to **1995**.

Publications

- **Satish Garre**, Todd Faner and Mary Kay H. Pflum* "Development of an ATP Analog to Identify Novel Kinases of P53 Substrate." (manuscript in preparation)
- **Satish Garre**, Sujit Suwal, Chamara Senevirathne, and Mary Kay H. Pflum* "Comparative Study of ATP Analogs for Kinase-Catalyzed Photocrosslinking." (manuscript in preparation)
- Geetha Padige, **Satish Garre**, Anton V. Bieliauskas, Sun Ea Choi, Sujith V. W. Weerasinghe and Mary Kay H. Pflum* "Synthesis and Biological Evaluation of C-7 Modified SAHA Analogs as HDAC Inhibitors." (manuscript in preparation)
- Sujit Suwal, Chamara Senevirathne, **Satish Garre** and Mary Kay H. Pflum* "Structural Analysis of ATP Analogues Compatible with Kinase-Catalyzed Labeling." Bioconjugate Chem., **2012**, *23* (12), 2386-2391.
- Bukuo Ni, Qianying Zhang, **Satish Garre** and Allan D. Headley* "Ionic Liquid (IL) as an Effective Medium for the Highly Efficient Hydroacylation Reaction of Aldehydes with Azodicarboxylates." *Adv Synth. & Catal.*, **2009**, 351, 6, 875.
- **Satish Garre**, Erica Parker, Bukuo Ni* and Allan D. Headley* "Design and Synthesis of Bistereogenic Chiral Ionic Liquids and Their Use as Solvents for Asymmetric Baylis-Hillman Reactions." *Org. Biomol. Chem.* **2008**, 6, 3041. (Highlighted by *SYNFACTS*).
- Bukuo Ni, **Satish Garre**, and Allan D. Headley* "Design and Synthesis of Fused-Ring Chiral Ionic Liquids from Amino acid Derivatives." *Tetrahedron Lett.*, **2007**, 48, 1999.